AN EMPIRICAL INVESTIGATION OF CATASTROPHIC AND PARTIAL FAILURES OF BULK STORAGE VESSELS AND SUBSEQUENT BUND WALL OVERTOPPING AND DYNAMIC PRESSURES

WILLIAM ATHERTON

BEng (Hons.)

A thesis submitted in partial fulfilment of the requirements of Liverpool John Moores University for the Degree of Doctor of Philosophy

This research was carried out as an extension of a project funded by the Health and Safety Executive

April 2008

ABSTRACT

The Methodology and Standards Development Unit of the Health and Safety Executive (HSE) commissioned Liverpool John Moores University (LJMU) to construct a laboratory facility to conduct a series of tests simulating the sudden failure of a tank such as is used industrially for the storage of hazardous liquids. Such failures are rare. However, history has shown that when they do occur a large proportion of the liquid is likely to escape over the surrounding bund wall or embankment, even if the force of the wave impact does not damage the retaining structures. This thesis introduces the background to the project, describes the new test facility, records the results of the investigation and shapes conclusions, which form partial fulfilment for the degree of Doctor of Philosophy. The results will be of value to the HSE in the performance of its statutory duties, and may be of value to tank storage operators in their consideration of the extent and severity of foreseeable major accidents, in their risk assessments and in their consideration of reasonably practicable measures to reduce those risks.

Tanks used for bulk storage of hazardous liquids are often completely surrounded by a wall or earth embankment with the aim of providing secondary containment for any spillage from the tank. If the walls of the bunded area have been designed, built and maintained in line with current standards then they will provide full containment of the likely spills. However, they will not contain the surge of liquid that would follow a catastrophic failure of the tank; even if the surge does not destroy the bund wall, the flood wave is likely to overtop it. Whilst catastrophic failure of bulk storage tanks is rare, the consequences for site personnel, any local community and the environment can be severe. Such accidents have occurred all around the world, such as in the USA, in Greece and in Lithuania, with colder climates being particularly at risk due to certain types of steel tanks becoming brittle with extended periods of exposure.

The laboratory facility was built to perform simulations of catastrophic and partial failures of a storage tank, covering a comprehensive range of tank and bund arrangements and to measure both the dynamic pressures that are exerted on the bund wall and the quantity of liquid that overtops it. Charts and correlating functions were derived, allowing interpolation to other tank and bund arrangements at full scale. The resulting empirical equations allow operators and other interested parties to quickly and easily assess the potential impact of various failure scenarios in terms of overtopping and to determine if the

structural integrity of the bund itself is a factor in the possible complete loss of secondary containment.

For overtopping, Equation 6.1:

$$Q = A\ exp\left[-B\left(\frac{h}{H}\right)\right]$$

With A and B taking values as recommended in Chapter 6

For dynamic pressures, Equation 6.2:

$$Dyn/Stat_{\ base} = C\ exp\left[-D\left(\frac{h}{H}\right)\right]$$

With C and D taking values as recommended in Chapter 6

The major extent of this work far exceeds previous attempts to quantify the extent of the problems experienced when a bulk storage vessel fails both in the types of failure modelled and in the range of configurations considered. A total of 183 different tank and bund configurations with various failure modes were investigated, with each individual test repeated at least five times. The novelty of this work is in the determination of the dynamic pressures associated with the bund overtopping and in evaluating any relationships between them.

Observations and measurements made during the testing programme determined the performance and integrity of bund walls to be in question given the force of the impounded wave in the event of a catastrophic failure of the primary containment. The findings clearly indicate that the vast majority of current installations are severely at risk in the event of catastrophic failures and various other forms of major leaks. The implications are that existing regulations and guidelines need to be re-evaluated to improve the assessment of potential risks and to recommend suitable mitigation measures in environmentally sensitive areas.

AKNOWLEDGEMENTS

I would like to thank the following people for their valued support and advice during the period of this research:

1.	My Wife	Elizabeth Atherton.
2.	My Parents	William Atherton and Sandra Iris Atherton.
3.	My Principal Supervisor	Dr. Rafid Alkhaddar.
4.	My supervision team	Dr. Neil Woolley and Dr. Aubrey Thyer.
5.	University Technical Staff	John Ash, Christopher Byrne, Malcolm Feegan, David Hewitt, Paul Hodgkinson, Alan Jones, Anthony Owens, John Sinclair.
6.	University Administration Staff	Steven Bennett and Katherine Griffiths
7.	Health and Safety Executive Staff	Ian Hirst, and Shaun Welsh

Thanks are also due to the United States Environmental Protection Agency for their kind permission to reproduce the photographic plate of the Ashland Oil incident (1988). In addition acknowledgement is due to the Office of Response and Restoration, National Ocean Service, National Oceanic and Atmospheric Administration, USA for their provision of access to incidents gallery.

CONTENTS

LIST OF CHARTS

LIST OF FIGURES

LIST OF PLATES

LIST OF TABLES

ABBREVIATIONS / ACRONYMS

A to D	Analogue to digital
API	American Petroleum Institute
bbl	blue barrel (42 US gallons)
BPA	British Pipeline Agency
CFD	Computational Fluid Dynamics
CIRIA	Construction Industry Research and Information Association
COAST	Catastrophic Overtopping Alleviation of Storage Tanks
COMAH	Control of Major Accident Hazards (Regulations)
EA	Environment Agency
EU	European union
HSE	Health and Safety Executive
HSL	Health and Safety Laboratory
LJMU	Liverpool John Moores University
MHIDAS	Major Hazard Investigation Database
MIT	Massachusetts Institute of Technology
MOTIF	Mitigation of Tank Instantaneous Failures
NACE	The National Association of Corrosion Engineers
NRC	National Response Center (USA)
PDA	Personal Data Assistant
RCM	Random Choice Method
'SPLOT'	HSE two-dimensional modelling software
UK	United Kingdom
US/USA	United States of America
USEPA	United States Environmental Protection Agency
VOF	Volume of Fluid
WAF	Wave Average Flux

NOMENCLATURE

R	Radius of tank
r	Bund radius
r_c	Corner radius
H	Height of fluid in tank
h	Height of bund
L	Tank to bund separation distance
θ	Angle of bund
d	Rectangular bund dimension
x	Rectangular bund dimension
y	Rectangular bund dimension
z	Rectangular bund dimension
Q	Experimental overtopping fraction
Q_f	Predicted overtopping using empirical formulae
Q_C	Predicted overtopping using Clark formula
Q_H	Predicted overtopping using Hirst formula
K	Overtopping conversion factor
Q_m	Modified overtopping fraction
V_{cap}	Bund capacity
V_{rel}	Volume released
V_{bund}	Volume retained
V_{slosh}	Volume overtopping
Dyn_{base}	Dynamic pressure at the base of the bund
$Stat_{base}$	Static pressure at the base of the bund
$Dyn/Stat_{base}$	Dynamic to static pressure ratio at the base of the bund
$Dyn/Stat_{cal}$	Calculated dynamic to static ratio at the base of the bund
u/v	Velocity
g	Acceleration due to gravity ($9.81ms^{-2}$)
R_e	Reynolds number
W_e	Webber number
ρ	Density
μ	Viscosity
σ	Surface tension
Dia	Diameter

Π	Pi (3.142)
A_{rel}	Release area
A_{tot}	Total area
$A_{\%}$	Percentage area of release
a	Acceleration
t	Time
s	Distance
u_m	Velocity for model
u_p	Velocity for prototype
l_m	Length for model
l_p	Length for prototype

GLOSSARY OF SYMBOLS

UNITS

m	Metres
s/secs	Seconds
Pa	Pascals
N	Newtons
g	Grammes
psi	Pounds per Square Inch
%	Percentage
°	Degrees (Angular)
°C	Degrees Centigrade, or Degrees Celsius

MULTIPLIER PREFIXES

M	Mega	$x10^{6}$
k	Kilo	$x10^{3}$
c	Centi	$x10^{-2}$
m	Milli	$x10^{-3}$
μ	Micro	$x10^{-6}$

CHAPTER 1

Introduction

1.1 Preface

Chemical storage of any kind gives rise to potential threats to the environment and poses health and safety issues, which require extensive consideration in terms of the management of design, manufacture, installation, operation, regular inspection and maintenance. There are numerous guidelines in existence to help give rise to standardised methods of work and to give recommendations on good practice, with slight variations depending upon the country of the installation. With regard to the UK the recent publication of the document *Chemical storage tank systems – good practice* CIRIA C598 (2003), aims to give guidance on design, manufacture, installation, operation, inspection and maintenance. The document is targeted at project promoters, designers, manufacturers, construction and maintenance engineers, construction project managers, site engineers and operatives as well as regulators (Cassie and Seale, 2003).

The 1999 Environment Agency (EA) report *Spotlight on business environmental performance* highlights the risks due to bad practice and outlines details on the prosecution of more than 100 companies for water pollution offences during that year. Although some improvements have been made over the last few years, there is still an urgent need for further improvement in the management of all areas of chemical storage.

Storage tanks are commonly surrounded by a catchment area in the form of a retaining wall, known as a bund, its function being to retain any spillages, which may occur. Bunds are a form of secondary containment sometimes used within plant buildings for reactors and other process vessels. It is normal to limit the number of tanks to 60,000 m^3 total capacity with incompatible materials having separate bunds as outlined in the Technical Measures Document on secondary containment issued by the Health and Safety Executive (2000).

Bunds are normally designed to hold 110 % of the volume of that of the largest tank, the excess height notionally to prevent stored liquid surging over the top of the bund in the event of a catastrophic failure of the primary containment. This allowance has proved to

be inadequate as, even with storage volume excess, large quantities of liquid can still overtop bunds as discussed by Thyer and Jagger (1997). This has been demonstrated by various researchers including Greenspan and Young (1978) and Greenspan and Johansson (1981), together with actual incidences of containment vessel failure e.g. at Ponca City in 1924 and Floreffe in 1988. Within the last decade, several incidents have occurred in which tanks have failed catastrophically involving flammable vapours inside an atmospheric storage tank exploding. This resulted in the tank splitting along the side seam or being propelled upward from its base (shell to base failure).

Welding operations are a common cause of catastrophic failure with vapours igniting outside the tank and flashback occurring into the tank itself. These incidents commonly result in serious injury or death to workers as well as environmental contamination as indicated by the United States Environmental Protection Agency (1997). Examples of the latter include:

- Floreffe, January 1988 – failure of a 4 million gallon tank of fuel oil at Ashland Oil released a wave of oil that surged through the bunded area damaging another tank, overtopping the bund and subsequently polluting major rivers (Plate 1.1).
- Iowa, March 1997 – failure of a 1 million gallon tank of ammonium phosphate.
- Michigan, July 1999 – a 1 million gallon tank of ammonium polyphosphate ruptured and damaged three other tanks.
- Ohio, August 2000 – a 1 million gallon tank of liquid fertilizer ruptured and damaged nearby tanks. The resulting wave of liquid broke through a concrete bund and hit five tractor-trailer rigs, pushing them into the Ohio River.
- Ohio, August 2000 – later that month a 1.5 million gallon tank of ammonium phosphate ruptured at the same storage facility. It damaged three other tanks causing them to leak, with liquid overflowing the bund. A total of 450,000 gallons of contaminated water was reclaimed from the sewers and the public drinking water system was feared contaminated, resulting in the widespread use of bottled water as reported by the United States Environmental Protection Agency (2001).

PAGE

EXCLUDED

UNDER

INSTRUCTION

FROM

UNIVERSITY

Later work carried out by Rouzsky (1983 cited in Thyer et al, 2002), led to the conclusion that these pressures may only be as high as 3 times the hydrostatic pressure at the base. An examination of bunding arrangements at numerous sites gave strength reserve factors, which varied greatly (factors of safety ranging from 600 down as low as 2), the lowest factors applying to larger bunds, where some risk of total failure was identified (Thyer and MacMillan, 1998). Due to the fact that bunds are normally designed to withstand the pressure due to a static head of fluid, a more accurate assessment of the resulting dynamic pressures is therefore needed. This will allow a more accurate analysis for the determination of safety factors for bunding and permit the design of adequate mitigation in the case of existing facilities.

The need for a more accurate assessment tool for the various bunding arrangements and the lack of available source data, particularly with respect to the possible magnitude of the dynamic pressures led to a detailed literature review. The literature clearly detailed a vast number of failures around the world, but the records of the quantities lost over the bund were poorly reported even though large quantities and huge surge waves were involved in almost every case. In terms of the research carried out in the area, the information was limited with the first seminal work on bund overtopping carried out in the late seventies (Greenspan and Young, 1978). Research data pertaining to the associated dynamic pressures was first presented by Cuperus (1980 cited in Thyer et al 2002) suggesting factors up to 6 times the static pressure at the base of the bund with later workers suggesting factors of between 2.5 and 3.5 (Trbojevic and Slater, 1989) and finally Rouzsky (1983) quoting a factor of 3. There are obvious discrepancies in the range of values quoted, mainly due to the different scenarios investigated, with limited range of configurations considered in each case. Such variation in the range of possible dynamic pressures exerted on the bunds was an area that clearly merited further, more detailed investigation, particularly in the area of possible bund capacity and the problems with large surface areas producing excessive evaporation.

1.3 Research Aim

The aim of this research is to investigate a substantial range of tank and bund configurations under various modes of failure to more accurately quantify the extent of the possible overtopping and the magnitudes of the dynamic pressures exerted on the bunds.

1.3.1 Objectives

- To produce data from experimental investigations, for percentage of tank contents overtopping model bund walls together with dynamic pressure profiles on the bund walls themselves.
- To perform a statistical analysis and derive charts or correlating functions for overtopping percentages and dynamic pressures in terms of dimensionless ratios of model bund and tank dimensions.
- To compare results with previous work using the dimensionless ratios referred to above.
- To apply findings to provide estimates of possible overtopping fractions and dynamic pressures in full size installations.
- To recommend improvements in bund design to incorporate adequate dynamic pressure strength reserve factors.

1.4 Organisation of the thesis

This thesis is arranged in a manner that reflects the order of the investigation, experimentation and analysis of the data collected.

Chapter 2 Covers the history of previous events and seeks to show that current thinking for the design of bund walls may not be suitable for all types of fluid release.

Chapter 3 Explains the construction of a test rig suitable for the investigation of catastrophic failures of bulk storage tanks and details the instrumentation used to measure the pressure effects on the bunds and the level of overtopping.

Chapter 4 Considers previous work and the correlations derived from the small-scale experimental results and provides an introduction to axisymmetric and asymmetric releases.

Chapter 5 Gives a summary of the results for axisymmetric and asymmetric modes of failure.

Chapter 6 Details the analysis of the axisymmetric and asymmetric test results and poses equations derived for the prediction of overtopping fractions together with expected dynamic pressures.

Chapter 7 Evaluates the performance of empirical formulae in relation to historical case studies including comparisons with associated wave impact research.

Chapter 8 Discusses the implications for stakeholders given the levels of overtopping and the extent of the dynamic pressures found during this investigation.

Chapter 9 Conclusions relating to the major implications for the bulk storage industry and the issues relating to regulators in the design of installations and land use planning together with recommendations for improved risk assessment and possible methods of mitigation.

1.5 Summary

The introduction clearly identifies the extent of the problem in the event of a failure of a bulk storage tank together with the extreme effects of such an incident. Statutory bodies responsible for safety at major facilities have stated a need for greater understanding in the areas of catastrophic and partial tank failures. The performance of secondary containment measures along with the possible extent of any losses is therefore central to any investigation and reliable data is paramount in any efforts to properly identify risk and implement effective mitigation.

The literature review examines a history of events and looks at the causes of bulk storage tank failures together with any 'domino' effects. A number of cases are discussed in further detail and the scope of the problem is explored in terms of the economic, social and environmental impact. Statutory regulations are an important factor in loss prevention in the process industries and the major Directives and Regulations relating to the design, operation and management of such facilities are outlined together with recommendations for the assessment of risk and the implementation of reasonably practicable measures for control of such risks. Limitations of previous research in the field is highlighted by a number of investigations undertaken by the HSE and a definitive need for review is established with the aim of gathering further data to quantify the level of possible losses in the event of a bulk storage tank failure.

CHAPTER 2

Literature Review

2.1 History of events

There have been a substantial number of failures in the primary containment leading to extensive loss of the fluids contained with varying levels of devastation. The modes of failure vary greatly as do the initial causes, however in the cases involving sudden catastrophic release, the bunds were found lacking in almost all instances.

The following examples are indicative of such failures, with a variety of causes listed including natural disasters and accidental releases. Some of the examples given are covered in more detail in order to convey the extent of the problem and to establish the need for a better understanding of the failure mechanisms and the magnitudes of the possible losses.

A selection of tank failures has been catalogued as an extract from a recent paper by Thyer et al (2005) with single tank failures illustrated in Table 2.1. In cases where a single tank failure has led to further tanks being damaged in a 'domino' effect, these have been listed separately in Table 2.2 (Thyer et al, 2005).

Table 2.1 Single tank failures (Thyer et al, 2005)

Date	Location	Contents	Inventory lost	Cause	Reference
1919	Boston USA	Molasses	12,300 tons	Inadequate design	Wilkinson 1991
December 1924	Ponca City, Oklahoma	Oil	8500 tons	Brittle fracture	MHIDAS Database record 2977
February 1952	Esso refinery, Fawley, UK	Water	Approx 21,500 m^3	Failed during hydrotest	Private correspondence
March 1952	Esso refinery, Fawley, UK	Water	Approx 21,500 m^3	Failed during hydrotest	Private correspondence
1957	Meraux, USA	Petrol	2220 m^3	Not known	Wilkinson 1991
January 1966	Feyzin, France	Propane	12000 m^3	-	Loss Prevention Bulletin
1967	North Tees, UK	Ethylene	Not reported	Over-pressurisation	Wilkinson 1991
1968	UK	Water	Not reported	Failed during hydrotest	Private correspondence
1970	Norfolk, USA	Petrol	2700 m^3	Tank collapsed following fire caused by lightning	MHIDAS database
1970	USA	Slop oil	2400 m^3	Internal explosion following lightning strike	IChemE accident database
January 1970	Varannes, Quebec Canada	Ethylene	70 tons	Over-pressurisation	MHIDAS database
December 1970	Netherlands	Fuel oil	19,000 m^3	Brittle fracture starting at corroded weld	Private correspondence
1971	Canada, USA?	Crude oil	Approx 9000 m^3	Brittle fracture	Glossop
1972	USA	Oil	66000 bbl	Brittle fracture	Wilkinson 1991
July 1973	Potchefstroom, S Africa	Ammonia	38 tons	Brittle fracture on domed end	Barnes, 1990
1976	Addyston, USA	Methanol	2275 m^3	Internal explosion following lightning strike	Wilkinson 1991
1976	USA	Asphalt	Not specified	-	Glossop
1977	Umm Said, Qatar	Propane	37000 m^3	Possibility of faulty welding	Lees 1996
1980	El Dorado, Kansas, USA	Solvents	2220 m^3	Mechanical failure	Wilkinson 1991
1981	Moose Jaw, USA	Crude oil	15,900 m^3	Defective welding	Private correspondence
1983	Canada?	Crude oil	Not known	Brittle fracture	Private correspondence
1983	USA	Sulphuric acid	1800 m^3	-	Glossop

1986	Colon, Panama	Light crude oil	38000 m^3	Not known	MHIDAS database
1986	Australia	C4 heavy ends	28 m^3	Internal explosion	Lees 1986
1987	Lyon, France	Multiple failures	-	Internal explosions due to fire in tank farm	Lees 1986
-	-	Lubricating oil	-	Failure at shell/bottom junction due to over-pressurisation	IChemE accident database
-	-	Fuel oil	-	Internal explosions due to fire in tank farm	IChemE accident database
1988	Brisbane, Australia	Petrol	5460 m^3	Mechanical failure	Wilkinson 1991
1988	Floreffe, Pennsylvania, USA	Diesel	14,630 m^3	Lack of full hydrotest for reassembled tank or brittle fracture	Laskowski, and Voltaggio in Bockholts and Heidebrink 1988
1989	USA	Oil	760 m^3	-	Glossop
1989	USA	Phosphoric acid	500 m^3	-	Glossop
1989	Richmond, California, USA	Petrol	3200 m^3	Earthquake	MHIDAS database
20 March 1989	Lithuania	Ammonia	7000 tons	Roll-over	Anderson & Lindley 1992
1992	USA	Water	1100 m^3	-	Glossop
1992	USA?	Undisclosed flammable liquid	Nil. (tank empty)	Ignition of flammable vapour in tank by external welding	USEPA
1993	El Segundo, California, USA	Fuel oil	830 tons	Not known	MHIDAS database
1993	Fawley, UK	Bunker oil	20,000 tons	Not known	MHIDAS database
1994	USA	Petroleum-based sludge	-	Internal explosion	USEPA
1995	USA	Asphalt	14,000 m^3	Internal explosion	Glossop
-	-	Flushing oil	77 tons	Spigot flow over bund following overheating of tank	Safety News
17 July 2001	Delaware USA	Petrol / sulphuric acid mixture	1.1 million gallons	Welding sparks ignited flammable vapours inside badly corroded tank	US Chemical Safety and Hazard Investigation Board
Oct 2004	Hamburg, Germany	Heating oil	500 m^3 in 50,000 m^3 tank	Internal explosion as demolition workers started demolishing the wrong tank	Internet news report.

Table 2.2 Catastrophic tank failure incidents resulting in damage to, or failure of, neighbouring tanks (Thyer et al, 2005)

Date	**Location**	**Contents**	**Inventory lost**		**Cause**	**Reference**
			Source tank	**Subsequent tanks**		
1949	Perth Amboy, USA	Asphalt	Not reported	Not reported	Overheating of asphalt tank caused explosion engulfing 4 adjacent tanks. One, containing naphtha rocketed.	Wilkinson 1991.
1970	USA	Creosote	-	-	-	Glossop
1978	US	Oil	72,000 m^3 - 3 tanks		Failure of three tanks in earthquake	Glossop
1979	USA	-	-		Internal explosion occurred in one tank lifting entire tank off foundations. 10 mins later a neighbouring tank exploded	Glossop
1990	Western Siberia	Crude oil	Not reported	10,000 tons (4 tank contents?)	Internal explosion following lightning strike	IChemE accident database
1995	US	Undisclosed flammable liquid	Approx 500 m^3	Approx 500 m^3	Internal explosion during welding on tank exterior	USEPA*
1997	Iowa, US	Ammonium phosphate solution	4550 m^3	9100 m^3 from 2 tanks	Defective welding	USEPA **
1999	Michigan US	Ammonium phosphate solution	4550 m^3	Damage to three other tanks, volume lost not reported	Defective welding	USEPA**
2000	Ohio, US	Liquid fertiliser	4550 m^3	4500 m^3 from 4 tanks	Defective welding	USEPA**
2000	Ohio, US	Ammonium Phosphate solution	6825 m^3	Approx 3400 m^3 from 3 tanks	Defective welding	USEPA**

(*) US EPA chemical safety alert, EPA 550-F-97-002b, May 1997.

(**) All of these incidents were listed in a USEPA chemical safety alert, EPA 550-F-01-001 January 2001, following a series of catastrophic tank failures. All the tanks were built either by the Carolyn Equipment Company of Fairfield Ohio, or Nationwide tanks Inc. of Hamilton Ohio. Both companies have since gone out of business.

2.2 Investigation of Causes

The failure of above ground atmospheric storage tanks (Tables 2.1 and 2.2), of which a variety of similar types are in use around the world, can be liable to failure in the same way. Types include open top tanks with or without floating roofs and closed-top tanks either with or without floating roofs. Within the European Union (EU) the specification for the design of such tanks is covered by BS EN 14015:2004.

The United States Environmental Protection Agency (USEPA) commissioned a study to investigate the common sources of failure and stated that a significant factor in tank farm accidents is human error. The study covering the ten-year period (1990 - 2000) highlighted that the number of accidents at long-term storage facilities had remained relatively constant. Of the 312 accidents at tank farms examined in this period it was found that operator error accounted for 22 %. Additionally, 55 % were attributable to tank failure, 10 % to valve failure, 4 % to pump failure and 3 % to bolted fitting failure. Human error also accounted for 100 % of accidents that resulted in fatalities, 88 % involving stock loss and 87 % of property damage, with the root cause attributed to overfilling/over-pressurisation (United States Environmental Protection Agency, 2000).

The failure of bulk storage tanks can be attributed to a number of causes including human error, poor maintenance, vapour ignition, differential settlement, earthquake, lightning strike, hurricane, flood damage and over-pressurisation. Such incidents have highlighted the need for the proper assessment of potential risks and the requirement for suitable methods of mitigation.

2.3 Natural disasters

The fact that most major facilities are exposed to the elements and that many countries experience severe climatic extremes and or geological phenomena makes for increased risk of failure at some point in time. Such natural disasters are not always predicable and suitable methods of construction may not always mitigate the most extreme of possible effects.

There have been numerous storage facilities around the world damaged by earthquakes including major incidents in Alaska USA 1964, Chile in 1960, and two in Japan, Niigata in 1964 and Tokachi in 2003. The incident in 1964 at Niigata resulted in the loss of

containment of several tanks due to damage sustained during the earthquake, which added to the ensuing inferno and continued to burn for 13 days. This incident highlighted several problems including that of floating roofs becoming dislodged and jamming, with the resulting fire being attributed to sparks from the damaged roof being shaken violently. More importantly, this was the first time that the phenomena of liquefaction had been observed, raising concerns over the integrity of storage tank foundations at similar coastal locations (Akatashi and Kobayashi, 2006).

It is estimated that lightning accounts for 61 % of all accidents in storage and processing activities, where natural events are identified as the root cause of the incidents. In North America, 16 out of 20 accidents involving petroleum products storage tanks were as a result of lightning strikes. Persson and Lönnormark (2004) in a review of fires in the petroleum industry claim there have been 150 tank fires in a 52-year period as a result of lightning. Some of the more recent incidents include Brisbane, Australia 4th June 2003, where a floating roof crude tank was struck by lightning. Nigeria, 20th July 2002, 180000 bbl (one blue barrel is equal to 42 US gallons) were lost when fire fighters failed to gain control of a rim fire caused by a lightning strike. Poland 5th May 2002, a 10,000 m^3 tank was destroyed as a result of being struck by lightning, this was compounded by the failure of the semi-fixed fire fighting system. Kansas, USA 21st August 2001, five tanks were destroyed in one incident after fire spread from a tank which had been struck by lightning.

2.3.1 Louisiana, USA, 3rd September 2005

Numerous refineries closed down production prior to Hurricane Katrina striking, however in the wake of the hurricane several refineries reported spills, the worst being at the Meraux Refinery operated by Murphy Oil. A crude oil storage tank holding 65,000 bbl was damaged during the storm and an estimated 25,110 bbl of oil was released. The surrounding dyke was damaged and large quantities of oil escaped into the local environment. The cause of the damage to the dyke is uncertain; it was either as a direct result of the storm or due to the force of material escaping from a tank. At least one tank was lifted and moved 10 metres away from its foundations by the immense power of the floodwaters (Murphy Oil Corporation, 2006), (MSN News, 2006).

2.4 Accidental releases

There are numerous causes for accidental releases to occur, most of them involving some form of human error or tank failure. Filling and emptying operations are particular sources for potential releases with structural failures mostly being traced back to poor construction or maintenance issues. In most instances, catastrophic failures can be attributed to material defects or extreme cold conditions leading to brittle fracture of the steel shell. A number of examples of such failures are listed below:

2.4.1 Naples, Italy, 21st December 1985

During a filling operation, fuel overflowed through the roof of a floating roof tank for almost an hour and a half. An estimated 700 tonnes of fuel escaped into the secondary containment. The pool of liquid covered the bund area of the tank and the adjacent pumping area, which was connected through a drain duct. The spill was followed by a vapour cloud, which rapidly formed and ignited, the source of the ignition being a pumping station. The explosion resulted in the injury of five personnel, and the destruction of the facility. Twenty-four tanks were destroyed in the fire, together with the failure of numerous pipelines, which contributed to the fire, and the loss of the main fire-fighting control centre. The fire lasted for seven days (Clark et al, 2001).

2.4.2 Floreffe, Pennsylvania, USA, 2nd January 1988

The Department of Environmental Protection (1988) reported a large aboveground fuel storage tank that suddenly failed as its shell rent completely from base to roof. The failure came completely without warning as the tank released a huge wave of Diesel fuel (3.5 to 3.9 million US gallons), which surged across the bunded area with the wave crest easily washing over the secondary containment systems in the form of earthen dykes (Plate 2.1). The intended design of the dykes was originally meant to deal with gradual releases with such an event never envisaged, leaving them unable to cope and totally inadequate. Figures on the amount of fuel escaping from the site vary with typical figures quoted as 750,000 US gallons leaving the storage terminal, owned and operated by Ashland Oil Inc. The pathways included underground wastewater systems operated by the nearby Elrama power generating station, which fed directly into the Monongahela River via a storm water discharge pipe.

PAGE/PAGES EXCLUDED UNDER INSTRUCTION FROM UNIVERSITY

Estimates of the amount of un-recovered material vary, however data suggests that over 511,000 gallons remain in the river systems. The effects of the release included the deaths of 11,000 fish and 2,000 birds with miles of contaminated shoreline reported. The short-term effects were merely the start of the problem with the log-term chronic effects on the environment persisting for many months. As well as the environmental impact, the socio-economic effects were just as widespread with businesses unable to operate properly and locals having their normal every day lives disrupted.

The investigation into the events leading up to the catastrophic failure and subsequent contamination found a flaw in the recently reconstructed 4,000,000-gallon bulk storage tank. The problem originated near the top edge of a steel plate in the fist level and with such low winter temperatures, the steel was prone to act in a brittle manner making it susceptible to the stresses imposed due to filling. The flaw was found to exist prior to the reassembly of the tank and had gone undetected for many years of previous operation.

The catastrophic failure should have been avoidable, as the existence of the flaw was detectable and the brittle nature of the steel during prolonged periods of cold weather was easily predicable. The errors in failing to detect the flaw and in the poor consideration of the material properties were considered serious deviations from good practice and compliance with the current codes. Further criticism was aimed at some of the company employees and contractors, where a pattern of bad practice and negligence in the reconstruction of the tank had been uncovered.

The reconstruction process did not conform to the industry standard practice or in some cases to the terms of the contract, however these discrepancies were not directly attributed to the ultimate failure of the tank. The neglect by Ashland, which led to the collapse caused extensive environmental and economic damage and exposed workers to unnecessary bodily harm, with one employee recorded as taking fluid level measurements from the roof only minutes prior to the event.

The lack of suitable statutory and regulatory programmes meant that the accident was unlikely to have been prevented, as there was no emphasis on the design and construction practices relating to such activities. The occurrence of sudden and extensive failures of bulk storage vessels is more frequent than commonly envisaged and legislation for construction and maintenance programmes is essential together with the apportioning of

financial responsibility for emergency response and recovery of associated costs (Department of Environmental Protection, 1988).

2.4.3 Lithuania, 20th March 1989

A large bulk storage vessel containing refrigerated liquid ammonia failed catastrophically without warning. The resulting sudden escape of the contents forced the tank to move sideways impacting and demolishing the concrete bund wall compromising the secondary containment and releasing 7000 tonnes of material, which ignited spreading fire across the site. The storage of 35,000 tonnes of fertiliser in a nearby warehouse added to the problem as the fire engulfed the facility. The combination with the solid material produced acid fumes from the burning mass for several days with the fume cloud visible form up to 45 km away. In terms of deaths, there were seven immediate fatalities with 57 gas related injuries reported on site due to the pools of ammonia that formed on the ground, however no deaths were reported off site.

The Azotas site was a large complex and employed many people from the local area with the main town of Jonova approximately 12 km from the facility having a population of about 40,000. At the time of the accident 3500 employees were on the site, which was with a restricted military zone. The tank was sited approximately 600 m from the main plant with rail tankers filled some 50 m from the storage tank. A control and operations room positioned nearby was completely destroyed along with all of the operations data.

The adjacent fertiliser plant transported product via conveyor belts to storage facilities with 15,000 and 20,000 tonnes of capacity with a further storage warehouse holding 20,000 tonnes of ammonium nitrate.

The tank itself had a diameter of 30 m and was about 20 m high, standing on a concrete plinth supported by columns. The base of the tank was fixed to the concrete base using 36 steel anchor straps welded to box section on the vertical shell, passing through the concrete and secured with welded steel cross plates. Carbon steel was used in the manufacture of the tank with a wall thickness of 200 mm at the top and 35 mm at the base. Thermal insulation was provided by 700 mm of perlite covered by a steel jacket. The condition of the perlite was not known with regard to moisture content at the time of installation and no record of base insulation could be found. The tank was of Japanese design and was

installed in 1979 surrounded by a 14 m high reinforced concrete bund with a 100 % capacity.

The incident was accompanied by a loud 'whooshing' noise as the shell of the tank was pushed through the bund by the force of the rapidly escaping liquid ammonia. It appeared that the tank had split open along one side extending to the base, breaking all of the holding straps. The extent of the damage was so great that the depth of the liquid ammonia around the fertiliser plant was up to 70 mm deep in some areas and evaporation soon allowed the build up of a large vapour cloud. The vapour was subsequently ignited by a nearby flare-stack and quickly advanced to include the nearby fertiliser storage areas.

The military responded in minutes and began to spray water, which only increased the evaporation rate fuelling the intensity of the fire. The toxic gas alarm sounded for several minutes after the release, yet the fire fighters were poorly equipped with no heat resistant suits or adequate air supplies. After about 12 hours all of the ammonia had evaporated, however the fertiliser continued to burn for many days, releasing vast quantities of nitrous fumes. Most of the deaths were attributed to inhalation of ammonia gas with victims concentrated in the storage area.

The root cause of the incident was later attributed to warm ammonia being delivered to the bottom of the tank due to an operational error. This led to the formation of an unstable layer at the base of the tank which later rose to surface causing violent evaporation to occur, which the pressure relief system was unable to cope with. The result was the sudden uplifting of the tank base and breaking of the straps along with the base to wall welds allowing the rapid release of the liquid ammonia (Anderson and Lindley, 1992).

2.4.4 Pennsylvania, USA, 16th October 1995

Five workers were killed when two tanks exploded at the Pennzoil Product Company Refinery. A welding operation was in progress on a service stairway sited between the two waste liquid storage tanks. One tank failed along its bottom seam, the shell being propelled vertically away from the base as a result of rapid over-pressurisation caused by ignition of combustible vapour. The tank contents were instantly released, igniting the contents of the second tank, this also exploded, releasing its entire contents. There was no secondary containment surrounding these tanks and the surge of burning liquid rapidly spread across the entire site, damaging another thirteen storage tanks. The contents of

another five other tanks were ignited, resulting in the loss of 95,000 gallons of solvent and fuel oil (United States Environmental Protection Agency, 1998).

2.4.5 Delaware, USA, 17th July 2001

One worker was killed and eight injured, when a large sulphuric acid tank exploded. The explosion was the result of sparks from hot work on a catwalk above one of several tanks on the site, entering a tank through corrosion holes. Due to the subsequent ignition of flammable vapours, the tank shell was propelled away from its base resulting in a significant volume of sulphuric acid being released into the environment. An estimated 660,000 gallons of acid was released, with extensive environmental damage including a large quantity of the escaping material entering the Delaware River killing thousands of fish and other wildlife. The operator, Motiva, part of the Premcor refining group were ordered to pay costs of $58 million, this included a sum of $36 million to the widow and family of the employee killed in the accident. An additional $24 million was also deemed payable in fines for various environmental violations (US Chemical Safety & Hazard Investigation Board, 2002).

2.4.6 Antwerp, Belgium, 25th October 2004

A storage tank failed catastrophically releasing its entire content of 37,000 m^3 of crude oil. It is estimated that only 3 m^3 escaped the secondary containment during this incident, this was a result of a combination of factors. The height of the containment dyke itself was in excess of 4 m and this combined with the unusual nature of the incident limited the extent of the losses. The mode of failure is best described, as a jetting release and it was this directionality, which possibly prevented further losses. One month prior to the incident a leak was detected in a neighbouring tank, which was consequently drained to allow for maintenance. Of seven tanks within the dyke at the time of the failure only three where in operation, the release being preceded by a low-level alarm indicator, which identified a change in content level. The incident began as a minor release rapidly changing to a major failure, with total loss of containment occurring within fifteen minutes of the alarm sounding. The release from the base was powerful enough to cause displacement and resulted in the tilting of the tank due to erosion of the foundation.

Primarily, the cause was traced to the construction process with similar problems later identified with the remaining tanks on the site. The tanks had been erected on a base of

sand with an outer annulus of compacted crushed rock acting as the foundation. This overlaid a layer of sand and soft clay with the tank bases designed to incorporate a 'dome-up' to allow run of any water. Upon initial fill, due to the soft ground conditions, all of the tanks experienced subsidence, which resulted in deformation of the bases. This allowed the formation of a 'gutter', which trapped and concentrated moisture away from the sump pumps. In the tank that failed this 'gutter' was some 35 m in length and 0.2 m in width and resulted in severe corrosion culminating in the breach of the primary containment (Federal Public Service – Employment, Labour and Social dialogue, 2006).

2.4.7 Buncefield, Hertfordshire, UK, 11th December 2005

The events at the Buncefield fuel depot in Hertfordshire saw what was possibly the largest explosion in Europe since the Second World War, as reported by BBC News (2005). The incident, which happened at around 0600 GMT on Sunday 11th December caused injuries to 43 people, two seriously and left a scene of devastation necessitating the closure of part of the M1 and M10 motorways. The surrounding area was evacuated leaving some 2,000 people displaced from their homes with thick clouds of smoke spreading to the south of the site.

The Buncefield site is operated by the Total Oil Company and is a major depot for the distribution of fuel, storing oil, petrol and kerosene. A total of 20 tanks were involved in the incident, each reported to hold three million gallons of fuel. There is a question as to the operational safety of the depot in terms of its size relative to operating capacity and the investigation will look at risk assessments made by Total and the British Pipeline Agency (BPA) (Buncefield Adeyfield Community Forum, 2006).

A tank overfilled at an estimated rate of 550 m^3 per hour for several hours overflowed into the bund generating vast quantities of vapour. This was a result of instrumentation failure, as high-level gauges failed to show that the tank was full. This was the second major catastrophe in less than 10 months, where vessels had been over-pressurised due to faulty instrumentation. In the first case the explosion and subsequent damage occurred at the BP America Refinery, Texas, where a distillation tower was over-pressurised during a start up operation and resulted in the loss of 15 lives with a further 170 injured (US Chemical Safety & Hazard Investigation Board, 2006). The devastation at Buncefield has been estimated at in excess of £10,000,000 in stored materials alone, in addition to the destruction of the site itself and the effect on surrounding businesses. The nearby

industrial estate housed some 630 businesses with at least 20 of these losing their premises, affecting the livelihood of some 500 people (Buncefield Major Incident Investigation Board, 2006).

The environmental issues related to the disaster do not appear to have long-term implications with regard to water pollution as the heavily contaminated firewater was contained on site. In terms of air quality, the smoke released was classified as an irritant, rather than being toxic and monitoring of both air and ground level contamination was used to inform on any public health issues (Environment Agency, 2005).

2.4.8 Mississippi, USA, 5th June 2006

Three contractors were killed and one was seriously injured in an explosion and fire at an oilfield. The contractors were stood on a gantry situated above four oil production tanks, preparing to weld piping, when it is assumed that a welding tool ignited flammable vapours from one of the tanks (US Chemical Safety & Hazard Investigation Board, 2006).

2.5 Current requirements

Two of the instruments on the control of major accident hazards involving dangerous substances are outlined below. The first is Council Directive 96/82/EC, which is known as the Seveso II Directive (1996) and applies to all activities within the European Communities. The second is the Control of Major Accident Hazards or COMAH Regulations (1999), which applies within the UK. Both instruments aim to ensure adequate control and build on the lessons learned from previous incidents, however such controls are limited to what is termed 'reasonably practicable'.

2.5.1 Seveso II Directive (1996)

The main issues relating to the bulk storage of hazardous materials include the following:

- A requirement to demonstrate that all possible steps have been taken to prevent major accidents including the preparation of contingency plans and response measures. The provision of a competent authority with information in the form of a safety report containing details of the establishments, the substances, the

installation and storage facilities, possible major accidents and the management systems in place to prevent/reduce risks of major incidents.

- To reduce the risk of domino effects so as not to increase the probability of major accidents by careful consideration to ensure establishments are not sited too closely and to provide the exchange of appropriate information.
- To Promote access to information on the environment with public access to safety reports and other information sufficient to allow correct actions to be taken.
- In the case installations where dangerous substances are present in significantly large quantities, it is necessary to institute internal and external emergency plans. This includes the establishment of systems to ensue monitoring and revisions as required to ensure proper implementation in the event of a major incident.
- With regard to internal emergency plans, staff must be properly consulted and with external plans the public suitably informed and consulted.
- For residential areas, areas of substantial public use and areas of natural/special interest it is necessary for land use and/or other policies to take account of the long-term need to maintain a suitable distance between these areas and establishments presenting major hazards. In the case of existing establishments to take account of additional/special technical measures so that the risk is not increased.
- To ensure adequate response measures are taken in the event of a major incident, whereas the operator immediately informs the competent authorities and provides sufficient information for the impact assessment to take place.
- The provision of information exchange to prevent future accidents of a similar nature with Member States communicating details of major accidents to the Commission to allow suitable analysis and dissemination of preventative measures.

2.5.2 COMAH Regulations (1999)

HSE has a statutory duty alongside the Environment Agencies as the Competent Authority under Statutory Instrument No. 743 - The Control of Major Accident Hazards (COMAH) Regulations (1999). As a part of this duty HSE must assess predictive aspects of COMAH safety reports. A failing of some such reports is the belief of their authors that because bunds satisfy current standards they do provide full secondary containment for all foreseeable failure modes; it follows that the estimates of the extent and severity of accidents in the reports may be seriously optimistic. It was foreseen that data from this project would greatly strengthen the technical basis of HSE's assessments. Moreover, data from the project would provide tank storage operators with a means of assessing the

current performance of their bunds, of assessing the extent and severity of accidents, and of considering the reasonable practicability of measures to reduce the risks.

COMAH regulations apply mainly to the chemical industry, but also to some storage activities, explosives and nuclear sites, and other industries where threshold quantities of dangerous substances identified in the Regulations are kept or used. Their main aim is to prevent and mitigate the effects of those major accidents involving dangerous substances, such as chlorine, liquefied petroleum gas, explosives and arsenic pentoxide which can cause serious damage/harm to people and/or the environment. The COMAH Regulations treat risks to the environment as seriously as those to people.

An ammendment to the COMAH regulations came into force on the 30th June 2005 realting to the notification of activities encompassed by the regulations including exploration, extraction, processing and storage of hazardous materials.

The bunds or earth banks that commonly surround tanks used for storing hazardous liquids are often designed with a capacity equal to 110 % of the capacity of the largest storage tank within the bund, the excess height being claimed in part to prevent liquid surging over the top of the bund following sudden failure of a tank. In reality, whilst a 110 % capacity bund will contain the release for less extreme modes of failure, it is unlikely to do so for more extreme modes. A series of experiments reported in HSE Contract Research Report 405/2002, in which the contents of a model storage tank were released gently into a 110 % bund over a period of 30 seconds, showed that the bund was overtopped in almost every case. More severe modes of release would clearly give more in terms of overtopping (Cronin and Evans, 2002).

2.6 Previous work

In the UK, the HSE has undertaken a number of experimental studies of bund overtopping, principally in its Health and Safety Laboratory (HSL) in Buxton. In 1997 an HSL report examined the totality of the work, alongside known work performed outside HSE, and concluded that whilst much had been done the work was generally piecemeal and was in some cases not well recorded; in consequence it did not form the coherent and comprehensive picture that HSE required (Thyer and Jagger, 1997).

An outcome of the 1997 review was focused on a particular set of overtopping experiments undertaken by Greenspan and Johansson at Massachusetts Institute of Technology (MIT) in 1981. Greenspan and Johansson performed some fifty- laboratory simulations of a catastrophic failure of a storage tank located centrally within a circular surrounding bund Greenspan and Johansson (1981). Their work has since formed the basis of derived overtopping correlations. However, their model tank had a diameter of only about 8 inches, leading to a suspicion that their results would be influenced by frictional effects to an extent that made them not applicable to full-scale tanks. A requirement of the test facility was that it should be sufficiently large that there should be no concern over scaling to full size (Thyer et al, 2002).

Trbojevic and Slater (1989) investigated the potential failure of the secondary containment given the sudden release of fluid and determined a real possibility of structural failure of the bund itself. Existing work on modelling has been split between (small scale) laboratory experimentation and pure mathematical and modelling with efforts made to combine the two made by Greenspan and Young (1978), Michels et al (1988) and Thyer and MacMillan (1998).

Based on these considerations the new facility was to have:

- A suitably large scale to reduce friction and losses associated with smaller models.
- A tank and bund quadrant representing a quarter of an axisymmetrical release.
- A system to lift the tank very rapidly leaving a column of unsupported liquid able to slump freely under gravity.
- A set of dynamic pressure transducers fixed to the bund wall at various heights to record the dynamic pressures acting on the bund due to the liquid impact.
- Systems for measuring the quantity of overtopped liquid.

To meet these requirements it was decided that the tank bursts would be modeled using a single quadrant of space in the corner of a square spill table with sides 2 m long. The effects of any friction against the smooth acrylic sheets that would form the sides of the spill table were to be regarded as negligible for the geometry applied in the analysis of the results, when considering a complete tank and bund arrangement. The quadrant-tank would have a radius of 300 mm.

The recent publication of the results based on the above work led to a number of recommendations for further investigation (Atherton, 2005). These recommendations are directed towards the mitigation of current storage facilities to reduce the risk of fluid escape and the subsequent contamination of the environment.

2.7 Need for review

There is clear historical evidence that the current design criteria fails to address the problems associated with the sudden release of the tank contents following a catastrophic failure. The bund arrangements for most installations will fail to contain such a release in some cases the design of the bund itself may be liable to complete structural failure leading to the total loss of secondary containment.

Given the substantial number of failures in the primary containment leading to extensive loss of the fluids, the need for further investigation into the performance and design of secondary containment was identified by current researchers. The modes of failure vary greatly as do the initial causes, however in the cases involving sudden catastrophic release, the bunds were found lacking in almost all instances. The overtopping of bunding is commonplace with the rapid escape of fluid from storage tanks. There is a particular need for hazard awareness in the area of defective welds, which have been identified as the cause of many failures. In terms of hazard identification there is a need to evaluate storage tanks for potential catastrophic failure with regard to the following (United States Environmental Protection Agency, 2001):

- Manufacturer's details and records of the levels for quality of workmanship and testing.
- Evidence for weakened or defective areas of weld.
- Indications of corrosion around the base and those areas in direct contact with the ground.
- Levels of exposure to heavy rainfall or high wind loading.
- Age and general condition of the tank.
- Close proximity to other bulk storage tanks, particularly those containing hazardous materials.

Hazard reduction/prevention is directly related to proper design and construction, with regular inspection and maintenance allowing early detection and repair of potentially

dangerous defects. Guidance on the scheduling of inspections can differ. API 653 (2001) recommends a full external inspection of tanks every five years, while NACE International suggest every two years (US Chemical Safety & Hazard Investigation Board, 2002). Such guidance and suggested 'good practice' rely on voluntary action rather than direct regulatory requirement. However, inadequate inspection is one of the root causes of a catastrophic tank failure, for example in Antwerp (Belgium) 2004. Examination of the failed tank and remaining tanks within the same containment area indicated that poor foundations had resulted in all of the tanks incurring damage to the bases. Large creases had been formed in their bases acting as channels that retained excess water, resulting in localised post-construction corrosion remaining undetected until failure.

In the UK, the HSE has considerable interest in predicting the consequence of releases of hazardous liquids from storage tanks, as indicated by Thyer, Hirst and Jagger (2002). HSE is a statutory body responsible for safety, and works alongside the various Environment Agencies. Regulation is mainly achieved via the implementation of the COMAH Regulations (1999) and the Seveso II Directive (1996). Under the UK regulations there is a need to perform suitable risk assessments and outline practicable measures to control the escape of materials from site. This requires the prediction of losses under various possible scenarios and leads to the requirement for realistic data on the performance of the secondary containment. The determination of common variables incorporated into an experimental database will facilitate the development of computer-based models as descried by Thyer and MacMillan (1998).

2.8 Summary

The history of events and the major incidents covered are only a few examples, which aim to highlight the extent of the problem the bulk storage industry faces with the containment of large volumes of mostly hazardous materials. Regulations can only go so far in providing a 'perceived' level of safety if the information upon which any assessment is based is reliable and covers all foreseeable modes of failure. A review of such work by the HSE has raised serious doubts over the validity of COMAH safety reports with misguided assumptions being made as to the performance of secondary containment at major installations. As a result of this work, a need for review was established and recommendations were made for possible further investigation of the problem based on information gathered from previous research and site assessments.

A suitable methodology has to be identified for a detailed investigation to be carried out and a review of the current literature is limited in terms of both the scope of the variables covered and the extent to which the data is recorded. A number of different approaches to the construction of a realistic test rig have been considered and the restrictions of various methods explored in some detail. The design of the test rig for this investigation is discussed as part of the methodology together with its functional requirements and performance in terms of repeatability.

CHAPTER 3

Methodology

3.1 Model Testing

The failure mode in the event of tank rupture is highly complex and involves the interaction between fracture propagation and the flow of a fluid with a free surface. The assumption is made that the cracks will propagate at a much higher velocity than that of the fluid motion, and that they propagate at the same time in the vertical and in the circumferential directions. Thus, the tank looses its integrity instantaneously and hence is considered to have been removed as far as any structural containment is concerned (Trbojevic and Slater, 1989). Hypothetically, this leaves a cylindrical column of liquid collapsing under gravity or an axisymmetric mode of failure. An alternative mode of failure has been considered based upon evidence that the crack will propagate much faster in the vertical than the circumferential direction, hence giving rise to a vertical gaping aperture with the liquid flowing directionally through the gap created. This would represent an asymmetric failure mode and could lead to a localised increase in the hydrodynamic loading on the bund. It is however, considered that a mixture of the two modes of failure is more likely to occur.

3.2 Axisymmetric releases

A water table was constructed together with a working model of a tank quadrant to simulate a catastrophic tank failure. The scale of the model used was 1:30 allowing a large enough model to overcome problems of excessive frictional effects, which could be detrimental to the results in terms of underestimating the level of overtopping. The type of tank failure modelled was to simulate a quadrant (90°) of cylindrical column of liquid collapsing under gravity within the secondary containment and can be considered to represent an axisymmetric mode of failure once transposed to 360° geometry as indicated in Fig. 3.1.

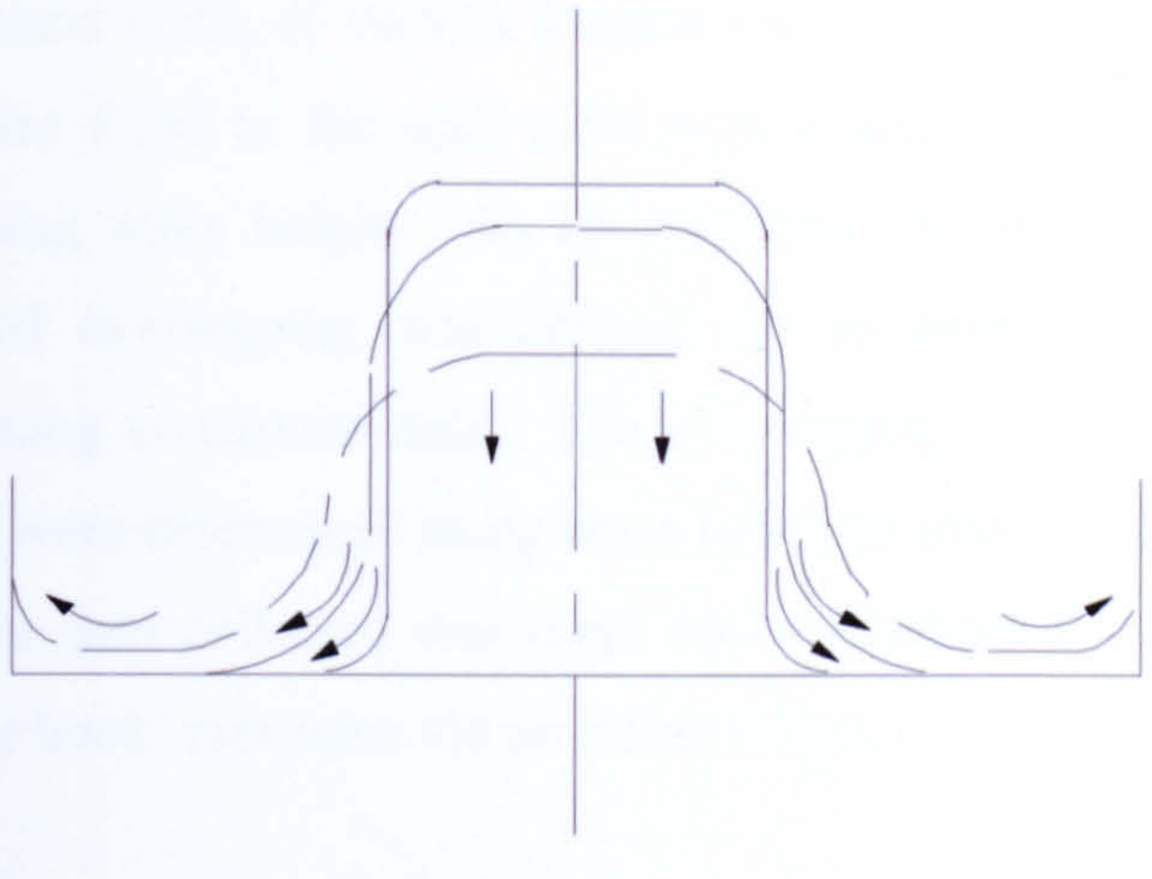

Figure 3.1 Typical axisymmetric release with the fluid collapsing under the action of gravity after the instantaneous removal of the tank

The tank quadrant was removed by accelerating it upwards using a power spring/cord at an initial rate of 250 ms^{-2} based upon a 440 mm extension with a stored force of 800 N accelerating a mass of 3.2 kg, allowing water to rapidly escape (Plate 3.1). Using the average force in the power spring of 560 N at half the extension over the total distance travelled a mean upwards velocity of 12.41 ms^{-1} is obtained using Newton's Laws of Motion. The velocity of the gate was measured using a magnetic pick-up connected to an oscilloscope, giving a peak to peak time of $8x10^{-5}$ sec for a screw pitch of 1 mm, leading to a mean upwards velocity of 12.5 ms^{-1}, giving a standing head of fluid. The initial fluid height in the tank and the wave height at the bund were recorded by capacitance probes.

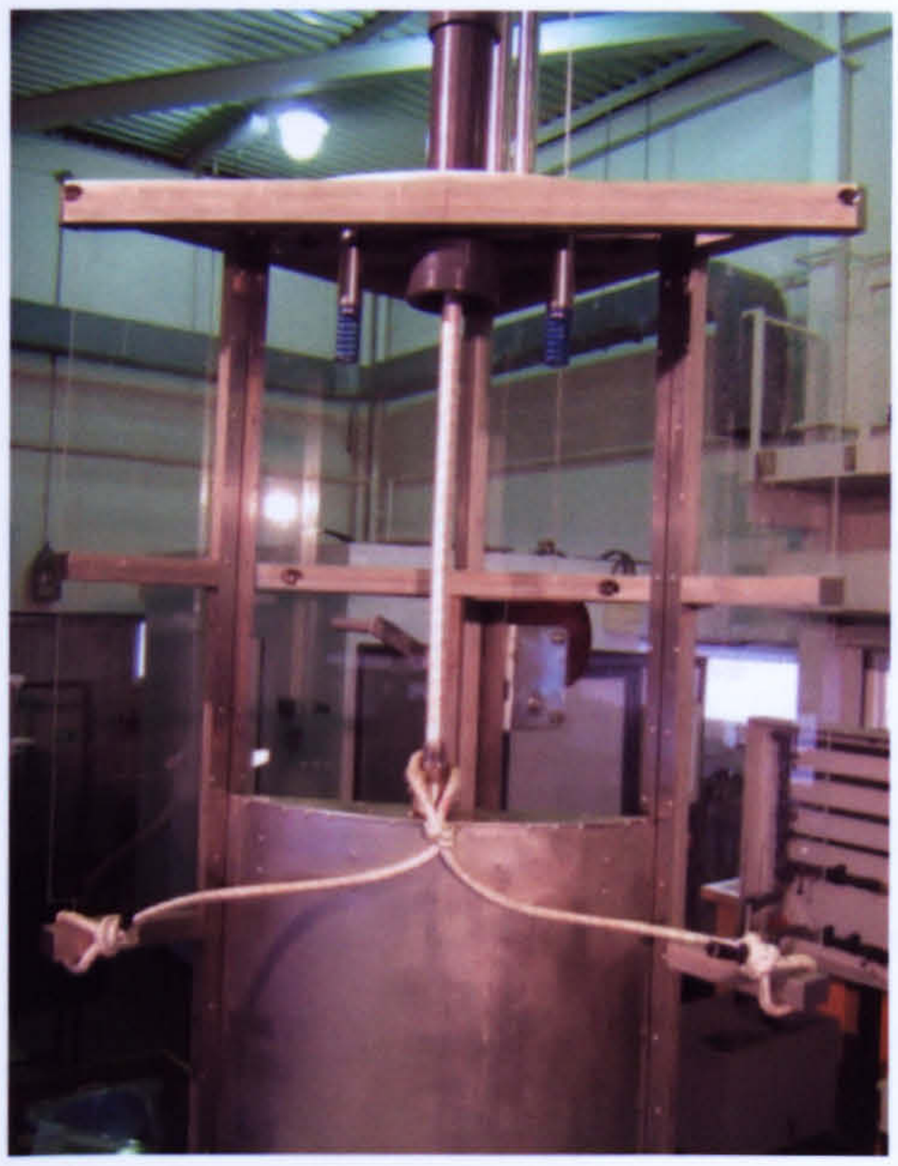

*Plate 3.1 Test rig with power spring/cord attached**

* *Plate source: LJMU*

A series of model bund walls of various heights and placements, incorporating dynamic pressure sensors were fixed to the spill table with a second capacitance probe used to record the overtopping wave height. An investigation into the repeatability of the tank bursts and levels of overtopping was carried out to determine a suitable operating procedure for obtaining consistent data. The overtopping fraction and volume of fluid retained in the bund were determined using mass balances after collecting the fluid through drainage points. The data collected was input into a Personal Data Assistant (PDA) and transferred to a 'note book' computer via an infrared link.

Raw data was collected via a National Instruments SCXI data logger used in conjunction with Labview virtual instrumentation software. The graphical programme written as part of this research enabled 'real time' visual data to be displayed on a computer screen as well as written to file for further processing in other software packages. Statistical analysis of the data was undertaken and dimensionless ratios were used to construct charts and correlating functions for the determination of overtopping percentages. The data from the dynamic pressure sensors was used to calculate the dynamic pressure profiles on the bund walls themselves and compare them to the hydrostatic profiles used for current design purposes.

3.3 Characteristics of the test programme

During the conceptual phase of development of the new test facility HSE undertook a survey of the storage tanks and bunding arrangements at sites where it may be required to give land-use advice or to assess operator's safety reports. With the results of this survey in mind the test programme was designed to embrace: -

Radius of model tank, R:	single radius of 300 mm.
Height of water in tank, H:	three ratios of (R/H): 0.5, 1.0 and 2.5.
Separation distance, L:	varies with radius of bund wall, r below.
Angle of bund, θ:	vertical bunds only ($\theta = 90°$).
Height of bund wall, h:	to cover (h/H) ranges from 0.05 to 0.4 and 1.0 to 1.2.
Radius of bund wall, r:	to cover the range of bunded volumes from 110 % to 200 % of the volume of water in the tank.

The nomenclature used for describing a 'circular' bund configuration is shown in Fig. 3.2 below:

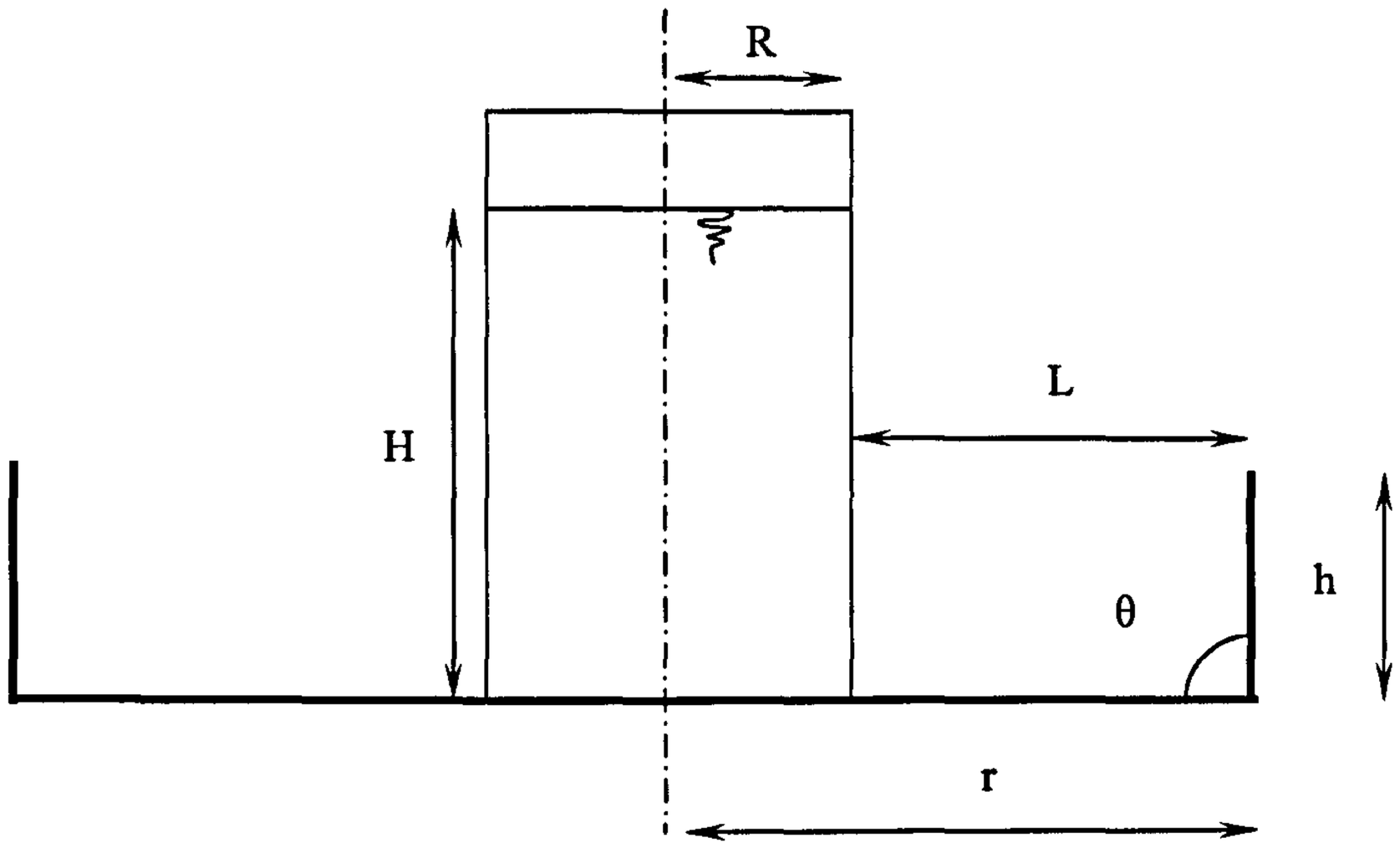

Figure 3.2 Tank and bund nomenclature for circular geometry

For the bunds with 'rectangular' geometries (Fig. 3.3) the key question to be addressed is whether a non-circular bund is systematically better or worse than a circular bund of the same area and height. The basis for testing was to use the 110 % bund capacity results from the circular configurations and identify the bund arrangement that gave the closest to 50 % overtopping for each tank type.

The tests were then to be repeated with the bund plan changed from circular to square, keeping the bund capacity at 110 %. Using symmetry in the quadrant of space there are two possibilities, one where the bund forms a 45° diagonal and one the bund consists of two equal walls parallel to the walls of the rig. Assuming no edge effects in the rig, then the two geometries should give similar values in overtopping. A rectangular bund with length/breadth = 2 was the final arrangement to be considered, again using the criteria as in the case of the square bund. In the case of the square and rectangular bunds small radii, r_c = 12 mm were used at the corners for fabrication purposes and to better introduce the threaded needle connectors of the dynamic pressure transducers.

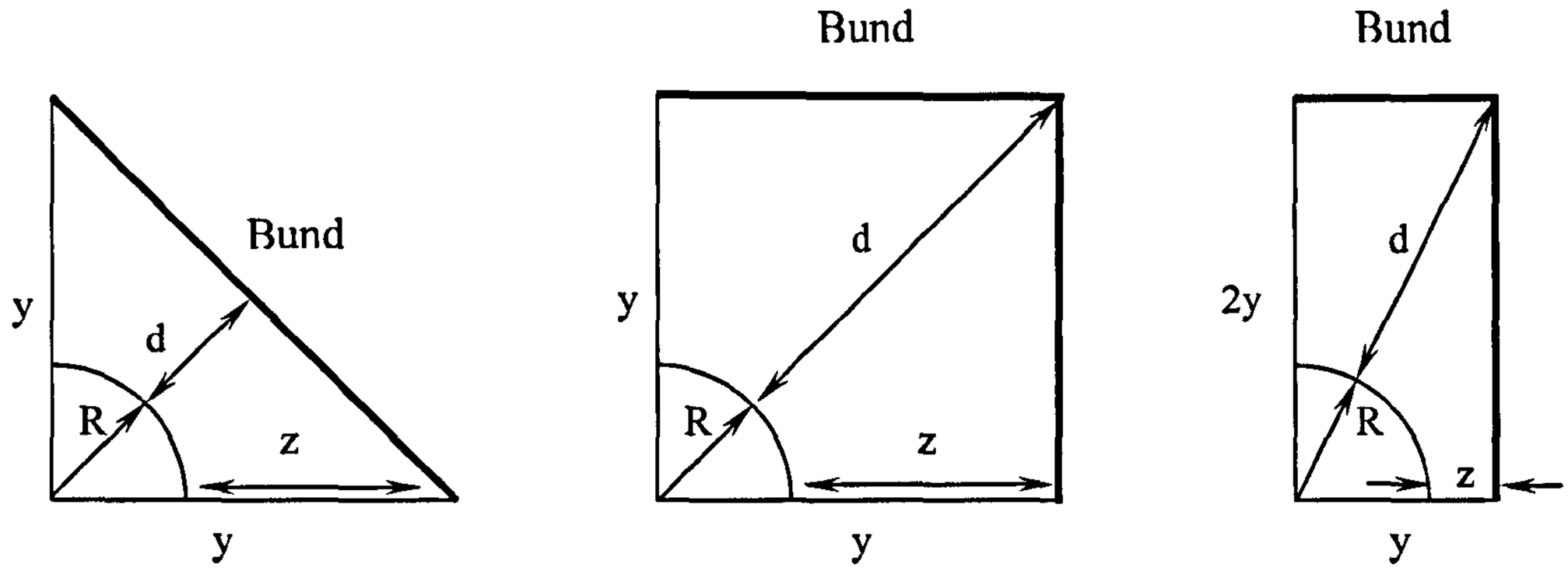

Triangular Square Rectangular

Figure 3.3 Tank and bund nomenclature for 'rectangular' geometries in plan

In the case of the triangular bunds the dynamic pressure transducers were placed at mid-span, with the square and rectangular bunds having the sensors located at the corners.

The total number of configurations investigated for the 'circular' bund geometry was 84 and for the 'rectangular' geometry 9 bund configurations were considered (Table 3.1) with each configuration tested a minimum of 5 times for repeatability purposes.

Table 3.1 HSE axisymmetric test matrix

CIRCULAR BUND CONFIGURATIONS
(3 values of R/H, 7 values of h/H and 4 values of Vtot/Vtank)

All dimensions in mm

Tests have R = 300 mm and maximum r < 2000 mm; vertical bund only

A. Tall Tank					
R	***300***	***H***	***600***	***R/H***	***0.5***

Radius of bund (in mm) for different values of h (in mm) and Vtot/Vtank

h/H	***h***	***Vtot/Vtank***			
		1.1	***1.2***	***1.5***	***2***
0.05	30	1407	1470	1643	1897
0.1	60	995	1039	1162	1342
0.2	120	704	735	822	949
0.3	180	574	600	671	775
0.4	240	497	520	581	671

Vtot/Vtank for different values of h and r (in mm)

h/H	***h***	***r***			
		315	***330***	***360***	***390***
1	600	1.10	1.21	1.44	1.69
1.2	720	1.32	1.45	1.73	2.03

B. "Middle" Tank					
R	***300***	***H***	***300***	***R/H***	***1***

Radius of bund (in mm) for different values of h (in mm) and Vtot/Vtank

h/H	***h***	***Vtot/Vtank***			
		1.1	***1.2***	***1.5***	***2***
0.05	15	1407	1470	1643	1897
0.1	30	995	1039	1162	1342
0.2	60	704	735	822	949
0.3	90	574	600	671	775
0.4	120	497	520	581	671

Vtot/Vtank for different values of h and r (in mm)

h/H	***h***	***r***			
		315	***330***	***360***	***390***
1	300	1.10	1.21	1.44	1.69
1.2	360	1.32	1.45	1.73	2.03

C. Squat Tank					
R	***300***	***H***	***120***	***R/H***	***2.5***

Radius of bund (in mm) for different values of h (in mm) and Vtot/Vtank

h/H	*h*	*Vtot/Vtank*			
		1.1	*1.2*	*1.5*	*2*
0.05	6	1407	1470	1643	1897
0.1	12	995	1039	1162	1342
0.2	24	704	735	822	949
0.3	36	574	600	671	775
0.4	48	497	520	581	671

Vtot/Vtank for different values of h and r (in mm)

h/H	*h*	*r*			
		315	*330*	*360*	*390*
1	120	1.10	1.21	1.44	1.69
1.2	144	1.32	1.45	1.73	2.03

TOTAL NUMBER OF TESTS REQUIRED = 84 (PLUS REPEATABILITY CHECKS)

RECTANGULAR BUND CONFIGURATIONS

All dimensions in mm

Tests have R = 300 mm and vertical bund only

A. Tall Tank					
R	***300***	***H***	***600***	***h***	***120***

Wall No	*Geometry type*	*y*	r_c	*z*	*d*
1	Triangular (tri)	882	Na	582	624
2	Square (squ)	624	12	324	582
3	Rectangular (rect)	441	12	141	686

B. "Middle" Tank					
R	***300***	***H***	***300***	***h***	***60***

Wall No	*Geometry type*	*y*	r_c	*z*	*d*
4	Triangular (tri)	882	Na	582	624
5	Square (squ)	624	12	324	582
6	Rectangular (rect)	441	12	141	686

C. Squat Tank						
R	***300***	***H***	***120***		***h***	***12***

Wall No	*Geometry type*	*y*	r_c	*z*	*d*
7	Triangular (tri)	1247	Na	947	882
8	Square (squ)	882	12	582	947
9	Rectangular (rect)	624	12	324	1095

TOTAL NUMBER OF TESTS REQUIRED = 9 (PLUS REPEATABILITY CHECKS)

3.4 Method of construction

The model tank wall, support frame, bearing rails and fittings for the swinging compression latching bar mechanism were all constructed from stainless steel, with the swinging arms made from lightweight aluminium tube. The power spring, effectively a giant rubber band was supplied by a manufacturer specialising in multi strand elastomeric material capable of delivering a high load to extension relationship with good repeatability and sustained durability.

The main tank and spill table (Plate 3.2) were manufactured using mild steel for the structural frame, with marine ply for the base of the spill table and two of the sides. The other two remaining sides were produced using laminated safety glass to enable video footage to be filmed through the main tank. One of the ply sides and one of the glass sides were then lined with Perspex to allow setscrews to be used for the bund wall fixings. The model bund walls were produced from polycarbonate to allow for the degree of bending required to form the smaller radii and to resist the impact loading produced by the rapidly released fluid.

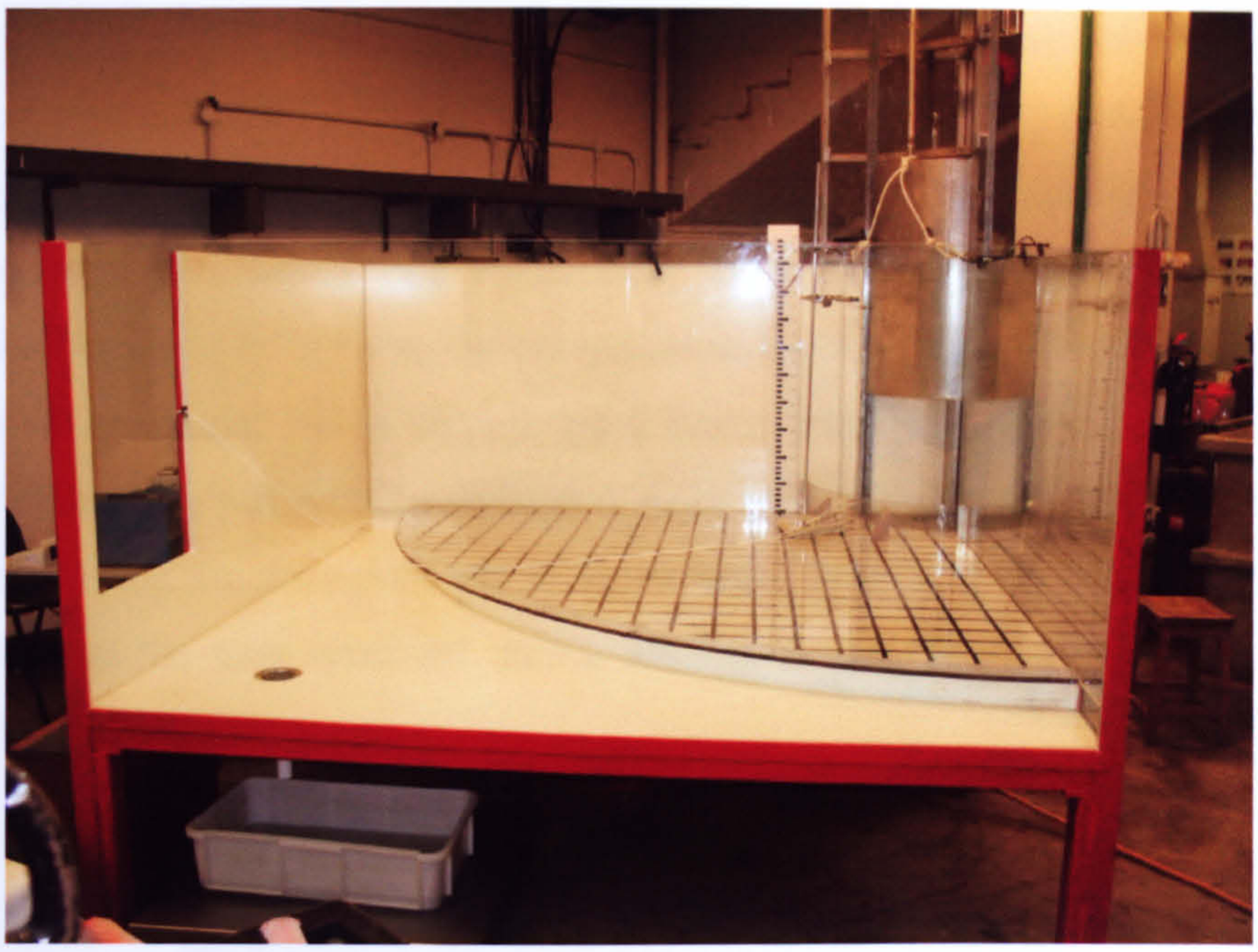

*Plate 3.2 Test rig with spill table and tank quadrant fitted**

3.5 Design considerations

The final design details were chosen for speed and ease of construction with as much as possible of the work performed in-house. Where equipment and tooling limitations existed, as in the manufacture of the tank quadrant and the frame incorporating the linear bearing rails, work was subcontracted to local specialist engineering companies. The resulting test rig design could thus be easily maintained in house with parts likely to be subject to wear and tear reproduced and installed relatively quickly, keeping any project delays to a minimum.

A number of design considerations led to the development of a basic model concept with three different methods of powering and triggering the rapid removal of the tank quadrant. Firstly a double acting arrangement of elastomeric power springs was considered using a twin catch release mechanism operated by a cam arrangement. This also incorporated a spring loaded latching system to prevent the tank quadrant from returning back down the bearing runners at high speed. Secondly, the same power spring arrangement was designed to be used in conjunction with a dual catching mechanism operated by a lever system. In the second case the non-return catching system was to be constructed using a 'butterfly' type spring opening mechanism designed to latch through a hole in the tank quadrant-loading beam.

* *Plate source: LJMU*

The final design, which was the one eventually constructed, used only a single power spring to accelerate the tank quadrant and a 'bungee' cord (Plate 3.3) to decelerate it before contracting a pair of safety compression spring buffers. The single power spring was extended using a mechanical bed winch once the tank quadrant had been locked and securely held in place by a swinging compression-latching bar. The 'firing' mechanism was designed to operate via a bicycle hand brake lever pulling down a spring-loaded stainless steel release pin running through a plain bronze bearing. The movement of the release pin allowed the swinging arm to move back, thus jumping off the roller bearing retaining bar on the tank quadrant, hence leading to the required rapid release of the contained liquid.

*Plate 3.3 Tank quadrant with bungee cord, dynamic pressure transducers and wave probes**

The resulting design gave rise to the required rapid removal of the tank quadrant and the standing head of liquid, as required for an axisymmetric mode of failure. Video footage was taken to show the tank side removal in an upward direction and to see the liquid released fall under gravity (Plate 3.4).

** Plate source: LJMU*

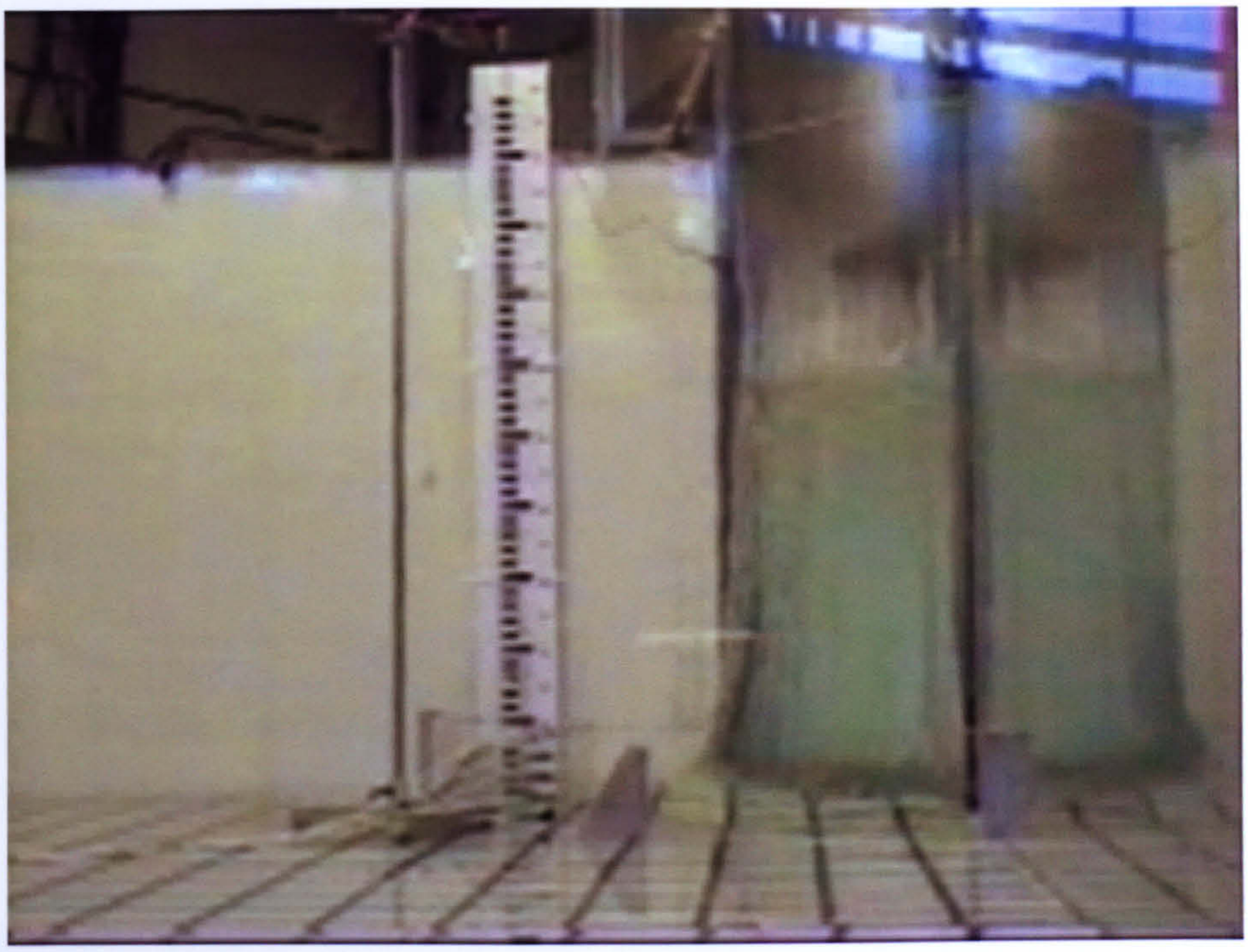

*Plate 3.4 Tank quadrant released with instantaneous standing head of fluid falling under gravity**

3.6 Asymmetric releases

Completion of the work for HSE has seen a change in focus to enable researchers to investigate alternative modes of failure, such as directional releases, which could be considered to be the more common mode of failure likely to be encountered. These failures represent situations such as low - level flange or pipe failure or the loss of integrity of a small section of the tank wall. Research suggests that this mode of failure can typically result in considerable loss of containment, together with the possibility of incurring failure to the bund or earthen dyke resulting from the prolonged and concentrated effects of a jet of fluid as indicated in Fig. 3.4.

* *Plate source: LJMU*

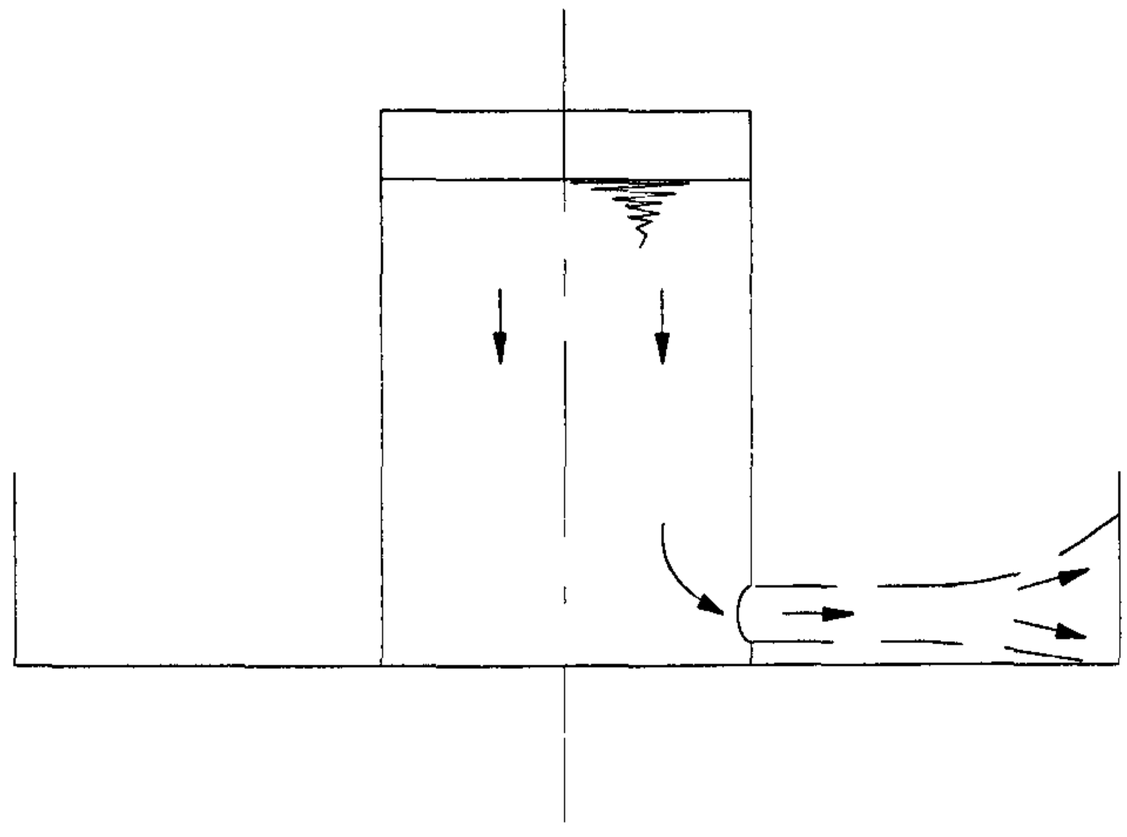

Figure 3.4 Typical asymmetric release with the fluid jet impacting the bund from a partial failure of the tank

The alternative mode of failure has been considered based upon evidence that the crack will propagate much faster in the vertical than the circumferential direction, hence giving rise to a vertical section of the tank being removed and the liquid flowing directionally through the gap created. This would represent an asymmetric failure mode and could lead to a localised increase in the dynamic loading on the bund. It is, however, considered that a mixture of the two modes of failure is more likely to occur as assumed by Trbojevic and Slater (1989).

While considerations are made for 'spigot flow' (Barnes, 1990) and the possibility of jetting failures in the design of bunds, most studies have examined sudden releases. This work has considered the effects of partial failures, which might be experienced through the loss of integrity of a flange or small section of the tank wall, as suggested in initial work by Greenspan & Johansson (1981).

To examine this mode of failure, modifications were required to the test facility. This was achieved by forming a second tank wall, which sat directly in front of the removable wall described above (axisymmetric releases). This contained guides, into which a series of interchangeable plates were inserted (Plate 3.5). A number of plates containing holes were used to represent flange failures and a moveable plate was positioned to represent the effect of removing a section of tank wall. The additional wall sat less than 0.2 mm in front of the original wall, allowing the original wall to be removed at the same velocities as with the axisymmetric releases. The test regime involved considering the 110 % bund capacity using three-tank radius to height ratios (R/H), three circular orifices, and three rectangular

(slot) openings (Plate 3.6). A total of 90 asymmetric test configurations were investigated with each configuration tested 5 times for repeatability checks to be carried out (Table 3.2).

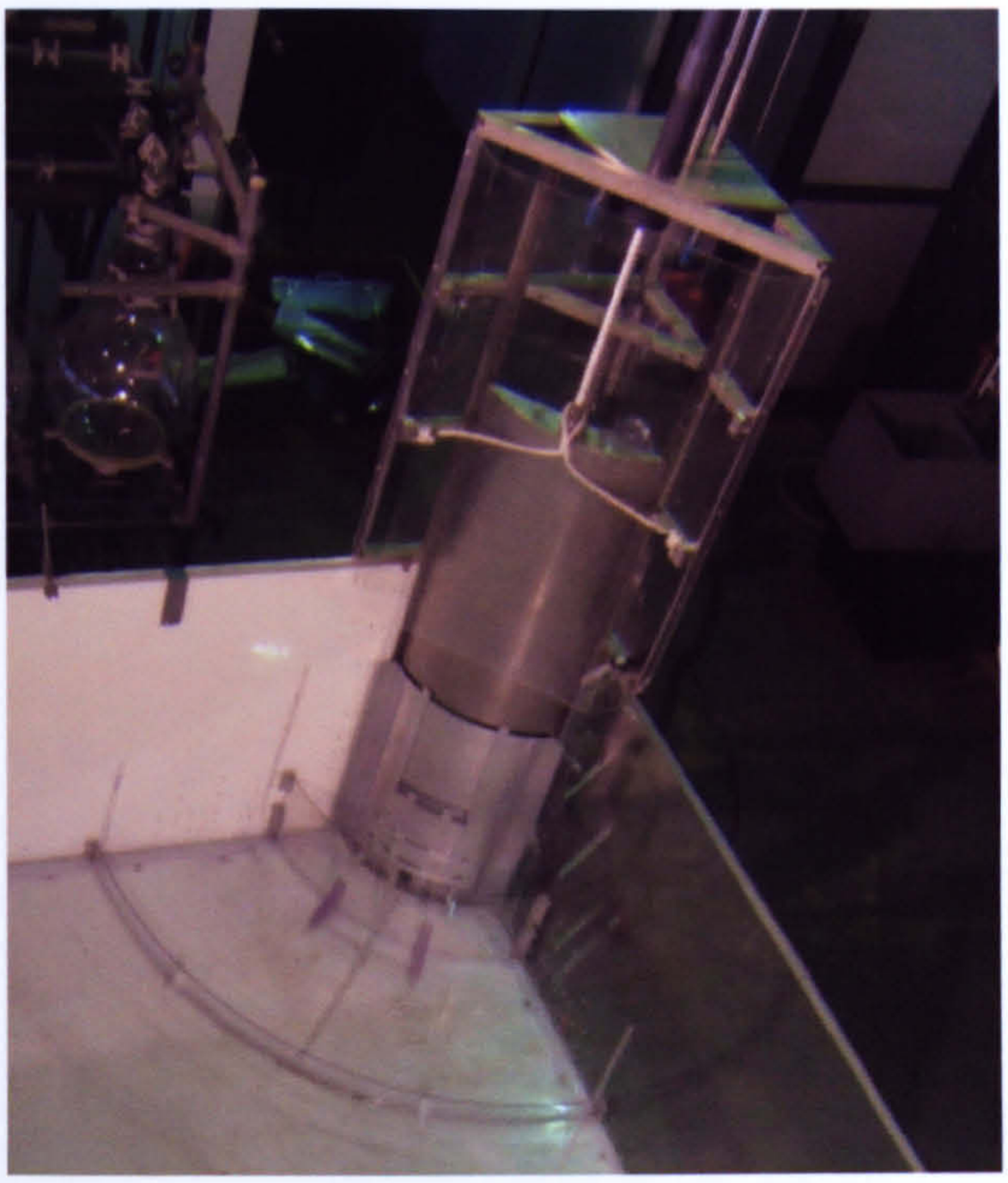

*Plate 3.5 Tank quadrant with second tank wall installed for asymmetric releases**

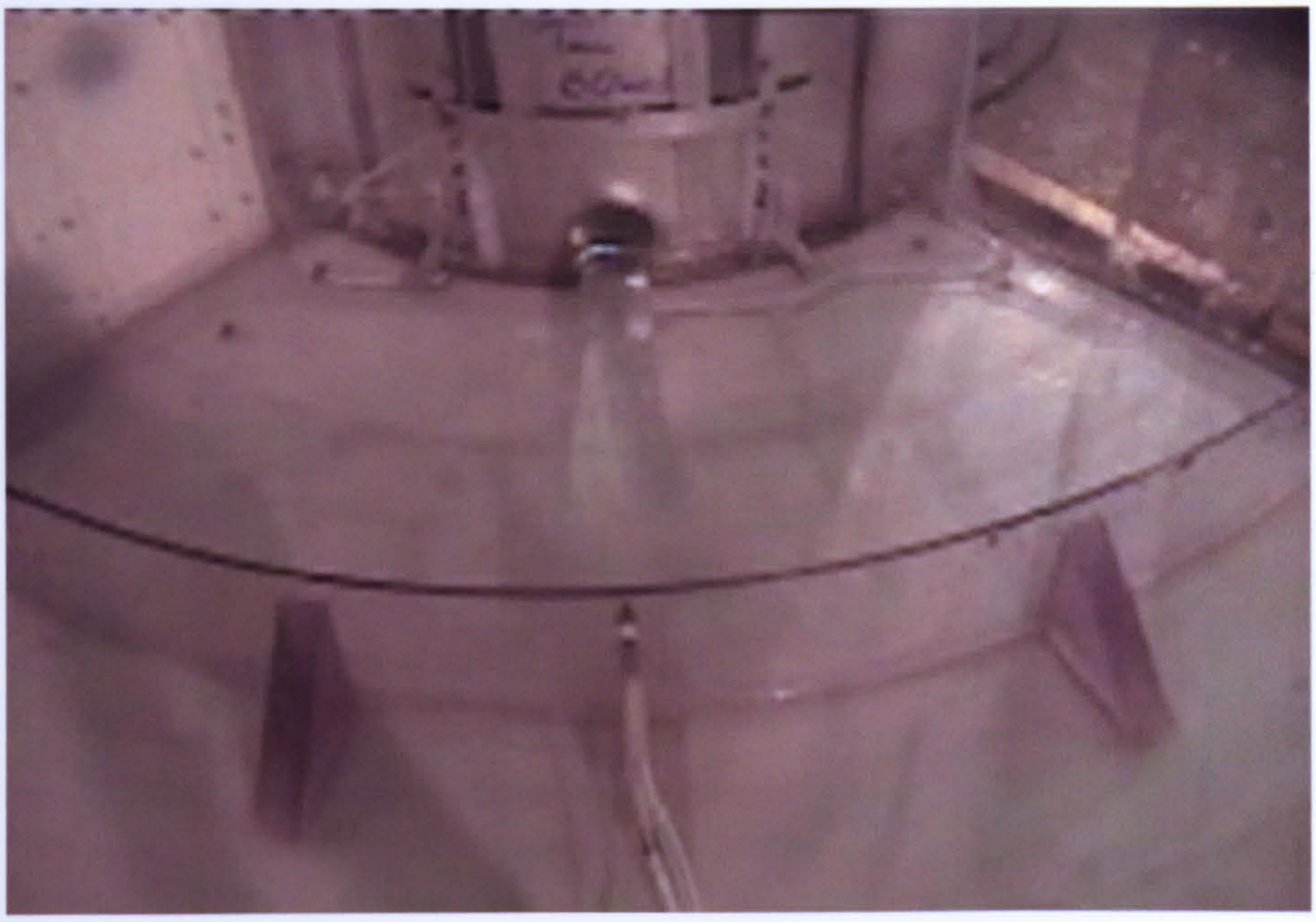

*Plate 3.6 Tank quadrant with asymmetric orifice release**

* *Plate source: LJMU*

Table 3.2 Asymmetric test matrix

CIRCULAR BUND CONFIGURATIONS (ASYMMETRIC RELEASES)

LJMU (2006)		
Angle of bund (°)	***Tank diameter (mm)***	***Tank fill level (mm)***
90	600	120
		300
		600

Orifice		***Squat***	***Medium***	***Tall***
	(% of surface area)	***Diameter (mm)***	***Diameter (mm)***	***Diameter (mm)***
	0.125	18.97	30.00	42.43
	0.250	26.83	42.43	60.00
	0.500	37.95	60.00	84.85

Slot		***(30°)***	***Squat***	***Medium***	***Tall***
	(% of surface area)	***Width (mm)***	***Height (mm)***	***Height (mm)***	***Height (mm)***
	0.500	157.08	7.20	18.00	36.00
	1.500	157.08	21.60	54.00	108.00
	2.500	157.08	36.00	90.00	180.00

TOTAL NUMBER OF TESTS REQUIRED = 90 (PLUS REPEATABILITY CHECKS)

3.7 Dynamic pressure transducers

The objectives required the determination of the dynamic pressure profiles on each of the bunds under test and in order to facilitate these, five piezotronic type pressure transducers were incorporated at predetermined percentage heights for each bund (Table 5.1 and Table 5.7). Kistler type 211B5 pressure transducers were selected powered by a type 5134A power supply/coupler and are illustrated below (Plate 3.7). These were specifically chosen because of their small size and high signal output, allowing them to be installed in the smaller height model bunds and respond effectively over the range of pressures expected. An additional aspect of these transducers is their ability to compensate for the acceleration produced by the physical movement of the model bund due to the impacting wave.

Model 211B5 piezotron pressure transducers are miniature, acceleration compensated instruments, which produce a high level, low impedance signal that is the voltage analogue of dynamic pressure input. Resolution is in the order of one part per 20,000 of full-scale range, in other words plus or minus 34.5 Pa for a 0 to 100 psi transducer. These transducers incorporate sensing elements of crystalline quartz and contain a solid-state impedance converter with sensitivity expressed in millivolts per unit of pressure.

The acceleration compensation is required as the mass of the diaphragm and sensing element produces an inherent acceleration sensitivity, which is eliminated by the embodiment of a quartz accelerometer whose output polarity is opposite to that of the pressure-sensing element. Thus, the accelerometer output nominally cancels or nulls what would otherwise be a component of the sensing element output attributed to the acceleration (Kistler Universal Pressure Transducer Manual, 2000).

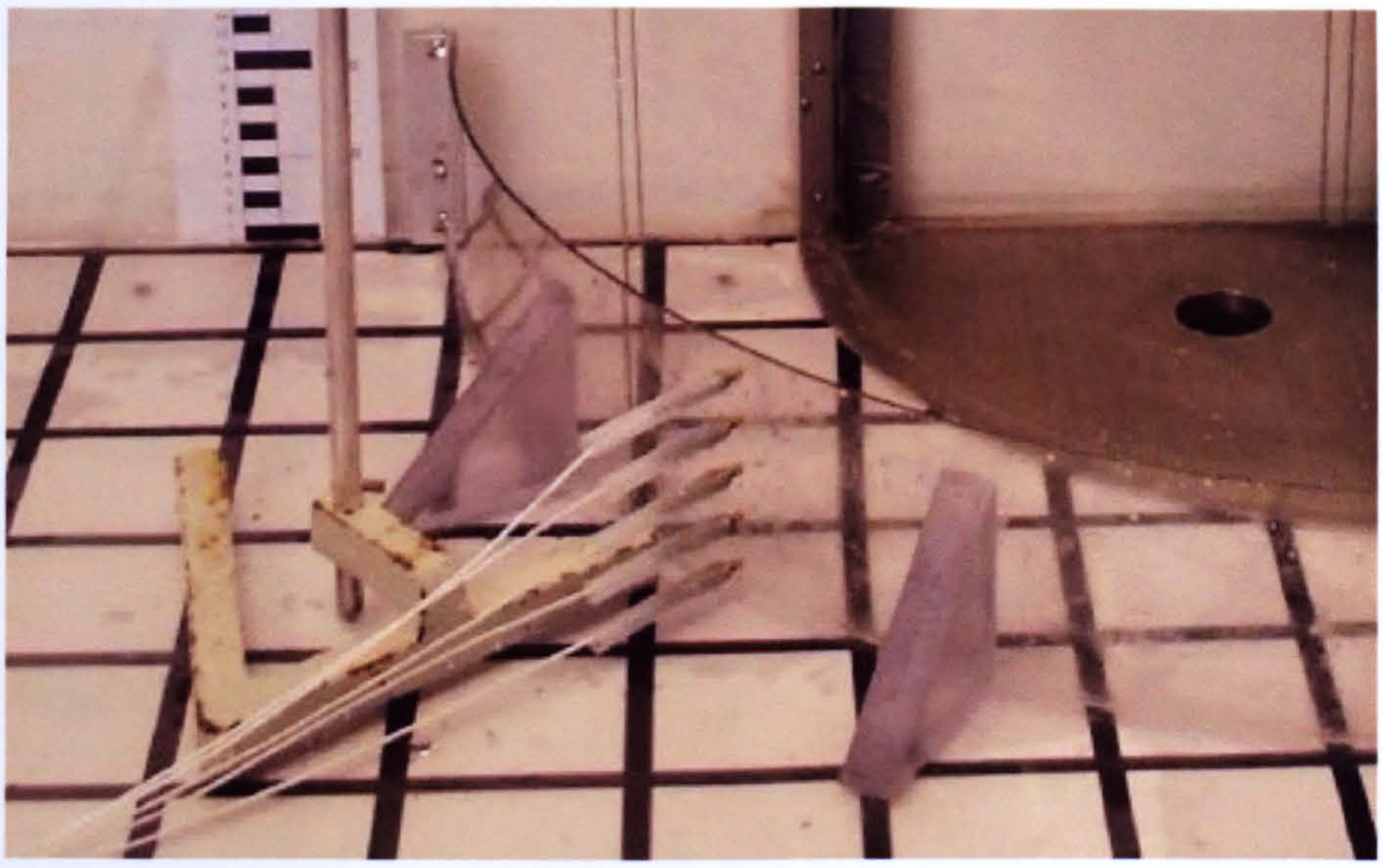

*Plate 3.7 Bund with dynamic pressure transducers installed**

3.8 Wave monitor

The wave monitoring equipment was supplied by Churchill Controls and comprises two probes and a wave monitor module. One probe was placed inside the tank quadrant to record the level as the tank emptied, the other being positioned adjacent to the inner face of the bund wall to monitor the wave height at the bund (Plate 3.3). This technology is well proven in the field of wave research and provides an output voltage that is directly proportional to the wave height, although regular calibration checks are required due to temperature changes in the fluid under investigation.

The system works on the principle of measuring the current flowing in a probe, which consists of a pair of stainless steel wires. The probe is energised with a high frequency square wave voltage to avoid polarisation effects at the wire surface. The wires dip into the water and the current that flows between them is proportional to the depth of immersion. The current is sensed by an electronic circuit, which provides an output voltage proportional to the instantaneous depth of immersion, or wave height, which can be used as input to a high-speed data logger (Churchill Controls Wave Monitor Manual, 1977).

* *Plate source: LJMU*

3.9 Electronic platform scales

The mass of the fluid overtopping the bund and the mass of the fluid retained by the bund were measured using Adam Equipment RFC/L series platform scales, one for each side of the bund. The capacity of each scale is 100 kg with readability of 10 g, the output received over the RS-232 interface. The balance data was then logged using A&D software and saved to file for later use in an Excel spreadsheet.

3.10 Magnetic pick-up

The speed of operation of the tank quadrant was determined using a fixed magnetic pick-up and a length of mild steel threaded studding of known pitch moving along with the tank quadrant. The device responds to the movement of ferrous parts past the pole-piece on the end of the unit. The passive nature of the device requires no external power and yields an output voltage in response to variations in a self induced magnetic field caused by proximity to moving ferrous metal parts. The output from this device was input into an oscilloscope and the time based used to determine the time between successive peaks on the 1mm pitch threaded studding.

3.11 Data logging

The data logger used for data collection from the pressure transducers and the wave monitoring probes was a National Instruments SCXI 1000 chassis with an SCXI 1200, 12-bit analogue to digital (A to D) converter with SCXI 1121 amplifier modules and SCXI 1321 terminal blocks. The data logger was then in turn connected to a computer and controlled through the use of Labview virtual instrumentation software, which is user programmable via a graphical programming language.

The resolution of the signals from the dynamic pressure transducers and the wave monitoring probes depends upon the gain used on the SCXI 1121 amplifier modules. For a chosen amplifier gain of 10 the resolution is 29 Pa/bit, for a gain of 100 this changes to 2.9 Pa/bit and for a gain of 200 this becomes 1.45 Pa/bit. A gain of 1 was used throughout for wave monitoring probes, with the probe length changing from 950 mm with a resolution of 0.29 mm/bit to 475 mm with a resolution of 0.145 mm/bit, depending upon the height of bund under test (Appendix 1, Table 1.1 and Appendix 4, Table 4.1).

The graphical programme (Figure 3.5) was written as part of this research enabled 'real time' visual data to be displayed on a computer screen as well as written to file for further processing in other software packages. Statistical analysis of the data was undertaken in Excel and dimensionless ratios were used to construct charts and correlating functions for the determination of empirical formulae for the prediction of the overtopping fractions and the dynamic/static pressure ratios. The empirical formulae were derived using the curve fitting techniques available in Excel with the level of fit determined using the square of the correlation coefficient or R^2. The derivation of the empirical formulae is more fully covered in chapter 5, section 5.6 with the performance investigated in chapter 7. The data from the dynamic pressure sensors was used to calculate the dynamic pressure profiles on the bund walls themselves and compare them to the hydrostatic profiles used for current design purposes.

Figure 3.5 Graphical computer programme

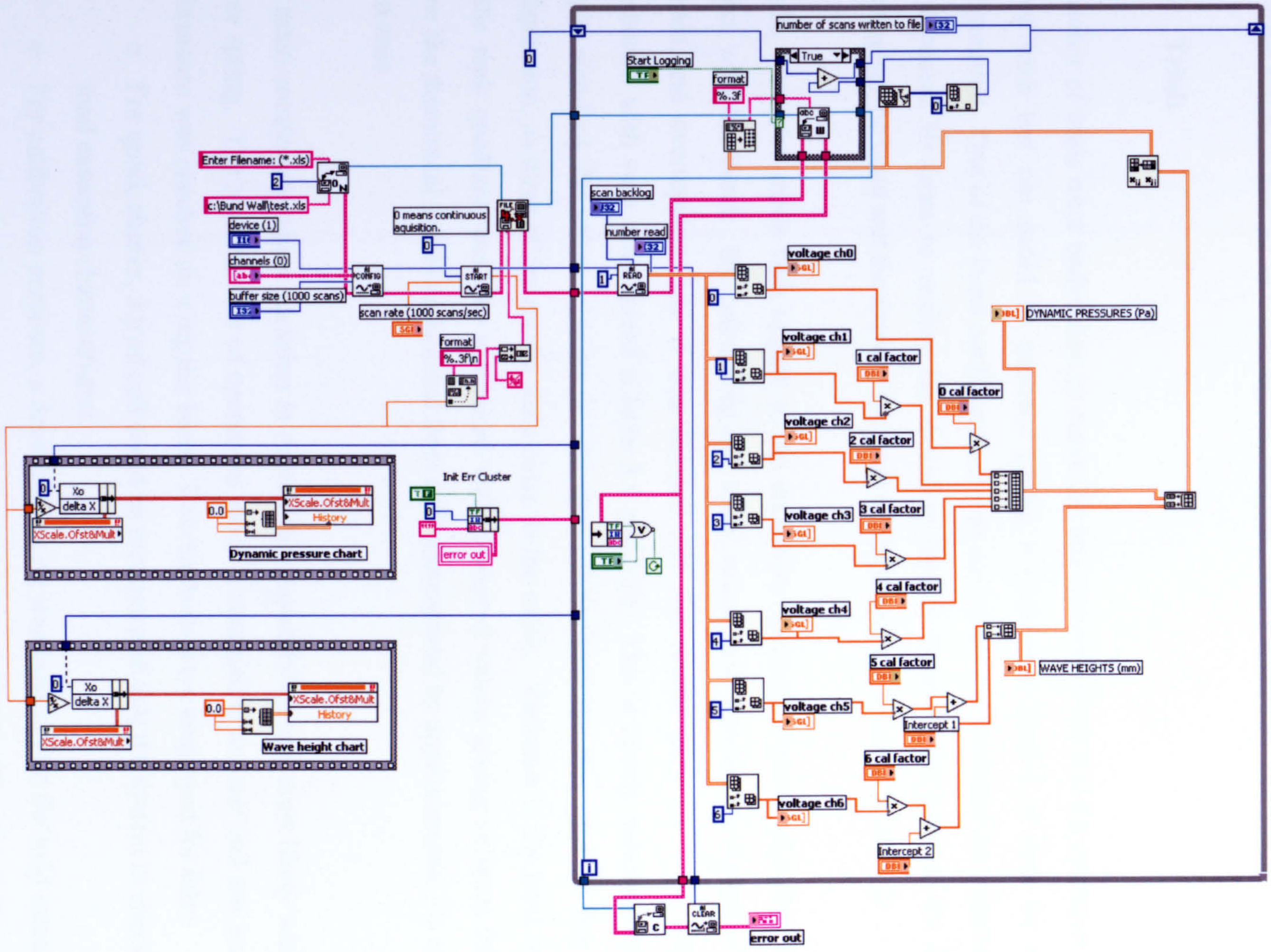

3.12 Video

Video footage was recorded for each of the bund configurations under test; the footage was then transferred to computer using video editing software. The video recordings were then used to monitor the movement of the tank quadrant and the subsequent motion of the fluid under the action of gravity as it approached and overtopped the bund.

3.13 Trials

A number of trials were undertaken to check the repeatability of the test rig operation and ensure each test run could be repeated giving a reasonable spread of data for each configuration. One of the bund configurations was chosen for the trials and the experiment was repeated 30 times to analyse the spread of data in terms of the mass of the fluid overtopping the bund and the mass of the fluid retained within the bund (Table 3.3).

Checks were also made with respect to the maximum dynamic pressure measured upon impact with the bund. By calculating the mean values and plotting the spread of the retained and overtopping data it was decided that the results gave rise to a normal distribution with very little spread (Charts 3.1 and 3.2). This is clearly indicated by the sample standard deviation. Hence it was decided to limit the test runs to five per configuration, as most of the results were close to the mean. Variation in the level of fill for the tank quadrant was also monitored with measured values giving volumes falling below the theoretical values (calculated from tank dimensions) by approximately 3% in the worst case.

The main component where variation in operational repeatability was most likely was the power spring. The high number of operations made it susceptible to wear and tear and its performance was checked on a regular basis. Two methods were employed for this:

- For quick checks, a load cell could be incorporated into the system to check the load extension characteristics.
- For calibration purposes, a dead loading rig was used to plot the load extension curve for the power spring and comparisons made to previous tests. The performance of the power spring was most satisfactory, even though some minor damage to the outer sheath became visible with repeated operations.

Table 3.3 Repeatability checks for axisymmetric overtopping

Date	*13/01/2004*	*Pipe & valve adjustment (kg)*		*0.40*
Test configuration id	*B1(h120)*			
Series id	*Temp (°C)*	*Mass retained (kg)*	*Mass overtopping (kg)*	*Overtopping (Ratio)*
1	14.4	15.58	5.83	0.28
2	14.0	15.62	5.94	0.28
3	13.9	15.63	5.73	0.27
4	13.7	15.41	5.79	0.28
5	13.9	15.66	5.59	0.27
6	14.0	15.58	5.75	0.27
7	13.9	15.61	5.74	0.27
8	13.7	15.79	5.60	0.27
9	13.4	15.69	5.69	0.27
10	13.4	15.63	5.61	0.27
11	18.2	15.56	5.62	0.27
12	17.5	15.49	5.91	0.28
13	17.4	15.65	5.67	0.27
14	17.1	15.53	5.86	0.28
15	16.9	15.67	5.85	0.28
16	16.7	15.83	5.71	0.27
17	16.8	15.56	5.92	0.28
18	16.9	15.5	5.8	0.28
19	16.9	15.45	5.93	0.28
20	16.8	15.68	5.69	0.27
21	17.8	15.69	5.56	0.27
22	17.7	15.67	5.68	0.27
23	17.5	15.47	5.78	0.28
24	17.4	15.44	5.84	0.28
25	17.4	15.52	5.8	0.28
26	16.9	15.46	5.85	0.28
27	18.2	15.59	5.58	0.27
28	17.9	15.55	5.73	0.27
29	17.6	15.64	5.68	0.27
30	17.5	15.47	5.82	0.28
Mean	16.18	15.59	5.75	0.27
Sample S.D.	1.73948	0.10242	0.11102	0.00475
Max overtopping				0.28

Chart 3.1 Frequency distribution of trial data for fluid retained in the bund

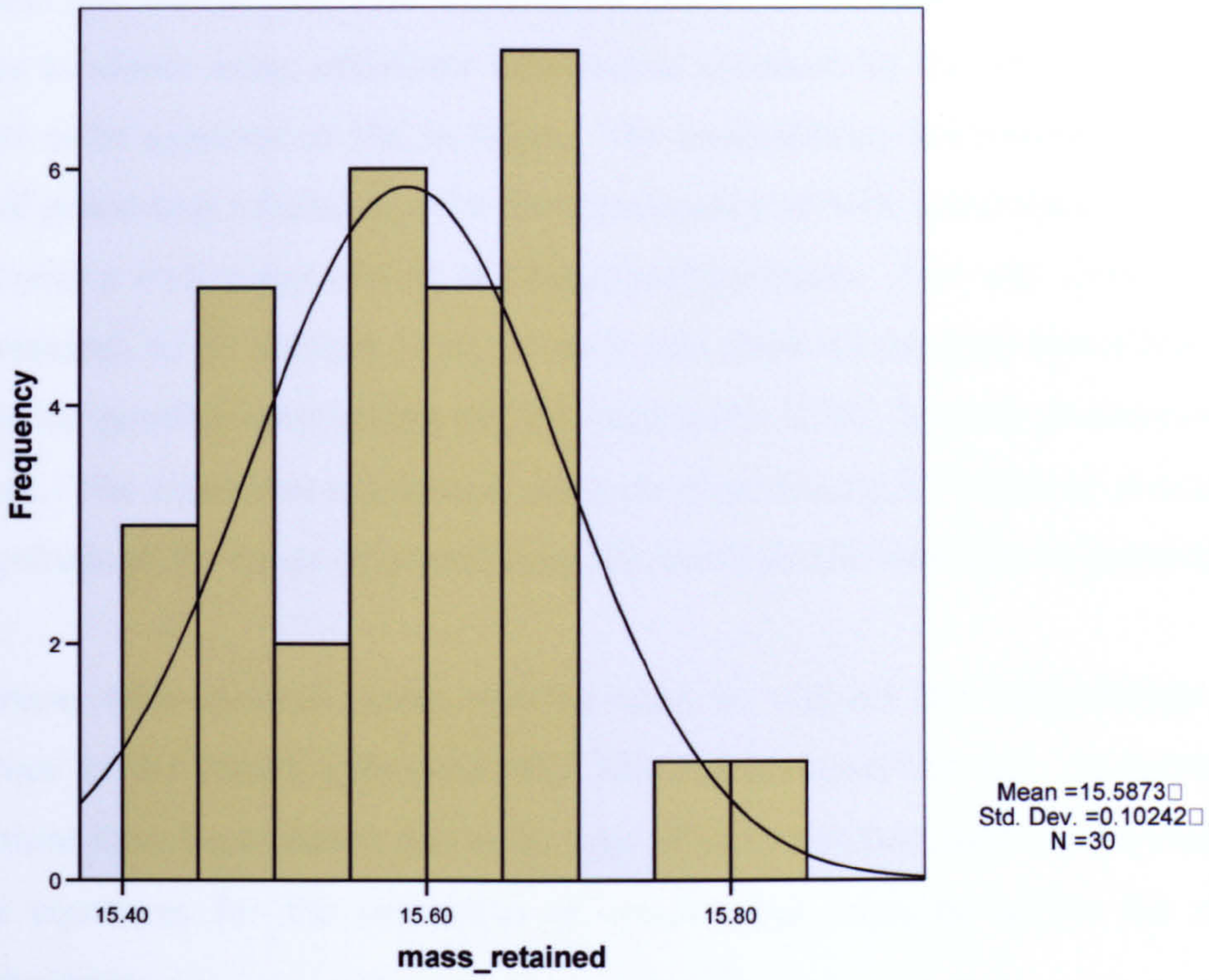

Chart 3.2 Frequency distribution of trial data for fluid overtopping the bund

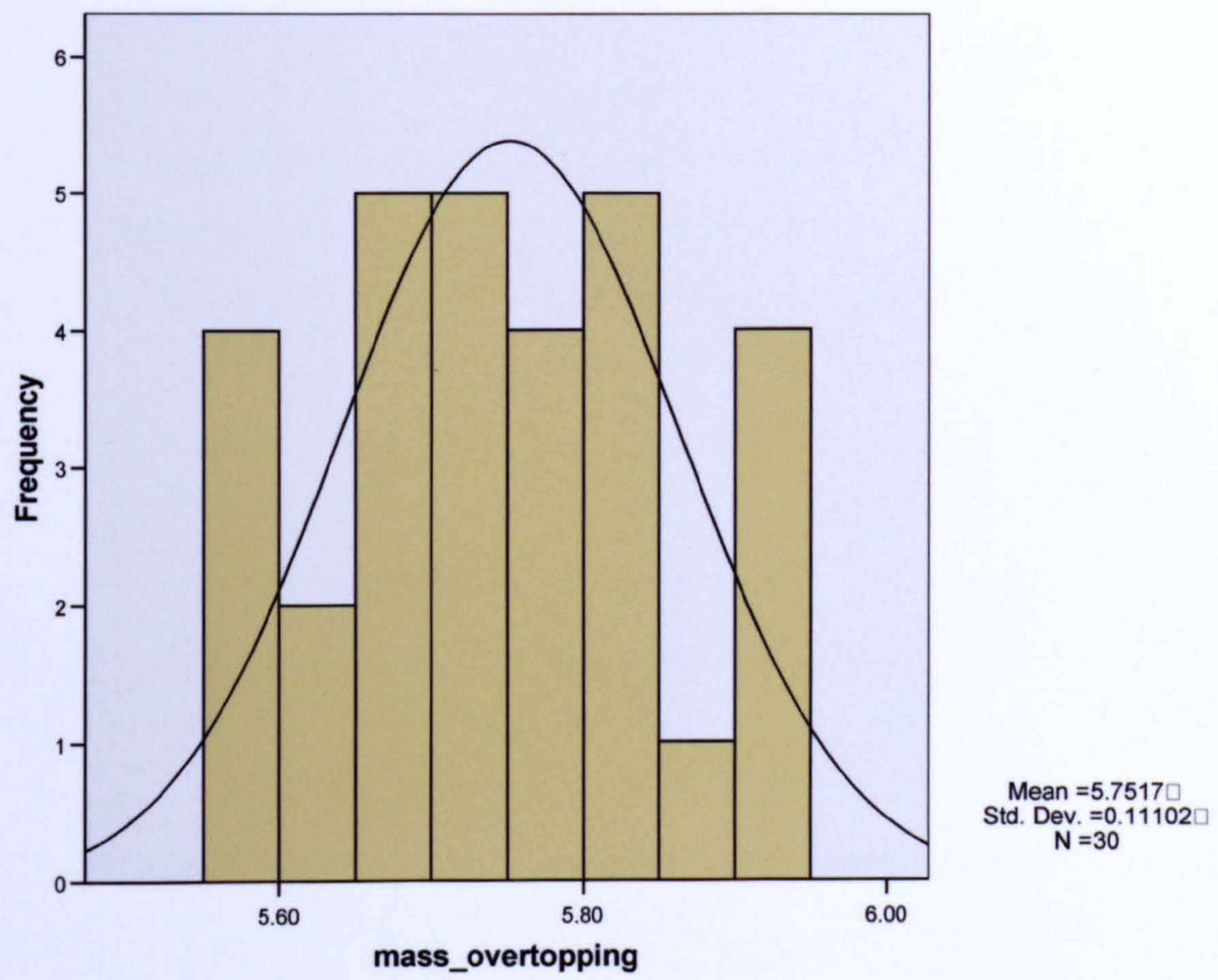

3.14 Summary

A suitable test facility has been constructed based on the detailed review of the limited literature available using additional information provided by the HSE as to the range of variables to be expected at UK facilities. The methodology has established a repeatable means of generating reliable data for the investigation of both catastrophic partial and tank failures over a wide range of tank and bund configurations. This will allow the main aim of the research to be realised in so far as it will allow an accurate quantification of the extent of the possible overtopping and the magnitudes of the dynamic pressures exerted on the bunds. The objectives to establish methods of predicting the levels of overtopping and the magnitude of the dynamic pressures on the bunds should therefore be possible.

Comparison with seminal works will be used to support the methodology and give confidence in the results generated from the experimental test rig. A number of key publications have been chosen due to the type of measurements taken or the availability of suitable equations for the estimation of overtopping fractions and/or the celerity of escaping waves.

CHAPTER 4

Comparative Seminal Works

4.1 Introduction

The following pieces of seminal work were chosen from the literature review due to the rigorous nature of their various methodologies and the fact that the data is reasonably recorded as to allow suitable comparison of the results produced from this investigation. There are certain limitations to the scope of the work in any one case, which is why such a range of work will be used for the purposes of testing any empirical formulae developed from the research. In some cases the work described is not directly associated with the failure of bulk storage tanks, yet it is possible to make certain assumptions in order to apply the findings.

4.2 Henderson (1966) and Featherstone (1988)

The basic design of the primary storage tanks is based on the hoop stress with the tank contents causing the shell of the vessel to be in constant tension. In the case of a failure, the integrity of the tank can be severely compromised and the ability to withstand the tensile forces vastly reduced. It is generally accepted that the failure will involve cracks rapidly propagating vertically up the shell, causing unwrapping at the base and allowing the contents to be spilled either in a directional asymmetric failure or in the case of a complete collapse, releasing fluid in all directions as an axisymmetric failure.

In the case of the axisymmetric failure mode, a comparison can be made with the classic dam-break failure scenario. This assumes that the failure will be the same throughout the 360° geometry of the tank and is considered as if the tank had suddenly been removed, leaving a free standing column of liquid, which then starts to fall under the action of gravity.

The fluid held against the dam wall is similar in nature to the fluid held by the tank shell with the failure allowing the flow to move horizontally away from the original position of the tank. The velocity of the flow post failure of the vessel is a major factor in the level of energy developed by the surge prior to impact with the bund. Henderson (1966) stated that

the 'Pivot' point at the intersection of the line of the dam and the parabolic curve if the liquid profile remains constant is at 4/9 times the original head of liquid behind the dam, as measured from the base. This is provided that the top surface remains at the same level at the top of the parabolic curve.

From Featherstone (1988) the velocity of the flow at the position of the dam wall can be approximated to:

$$V_1 = \frac{2}{3} g^{1/2} H^{1/2} \qquad (4.1)$$

The reality of this concept will not produce a true parabolic curve and the downstream wave profile will not comply to a featheredge, as the frictional effects with the ground interface will produce a bore (Fig. 4.1).

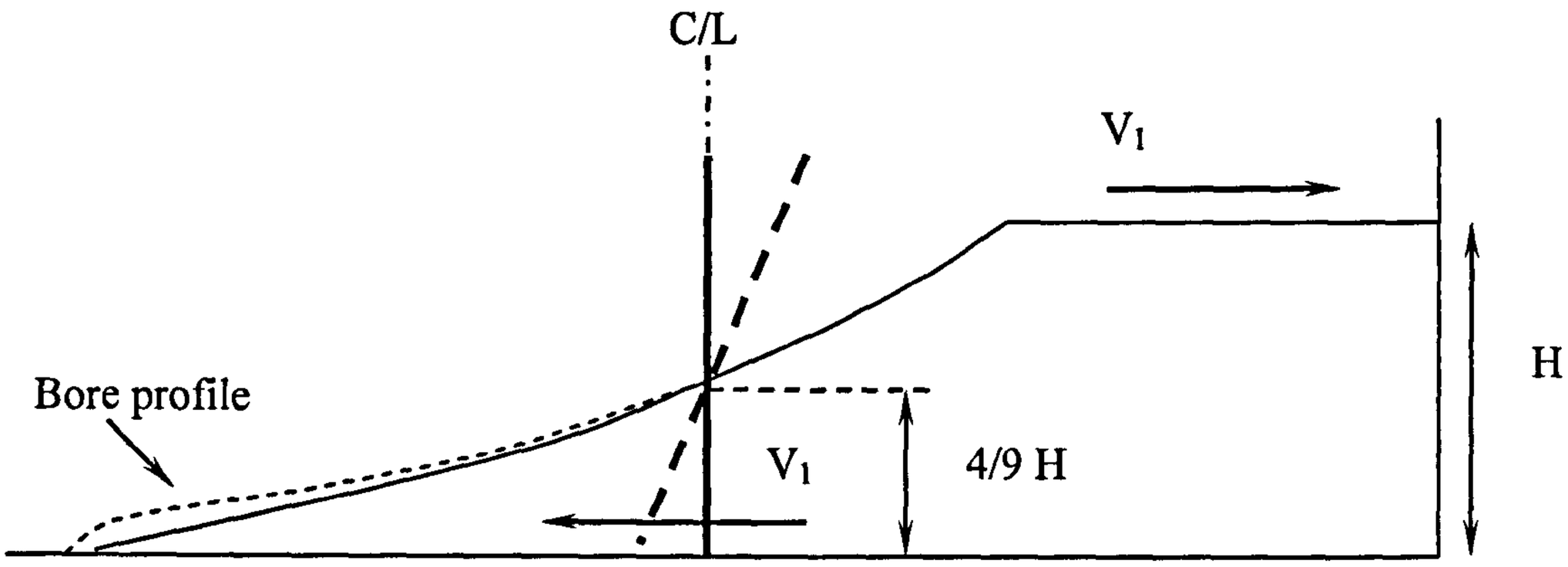

Figure 4.1 Dam-break scenario

4.3 Greenspan and Young (1978)

The consequences of the sudden release of a large volume of fluid within a relatively short period of time were investigated by Greenspan and Young (1978). They realised that very little was actually known about the problem of fluid impact against and over a barrier and attempted to investigate the problem both theoretically and experimentally. The aim was to establish the overflow fraction of the original fluid volume that escapes on impact using non-linear shallow-water equations, which were originally applied to 'dam-break' problems.

They found that upon collision of the fluid with the vertical face of the barrier, liquid accumulates rapidly to a great height, forming a shock wave, which moves back towards the tank. Fluid starts to pile up behind the shock and rapidly begins to overtop the barrier with reflected waves interacting with the propagating shock. The numerical analysis was carried out using a two dimensional approach, which once revolved about the vertical axis equates to the normal three dimensional geometry relating to a cylindrical storage tank surrounded by a concentric circular bund.

For the analysis the wall of the tank is considered to have disappeared at time zero with the resulting flow directed towards the bund. The impact with the bund and the resulting overtopping is only discussed in terms of vertical bunds with the spillage determined using accurate qualitative and quantitative descriptions of the events using a series of parameters as employed in the non-linear shallow water theory. This theory uses depth-averaged versions of the conservation laws involving mass and momentum with dependant variables being free-surface height and the mean horizontal velocity. Other assumptions made relate to the running surface being smooth and level with viscosity, turbulence and frictional ground effects ignored with escaping liquid no longer influencing the main body within the bund.

The basic description is typically described as the tank wall being removed, the liquid rushing to meet the bund and the rarefaction wave moving into the tank. Eventually the leading edge of the liquid is considered to move at constant dimensionless speed with a rarefaction wave moving in the opposite direction and reflecting off the rear wall. The impact with the bund causes a rapid accumulation of liquid, capable of reaching extreme height with the subsequent formation of a strong shock wave moving back towards the tank. Liquid continues to accumulate at the bund behind the shock wave with fluid flow eventually overtopping the bund and/or reflected waves interacting with the shock wave. The free surface behind the bore is almost uniform at any instant in time and this forms the basis of the analytical approach, allowing for the evaluation of the motion even when the bund is too high to allow overtopping. The complexity of the problem required the use of a computer to carry out the numerical analysis based on linear interpolations to define points between nodes based on small increments in time using central differences.

Experiments were carried out using a sliding wall in a Plexiglas tank (9 x 9 x 48 inch) with the slide positioned 9 inches from one end of the tank forming a reservoir and a spillage channel with dykes placed at various positions along the channel with inclinations of 90°,

60° and 30°. The reservoir was filled to a fluid height of less than 8 inches and the rapid removal of the sliding wall used to generate the surge. The motion of the wave was recorded on videotape and examined using slow motion playback. As the flow builds behind the vertical wall, some of the fluid is thrown to great height as a plume, which subsequently collapses into the main body of the fluid that accumulates behind the shock and then flows over the barrier.

The problem of the reflected waves led to the investigation of overtopping due to initial impact only. This was achieved by replacing the siding wall before the reflected wave could escape the tank thus preventing additional overtopping due to successive impacts. The total amount overtopping the barrier due to reflected waves was found to be a maximum of an additional 5 % with 'sloshing' being an important factor for a high barrier close to the tank.

The main finding indicated that the overtopping was dependant mainly on h/H, the ratio of the height of the barrier to the height of the fluid released from the tank with little dependence on L/R, the ratio of tank wall/barrier separation and the distance from the back of the tank to the sliding wall. This was found to be true for all combinations of barrier and tank heights in the range $0.33 \leq L/R \leq 4$. The overtopping fraction increases as the bund/dyke is sited further from the tank, with the height of the bund decreasing to maintain the storage capacity. This is true within certain limits, as frictional effects would limit overtopping with increasingly large values of L/H, however this is not generally the case in practice. The other obvious effect is the angle of the dyke with any decrease from the vertical allowing a greater percentage of spillage, due to the greater forward momentum being maintained over the dyke.

With regard to the performance of the mathematical model based on the shallow water equations, the physical model generated measured fluid heights adjacent to the bund in the order of approximately 15 % greater than the theoretical predictions. The flight of fluid droplets was also an issue with the theory unable to account for the droplet formation. It was determined that the height of the fluid plume exceeded the initial height of fluid in the tank with the flight of particles from the leading edge of the surge reaching three times the height of the tank fill level.

When transcribing the results to circular tank/barrier configurations it was found that the volume of overtopping was of the same order of magnitude as in the unidirectional releases

originally investigated. It was estimated that up to 25 % of the volume stored would be lost in the event of a sudden failure for a bunded area corresponding to a volume equal to that of the initial tank capacity.

4.4 Greenspan and Johansson (1981)

In their 1981 publication, the manner in which the wave overtops the barrier depends upon the shape of the dyke or bund. The fluid may vault an inclined embankment or accumulate rapidly behind a vertical bund and then overtop. The experimental apparatus consisted of an aluminium cylinder 7.5 inches in diameter and 11 inches in height surrounded by a circular barrier constructed from Plexiglas and clay. The barriers were placed at 5,7,9 or 11 inches from the centre with dyke inclinations of 30°, 60° or 90° measured from the horizontal. The tests were axisymmetric in nature with an instantaneous release of fluid from the storage tank, whereby a stationary column of fluid was allowed to fall and spread under the action of gravity. This was achieved using compressed air to operate a piston, which rapidly lifted the containment vessel. The overtopping fraction was determined by measuring the height of the fluid retained within the barrier using a needle depth gauge.

Video recordings were taken and viewed in slow motion playback to observe the falling column of fluid and the subsequent overtopping of the barrier. A source of error was identified as the sudden impulsive motion of the containment vessel, which produced drag on the outer surface of the fluid column. This effect on the final level of overtopping was considered minimal due to the relatively small volume of fluid involved. The overtopping due to 'sloshing' was considered not to be significant with most of the fluid escaping in the first impact of the wave with the barrier.

Partial tank ruptures were also modelled using an inner wall with various rectangular holes (1 to 3 inches high) over a 30° arc length. The influence of the barrier shape was further investigated using the two-dimensional tank as described in the earlier experiments.

The Greenspan and Johansson (1981) experiments, led to a conclusion that simple formulae to estimate the overtopping fraction could probably be based on dimensionless combinations of parameters:

$$Q = f\left(\frac{h}{H}, \frac{r}{H}, \frac{R}{H}, \theta\right) \tag{4.2}$$

with h/H as the main variable and r/H, R/H and the angle of inclination of the bund, θ, as subsidiary parameters.

Comparisons between axisymmetric configurations and the channel experiments indicated that in both cases the level of overtopping Q, was mainly dependant upon h/H, the ratio of the height of the barrier, h to the height of the original fluid column, H. In all cases the overtopping of the barrier was substantial with reduced levels of overtopping occurring with increased distance of the barrier from the tank. Reducing the angle of the barrier also led to increased values of overtopping. The level of agreement between the cylindrical and channel experiments was generally good with some variation at increased separation distances. This meant that the simplified experimental channel results could be used to gain meaningful overtopping fractions that could be applied to axisymmetric releases.

The directional releases indicated that spillages from small holes were comparable to full column releases, especially in the case of the inclined dykes. It was therefore demonstrated that the two-dimensional channel releases were sufficient to model the effects of a catastrophic failure of a containment vessel. The investigation was then centred on various designs of barrier with the aim of reducing the overtopping fraction. Designs included reversed tops on the inclined dykes, where the escaping fluid is thrown back to interfere with the approaching flow. The reduction in forward momentum resulted in lower levels of overtopping and this led to the use of fluid 'trip' control devices to further reduce the forward momentum. Other methods included the use of forward facing angled bunds, which proved effective, but would be difficult to construct in terms of any full-scale mitigation.

The mitigation methods used reduced the overtopping fraction in the range of 25 to 35 % of the values originally obtained while maintaining the equal tank storage to containment volumes. In terms of a real life solution the mitigation would most probably take the form of an additional deflector fixed to the top of the original bund. When this proposal was investigated the deflector along with the increased capacity of the bund led to a much reduced overtopping fraction in the order of a factor of ten. Such methods of mitigation should therefore be considered for further investigation, both in terms of optimisation and reasonably practicable installation.

4.5 Michels et al (1988)

One of the most important factors in the design of a bulk storage facility must be its "total and immediate containment capability." This means that even a large spill can be dealt with and limited to enclosed predetermined area, normally achieved via the construction of a suitable bund/dyke. Experience has indicated that the tank needs to be encompassed by a surround at least as high as the tank itself to achieve protection from catastrophic tank failure. The determining influence for level of overtopping is related to the rate of release rather than the volume of release, with the possibility of earthen dykes being simply washed away.

A combined theoretical and physical modelling programme was established to investigate the problem with the starting point being that once failed, the storage tank is largely irrelevant to the subsequent flow, due relative mass of the tank walls compared to that of the liquid contents, typically around 1%. Hence, the assessment of a freestanding column of liquid falling under the action of gravity was used in the analysis.

Typically, Reynolds number, R_e:

$$R_e = \frac{\rho g^{1/2} H^{3/2}}{\mu} >> 1 \qquad (4.3)$$

with the Weber number, W_e:

$$W_e = \frac{\rho g H^2}{\sigma} >> 1 \qquad (4.4)$$

where, ρ = density of liquid, μ = viscosity, σ = surface tension & g = acceleration due to gravity

Theoretically, the viscous and surface tension effects are negligible compared to the inertial and gravitational forces. This leads to the equations of motion being modified from the Navier-Stokes equations immediately after the tank failure to Euler's equations. If the vertical acceleration in the liquid is neglected together with the immediate failure, then the equations further simplify to the shallow water equations. These are hyperbolic partial differential equations with dependent variables being the horizontal liquid velocity and the local height of the fluid. The solution is again obtained via the use of a computer based on discrete changes in radial position and time.

The flow near the bund/dyke is of importance due to the surging liquid being slowed down by contact with the bund and the rise in fluid level. The increase in level can be sufficient to cause overtopping of the bund, which is assumed to take place with a horizontal velocity equivalent to that of long waves of small amplitude based on the localised depth. There is also consideration of reflected waves travelling back towards the original tank position and the formation of a hydraulic jump allows analysis using conservation of momentum. Hence the velocity near the leading edge of the moving liquid is given by:

$$u = 2g^{1/2}H^{1/2} \tag{4.5}$$

The physical model comprised a horizontal water table made from plate glass, illuminated from below in order to allow viewing through the flow. A vertical open-ended cylinder was used to contain the liquid under test with a mechanism for providing a rapid vertical lift. The resulting flow was photographed and the progress of the wave monitored as the flow travelled over a series of photodiodes placed at known positions along the water table in order to determine the velocities. Experimentally, from the physical modelling for the velocity near the leading edge of the liquid, it was found that:

$$u = 1.4g^{1/2}H^{1/2} \tag{4.6}$$

The overtopping fraction was also determined, with the percentage overtopping expressed versus h/H and r/R. The importance of scale is highlighted due to the fact that Reynolds number, R_e varies with $H^{3/2}$ (Equation 4.3) and that the Weber number, W_e varies with H^2 (Equation 4.4). Thus, if the height of liquid stored in the tank is too small, it possible to get values such that R_e and W_e are not very much greater than 1 and it is recommended that H is at least 0.1 m, which determines the lower limit on the length scale for any investigation. The difference between Equations 4.5 and 4.6 is due to the neglect of viscous and surface tension effects as assumed in the mathematical model.

4.6 Trbojevic and Slater (1989)

There is considerable interest in the loading that would occur on the bund/dyke given the sudden failure of the bulk storage tank. In the event of a failure, the consequences of large volumes of fuel being released and the possibility of fire, explosion and the ultimate widespread pollution means that the probability of failure is required to be very low. The

problem currently facing designers is that existing facilities may not provide the necessary levels of protection, especially with land use planning issues and the locality of densely populated areas.

Due to the complexity of the problems associated with tank failures there are various views as to the modes of credible failure. A widely accepted possibility is the rapid propagation of cracks in the primary containment (storage tank), leading to large dynamic loading on the secondary containment (bund). Reliable and sensible estimates of these dynamic pressures are needed to evaluate existing bunds as well as to aid the design of new facilities. The use of complex numerical methods needs to be considered to obtain a better understanding of the overall system behaviour both to evaluate existing levels of risk and to reduce such risks in new designs.

There are many arguments as to the speed of crack propagation in bulk storage tanks and a worst-case option is often adopted, where the vertical propagation is considered along with crack propagation around the base of the tank. During any sudden release, the tank will move due to the escaping liquid and cases have been recorded, where the tank has been forced backwards from its base in reaction to the instantaneous release and rapid forward motion of the liquid. Even with such complexity, a suitable mathematical model can offer considerable flexibility provided a reasonable representation of the physical problem could be achieved. This would undoubtedly require validation using physical scale modelling to confirm the necessary performance and suitability across a range of usual parameters.

The highly complex nature of the interaction between the fracture propagation and the rapid fluid flow under free-surface conditions has to be simplified for the analysis and it is assumed that the tank loses integrity instantaneously with cracks propagating much faster than the motion of the escaping fluid. This gives rise to the collapsing cylindrical column as previously discussed, with liquid rapidly directed towards the bund in an axisymmetric mode of failure. It is this failure mode that is modelled mathematically using a finite difference programme based on Eulerian theory and run on a computer. The volume of fluid (VOF) technique is employed at the boundaries with the computational grid fixed allowing flow through the mesh in discrete intervals of time. This offers certain advantages over the integration of the Navier-Stokes equations as the VOF method allows for discontinuities (droplet formation) and large deformations of the free surface during release and overtopping.

Results from the modelling indicated dynamic pressures at the bunds to be between 2.5 and 3.5 times the normal static head with local conditions more than four times that normally experienced. Velocities were also determined and for a tank of 30 m diameter with a 10.5 m head of fluid it was shown that the velocity reached a value of up to 14.6 ms^{-1} after a time of 2 seconds, just prior to impacting the bund/dyke. It was estimated that approximately 30 % of the initial contents of the tank overtopped the secondary containment, assuming no physical damage to the bund/dyke was sustained due to the dynamic loading.

The overall conclusions indicated good levels of fit with existing small-scale models and highlighted the need for careful consideration of the dynamic pressures in the design of secondary containment. The speed of determination of results and the usefulness in assessment of mitigation was discussed given the limitations of scale using physical modelling.

4.7 Clark et al (2001)

For a cylindrical tank surrounded by a concentric circular bund, the following relationship is suggested for the height of the bund wall required to provide 100 % containment, this of course assumes that bund overtopping or spigot flow (jetting) does not occur:

$$h \geq \frac{\left(R^2 H\right)}{\left(R+L\right)^2} \quad or \quad h \geq \frac{\left(R^2 H\right)}{r^2} \quad as \ r = \left(R+L\right) \tag{4.7}$$

Thus, for 110% containment:

$$h \geq \frac{\left(1.1 R^2 H\right)}{\left(R+L\right)^2} \quad or \quad h \geq \frac{\left(1.1 R^2 H\right)}{r^2} \tag{4.8}$$

Similarly, for a rectangular bund with dimensions x and y 100 % capacity is given by:

$$h \geq \frac{\left(\pi R^2 H\right)}{xy} \tag{4.9}$$

Thus, for 110 % containment:

$$h \geq \frac{(1.1\pi R^2 H)}{xy} \tag{4.10}$$

Bunds should be capable of limiting the contamination of the soil and groundwater along with preventing running pool fires by providing adequate containment and at the same time, minimising vapour production due to evaporation. The main contributors to evaporation are vapour pressure, the exposed surface area of the spill, the velocity of the passing wind and the ambient temperature of the contact materials including the air interface. Hence, effective bund design should limit the exposed surface area in an effort to minimise evaporation and the generation of excessive amounts of vapour. The method of construction of the bund itself is also of importance in terms of the material properties, such as thermal insulation, which can be used to inhibit vapour production due to heat transfer characteristics.

It is essential that the effectiveness of any secondary containment system be properly considered in terms of the possible scenarios that may render its design ineffective. A number of possibilities exist where problems may arise including overtopping, rainwater build-up, spigot or jetting failure, accidental drainage and bund collapse due to excessive dynamic loading.

Overtopping due to sudden failures of the primary containment (tank) should be taken seriously with the severity of such an event depending on factors such as the bund capacity, the structural integrity of the design and the severity of the release dynamics due to the catastrophic failure mode. Both mathematical and physical modelling techniques have indicated that, for vertical bunding arrangements, the volume overtopping the bund depends principally on the parameter h/H.

Clark (2001) put forward the following relationship to predict the overtopping fraction, Q_C:

$$Q_C = exp\left[-p\left(\frac{h}{H}\right)\right] \tag{4.11}$$

where p = 3.89, 2.43 or 2.28 when $\theta = 90^\circ$, 60° or 30°.

Generally, it was found that the overtopping fraction Q_C and the relationship with h/H held true over the range $0.33 \leq (r - R) / R \leq 4$, with an intercept at h/H = 0 when Q = 1.

It is clear that the angle of inclination of the bund/dyke has a definite effect on the overtopping fraction with a positive slope angle, the surge retains more of its horizontal momentum both pre and post impact. This allows a greater spread of fluid than that typically observed for a vertical bund wall with a 30° slope giving values of overtopping approximately twice that expected for the equivalent vertical bund. A negative angle of slope can be beneficial, with a backward facing wall giving significant reductions in overtopping fraction. In situations where the shock wave is reflected back from the bund wall post impact, returning to the storage vessel and then continues to reverberate, additional overtopping can occur. In such cases it has been shown that these effects typically contribute only 5 % of the fluid lost over the bund.

The proper management of bunded areas is essential and careful planning is needed in the removal of water build-up from precipitation. This normally involves drain down valves and surface water may need to go through separation procedures depending on the presence of any previous minor spillages and the nature of the liquid involved. If this process is not properly managed then a major spill could easily result in the capacity of the secondary containment being exceeded or seriously limit the capability of dealing with fire fighting water or chemical agents. There is also the possibility of a spill being accidentally released due to failure in the drainage management system with control valves being left open.

Spigot flow or 'jetting' is a possible mode of partial failure and the bund can largely be bypassed by such an event if not properly designed to cope. It is possible to perform relatively simple calculations to determine if such a scenario is credible for a give tank and bund configuration. The various factors involved are based on the minimum distance from a credible position of release, the operating pressure of the containment vessel and the head of the liquid in the tank.

For atmospheric conditions, spigot flow is prevented using the relationship:

$$L + h > H \quad or \quad L \geq H - h \tag{4.12}$$

In the case of pressurised liquids, the formation of a high-speed jet is probable and due to the horizontal orientation of such storage vessels it is not normally possible to prevent fluid escaping unless high collar bunds are employed. Due to the pressurised nature of such tanks, a partial breach of containment could propagate resulting in an explosion and a total loss of containment.

A more serious scenario is the possibility of a total bund collapse due to excessive dynamic loading conditions or the impact of tank debris following the catastrophic failure of the bulk storage tank. Other possibilities include thermal shock in the case of cryogenic liquids, earthquake and differential settlement due to poor foundation design or impact damage from moving vehicles.

4.8 Thyer et al (2002)

A number of experimental studies are discussed including the work of Greenspan and Young (1978) and Greenspan and Johansson (1981). Two studies carried out at the Health and Safety Laboratory using hydraulically lifted storage tanks in water channels are described with the results indicating good agreement with that of Greenspan and Young (1978).

The simple approach above was improved upon using three-dimensional models of both small and large scale. The large-scale tests employed either a 'petal' opening arrangement or a 'split-skin' approach with the tank opening along a vertical split in one face. The size of the test area for the experiments was a 10m square concrete pad using a square bund and central circular tank. This arrangement allowed the corner effects to be investigated with interfering wave fronts giving rise to localised increased overtopping. The fluid flow was monitored using video cameras with the overtopping fraction determined from measurements of liquid collected in a series of trays laid out behind the bund.

The smaller-scale testing was carried out using a similar 'split-skin' tank arrangement with water released onto a smooth table with overtopping determined by collecting the overflow into a number of trays located behind the model bund with quantification via measuring cylinder. A rather crude attempt was made at determining the wave height employing strips of tissue paper suspended directly behind the bunds. The combined results of these tests were analysed in terms of the overtopping as a function of the parameter h/H with varied r/H and r/R.

Work by Cronin and Evans (2002) was described, where water was released through a 25 mm high circumferential slot at the base of a 'quadrant' tank with a diameter of 3.5 m and a fill height of approximately 2 m and allowed to flow over a concrete base surrounded by various bund configurations. On average, the release time was 30 seconds with the flow of the fluid monitored and the overtopping estimated.

Some comparison of the various data sets is possible as the overtopping fraction, Q was normally expressed in terms of varying h/H, as a function of r/H however there are limitations as the parameter r/R was also varied. Where the differences in r/R are minor it is possible to obtain comparisons with some level of confidence.

In the case of predictive models, a number of researchers have attempted to quantify the bund overtopping for various configurations this included Clark et al (2001), where an equation was fitted to the data complied by Greenspan and Johansson (1981). Independently, Hirst in Thyer et al (2002) derived formulae fitted to the same test data to predict the overtopping fraction, Q_H:

$$Q_H = A + B\,ln\left(\frac{h}{H}\right) + C\,ln\left(\frac{r}{H}\right) \qquad (4.13)$$

where $A = 0.044$, $B = -0.264$ & $C = -0.116$ for $\theta = 90^\circ$

$A = 0.287$, $B = -0.229$ & $C = -0.191$ for $\theta = 60^\circ$

$A = 0.155$, $B = -0.360$ & $C = -0.069$ for $\theta = 30^\circ$

The proposed equation permits estimates of the bund retention capabilities; this may be limited in terms of performance when transposed to larger scale facilities due to the small scale of the models used. It is suggested that scaling issues relating to surface roughness in the models may cause the equation to under estimate the overtopping fraction when applied to full scale.

In conclusion, there are limitations as to the range of available data sets and a definitive investigation is still required using medium scale laboratory models in order to validate any computer based mathematical models. Both the Clark and Hirst equations gave good fits to the data of Greenspan and Johansson on which they were based. However, as the test data did not include high collar bunds, neither Clark nor Hirst claimed that their functions could be used for such cases. Moreover, the Greenspan and Johansson tests were

performed at very small scale so may systematically underestimate the overtopping fraction due to the spill surfaces not being suitably smooth enough. The performance of both Equations 4.11 and 4.13 are tested in this research against the newly obtained test data. Failure to perform well would indicate a systematic difference between the small-scale test data and the new larger scale data.

4.9 Pettitt and Waite (2003)

A series of experiments were carried out to determine the effects of placing a vertical section of wall on top of an existing sloping dyke with the aim of providing suitable mitigation of overtopping. Observations made on the performance of sea wall defences indicated considerable reduction in overtopping could be achieved by deflecting high velocity waves and associated splash back into the sea. This influenced the decision in providing a horizontal 'lip' at the inside face on the top of the sloping dyke with the aim of investigating its performance in terms of reduced overtopping. A series of experiments were undertaken using physical modelling at a scale of 1:30 based on a bund capacity of 170% of the maximum tank capacity used during testing.

The release of fluid was achieved using a sliding plate behind a polypropylene block with a series of profiled apertures cut into the block, a second much larger opening in another block sandwiched the sliding plate allowing a suitable seal to be formed. Hence, the investigation was focused on asymmetric releases associated with the spigot failure mode. The fluid used was water with a specific gravity of 1 rather than the typical specific gravity of 0.83 for a hydrocarbon fuel.

Various combinations of sloping dyke profiles; apertures, separation distances and fluid heads were investigated with a video camera used to record the escaping fluid motion. Release quantities were calculated from the tank geometry with overtopping fractions determined by weighing the contents of a series of catch trays. The results indicated that the tanks typically emptied in 10 to 20 seconds depending on the fill height and aperture size with the virtual elimination of overtopping when employing the deflector plate modification. Comparison with other data for the sloping dykes highlighted discrepancies, probably due to the geometry of the comparison test regime, which was based on releases in a channel rather than similar spigot flow.

In terms of the civil engineering issues, the possibility of bund failure was considered due to the nature of the dynamic loading upon impact by the rapidly approaching surge. Any

retrofitted deflector would therefore have to be suitably designed with these pressures carefully considered.

4.10 Kleefsman et al (2004)

Confidence in computational fluid dynamics (CFD) modelling is building as improved methods are developed with increasing computer speed and memory capacity enabling millions of calculations to take place in shorter periods of time with high mesh densities giving a high degree of resolution to free surface flow simulations. A common theme is the use Navier-Stokes equations with improvement in the VOF method used for the displacement of the free surface. A dam break scenario is used for simulation purposes with experimental results used for validation purposes.

The area of interest lies in the physical modelling of breaking dam flows over the deck of a cargo ship. A large tank of 3.22 m x 1.00 m x 1.00 m was used with 0.55 m head of water retained behind a release door, which when release allowed water to rapidly flow along the tank. At a known position along the tank, a model container was position to represent full size container sited on the deck of a large ship. The instrumentation employed allowed collection of wave profile data and more importantly the dynamic pressures generated on the front face and top of the model container. Four pressure sensors were fitted to the front face and four to the top surface with the wave velocity determined using a horizontal wave probe located near the sidewall of the tank. Although velocities are not directly quoted in the paper, it is possible to elicit data from the scale drawings and plates using the impact times to estimate the celerity of the wave.

For the wave impacts on the model containers, the dynamic pressure are shown graphically against time for two of the sensors on the front face and two on the upper surface. The front face dynamic pressures indicate instantaneous peak values of 11400 Pa close to the base (Chart 4.1) and 6500 Pa in the region of the upper third (Chart 4.2), however these values quickly fall to post peak values of 4000 and 3900 Pa respectively.

Chart 4.1 Kleefsman et al (2004) results - front face base pressure

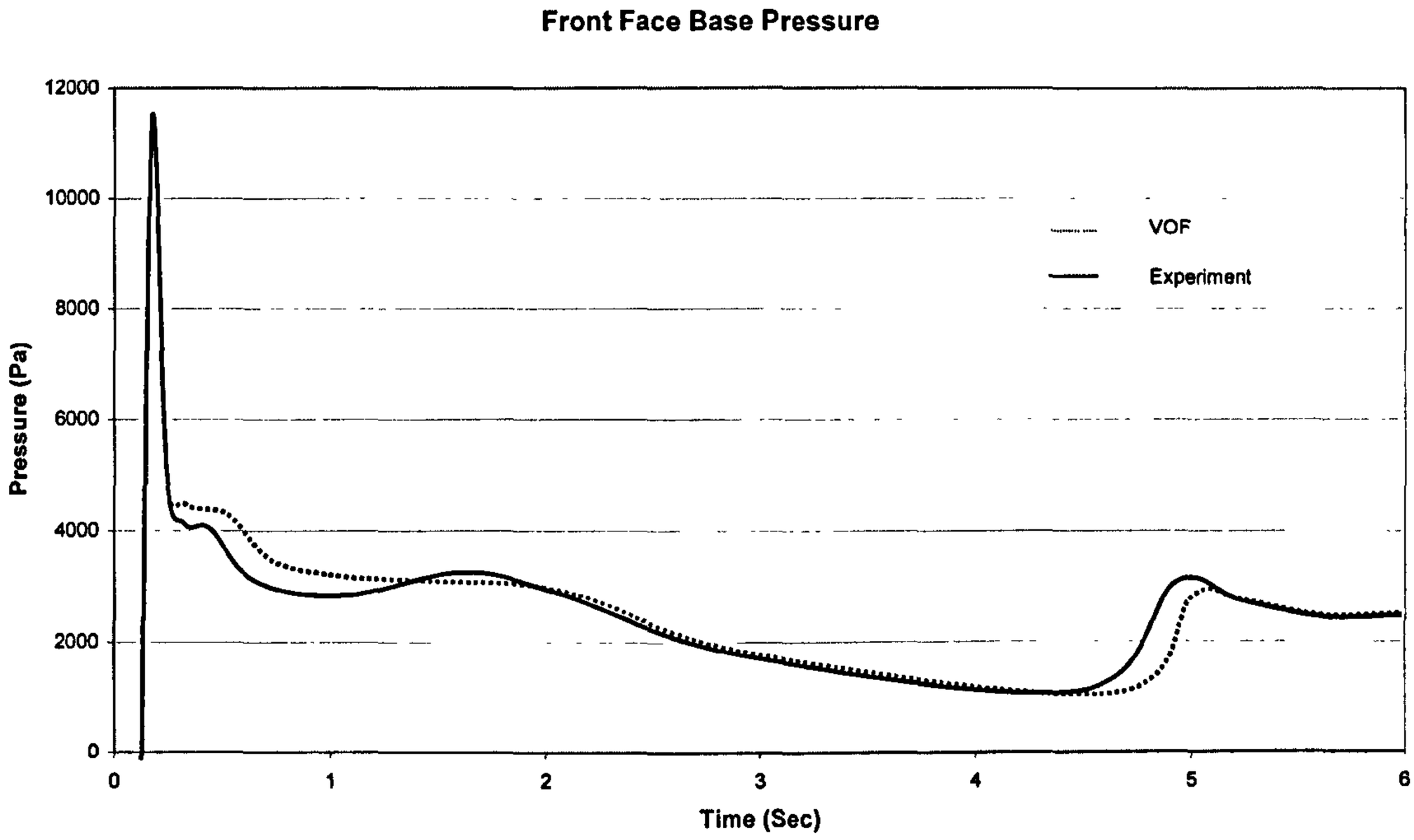

Chart 4.2 Kleefsman et al (2004) results – front face upper third pressure

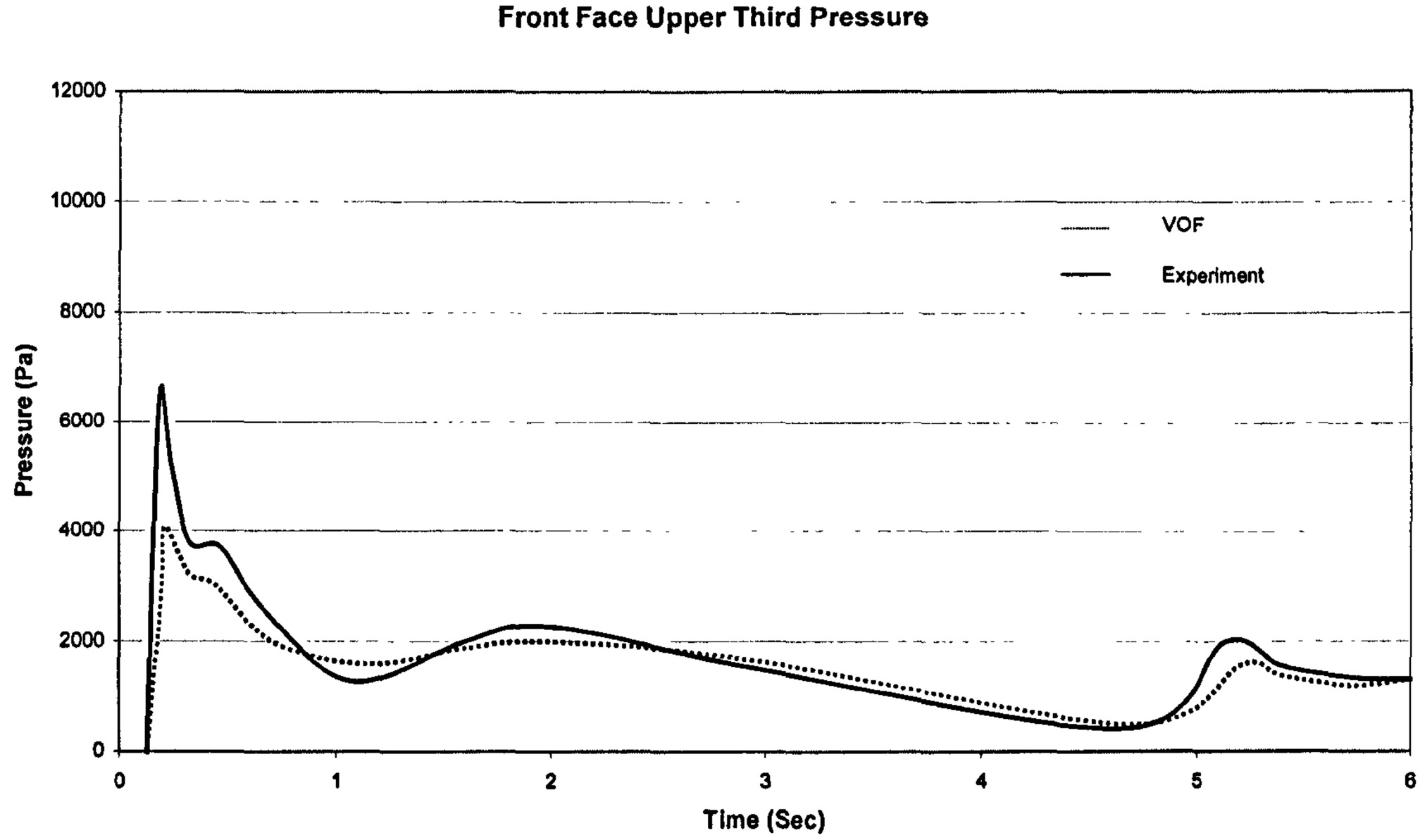

The final conclusion relates to the overall validation of the improved VOF method with the global agreement of results between mathematical and physical models. One of the main uses of the results relating to this work will be in comparison of the velocity and dynamic pressure values with those recorded on bunds of similar geometry with similar dimensionless ratios in terms of h/H at suitable separation distances, L.

4.11 Ivings and Webber (2007)

Ivings and Webber (2007) further extended the work on CFD modelling with the development of a bespoke method of assessing the hazards arising from liquid spills from bulk storage tanks eliciting data produce by Atherton (2005). The CFD model again made use of the solution of shallow water equations with the ability to account for the interaction of the flow with sloping ground and bund/dykes. In terms of risk assessment, one of the major requirements is the determination of the quantity of fluid that might conceivably overtop the secondary containment or bund/dyke. This specific requirement led to the development of a 'sub model' to analyse the three-dimensional nature of the problem within the two-dimensional model. The methodology employed the solution of the shallow water equations with an adaptive element incorporating two shock-capturing numerical techniques known as the weighted average flux (WAF) and the random choice methods (RCM).

In real terms tank and bund configurations are complex, requiring much more complex algorithms with various levels of input information required, depending on the level of complexity. The time and extreme effort required to input data and model the scenarios to the desired level of output are demanding and for practicality an acceptable approach has to be determined, allowing as suitable degree of confidence in the results to be achieved. Hence the development of 'SPLOT', allowing necessary degrees of complexity with reduced functionality in comparison to full three-dimensional CFD modelling software.

The shallow water equations are unable to account for three-dimensional behaviour of the fluid bund interface and subsequent overtopping. To describe the physical behaviour, the model was based on certain assumptions including representing the bund as a thin wall between computational cells with the flow subdivided vertically at the top of the bund, solving the resulting shallow water equations in two layers. The lower layer is considered to interact with the bund as a solid wall with the upper layer free to travel over the bund. The bottom layer is updated using a reflective boundary condition in the cells immediately adjacent to the bund and the upper layer is analysed using a modified liquid height (liquid height – bund height). The overall solution is a recombination of the separate solutions to give the depth-averaged flow variables in that cell, which leads to a reasonable solution to the problem without having to take account of the complexity of the three-dimensional flow.

In a typical test run, a single tank of radius 8 m is filled to a height of 10 m giving a volume of just over 2000 m^3 with a rectangular bund 24 m x 44 m x 2 m with a volume of 2100 m^3. The results in terms of general observation show that overtopping takes place at the nearest section of wall to the release through a 25 % area of the tank. The impact generates splashing to a considerable height and overtopping is significant before the volume of fluid released ever becomes an issue in terms of the bund capacity. Thus, the bund capacity is not a determining factor in the magnitude of the overtopping fraction.

The application of the model has been validated using more exacting numerical methods as well as experimental work including the overtopping results obtained by Atherton (2005). In conclusion, the model is sufficiently accurate to predict overtopping in the event of a sudden release due to the catastrophic failure of the primary storage vessel and as such, is able to adequately assess the risks associated with this type of potential hazard.

4.12 Summary

A number of previous researchers have attempted to address some of the problems highlighted using a range of different approaches including dam-break analogies, channel releases, small-scale cylinder models and CFD techniques. In each case it has been difficult to make exact comparisons between the results due to the different ranges in the parameters used in each of the investigations. There is one overall commonality between all works considered, in so far as the conclusions lead to an undeniable shortcoming of the vast majority of bund walls. This is particularly evident in the case of bunds providing proper containment for the more extreme modes of failure. For the purposes of validation of the results from this research, the work described in this chapter will provide sufficient information for the performance of any empirical formulae to be evaluated. This is possible, as over the range of work considered there are a number of suitable cases that are relatively similar dimensionally to those investigated.

The summary of results aims to confirm the extent of the problem of bund wall overtopping and dynamic pressures over a wide range of possible tank and bund configurations for both catastrophic (axisymmetric) and partial (asymmetric) releases. The results are presented in both table and chart format, making use of non-dimensional parameters to illustrate the magnitudes of both overtopping and dynamic pressures. Comparisons between types of failure and the effects of aperture size and shape are also presented for consideration.

CHAPTER 5

Summary of Results

5.1 Data processing

The data collected from each test run were imported into a Microsoft Excel spreadsheet for statistical analysis. For each configuration examined the maximum, minimum, mean and sample standard deviation for the masses overtopping the bund and retained by the bund in each of the five test runs were calculated to check the spread of the data about the mean. The spread was found to be small, usually within 1 % of the mean. The maximum value of the overtopping fraction, Q, over the five test runs was taken forward as the overtopping fraction for the configuration.

Dynamic pressures and fluid heights were plotted against time to allow comparison of results and permit the evaluation of values such as the average speed of the approaching wave. The dynamic pressure profiles were plotted and the maximum dynamic pressure at the base was estimated using linear extrapolation of the signals from the two sensors nearest to the base. The majority of tests had these sensors at 10 % of the bund height, but the physical size of the sensors meant that for bund heights of 36 mm and below greater heights had to be used to accommodate the sensor body adjacent to the base. The extrapolation is therefore less reliable for the lower bunds (and indeed is not available for the 6 mm bund as only one sensor could be used in that case). The sensor positions are recorded in Tables 5.1and 5.7. The extrapolated pressure could then be compared to the wave height measured at the bund in the vicinity of the transducers.

Table 5.1 Dynamic pressure sensor positions for axisymmetric tests

Bund height (mm)	*Sensor positions (% from base)*	*Sensor position (mm from base)*
6	75	4.5
12	40	4.8
	50	6
	60	7.2
	70	8.4
	80	9.6
15	30	4.5
	50	7.5
	70	10.5
	80	12
	90	13.5
24	20	4.8
	30	7.2
	50	12
	70	16.8
	90	21.6
30	20	6
	30	9
	50	15
	70	21
	90	27
36	20	7.2
	30	10.8
	50	18
	70	25.2
	90	32.4
48	10	4.8
	30	14.4
	50	24
	70	33.6
	90	43.2
60	10	6
	30	18
	50	30
	70	42
	90	54
90	10	9
	30	27
	50	45
	70	63
	90	81

Bund height (mm)	*Sensor positions (% from base)*	*Sensor position (mm from base)*
120	10	12
	30	36
	50	60
	70	84
	90	108
144	10	14.4
	30	43.2
	50	72
	70	100.8
	90	129.6
180	10	18
	30	54
	50	90
	70	126
	90	162
240	10	24
	30	72
	50	120
	70	168
	90	216
300	10	30
	30	90
	50	150
	70	210
	90	270
360	10	36
	30	108
	50	180
	70	252
	90	324
600	10	60
	30	180
	50	300
	70	420
	90	540
720	10	72
	30	216
	50	360
	70	504
	90	648

Example results for the axisymmetric 'circular' configurations are given in Tables 5.2 and 5.3 with full results given in Appendix 2. For each of the 84 configurations studied the appendix shows a table of measured variables in each of the five test runs and their

statistical analysis, followed by a table showing extrapolation of the worst-case dynamic pressures and their analysis alongside wave heights.

Table 5.2 Series results for configuration identity B2 (h240)

Configuration identity	*series identity*	M_{bund} *(kg)*	M_{slosh} *(kg)*	*temp (°C)*	M_{bund} *correction (kg)*	V_{bund} *(m^3)*	V_{slosh} *(m^3)*	*Overtopping fraction*
B2(h240)	A	33.38	8.63	18.4	0.4	0.13192	0.03452	0.2074
	B	33.62	8.55	15.6		0.13288	0.03420	0.2047
	C	33.55	8.68	14.3		0.13260	0.03472	0.2075
	D	33.20	8.95	14.6		0.13120	0.03580	0.2144
	E	33.48	8.86	14.0		0.13232	0.03544	0.2113
Max		33.62	8.95	18.4		0.13288	0.03580	0.2144
Min		33.20	8.55	14.0		0.13120	0.03420	0.2047
Mean		33.45	8.73	15.4		0.13218	0.03494	0.2090
Sample sd		0.16365	0.16592	1.7922		0.00065458	0.00066369	0.0037835

Height from base (%)	*Series dynamic pressures (Pa)* *A*	*B*	*C*	*D*	*E*	*Max dynamic pressure (Pa)*
10	3779	3808	3750	3808	3808	3808
30	2922	2840	2977	2867	2895	
50	1350	1292	1206	1292	1264	
70	403	317	317	288	317	
90	137	-82	-82	137	-82	

Table 5.3 Worst-case dynamic pressures for configuration identity B2 (h240)

Configuration identity	*Test Series identity*	*Tank radius, R (mm)*	*Tank fluid depth, H (mm)*	*Bund radius, r (mm)*	*Bund height, h (mm)*
B2(h240)	B	300	600	520	240

Estimated dynamic base pressure (Pa)	*Estimated Wave intercept height (mm)*	*Equivalent wave intercept pressure (Pa)*	*Max integral wave height (mm)*	*Equivalent integral wave pressure (Pa)*
4292	288	2830	552	5418

Height from base (%)	*Static pressure (Pa)*	*Dynamic pressure (Pa)*	*Local difference (Pa)*	*Local dynamic/static ratio*
0	2354	4292	1937	1.82
10	2119	3808	1689	1.80
30	1648	2840	1192	1.72
50	1177	1292	115	1.10
70	706	317	-390	0.45
90	235	-82	-317	-0.35
100	0			

Release time (sec)	*Impact time (sec)*	*Time taken (sec)*	*Impact Velocity (m/s)*
0.184	0.301	0.117	3.76

Example Charts 5.1 and 5.2 indicate variation of dynamic pressures and fluid depths against time, and best-fit curves to the pressure data with variation in percentage bund height with. Complete chart sets are given in Appendix 2.

Chart 5.1 Plot of dynamic pressures and wave heights for configuration identity B2 (h240)

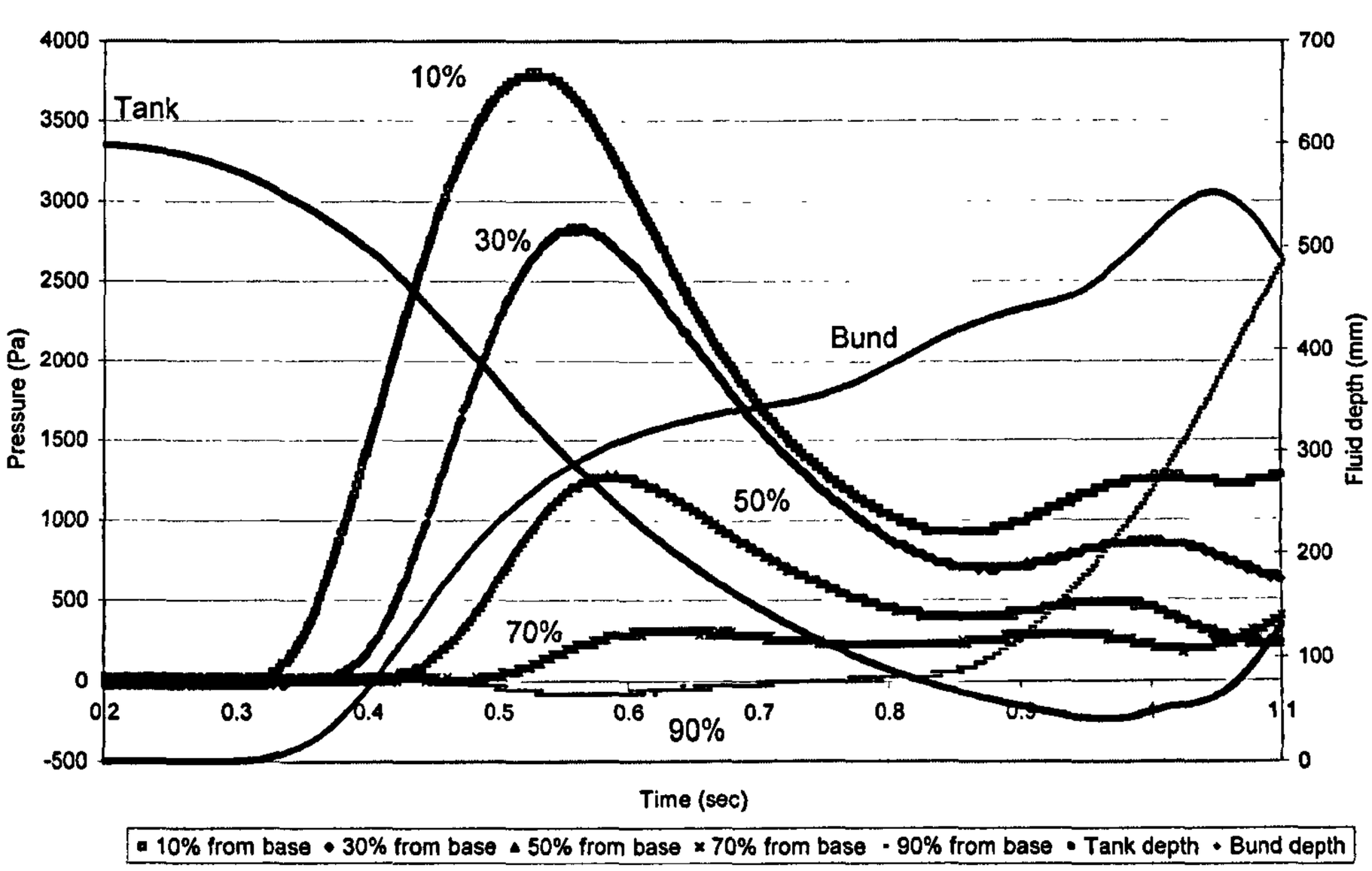

Chart 5.2 Plot of static and dynamic pressures for configuration identity B2 (h240)

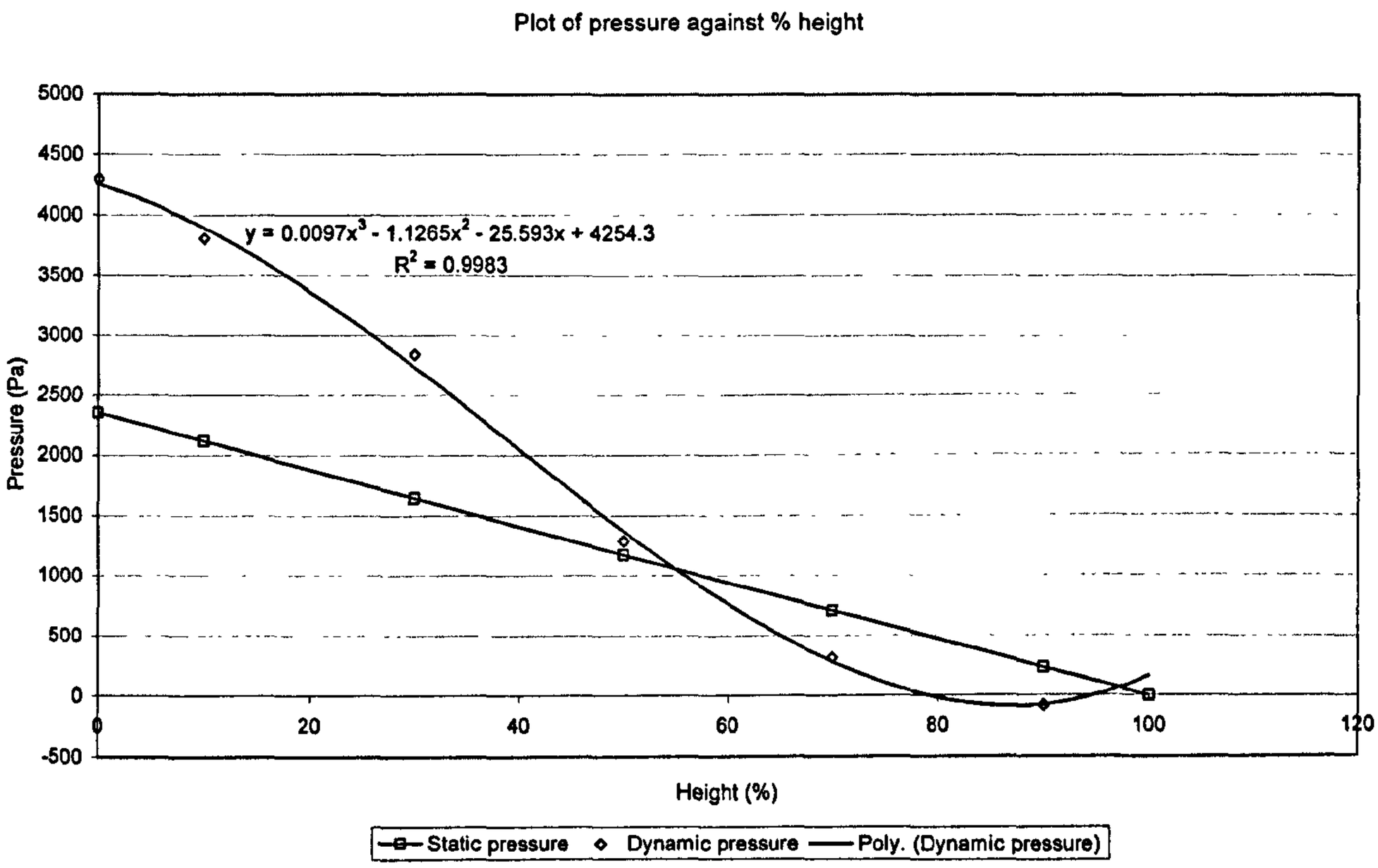

During the testing of the axisymmetric 'circular' configurations, the phenomenon of reflected wave overtopping was observed and subsequently investigated. Table 5.4 indicates the extent of the first wave and subsequent reflected wave overtopping.

Table 5.4 First wave overtopping for axisymmetric 'circular' releases

Date	***13/01/2004***	***Pipe & valve adjustment (kg)***		***0.40***	
Test configuration id B1(h120)					
Series id	***Temp (°C)***	***Mass retained (kg)***	***Mass overtopping (kg)***	***Overtopping (Ratio)***	***Percentage of total (%)***
1	14.6	15.91	5.29	0.25	92.6
2	14.7	16.31	4.89	0.24	85.6
3	14.7	15.85	5.41	0.26	94.4
4	14.5	15.81	5.42	0.26	94.7
5	14.4	15.64	5.61	0.27	98.0
6	14.2	15.75	5.42	0.26	95.0
7	13.8	15.84	5.36	0.26	93.8
8	13.9	15.84	5.35	0.26	93.7
9	13.7	15.73	5.62	0.27	97.7
10	13.7	15.88	5.33	0.26	93.2
Mean	14.22	15.86	5.37	0.26	93.9
sample S.D.	0.41312	0.17828	0.20155	0.00934	3.39985
Max overtopping				0.27	

Tables 5.5 and 5.6 indicate example results for the axisymmetric 'rectangular' configurations with full results for each of the nine test configurations shown in Appendix 3.

Table 5.5 Series results for configuration identity Wall 3 (rect)

Configuration identity	*series identity*	M_{bund} *(kg)*	M_{slosh} *(kg)*	*temp (°C)*	M_{bund} *correction (kg)*	V_{bund} *(m^3)*	V_{slosh} *(m^3)*	*Overtopping fraction*
Wall 3 (rect)	A	22.23	19.71	20.6	0.4	0.08732	0.07884	0.4745
	B	22.14	19.95	20.1		0.08696	0.07980	0.4785
	C	22.51	19.63	19.7		0.08844	0.07852	0.4703
	D	22.22	19.92	19.3		0.08728	0.07968	0.4772
	E	22.42	19.88	19.2		0.08808	0.07952	0.4745
Max		22.51	19.95	20.6		0.08844	0.07980	0.4785
Min		22.14	19.63	19.2		0.08696	0.07852	0.4703
Mean		22.30	19.82	19.8		0.08762	0.07927	0.4750
Sample sd		0.15437	0.14025	0.5805		0.00061748	0.00056100	0.0031706

Height from base (%)	*Series dynamic pressures (Pa)* *A*	*B*	*C*	*D*	*E*	*Max dynamic pressure (Pa)*
10	3953	3663	3837	3866	3517	3953
30	3523	3441	3741	3414	3496	
50	3274	3504	3274	3360	3274	
70	2793	2764	2994	2649	2677	
90	2377	1885	2049	1830	1666	

Table 5.6 Worst-case dynamic pressures for configuration identity Wall 3 (rect)

Configuration identity	*Test Series identity*	*Tank radius, R (mm)*	*Tank fluid depth, H (mm)*	*Multiple of length, y (mm)*	*Bund diagonal, d (mm)*	*Bund height, h (mm)*
Wall 3 (rect)	A	300	600	441	686	120

Estimated dynamic base pressure (Pa)	*Estimated Wave intercept height (mm)*	*Equivalent wave intercept pressure (Pa)*	*Max integral wave height (mm)*	*Equivalent integral wave pressure (Pa)*
4168	122	1197	128	1259

Height from base (%)	*Static pressure (Pa)*	*Dynamic pressure (Pa)*	*Local difference (Pa)*	*Local dynamic/static ratio*
0	1177	4168	2991	3.54
10	1059	3953	2894	3.73
30	824	3523	2699	4.28
50	589	3274	2685	5.56
70	353	2793	2439	7.91
90	118	2377	2259	20.19
100	0			

Release time (sec)	*Impact time (sec)*	*Time taken (sec)*	*Impact Velocity (m/s)*
0.742	1.094	0.352	2.19

Example Charts 5.3 and 5.4 indicate variation of dynamic pressures and fluid depths against time, and best-fit curves to the pressure data with variation in percentage bund height with for 'rectangular' bunding arrangements. Complete chart sets are given in Appendix 3.

Chart 5.3 Plot of dynamic pressures and wave heights for configuration identity Wall 3 (rect)

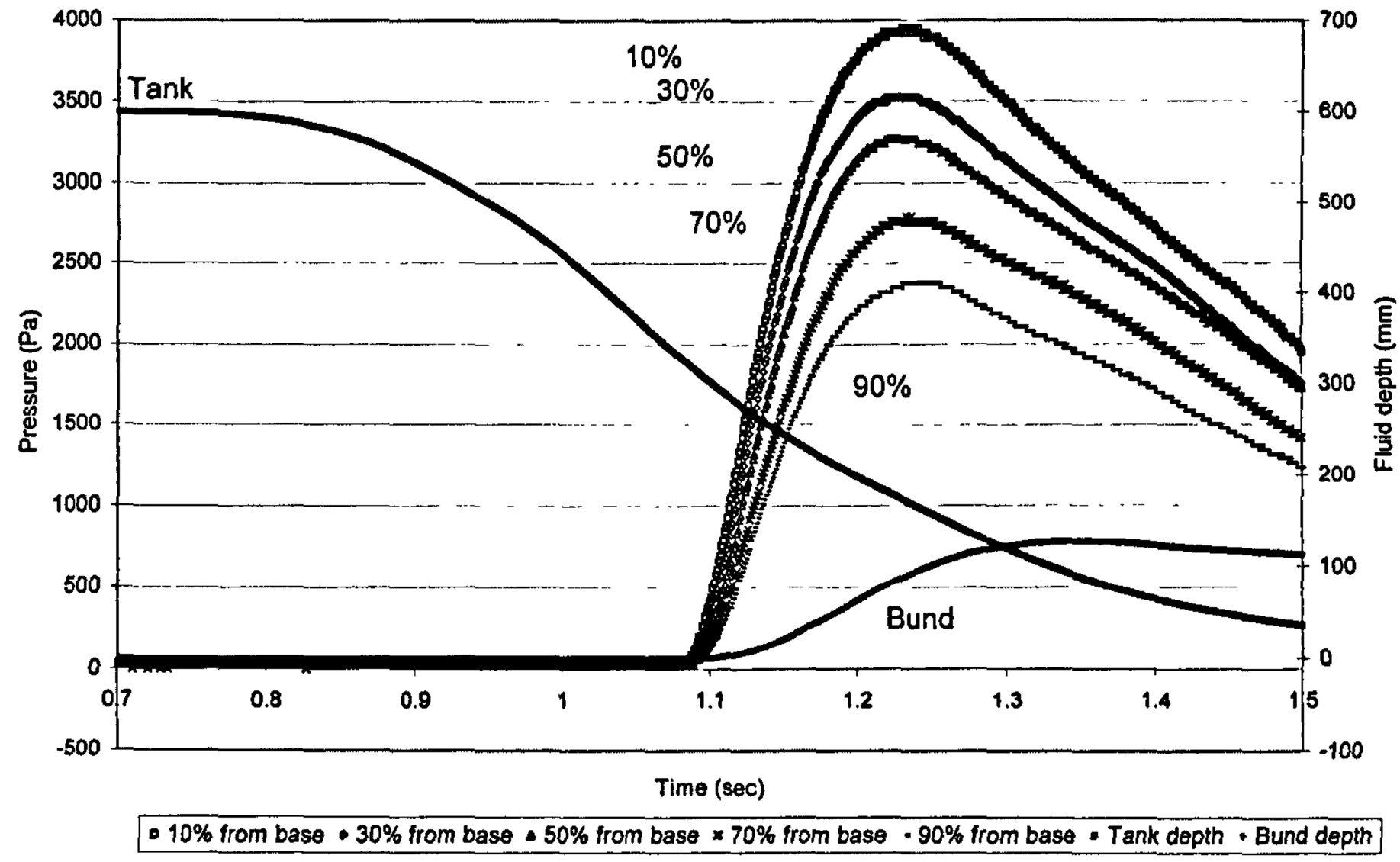

Chart 5.4 Plot of static and dynamic pressures for configuration identity Wall 3 (rect)

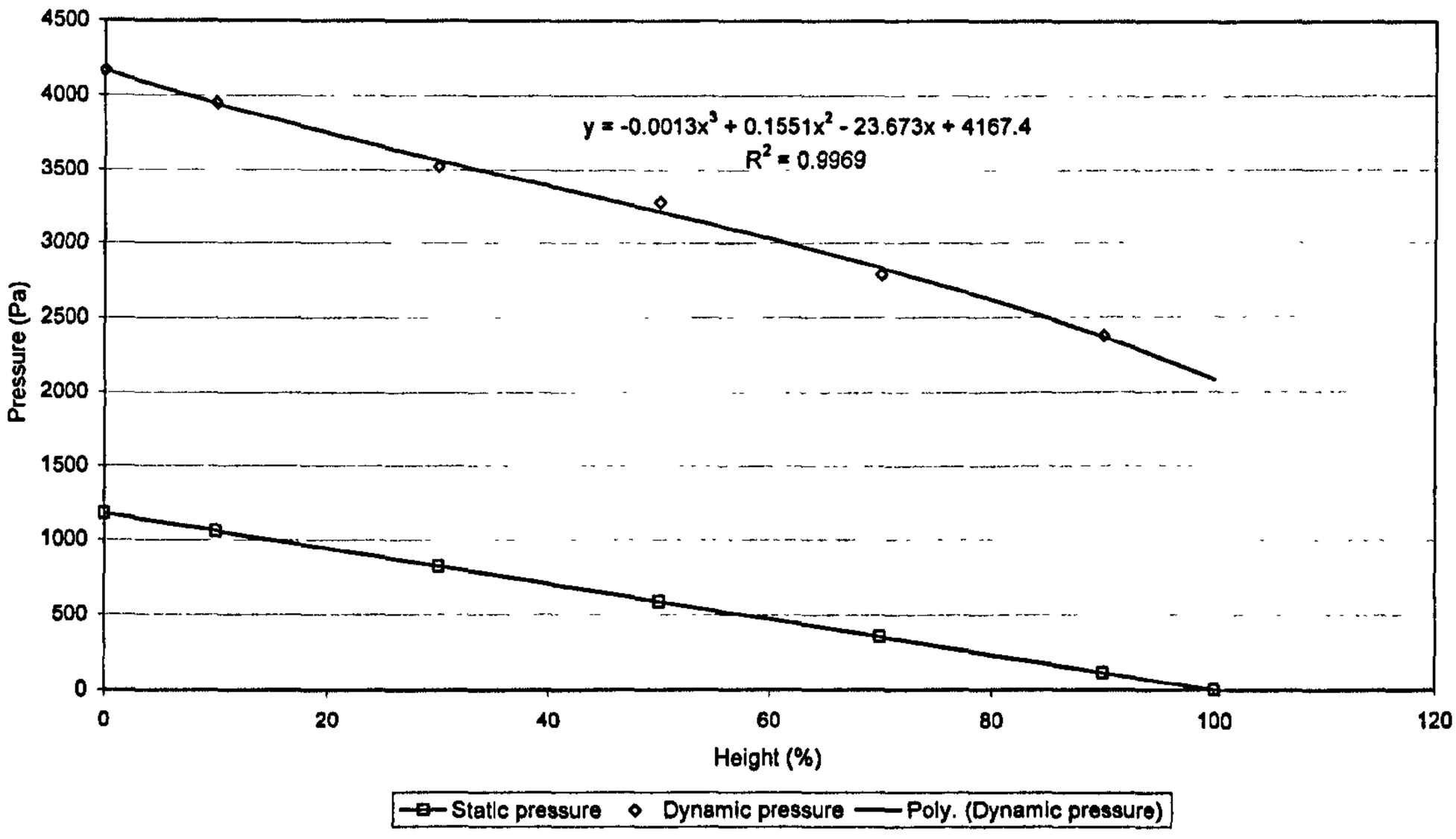

Table 5.7 Dynamic pressure sensor positions for asymmetric tests

Bund height (mm)	*Sensor positions (% from base)*	*Sensor position (mm from base)*
6	75	4.5
12	40	4.8
	50	6
	60	7.2
	70	8.4
	80	9.6
15	30	4.5
	50	7.5
	70	10.5
	80	12
	90	13.5
24	20	4.8
	30	7.2
	50	12
	70	16.8
	90	21.6
30	20	6
	30	9
	50	15
	70	21
	90	27
36	20	7.2
	30	10.8
	50	18
	70	25.2
	90	32.4
48	10	4.8
	30	14.4
	50	24
	70	33.6
	90	43.2
60	10	6
	30	18
	50	30
	70	42
	90	54
90	10	9
	30	27
	50	45
	70	63
	90	81
120	10	12
	30	36
	50	60
	70	84
	90	108
180	10	18
	30	54
	50	90
	70	126
	90	162
240	10	24
	30	72
	50	120
	70	168
	90	216

Tables 5.8 and 5.9 indicate example results for the asymmetric 'circular' configurations with full results for each of the nine test configurations shown in Appendix 5.

Table 5.8 Series results for configuration identity B1JS3 (h48)

Configuration identity	*series identity*	M_{bund} *(kg)*	M_{slosh} *(kg)*	*temp (°C)*	M_{bund} *correction (kg)*	V_{bund} *(m^3)*	V_{slosh} *(m^3)*	*Overtopping fraction*
B1JS3(h48)	A	7.11	1.08	21.6	0.0	0.02844	0.00432	0.1319
	B	7.11	1.10	21.8		0.02844	0.00440	0.1340
	C	7.18	1.07	21.9		0.02872	0.00428	0.1297
	D	7.09	1.07	22.0		0.02836	0.00428	0.1311
	E	7.13	1.07	22.0		0.02852	0.00428	0.1305
Max		7.18	1.10	22.0		0.02872	0.00440	0.1340
Min		7.09	1.07	21.6		0.02836	0.00428	0.1297
Mean		7.12	1.08	21.9		0.02850	0.00431	0.1314
Sample sd		0.03435	0.01304	0.1673		0.00013740	0.00005215	0.0016349

Height from base (%)	*Series dynamic pressures (Pa)* *A*	*B*	*C*	*D*	*E*	*Max dynamic pressure (Pa)*
10	748	730	657	641	668	748
30	677	591	594	613	707	
50	531	514	538	573	430	
70	367	363	384	417	439	
90	232	191	200	194	240	

Table 5.9 Worst-case dynamic pressures for configuration identity B1JS3 (h48)

Configuration identity	*Test Series identity*	*Tank radius, R (mm)*	*Tank fluid depth, H (mm)*	*Bund radius, r (mm)*	*Bund height, h (mm)*
B1JS3(h48)	A	300	120	497	48

Estimated dynamic base pressure (Pa)	*Orifice diameter (mm)*	*Slot width (mm)*	*Slot height (mm)*	*Area of jet (mm^2)*
784		157.08	36.00	5654.88

Height from base (%)	*Static pressure (Pa)*	*Dynamic pressure (Pa)*	*Local difference (Pa)*	*Local dynamic/static ratio*
0	471	784	313	1.67
10	424	748	325	1.77
30	330	677	348	2.05
50	235	531	296	2.26
70	141	367	226	2.60
90	47	232	185	4.93
100	0			

Release time (sec)	*Impact time (sec)*	*Time taken (sec)*	*Impact Velocity (m/s)*
0.818	0.979	0.161	2.45

Example Charts 5.5 and 5.6 indicate variation of dynamic pressures and fluid depths against time, and best-fit curves to the pressure data with variation in percentage bund height with for asymmetric 'circular' bunding arrangements. Complete chart sets are given in Appendix 5.

Chart 5.5 Plot of dynamic pressures and tank contents for configuration identity B1JS3 (h48)

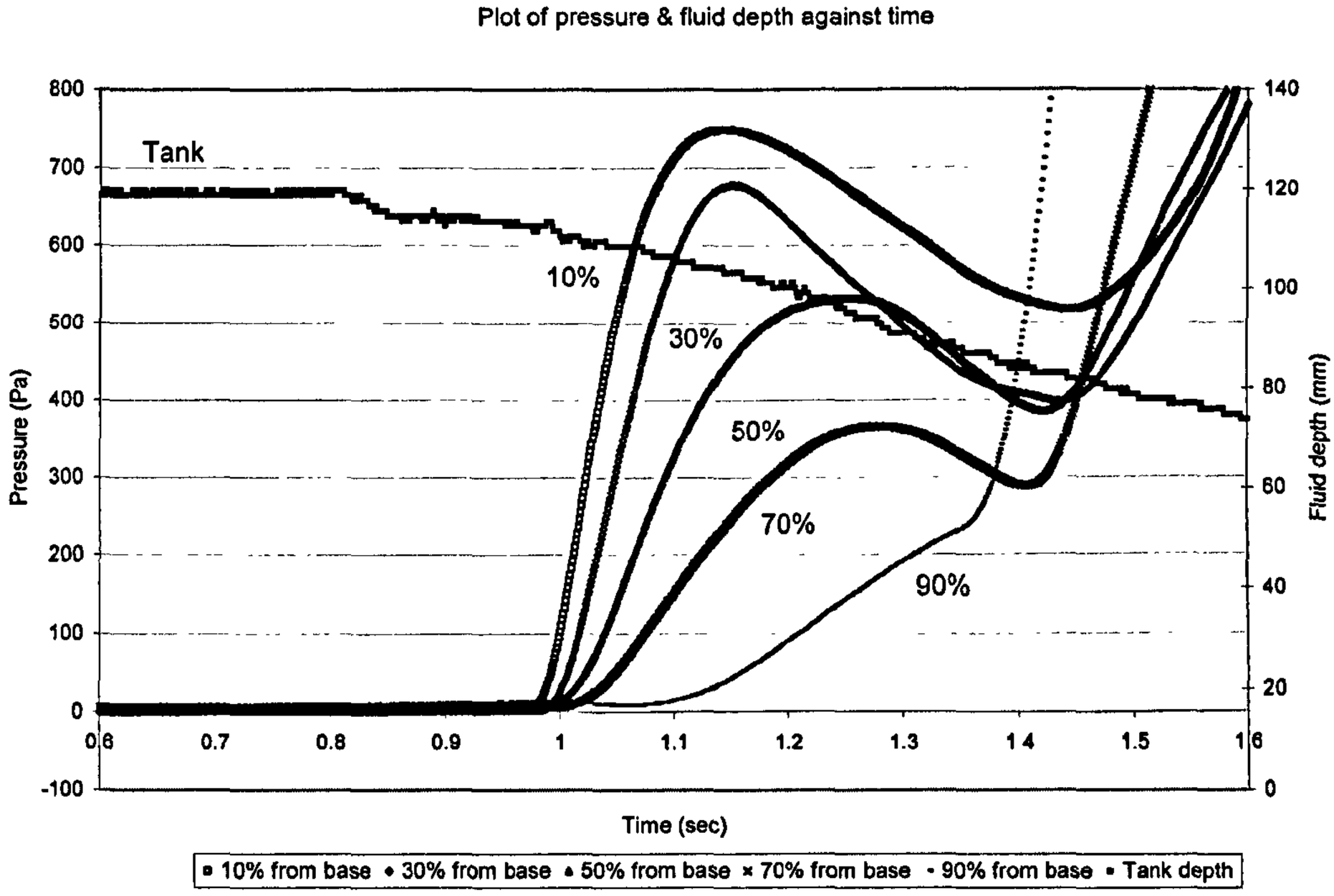

Chart 5.6 Plot of static and dynamic pressures for configuration identity B1JS3 (h48)

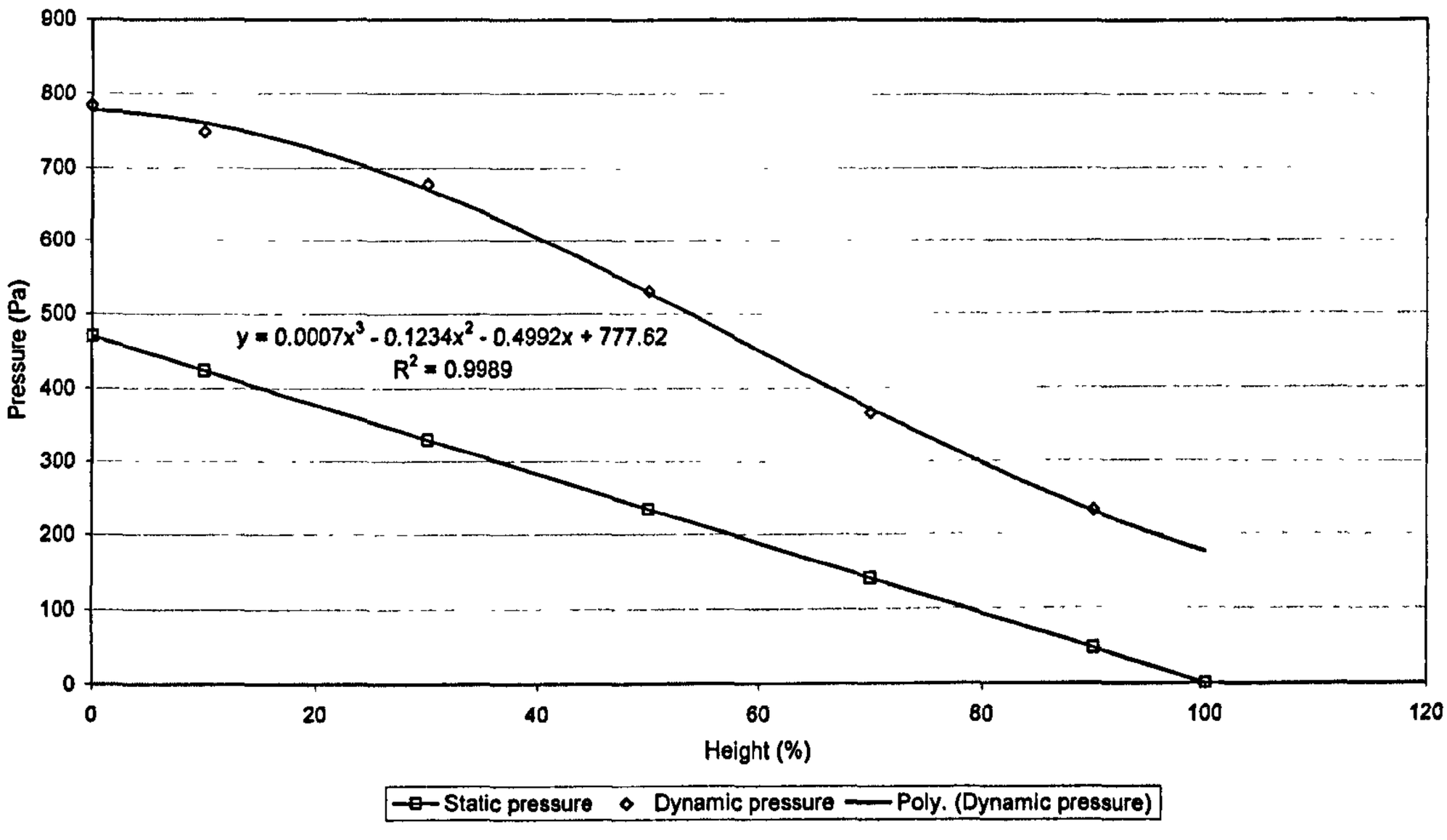

5.2 Axisymmetric overtopping

Along with the total overtopping for axisymmetric 'circular' configurations, a comparison between the total overtopping and the overtopping due to the first wave impact was also considered and an experimental procedure developed to investigate the relationship. By repeating the same tests, only this time suddenly opening the tank drain before any reflected wave could overtop the bund, a series of first wave overtopping results were obtained. The values were compared and it was found that a reduced overtopping fraction resulted, indicating that 94 to 95 % of the total overtopping takes place with the impact of the first wave (Table 5.4). A short summary of all axisymmetric results both 'circular and 'rectangular' can be found in Table 5.10.

Table 5.10 Short summary of axisymmetric results

	R = 300 mm						*R = 300 mm*						*R = 300 mm*				
	H ***(mm)***	***r*** ***(mm)***	***h*** ***(mm)***	***Q*** ***(%)***	***Dyn/Stat*** ***base***		***H*** ***(mm)***	***r*** ***(mm)***	***h*** ***(mm)***	***Q*** ***(%)***	***Dyn/Stat*** ***base***		***H*** ***(mm)***	***r*** ***(mm)***	***h*** ***(mm)***	***Q*** ***(%)***	***Dyn/Stat*** ***base***
Squat tank	120	1407	6	48	Na	***Middle tank***	300	1407	15	62	6.50	***Tall tank***	600	1407	30	70	7.33
110% bund	120	995	12	49	16.45	***110% bund***	300	995	30	62	9.78	***110% bund***	600	995	60	70	9.19
	120	704	24	41	4.80		300	704	60	52	2.53		600	704	120	49	2.42
	120	574	36	32	1.32		300	574	90	38	1.97		600	574	180	34	1.79
	120	497	48	24	1.55		300	497	120	28	1.92		600	497	240	25	1.89
Squat tank	120	1470	6	44	Na	***Middle tank***	300	1470	15	59	7.31	***Tall tank***	600	1470	30	68	9.47
120% bund	120	1039	12	43	6.64	***120% bund***	300	1039	30	59	5.76	***120% bund***	600	1039	60	68	3.68
	120	735	24	38	2.97		300	735	60	50	2.83		600	735	120	47	2.44
	120	600	36	30	1.51		300	600	90	36	1.66		600	600	180	32	1.65
	120	520	48	22	2.01		300	520	120	26	1.65		600	520	240	21	1.82
Squat tank	120	1643	6	32	Na	***Middle tank***	300	1643	15	51	4.46	***Tall tank***	600	1643	30	63	7.48
150% bund	120	1162	12	36	6.64	***150% bund***	300	1162	30	50	5.63	***150% bund***	600	1162	60	64	5.50
	120	822	24	28	4.12		300	822	60	45	2.80		600	822	120	43	2.22
	120	671	36	24	2.05		300	671	90	31	1.62		600	671	180	29	1.46
	120	581	48	16	1.51		300	581	120	22	1.23		600	581	240	20	1.47
Squat tank	120	1897	6	14	Na	***Middle tank***	300	1897	15	39	6.75	***Tall tank***	600	1897	30	55	8.33
200% bund	120	1342	12	22	2.92	***200% bund***	300	1342	30	40	3.95	***200% bund***	600	1342	60	57	3.63
	120	949	24	18	5.08		300	949	60	36	2.58		600	949	120	39	2.20
	120	775	36	15	2.09		300	775	90	24	1.35		600	775	180	24	1.23
	120	671	48	14	1.44		300	671	120	19	1.10		600	671	240	18	1.24
Squat tank	120	315	120	1	1.00	***Middle tank***	300	315	300	1	0.94	***Tall tank***	600	315	600	1	0.92
hi-collar bund	120	315	144	0	0.82	***hi-collar bund***	300	315	360	1	0.75	***hi-collar bund***	600	315	720	1	0.75
	120	330	120	2	0.99		300	330	300	3	0.92		600	330	600	1	0.91
	120	330	144	0	0.76		300	330	360	1	0.72		600	330	720	2	0.81
	120	360	120	3	0.84		300	360	300	5	0.92		600	360	600	2	0.96
	120	360	144	2	0.71		300	360	360	4	0.81		600	360	720	3	0.81
	120	390	120	2	0.78		300	390	300	4	0.87		600	390	600	5	0.94
	120	390	144	1	0.55		300	390	360	3	0.77		600	390	720	3	0.81
Squat tank	120	Tri	12	55	3.42	***Middle tank***	300	Tri	60	50	2.94	***Tall tank***	600	Tri	120	50	2.74
110% bund	120	Squ	12	52	6.90	***110% bund***	300	Squ	60	50	3.20	***110% bund***	600	Squ	120	49	3.01
(non-circular)	120	Rect	12	54	5.51	***(non-circular)***	300	Rect	60	47	3.39	***(non-circular)***	600	Rect	120	48	3.54

5.3 Asymmetric overtopping

Due to the physical nature of the impinging jet of fluid in the case of an asymmetric directional release or 'spigot/jetting' failure, the resulting overtopping can be very different than that for an axisymmetric release. For experimental purposes the apertures used for the partial failures were split into two types, namely 'orifice' and 'slot' as detailed in Table 3.2. These apertures were further sub divided into different surface areas of release of 0.125, 0.250 and 0.500 % of tank surface area for orifice releases and 0.500, 1.500 and 2.500 % for slot releases. The bund capacity investigated was limited to 110 %, due the increased number of variations of aperture under evaluation. In terms of fluid height, the same ratios of R/H (0.5. 1.0 and 2.5) or 'squat', 'middle' and 'tall' were used to determine the effects of the partial releases. A short summary of all asymmetric results can be found in Table 5.11.

Table 5.11 Short summary of asymmetric results

	R = 300 mm						R = 300 mm						R = 300 mm				
	H (mm)	*r (mm)*	*h (mm)*	*Q (%)*	*Dyn/Stat base*		*H (mm)*	*r (mm)*	*h (mm)*	*Q (%)*	*Dyn/Stat base*		*H (mm)*	*r (mm)*	*h (mm)*	*Q (%)*	*Dyn/Stat base*
Squat tank	120	1407	6	0	Na	*Middle tank*	300	1407	15	6	0.46	*Tall tank*	600	1407	30	26	7.99
110% bund	120	995	12	0	Na	*110% bund*	300	995	30	13	1.02	*110% bund*	600	995	60	17	5.01
Orifice	120	704	24	0	1.35	*Orifice*	300	704	60	2	3.29	*Orifice*	600	704	120	12	5.09
Dia 18.97mm	120	574	36	0	1.39	*Dia 30.00mm*	300	574	90	8	2.52	*Dia 42.43mm*	600	574	180	10	4.22
	120	497	48	1	0.76		300	497	120	8	2.44		600	497	240	4	2.53
Squat tank	120	1407	6	0	Na	*Middle tank*	300	1407	14	6	0.52	*Tall tank*	600	1407	30	24	10.27
110% bund	120	995	12	0	Na	*110% bund*	300	995	30	14	5.42	*110% bund*	600	995	60	22	3.56
Orifice	120	704	24	0	0.21	*Orifice*	300	704	60	9	2.74	*Orifice*	600	704	120	21	4.56
Dia 26.83mm	120	574	36	0	2.08	*Dia 42.43mm*	300	574	90	13	2.41	*Dia 60.00mm*	600	574	180	12	4.29
	120	497	48	0	1.10		300	497	120	10	2.74		600	497	240	4	2.83
Squat tank	120	1407	6	0	Na	*Middle tank*	300	1407	15	14	4.93	*Tall tank*	600	1407	30	30	7.08
110% bund	120	995	12	0	Na	*110% bund*	300	995	30	15	3.92	*110% bund*	600	995	60	26	2.90
Orifice	120	704	24	1	1.21	*Orifice*	300	704	60	14	2.18	*Orifice*	600	704	120	25	2.60
Dia 37.95mm	120	574	36	1	4.38	*Dia 60.00mm*	300	574	90	18	1.42	*Dia 84,85mm*	600	574	180	16	3.13
	120	497	48	2	1.43		300	497	120	12	2.14		600	497	240	8	2.55
Squat tank	120	1407	6	11	Na	*Middle tank*	300	1407	15	33	3.28	*Tall tank*	600	1407	30	41	4.38
110% bund	120	995	12	1	Na	*110% bund*	300	995	30	26	3.44	*110% bund*	600	995	60	28	3.48
Slot	120	704	24	3	3.58	*Slot*	300	704	60	12	3.24	*Slot*	600	704	120	18	1.63
Width 157.08mm	120	574	36	1	3.47	*Width 157.08mm*	300	574	90	5	1.26	*Width 157.08mm*	600	574	180	14	1.66
Height 7.20mm	120	497	48	1	0.79	*Height 18.00mm*	300	497	120	5	1.40	*Height 36.00mm*	600	497	240	11	1.75
Squat tank	120	1407	6	31	Na	*Middle tank*	300	1407	15	44	7.42	*Tall tank*	600	1407	30	48	8.47
110% bund	120	995	12	22	0.57	*110% bund*	300	995	30	37	3.40	*110% bund*	600	995	60	42	5.43
Slot	120	704	24	17	1.34	*Slot*	300	704	60	30	4.24	*Slot*	600	704	120	32	2.92
Width 157.08mm	120	574	36	15	3.17	*Width 157.08mm*	300	574	90	22	2.11	*Width 157.08mm*	600	574	180	26	2.19
Height 21.60mm	120	497	48	8	1.80	*Height 54.00mm*	300	497	120	19	1.87	*Height 108.00mm*	600	497	240	18	2.17
Squat tank	120	1407	6	31	Na	*Middle tank*	300	1407	15	42	8.59	*Tall tank*	600	1407	30	50	7.33
110% bund	120	995	12	26	2.53	*110% bund*	300	995	30	40	3.49	*110% bund*	600	995	60	49	5.70
Slot	120	704	24	24	2.77	*Slot*	300	704	60	38	3.31	*Slot*	600	704	120	37	3.55
Width 157.08mm	120	574	36	21	3.17	*Width 157.08mm*	300	574	90	28	2.20	*Width 157.08mm*	600	574	180	26	2.56
Height 36.00mm	120	497	48	13	1.67	*Height 90.00mm*	300	497	120	22	1.90	*Height 180.00mm*	600	497	240	16	1.93

5.4 Axisymmetric dynamic pressures

An estimate of the maximum dynamic pressure at the base of the bund was obtained by extrapolating the pressure profiles, and comparisons were then made with the pressures that would apply if the bund were just full of static water. For the non high-collar bunds, it was found that the actual pressure experienced in the event of a catastrophic failure was higher than that normally employed for design purposes. For high-collar bunds the dynamic pressures were lower than the static pressure.

Further comparisons between the fluid levels and the maximum dynamic pressures led to the investigation of the crossover points (that is, the moment in time when the fluid level in the tank and that at the bund are equal) and the instantaneous pressure heads corresponding to the positions of local maxima. The wave-monitoring probe was repositioned to be as close as possible to the dynamic pressure transducers in order to obtain more accurate correlations.

As work progressed it was consistently apparent that the maximum wave height did not correspond to the timings or magnitudes of the maximum dynamic pressures. Video footage allowed an upward and forward momentum to be identified along with the formation of a separation layer, which having a higher energy level, starts to rapidly rise upwards and forwards to leave the main body of fluid (Plate 5.1).

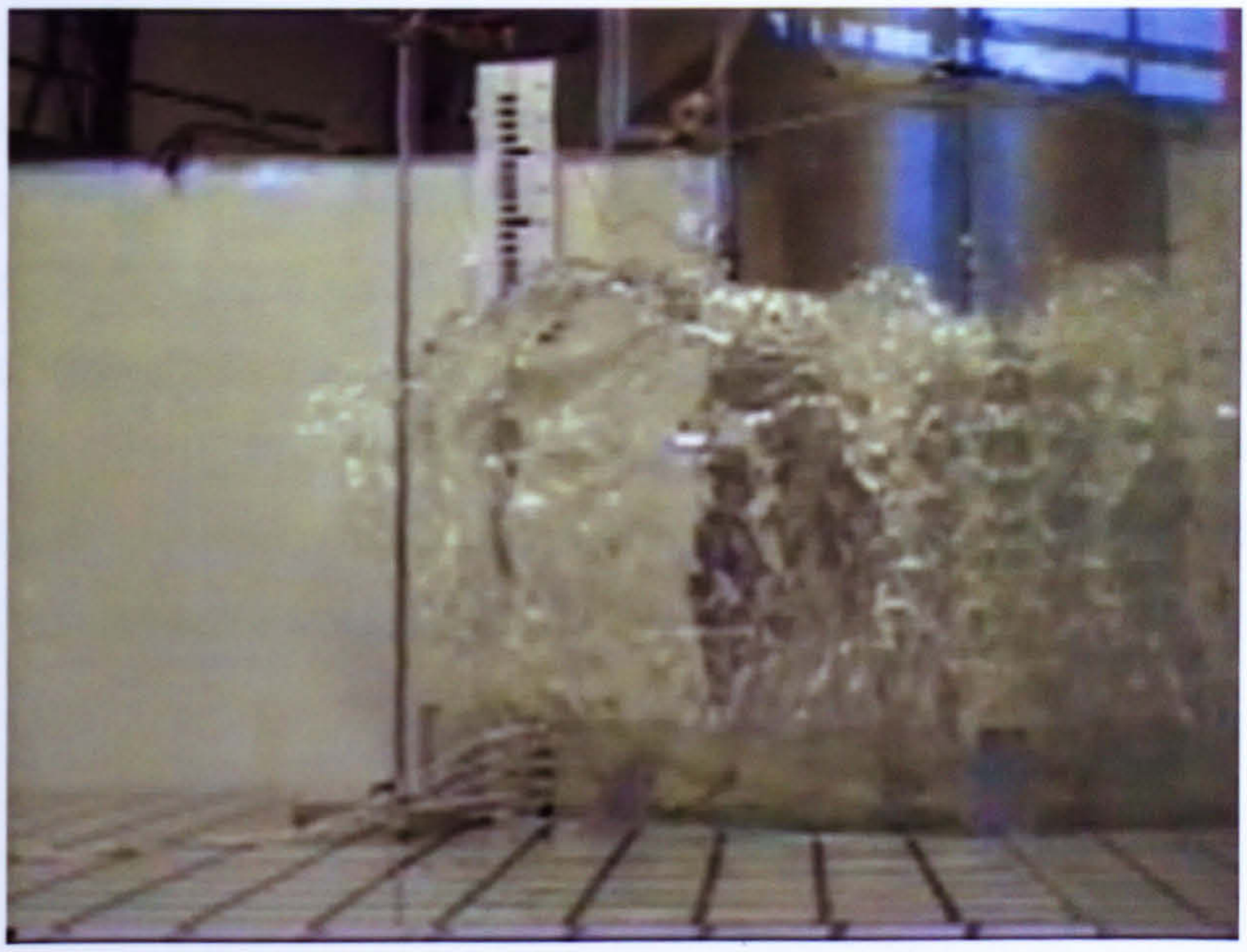

*Plate 5.1 Wave breaking over model bund showing separation layer**

** Plate source: LJMU*

High-speed camera footage was used to further confirm the behaviour of the fluid at the point of contact with the bund. The same characteristics were observed with the separation layer further forming droplets, which separate and fly through the air. It is therefore concluded that the full wave height, including the separation layer does not fully contribute to the maximum dynamic pressure at the base of the bund wall due to the vertical component of the upward moving fluid as it separates from the main fluid body.

The ratios of maximum dynamic pressures to hydrostatic pressure obtained in this work are mostly in keeping with the results reported by Trbojevic and Slater (1989), where a ratio of 2.5 is quoted for a typical liquefied fuel gas and a ratio of 3.5 for Diesel fuel. Atherton (2005) has, however, shown much higher values in some cases, generally for the lower bunds. The values for lower bunds may have been exaggerated by the need to extrapolate data from sensors whose placement was not ideal, and it has to be noted that the dynamic pressures obtained in nominally identical tests showed a substantial variability (h = 12 mm - $Dyn/Stat_{base}$ = 16.45 for a squat tank 110% bund and $Dyn/Stat_{base}$ = 6.64 for a squat tank 120% bund). Other workers have stated higher values than did Trbojevic and Slater (1989), for example Cuperus (1980) quoted a ratio of six, but the basis of the Cuperus data is unknown. The ratios obtained in this research are shown in the "Short summary of axisymmetric results" Table 5.10 in the columns headed "$Dyn/Stat_{base}$".

Impact velocities, as shown in example Table 5.3 (fully in Appendix 2) for circular bunds and in example Table 5.6 (fully in Appendix 3) for rectangular bunds are calculated from Newton's Laws of Motion considering the fluid to be accelerated uniformly from rest over a known distance in known time. There are inherent inaccuracies in the calculation of velocities, as the horizontal acceleration is not uniform as the standing head of fluid falls and spreads over the bunded area and friction acts to slow the motion, especially over the larger distances travelled. The transit times are also shown and these are more reliable as they are inferred directly from the recorded data. A range of video stills (Plate set 5.2) are shown with the fluid (water dyed blue) tracked across the flow table from initial release to impact with the bund and eventual overtopping.

1. Firing mechanism released

2. Free standing water

3. Initial impact with bund

4. Fluid clears bund

5. Fluid gains height

6. Separation layer forms

7. Separate components visible

8. Fluid moves up & forward

9. Height in excess of fill level

10. Fluid starts to fall

11. Separation layer clears bund

12. First wave overtopping

13. Overtopping continues

14. Reflected wave forming

15. Reflected wave gains height

16. Reflected wave returns

*Plate set 5.2 Video frames showing wave tracking and bund impact for axisymmetric releases**

* *Plate source: LJMU*

5.5 Asymmetric dynamic pressures

It has been suspected for some time that a concentrated jet of fluid acting on the bund would cause high levels of dynamic loading in excess of those generated by a catastrophic failure (Plate 5.3). The results in the short summary Table 5.11 indicate that this in not universally true and the dynamic pressure at the base of the bund depends on a number of factors including the size and shape of the aperture, the tank to bund separation distance and the height of the bund. The effect of the separation distance, L may appear obvious, as with an increasing value of L, the jet tends to impact the floor of the bund and spreads out prior to impact with the bund wall. An example impact velocity is indicated in Table 5.9 and more detailed information can be found for individual configurations in Appendix 5.

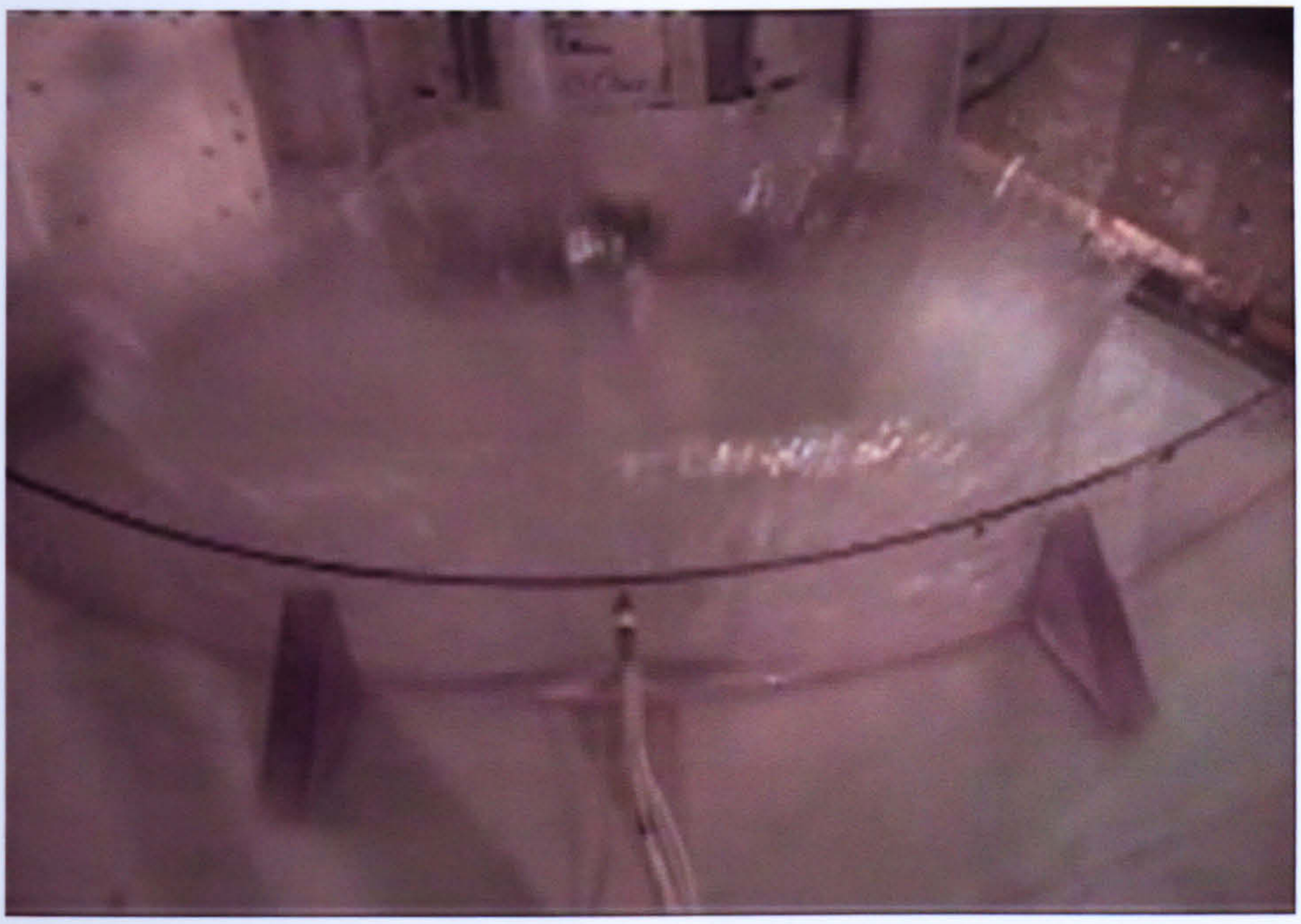

*Plate 5.3 Asymmetric orifice release with jet impacting model bund wall**

A range of video stills (Plate set 5.4) are shown with the fluid tracked from initial release to sustained impact with the bund and continual overtopping.

* *Plate source: LJMU*

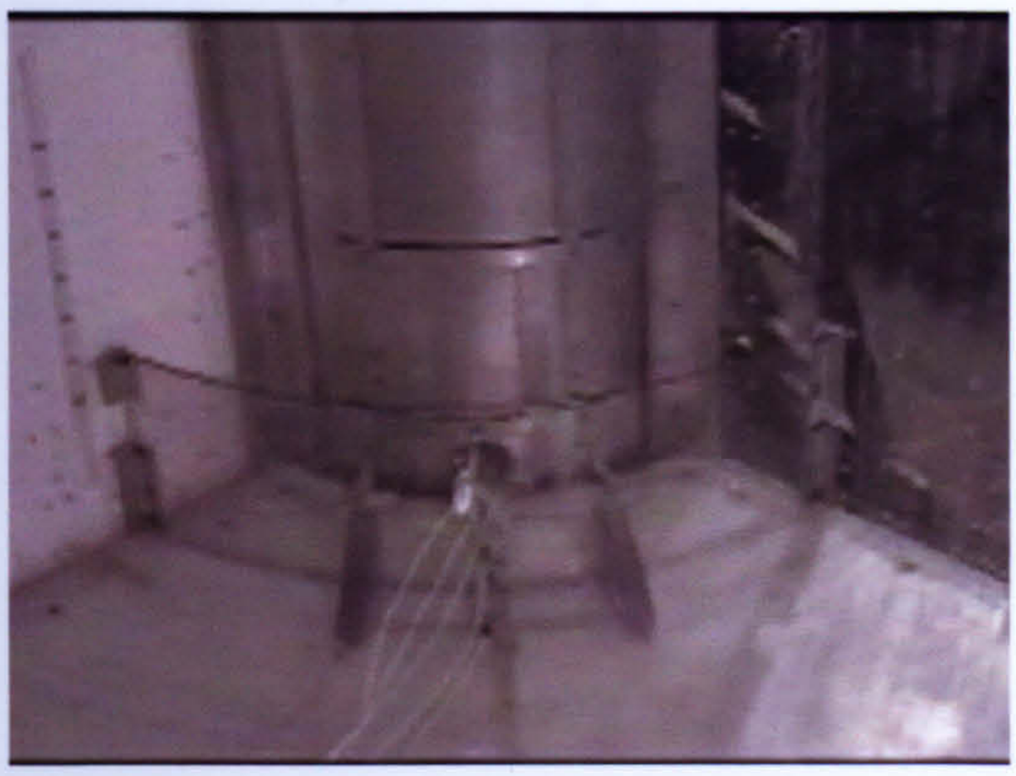

1. Initial release

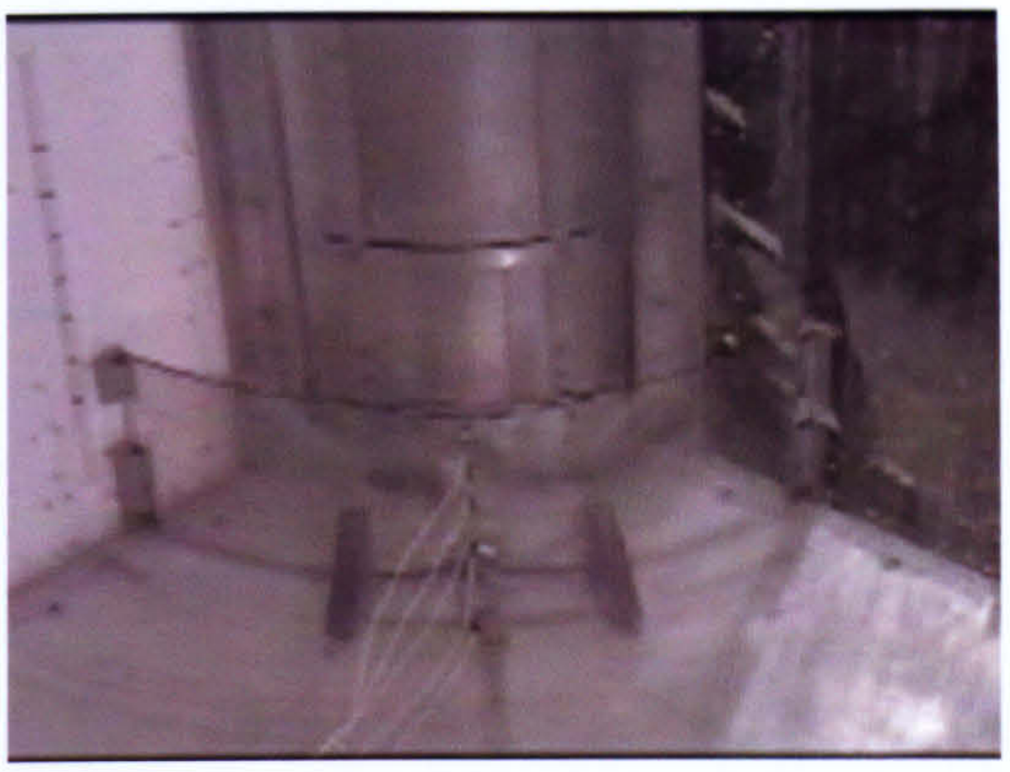

2. Impact with bund

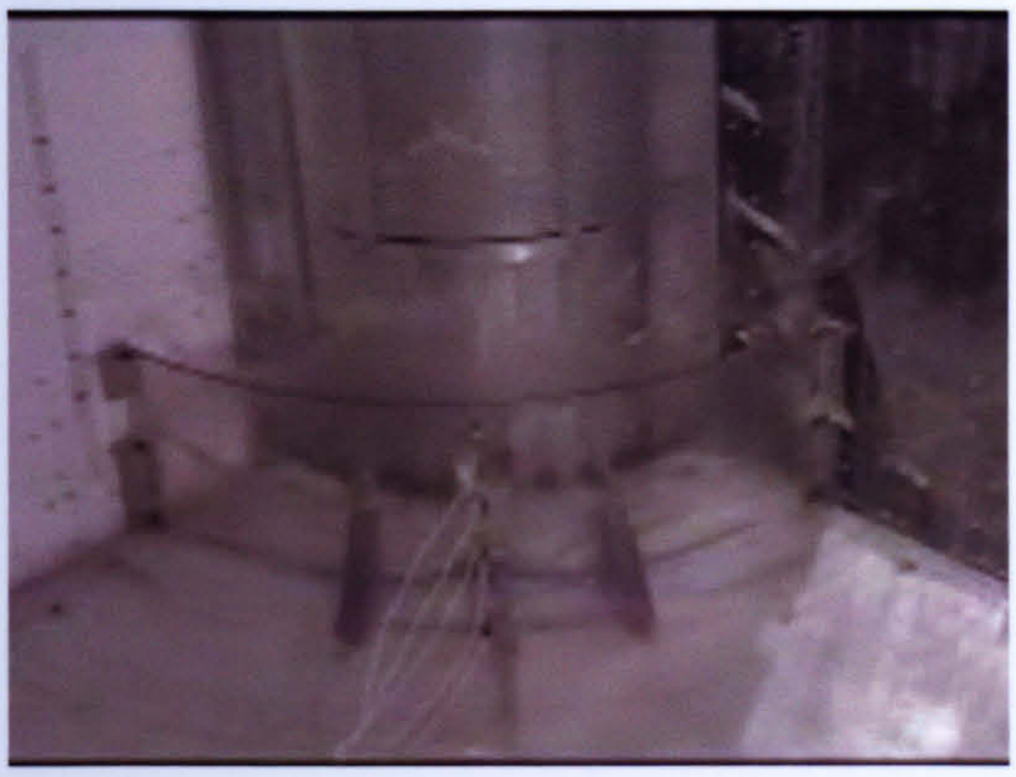

3. Spreading starts

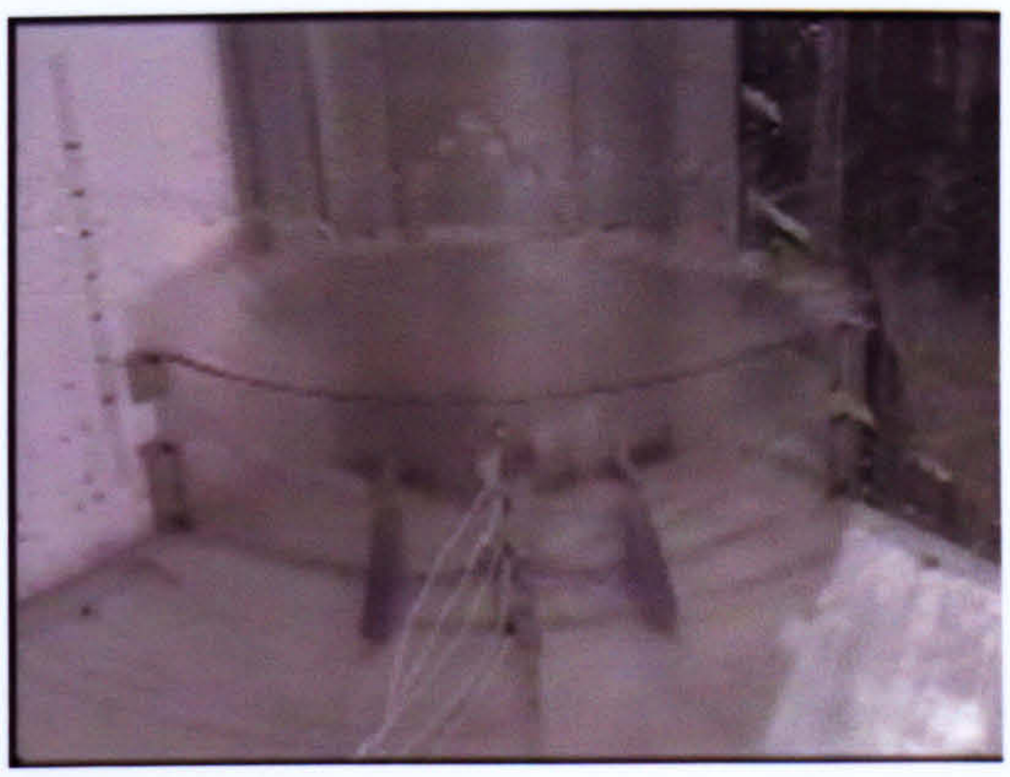

4. Spreading continues

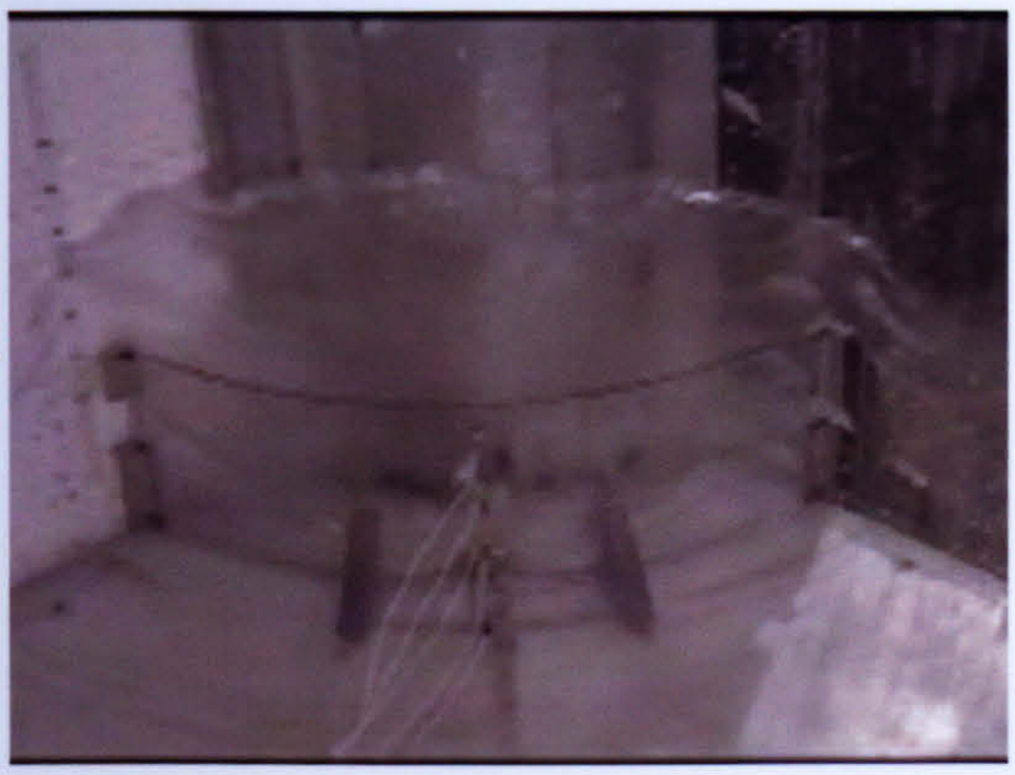

5. Upward & forward motion

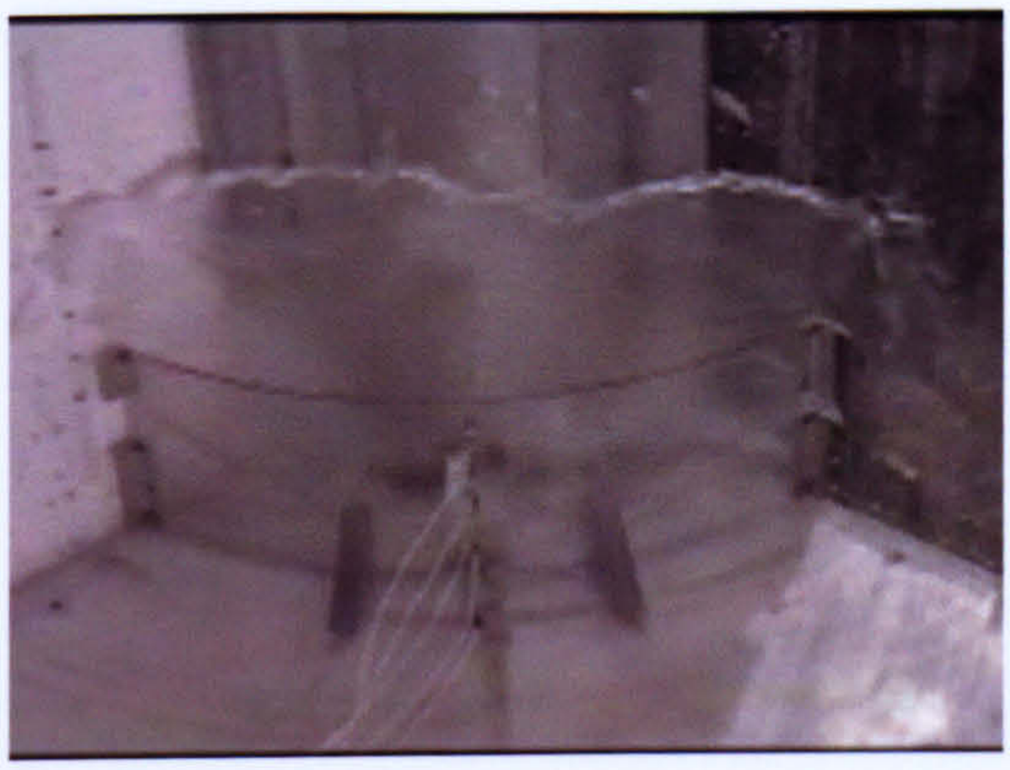

6. Droplets start to fall

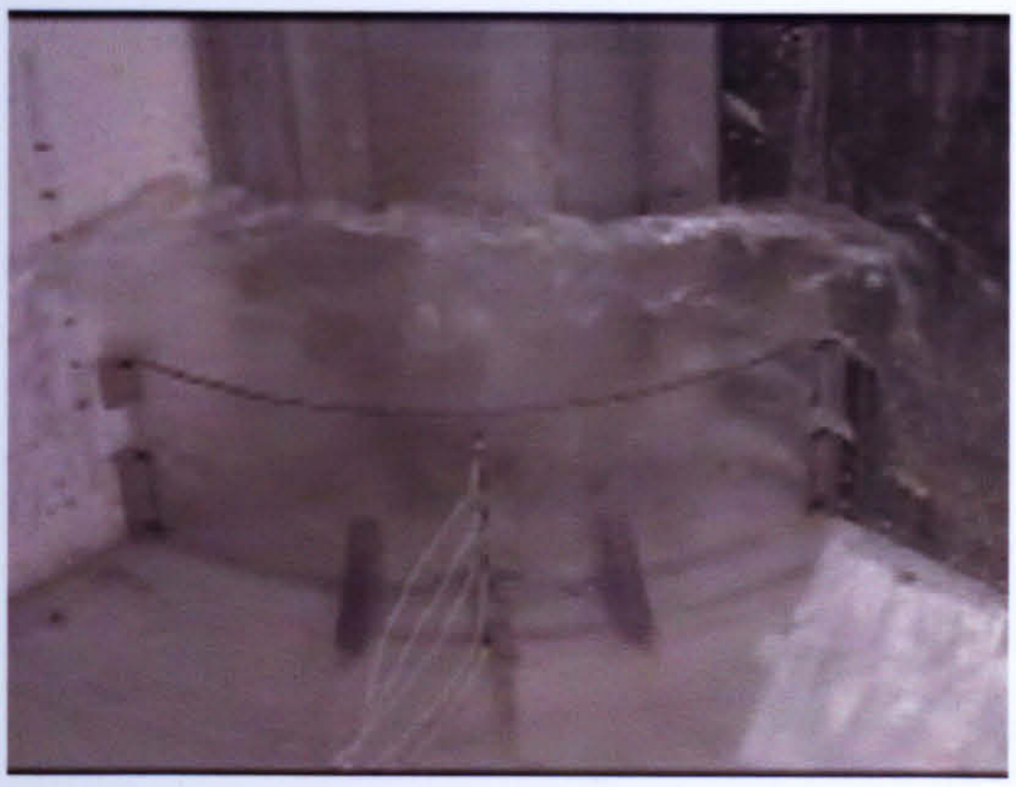

7. Overtopping starts

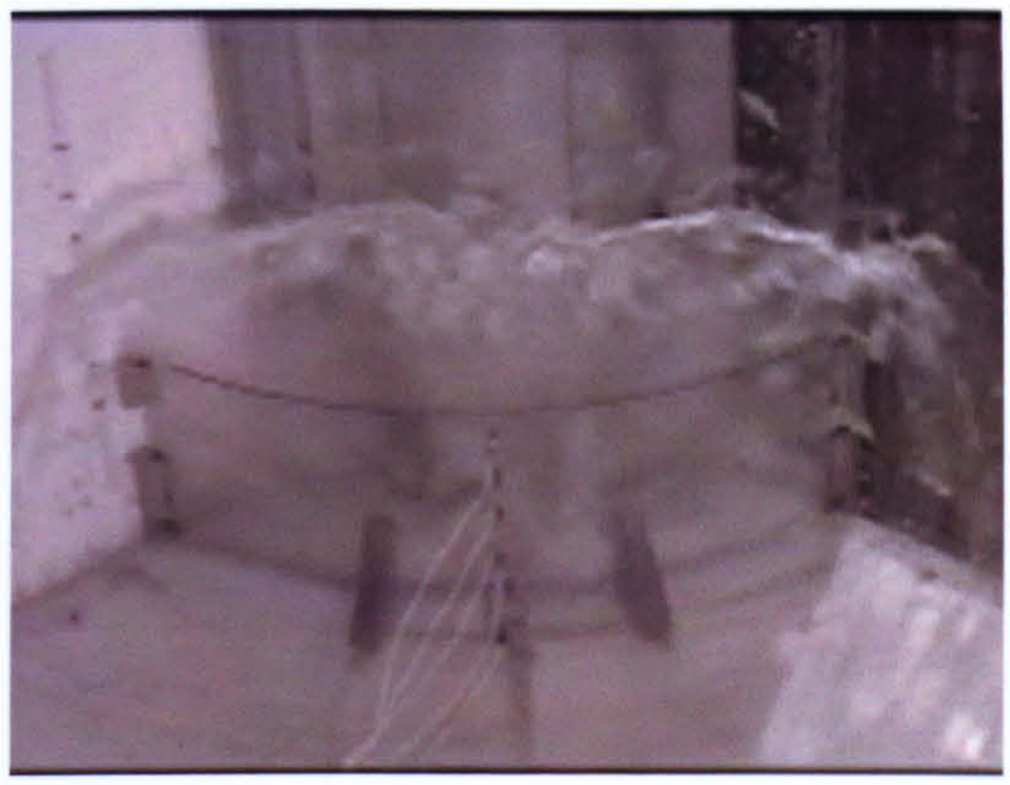

8. Overtopping continues

9. Overtopping builds

10. Impact with spill table

11. Wave height starts to fall

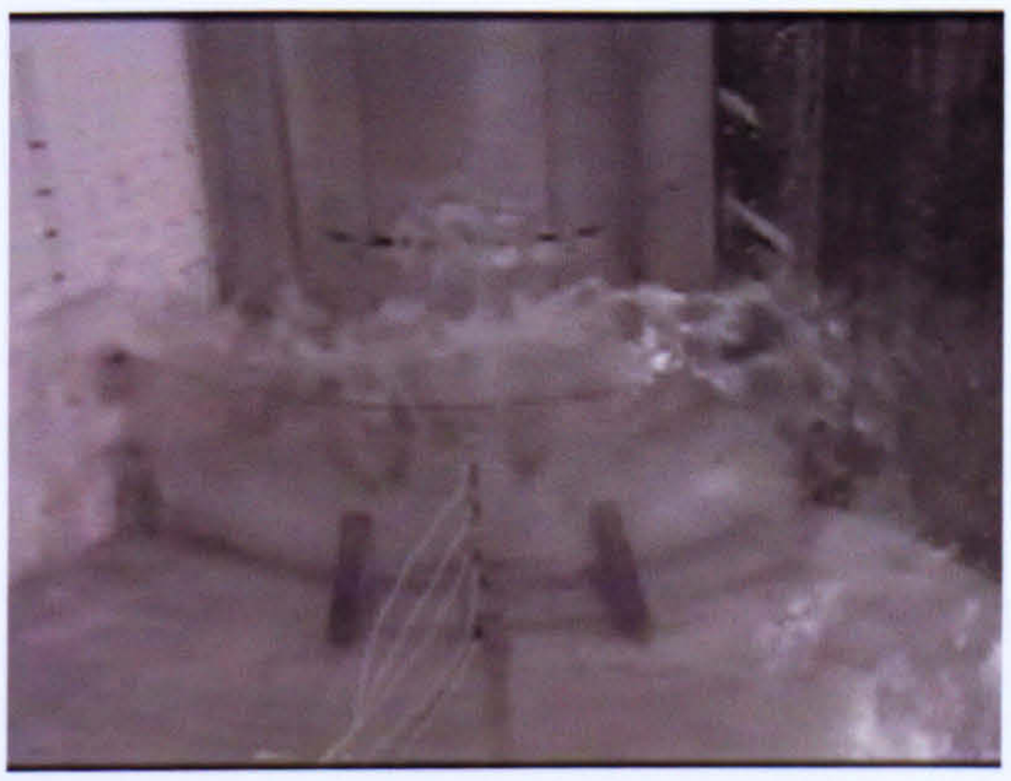

12. Wave height reduces further

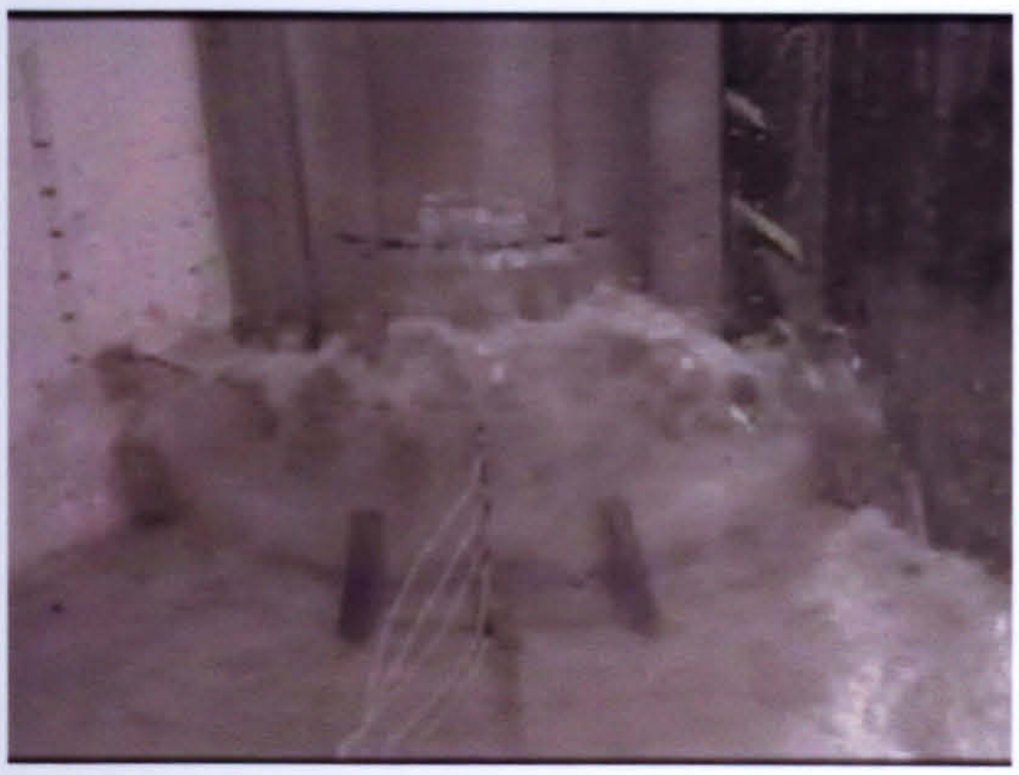

13. Overtopping stabilises

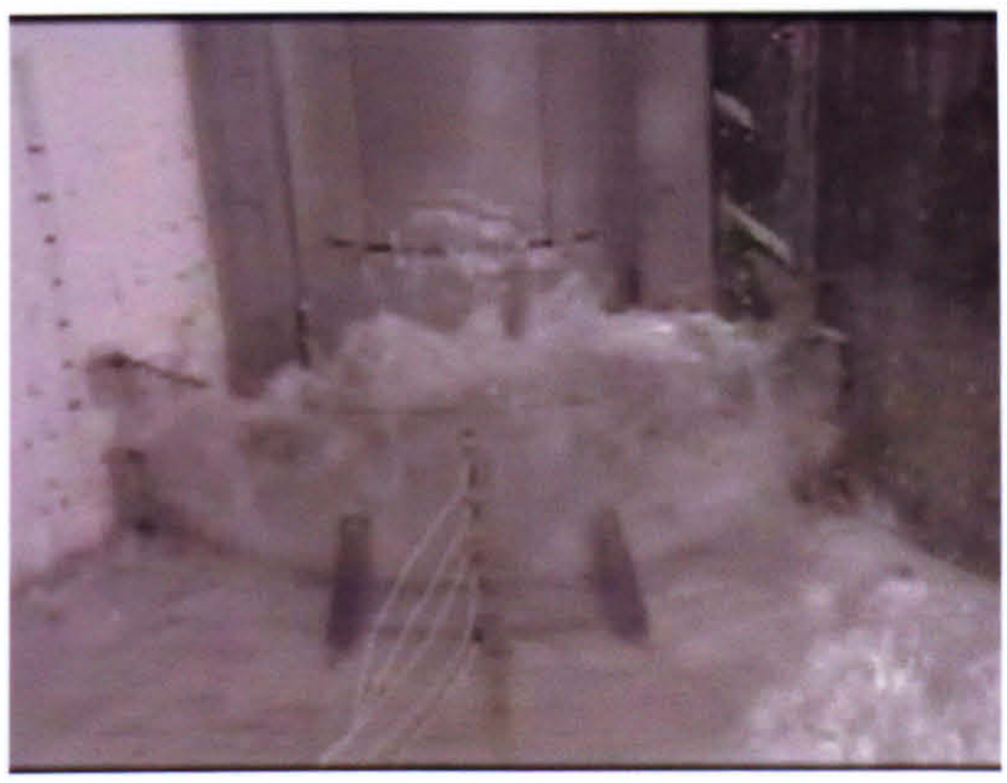

14. Overtopping continues

15. Overtopping continues

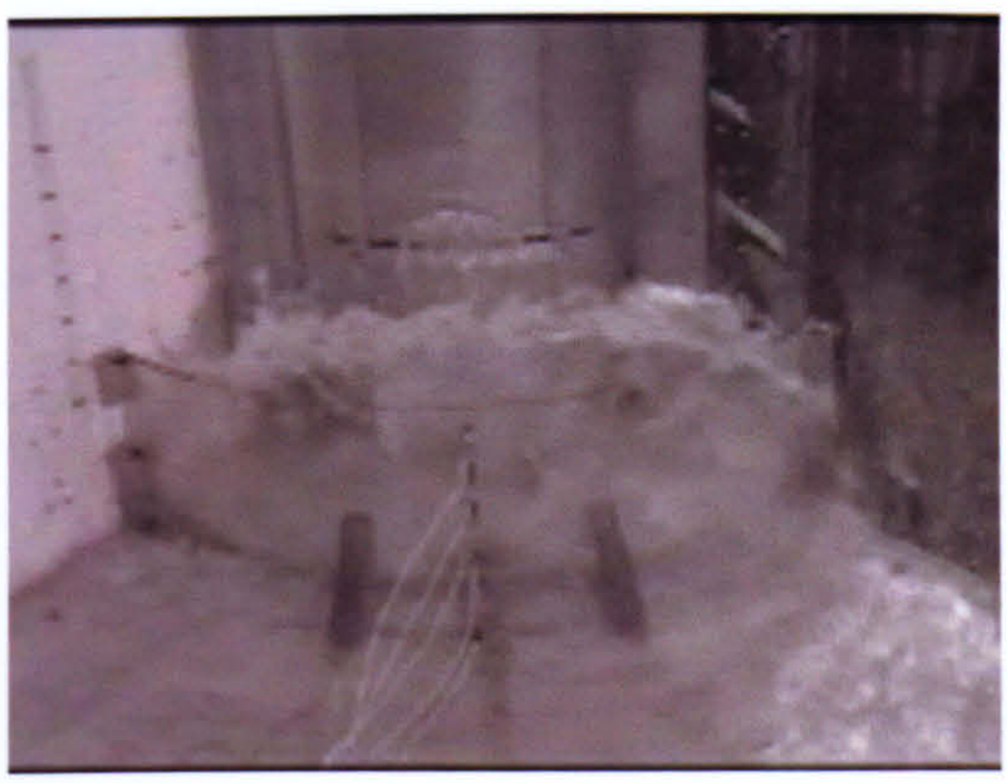

16. Overtopping continues

17. Overtopping continues

18. Overtopping continues

19. Overtopping continues

20. Overtopping continues

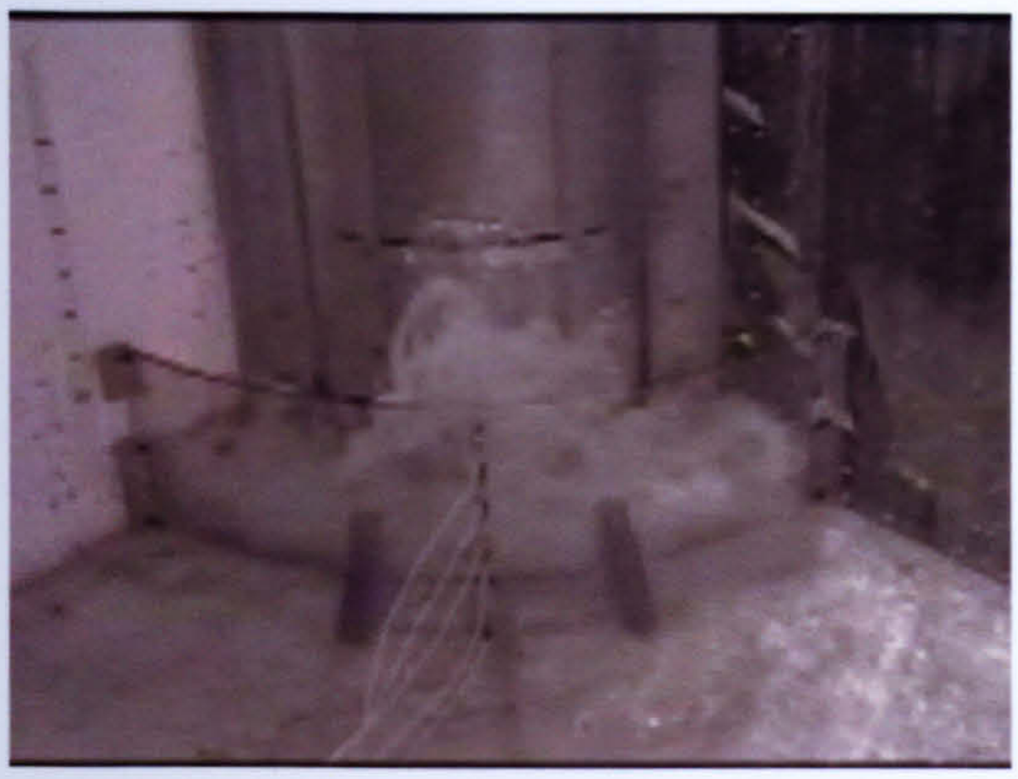

21. Overtopping starts to diminish

22. Overtopping subsides

23. Overtopping ends

24. Bund starts to fill

*Plate set 5.4 Video frames showing wave tracking and bund impact for asymmetric releases**

* *Plate source: LJMU*

In the Summary of Results Tables 5.12 to 5.23 below the column headed 'Q' shows the measured overtopping fractions, those headed Q_f, Q_C, and Q_H show the overtopping fractions predicted using the equations of Atherton, Clark (2001) and Hirst in Thyer et al (2002) respectively.

Table 5.12 Summary of results for axisymmetric squat tank releases (110% and 120% nominal bund capacity)

R	*300*	*mm*	*H*	*120*	*mm*			*R/H*	*2.5*				*V_{rel}*	*0.03393*	*(m^3)*	*Theoretical*

h (Θ=90°) (mm)	*h/H*	*r (mm)*	*r/H*	*r/R*	*L (mm)*	*V_{cap} (m^3)*	*V_{cap}/V_{rel}*	*V_{bund} (m^3)*	*V_{slosh} (m^3)*	*$V_{bund}+V_{slosh}$ (m^3)*	*Q*	*Q_f*	*Q_C*	*Q_H*	*Dyn_{base} (Pa)*	*$Stat_{base}$ (Pa)*	*Dyn/Stat base*	*Dyn/Stat cal*
6	0.05	1407	11.73	4.69	1107	0.0373	1.10	0.01720	0.01572	0.03292	0.48	0.52	0.82	0.55	Na	59	Na	Na
12	0.10	995	8.29	3.32	695	0.0373	1.10	0.01696	0.01644	0.03340	0.49	0.47	0.68	0.41	1937	118	16.45	12.52
24	0.20	704	5.87	2.35	404	0.0374	1.10	0.01928	0.01352	0.03280	0.41	0.38	0.46	0.26	1131	235	4.80	5.42
36	0.30	574	4.78	1.91	274	0.0373	1.10	0.02272	0.01048	0.03320	0.32	0.31	0.31	0.18	466	353	1.32	2.35
48	0.40	497	4.14	1.66	197	0.0372	1.10	0.02536	0.00796	0.03332	0.24	0.25	0.21	0.12	732	471	1.55	1.02
120	1.00	315	2.63	1.05	15	0.0374	1.10	0.03288	0.00036	0.03324	0.01	Na	0.02	-0.07	1174	1177	1.00	Na
144	1.20	315	2.63	1.05	15	0.0449	1.32	0.03300	0.00012	0.03312	0.00	Na	0.01	-0.12	1157	1413	0.82	Na

h (Θ=90°) (mm)	*h/H*	*r (mm)*	*r/H*	*r/R*	*L (mm)*	*V_{cap} (m^3)*	*V_{cap}/V_{rel}*	*V_{bund} (m^3)*	*V_{slosh} (m^3)*	*$V_{bund}+V_{slosh}$ (m^3)*	*Q*	*Q_f*	*Q_C*	*Q_H*	*Dyn_{base} (Pa)*	*$Stat_{base}$ (Pa)*	*Dyn/Stat base*	*Dyn/Stat cal*
6	0.05	1470	12.25	4.90	1170	0.0407	1.20	0.01868	0.01464	0.03332	0.44	0.47	0.82	0.54	Na	59	Na	Na
12	0.10	1039	8.66	3.46	739	0.0407	1.20	0.01892	0.01440	0.03332	0.43	0.43	0.68	0.40	782	118	6.64	5.27
24	0.20	735	6.13	2.45	435	0.0407	1.20	0.02060	0.01260	0.03320	0.38	0.35	0.46	0.26	699	235	2.97	3.44
36	0.30	600	5.00	2.00	300	0.0407	1.20	0.02316	0.00992	0.03308	0.30	0.29	0.31	0.18	532	353	1.51	2.25
48	0.40	520	4.33	1.73	220	0.0408	1.20	0.02588	0.00736	0.03324	0.22	0.24	0.21	0.12	948	471	2.01	1.47
120	1.00	330	2.75	1.10	30	0.0411	1.21	0.03284	0.00056	0.03340	0.02	Na	0.02	-0.07	1168	1177	0.99	Na
144	1.20	330	2.75	1.10	30	0.0493	1.45	0.03304	0.00012	0.03316	0.00	Na	0.01	-0.12	1068	1413	0.76	Na

Table 5.13 Summary of results for axisymmetric squat tank releases (150% and 200% nominal bund capacity)

R	*300*	*mm*	*H*	*120*	*mm*			*R/H*	*2.5*				*V_{rel}*	*0.03393*	*(m^3)*	*Theoretical*

h (Θ=90°) (mm)	*h/H*	*r (mm)*	*r/H*	*r/R*	*L (mm)*	*V_{cap} (m^3)*	*V_{cap}/V_{rel}*	*V_{bund} (m^3)*	*V_{slosh} (m^3)*	*$V_{bund}+V_{slosh}$ (m^3)*	*Q*	*Q_f*	*Q_C*	*Q_H*	*Dyn_{base} (Pa)*	*$Stat_{base}$ (Pa)*	*Dyn/Stat base*	*Dyn/Stat cal*
6	0.05	1643	13.69	5.48	1343	0.0509	1.50	0.02256	0.01040	0.03296	0.32	0.36	0.82	0.53	Na	59	Na	Na
12	0.10	1162	9.68	3.87	862	0.0509	1.50	0.02140	0.01180	0.03320	0.36	0.33	0.68	0.39	782	118	6.64	6.56
24	0.20	822	6.85	2.74	522	0.0509	1.50	0.02380	0.00936	0.03316	0.28	0.27	0.46	0.25	971	235	4.12	3.93
36	0.30	671	5.59	2.24	371	0.0509	1.50	0.02520	0.00780	0.03300	0.24	0.22	0.31	0.16	724	353	2.05	2.35
48	0.40	581	4.84	1.94	281	0.0509	1.50	0.02748	0.00532	0.03280	0.16	0.18	0.21	0.10	713	471	1.51	1.41
120	1.00	360	3.00	1.20	60	0.0489	1.44	0.03240	0.00096	0.03336	0.03	Na	0.02	-0.08	983	1177	0.84	Na
144	1.20	360	3.00	1.20	60	0.0586	1.73	0.03352	0.00060	0.03412	0.02	Na	0.01	-0.13	1010	1413	0.71	Na

h (Θ=90°) (mm)	*h/H*	*r (mm)*	*r/H*	*r/R*	*L (mm)*	*V_{cap} (m^3)*	*V_{cap}/V_{rel}*	*V_{bund} (m^3)*	*V_{slosh} (m^3)*	*$V_{bund}+V_{slosh}$ (m^3)*	*Q*	*Q_f*	*Q_C*	*Q_H*	*Dyn_{base} (Pa)*	*$Stat_{base}$ (Pa)*	*Dyn/Stat base*	*Dyn/Stat cal*
6	0.05	1897	15.81	6.32	1597	0.0678	2.00	0.02832	0.00452	0.03284	0.14	0.18	0.82	0.51	Na	59	Na	Na
12	0.10	1342	11.18	4.47	1042	0.0679	2.00	0.02584	0.00736	0.03320	0.22	0.17	0.68	0.37	344	118	2.92	4.06
24	0.20	949	7.91	3.16	649	0.0679	2.00	0.02716	0.00608	0.03324	0.18	0.17	0.46	0.23	1197	235	5.08	3.01
36	0.30	775	6.46	2.58	475	0.0679	2.00	0.02788	0.00496	0.03284	0.15	0.16	0.31	0.15	739	353	2.09	2.23
48	0.40	671	5.59	2.24	371	0.0679	2.00	0.02824	0.00468	0.03292	0.14	0.15	0.21	0.09	678	471	1.44	1.65
120	1.00	390	3.25	1.30	90	0.0573	1.69	0.03252	0.00076	0.03328	0.02	Na	0.02	-0.09	920	1177	0.78	Na
144	1.20	390	3.25	1.30	90	0.0688	2.03	0.03284	0.00028	0.03312	0.01	Na	0.01	-0.14	776	1413	0.55	Na

Chart 5.7 Axisymmetric test results and empirical equations for overtopping for squat tank releases (various bund capacities)

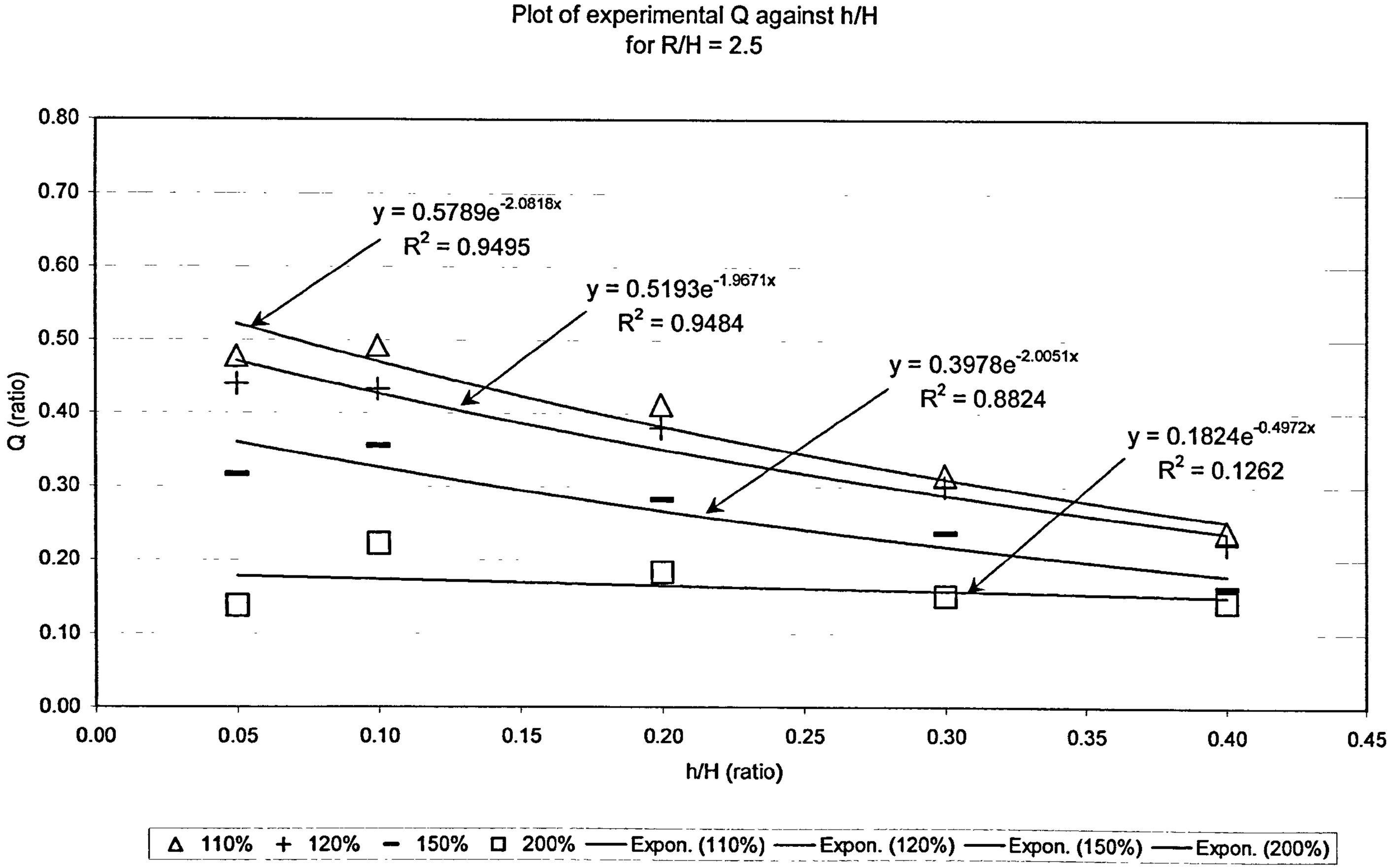

Chart 5.8 Axisymmetric test results and empirical equations for the ratio Dyn/$Stat_{base}$ for squat tank releases (various bund capacities)

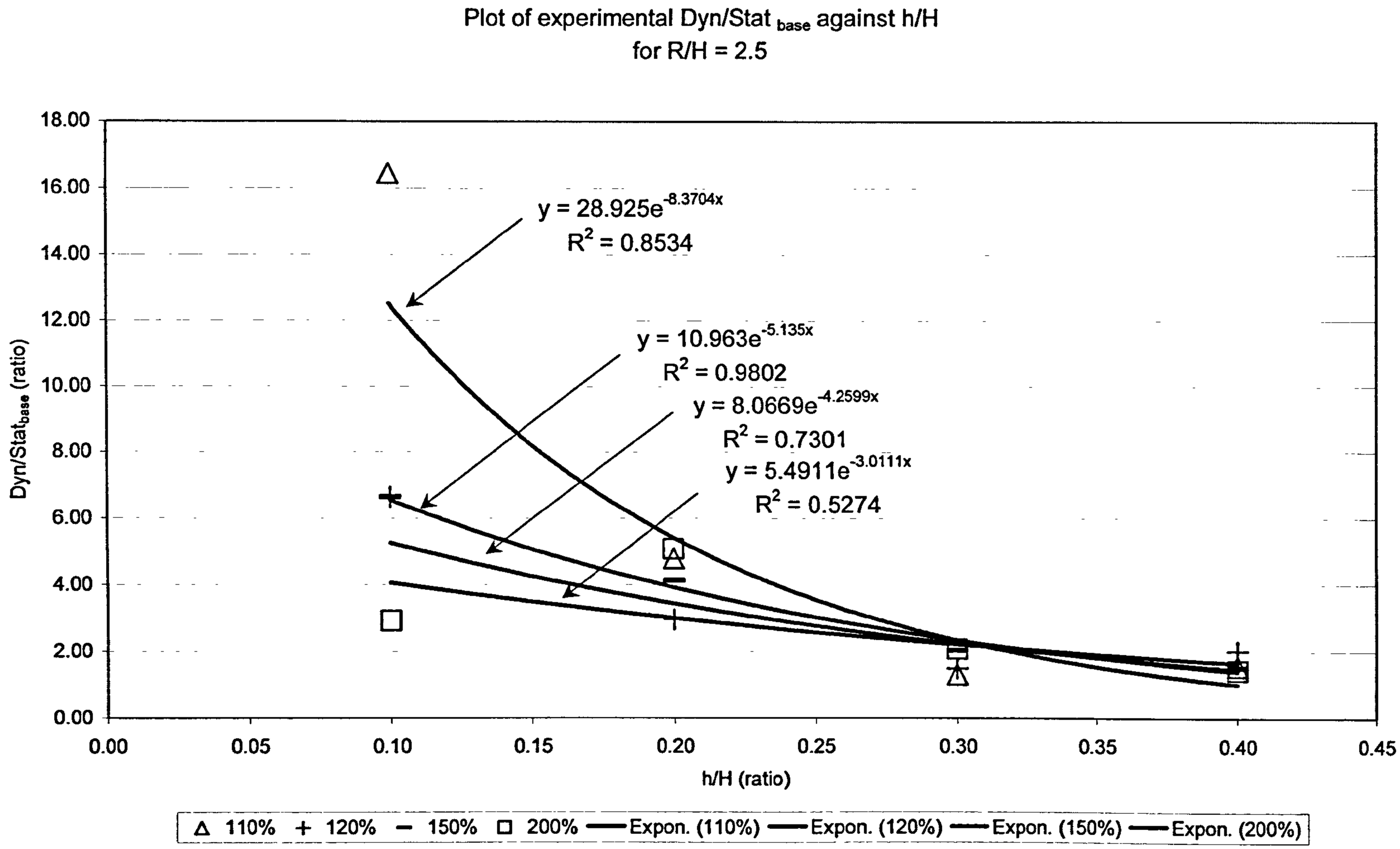

Table 5.14 Summary of results for axisymmetric middle tank releases (110% and 120% nominal bund capacity)

R	*300*	*mm*	*H*	*300*	*mm*			*R/H*	*1.0*				*V_{rel}*	*0.08482*	*(m^3)*	*Theoretical*

h (Θ=90°) (mm)	*h/H*	*r (mm)*	*r/H*	*r/R*	*L (mm)*	*V_{cap} (m^3)*	*V_{cap}/V_{rel}*	*V_{bund} (m^3)*	*V_{slosh} (m^3)*	*$V_{bund}+V_{slosh}$ (m^3)*	*Q*	*Q_f*	*Q_C*	*Q_H*	*Dyn_{base} (Pa)*	*$Stat_{base}$ (Pa)*	*Dyn/Stat base*	*Dyn/Stat cal*
15	0.05	1407	4.69	4.69	1107	0.0933	1.10	0.03148	0.05168	0.08316	0.62	0.67	0.82	0.66	956	147	6.50	7.49
30	0.10	995	3.32	3.32	695	0.0933	1.10	0.03164	0.05104	0.08268	0.62	0.60	0.68	0.51	2879	294	9.78	5.96
60	0.20	704	2.35	2.35	404	0.0934	1.10	0.04012	0.04300	0.08312	0.52	0.47	0.46	0.37	1489	589	2.53	3.77
90	0.30	574	1.91	1.91	274	0.0932	1.10	0.05124	0.03196	0.08320	0.38	0.37	0.31	0.29	1743	883	1.97	2.39
120	0.40	497	1.66	1.66	197	0.0931	1.10	0.06008	0.02324	0.08332	0.28	0.30	0.21	0.23	2255	1177	1.92	1.51
300	1.00	315	1.05	1.05	15	0.0935	1.10	0.08228	0.00096	0.08324	0.01	Na	0.02	0.04	2756	2943	0.94	Na
360	1.20	315	1.05	1.05	15	0.1122	1.32	0.08180	0.00064	0.08244	0.01	Na	0.01	-0.01	2666	3532	0.75	Na

h (Θ=90°) (mm)	*h/H*	*r (mm)*	*r/H*	*r/R*	*L (mm)*	*V_{cap} (m^3)*	*V_{cap}/V_{rel}*	*V_{bund} (m^3)*	*V_{slosh} (m^3)*	*$V_{bund}+V_{slosh}$ (m^3)*	*Q*	*Q_f*	*Q_C*	*Q_H*	*Dyn_{base} (Pa)*	*$Stat_{base}$ (Pa)*	*Dyn/Stat base*	*Dyn/Stat cal*
15	0.05	1470	4.90	4.90	1170	0.1018	1.20	0.03384	0.04892	0.08276	0.59	0.65	0.82	0.65	1075	147	7.31	6.68
30	0.10	1039	3.46	3.46	739	0.1017	1.20	0.03384	0.04952	0.08336	0.59	0.58	0.68	0.51	1695	294	5.76	5.30
60	0.20	735	2.45	2.45	435	0.1018	1.20	0.04120	0.04200	0.08320	0.50	0.45	0.46	0.36	1663	589	2.83	3.33
90	0.30	600	2.00	2.00	300	0.1018	1.20	0.05300	0.03024	0.08324	0.36	0.36	0.31	0.28	1470	883	1.66	2.10
120	0.40	520	1.73	1.73	220	0.1019	1.20	0.06112	0.02200	0.08312	0.26	0.28	0.21	0.22	1939	1177	1.65	1.32
300	1.00	330	1.10	1.10	30	0.1026	1.21	0.08136	0.00232	0.08368	0.03	Na	0.02	0.03	2699	2943	0.92	Na
360	1.20	330	1.10	1.10	30	0.1232	1.45	0.08256	0.00116	0.08372	0.01	Na	0.01	-0.02	2533	3532	0.72	Na

Table 5.15 Summary of results for axisymmetric middle tank releases (150% and 200% nominal bund capacity)

R	*300*	*mm*	*H*	*300*	*mm*			*R/H*	*1.0*					*V_{rel}*	*0.08482*	*(m^3)*	*Theoretical*
h (Θ=90°) (mm)	*h/H*	*r (mm)*	*r/H*	*r/R*	*L (mm)*	*V_{cap} (m^3)*	*V_{cap}/V_{rel}*	*V_{bund} (m^3)*	*V_{slosh} (m^3)*	*$V_{bund}+V_{slosh}$ (m^3)*	*Q*	*Q_f*	*Q_C*	*Q_H*	*Dyn_{base} (Pa)*	*$Stat_{base}$ (Pa)*	*Dyn/Stat base*	*Dyn/Stat cal*
15	0.05	1643	5.48	5.48	1343	0.1272	1.50	0.04064	0.04240	0.08304	0.51	0.56	0.82	0.64	657	147	4.46	5.39
30	0.10	1162	3.87	3.87	862	0.1273	1.50	0.04112	0.04168	0.08280	0.50	0.50	0.68	0.49	1658	294	5.63	4.34
60	0.20	822	2.74	2.74	522	0.1274	1.50	0.04576	0.03712	0.08288	0.45	0.39	0.46	0.35	1646	589	2.80	2.81
90	0.30	671	2.24	2.24	371	0.1273	1.50	0.05720	0.02628	0.08348	0.31	0.31	0.31	0.27	1426	883	1.62	1.82
120	0.40	581	1.94	1.94	281	0.1273	1.50	0.06504	0.01836	0.08340	0.22	0.24	0.21	0.21	1451	1177	1.23	1.18
300	1.00	360	1.20	1.20	60	0.1221	1.44	0.07960	0.00420	0.08380	0.05	Na	0.02	0.02	2707	2943	0.92	Na
360	1.20	360	1.20	1.20	60	0.1466	1.73	0.08040	0.00324	0.08364	0.04	Na	0.01	-0.03	2846	3532	0.81	Na

h (Θ=90°) (mm)	*h/H*	*r (mm)*	*r/H*	*r/R*	*L (mm)*	*V_{cap} (m^3)*	*V_{cap}/V_{rel}*	*V_{bund} (m^3)*	*V_{slosh} (m^3)*	*$V_{bund}+V_{slosh}$ (m^3)*	*Q*	*Q_f*	*Q_C*	*Q_H*	*Dyn_{base} (Pa)*	*$Stat_{base}$ (Pa)*	*Dyn/Stat base*	*Dyn/Stat cal*
15	0.05	1897	6.32	6.32	1597	0.1696	2.00	0.05084	0.03208	0.08292	0.39	0.43	0.82	0.62	993	147	6.75	5.74
30	0.10	1342	4.47	4.47	1042	0.1697	2.00	0.04996	0.03336	0.08332	0.40	0.39	0.68	0.48	1163	294	3.95	4.44
60	0.20	949	3.16	3.16	649	0.1698	2.00	0.05364	0.03036	0.08400	0.36	0.31	0.46	0.34	1517	589	2.58	2.65
90	0.30	775	2.58	2.58	475	0.1698	2.00	0.06296	0.02036	0.08332	0.24	0.25	0.31	0.25	1190	883	1.35	1.59
120	0.40	671	2.24	2.24	371	0.1697	2.00	0.06776	0.01592	0.08368	0.19	0.20	0.21	0.19	1292	1177	1.10	0.95
300	1.00	390	1.30	1.30	90	0.1434	1.69	0.07968	0.00368	0.08336	0.04	Na	0.02	0.01	2571	2943	0.87	Na
360	1.20	390	1.30	1.30	90	0.1720	2.03	0.08108	0.00252	0.08360	0.03	Na	0.01	-0.03	2730	3532	0.77	Na

Chart 5.9 Axisymmetric test results and empirical equations for overtopping for middle tank releases (various bund capacities)

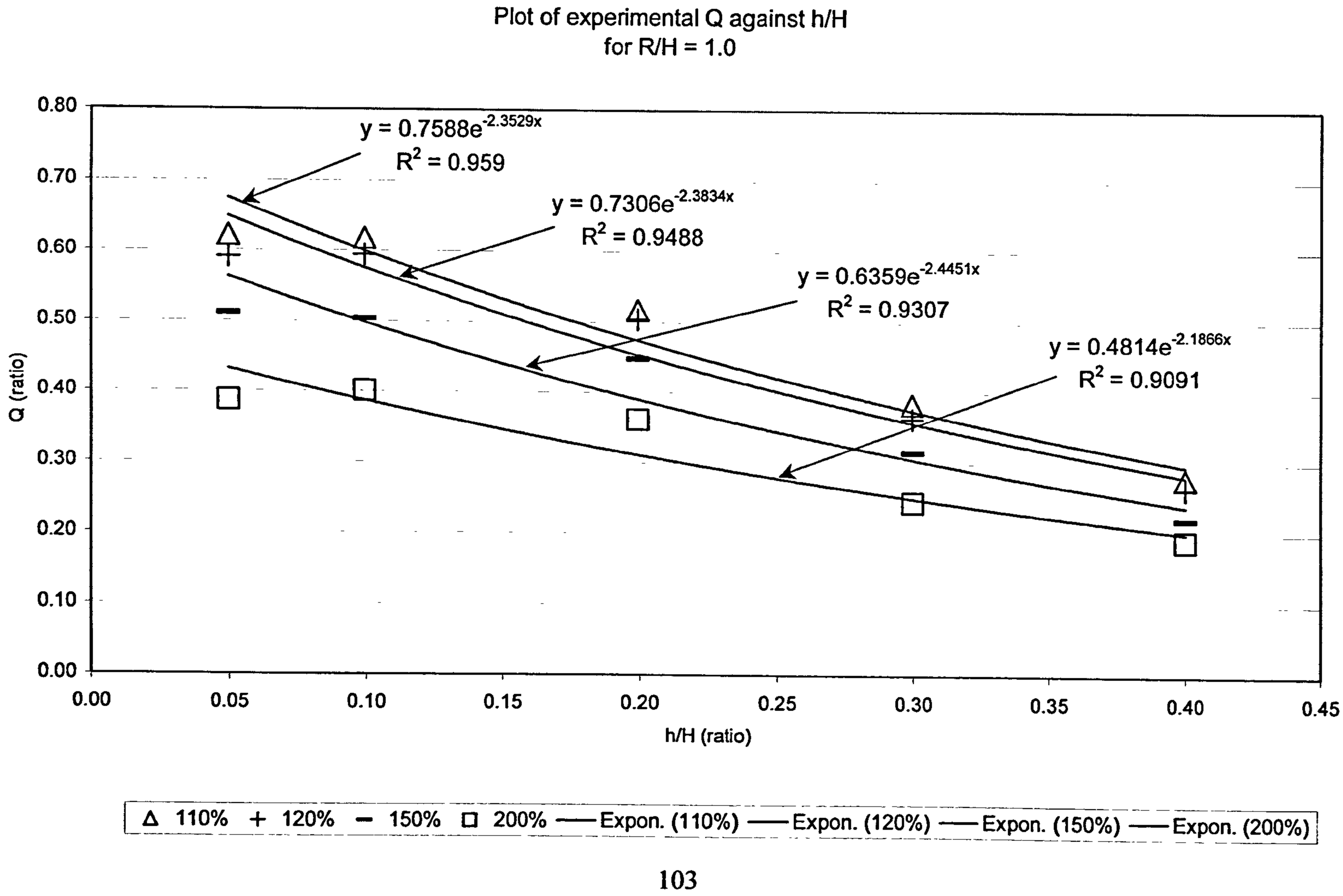

Chart 5.10 Axisymmetric test results and empirical equations for the ratio Dyn/$Stat_{base}$ for middle tank releases (various bund capacities)

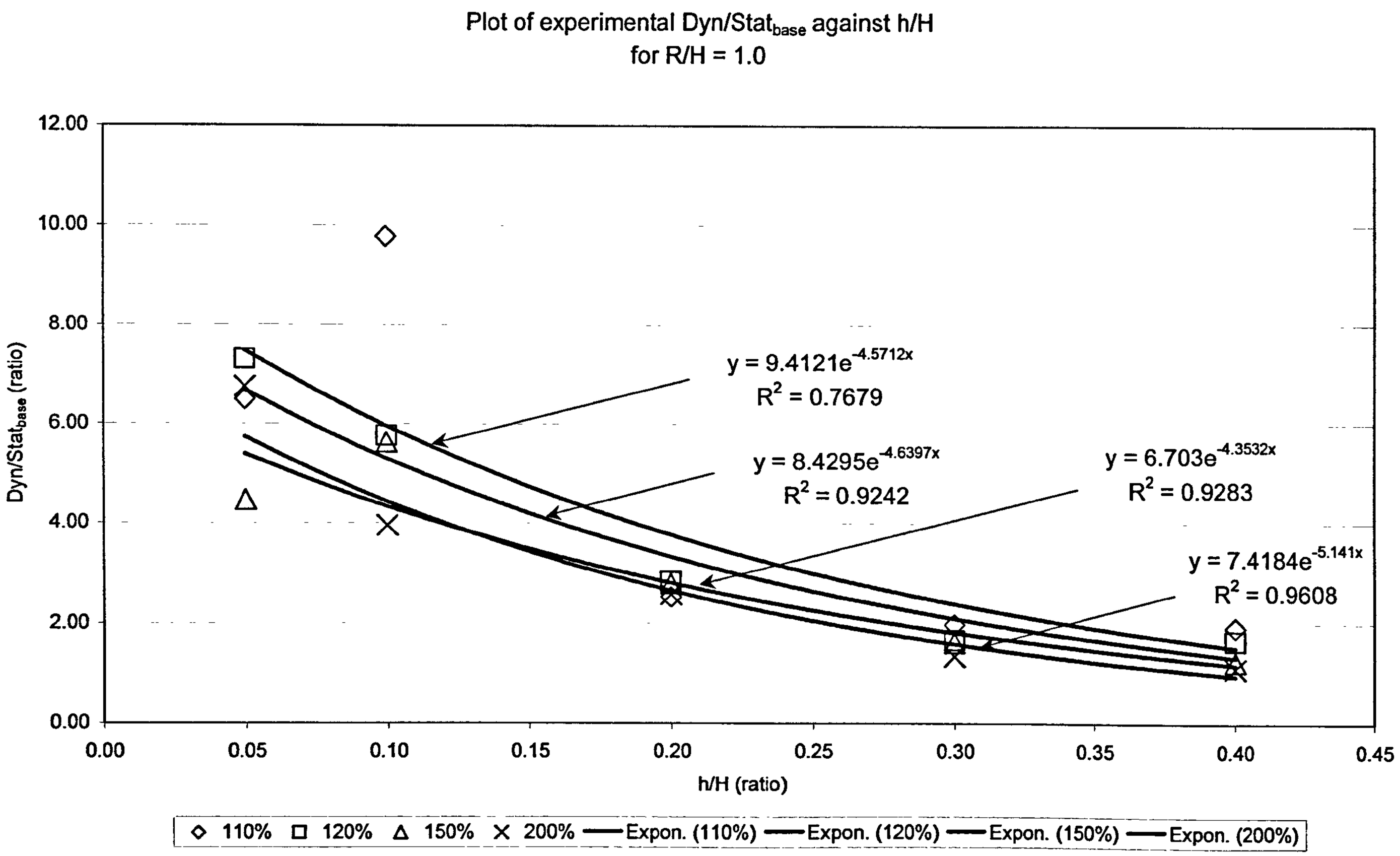

Table 5.16 Summary of results for axisymmetric tall tank releases (110% and 120% nominal bund capacity)

R	*300*	*mm*	*H*	*600*	*mm*			*R/H*	*0.5*					*V_{rel}*	*0.16965*	*(m^3)*	*Theoretical*
h (Θ=90°) (mm)	*h/H*	*r (mm)*	*r/H*	*r/R*	*L (mm)*	*V_{cap} (m^3)*	*V_{cap}/V_{rel}*	*V_{bund} (m^3)*	*V_{slosh} (m^3)*	*$V_{bund}+V_{slosh}$ (m^3)*	*Q*	*Q_f*	*Q_C*	*Q_H*	*Dyn_{base} (Pa)*	*$Stat_{base}$ (Pa)*	*Dyn/Stat base*	*Dyn/Stat cal*
30	0.05	1407	2.35	4.69	1107	0.1866	1.10	0.04996	0.11648	0.16644	0.70	0.76	0.82	0.74	2158	294	7.33	7.69
60	0.10	995	1.66	3.32	695	0.1866	1.10	0.05032	0.11596	0.16628	0.70	0.65	0.68	0.59	5411	589	9.19	6.03
120	0.20	704	1.17	2.35	404	0.1868	1.10	0.08588	0.08120	0.16708	0.49	0.47	0.46	0.45	2848	1177	2.42	3.71
180	0.30	574	0.96	1.91	274	0.1863	1.10	0.11072	0.05648	0.16720	0.34	0.34	0.31	0.37	3165	1766	1.79	2.28
240	0.40	497	0.83	1.66	197	0.1862	1.10	0.12644	0.04136	0.16780	0.25	0.25	0.21	0.31	4444	2354	1.89	1.40
600	1.00	315	0.53	1.05	15	0.1870	1.10	0.16456	0.00108	0.16564	0.01	Na	0.02	0.12	5389	5886	0.92	Na
720	1.20	315	0.53	1.05	15	0.2244	1.32	0.16436	0.00108	0.16544	0.01	Na	0.01	0.07	5264	7063	0.75	Na

h (Θ=90°) (mm)	*h/H*	*r (mm)*	*r/H*	*r/R*	*L (mm)*	*V_{cap} (m^3)*	*V_{cap}/V_{rel}*	*V_{bund} (m^3)*	*V_{slosh} (m^3)*	*$V_{bund}+V_{slosh}$ (m^3)*	*Q*	*Q_f*	*Q_C*	*Q_H*	*Dyn_{base} (Pa)*	*$Stat_{base}$ (Pa)*	*Dyn/Stat base*	*Dyn/Stat cal*
30	0.05	1470	2.45	4.90	1170	0.2037	1.20	0.05308	0.11324	0.16632	0.68	0.75	0.82	0.73	2787	294	9.47	6.03
60	0.10	1039	1.73	3.46	739	0.2035	1.20	0.05260	0.11412	0.16672	0.68	0.63	0.68	0.59	2168	589	3.68	4.87
120	0.20	735	1.23	2.45	435	0.2037	1.20	0.08832	0.07792	0.16624	0.47	0.45	0.46	0.45	2872	1177	2.44	3.17
180	0.30	600	1.00	2.00	300	0.2036	1.20	0.11340	0.05328	0.16668	0.32	0.32	0.31	0.36	2916	1766	1.65	2.06
240	0.40	520	0.87	1.73	220	0.2039	1.20	0.13120	0.03580	0.16700	0.21	0.22	0.21	0.30	4292	2354	1.82	1.34
600	1.00	330	0.55	1.10	30	0.2053	1.21	0.16568	0.00224	0.16792	0.01	Na	0.02	0.11	5337	5886	0.91	Na
720	1.20	330	0.55	1.10	30	0.2463	1.45	0.16312	0.00312	0.16624	0.02	Na	0.01	0.07	5733	7063	0.81	Na

Table 5.17 Summary of results for axisymmetric tall tank releases (150% and 200% nominal bund capacity)

R	*300*	*mm*	*H*	*600*	*mm*			*R/H*	*0.5*				*V_{rel}*	*0.16965*	*(m^3)*	*Theoretical*
h (Θ=90°) (mm)	*h/H*	*r (mm)*	*r/H*	*r/R*	*L (mm)*	*V_{cap} (m^3)*	*V_{cap}/V_{rel}*	*V_{bund} (m^3)*	*V_{slosh} (m^3)*	*$V_{bund}+V_{slosh}$ (m^3)*	*Q*	*Q_f*	*Q_C*	*Q_H*	*Dyn_{base} (Pa)*	*$Stat_{base}$ (Pa)*	*Dyn/Stat base*	*Dyn/Stat cal*
30	0.05	1643	2.74	5.48	1343	0.2544	1.50	0.06192	0.10440	0.16632	0.63	0.69	0.82	0.72	2200	294	7.48	6.39
60	0.10	1162	1.94	3.87	862	0.2545	1.50	0.06040	0.10642	0.16682	0.64	0.58	0.68	0.58	3238	589	5.50	4.98
120	0.20	822	1.37	2.74	522	0.2547	1.50	0.09452	0.07160	0.16612	0.43	0.41	0.46	0.43	2608	1177	2.22	3.02
180	0.30	671	1.12	2.24	371	0.2546	1.50	0.11888	0.04764	0.16652	0.29	0.29	0.31	0.35	2580	1766	1.46	1.83
240	0.40	581	0.97	1.94	281	0.2545	1.50	0.13316	0.03360	0.16676	0.20	0.21	0.21	0.29	3461	2354	1.47	1.11
600	1.00	360	0.60	1.20	60	0.2443	1.44	0.16252	0.00352	0.16604	0.02	Na	0.02	0.10	5670	5886	0.96	Na
720	1.20	360	0.60	1.20	60	0.2931	1.73	0.16176	0.00432	0.16608	0.03	Na	0.01	0.06	5725	7063	0.81	Na

h (Θ=90°) (mm)	*h/H*	*r (mm)*	*r/H*	*r/R*	*L (mm)*	*V_{cap} (m^3)*	*V_{cap}/V_{rel}*	*V_{bund} (m^3)*	*V_{slosh} (m^3)*	*$V_{bund}+V_{slosh}$ (m^3)*	*Q*	*Q_f*	*Q_C*	*Q_H*	*Dyn_{base} (Pa)*	*$Stat_{base}$ (Pa)*	*Dyn/Stat base*	*Dyn/Stat cal*
30	0.05	1897	3.16	6.32	1597	0.3392	2.00	0.07480	0.09232	0.16712	0.55	0.62	0.82	0.70	2452	294	8.33	5.82
60	0.10	1342	2.24	4.47	1042	0.3395	2.00	0.07216	0.09560	0.16776	0.57	0.52	0.68	0.56	2134	589	3.63	4.48
120	0.20	949	1.58	3.16	649	0.3395	2.00	0.10132	0.06604	0.16736	0.39	0.36	0.46	0.42	2584	1177	2.20	2.65
180	0.30	775	1.29	2.58	475	0.3396	2.00	0.12644	0.04044	0.16688	0.24	0.26	0.31	0.33	2177	1766	1.23	1.57
240	0.40	671	1.12	2.24	371	0.3395	2.00	0.13724	0.02980	0.16704	0.18	0.18	0.21	0.27	2925	2354	1.24	0.93
600	1.00	390	0.65	1.30	90	0.2867	1.69	0.15772	0.00752	0.16524	0.05	Na	0.02	0.09	5532	5886	0.94	Na
720	1.20	390	0.65	1.30	90	0.3440	2.03	0.15944	0.00496	0.16440	0.03	Na	0.01	0.05	5696	7063	0.81	Na

Chart 5.11 Axisymmetric test results and empirical equations for overtopping for tall tank releases (various bund capacities)

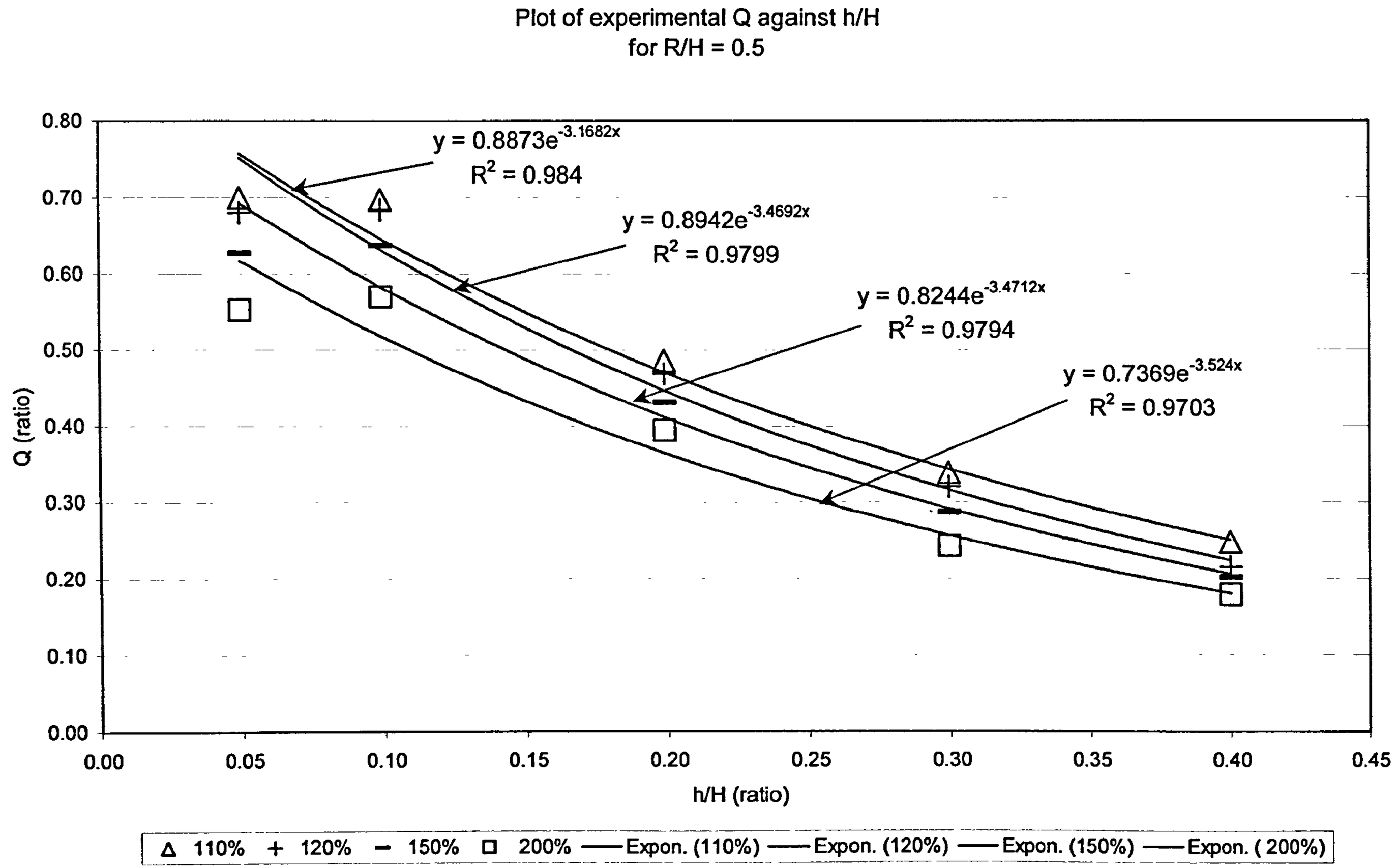

Chart 5.12 Axisymmetric test results and empirical equations for the ratio Dyn/$Stat_{base}$ for tall tank releases (various bund capacities)

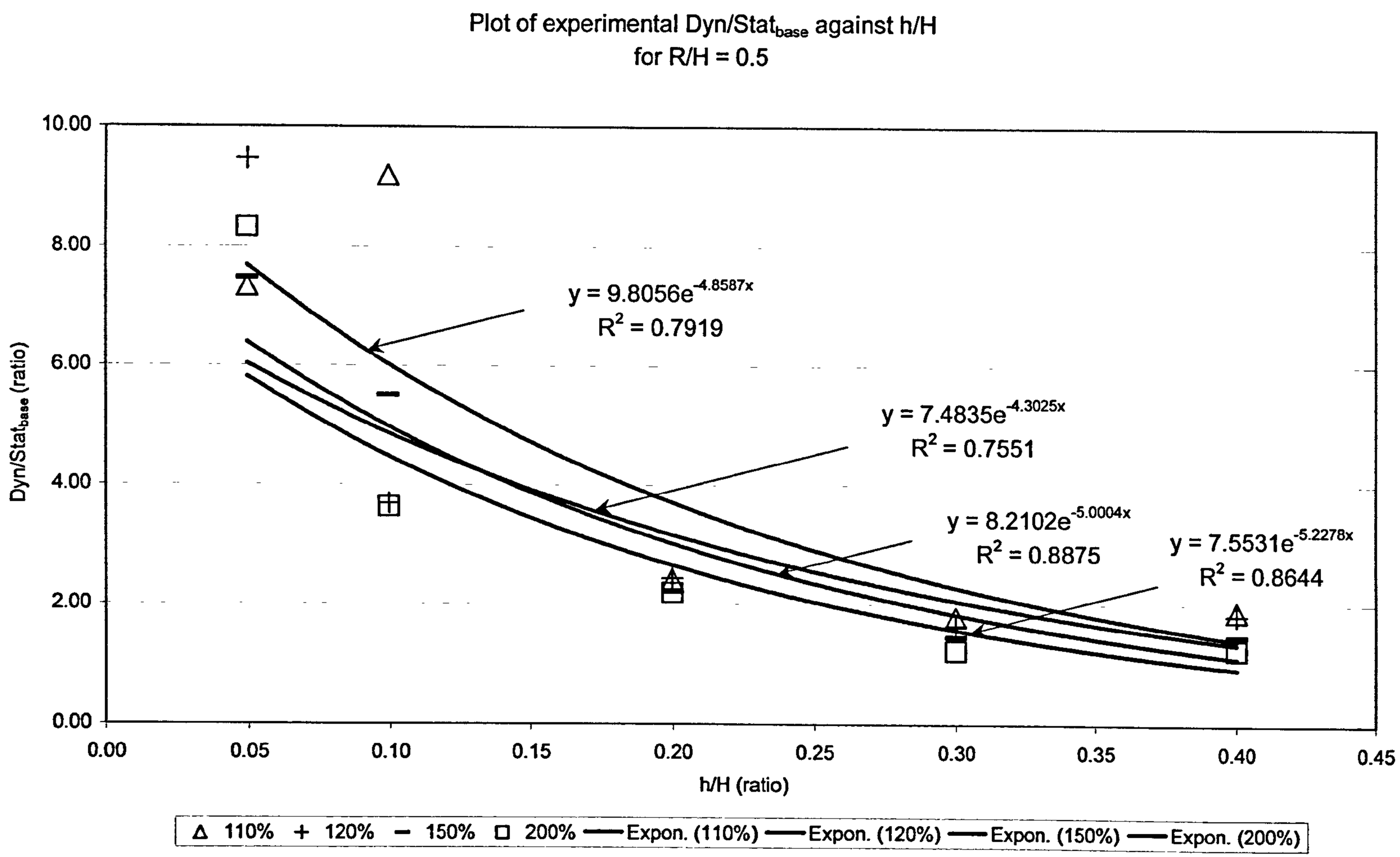

5.6 Interpretation of graphical results for axisymmetric releases

The Charts 5.7 to 5.12 indicate both the quantity overtopping the bunds and the magnitudes of the dynamic pressures in terms of non-dimensional parameters for bund capacities ranging from 110 % to 200 %. The curves are derived from the best fit to the experimental data using the standard curve-fitting techniques available in Excel and the equations of the curve are shown along with the degree of fit, as indicated by R^2, the correlation coefficient squared. The degree of fit is deemed perfect $R^2 = 1$, with deviations of fit determined by values of $R^2 < 1$.

The dimensionless ratios used in the charts allow the equations to be used at any scale to predict both the amount of overtopping and the magnitude of the ratio of the dynamic to static pressures experienced due to an axisymmetric failure of a bulk storage tank. It can be seen for the results that the degree of fit for both overtopping and dynamic pressures is less good for squat tanks with bunds of larger capacity (200 %). The middle and tall tank configurations are fairly consistent with regard the degree of fit, however there are a couple of anomalous results in the pressure data at smaller ratios of h/H.

Generally, the greater the tank height, the greater the overtopping and the pressure ratio obtained due the increase in potential energy. In terms of bund capacity, smaller capacity bunds tend to have increased pressure ratios, although there are slight variations with specific configurations of tank and bund.

Table 5.18 Summary of results for asymmetric squat tank releases (orifice with 110% nominal bund capacity)

R	*300*	*mm*	*H*	*120*	*mm*				*R/H*	*2.5*			*V_{rel}*	*0.03393*	*(m^3)*	*Theoretical*
Orifice	*Dia*	*18.97*	*mm*													
h (Θ=90°) (mm)	*h/H*	*r (mm)*	*r/H*	*r/R*	*L (mm)*	*V_{cap} (m^3)*	*V_{cap}/V_{rel}*	*V_{bund} (m^3)*	*V_{slosh} (m^3)*	*$V_{bund}+V_{slosh}$ (m^3)*	*Q*	*Q_f*	*Dyn_{base} (Pa)*	*$Stat_{base}$ (Pa)*	*Dyn/Stat base*	*Dyn/Stat cal*
6	0.05	1407	11.73	4.69	1107	0.0373	1.10	0.03208	0.00000	0.03208	0.00	<0.01	Na	59	Na	Na
12	0.10	995	8.29	3.32	695	0.0373	1.10	0.03296	0.00000	0.03296	0.00	<0.01	Na	118	Na	Na
24	0.20	704	5.87	2.35	404	0.0374	1.10	0.03268	0.00000	0.03268	0.00	<0.01	318	235	1.35	Na
36	0.30	574	4.78	1.91	274	0.0373	1.10	0.03244	0.00000	0.03244	0.00	<0.01	493	353	1.40	Na
48	0.40	497	4.14	1.66	197	0.0372	1.10	0.03220	0.00020	0.03240	0.01	<0.01	359	471	0.76	Na
Orifice	*Dia*	*26.83*	*mm*													
h (Θ=90°) (mm)	*h/H*	*r (mm)*	*r/H*	*r/R*	*L (mm)*	*V_{cap} (m^3)*	*V_{cap}/V_{rel}*	*V_{bund} (m^3)*	*V_{slosh} (m^3)*	*$V_{bund}+V_{slosh}$ (m^3)*	*Q*	*Q_f*	*Dyn_{base} (Pa)*	*$Stat_{base}$ (Pa)*	*Dyn/Stat base*	*Dyn/Stat cal*
6	0.05	1407	11.73	4.69	1107	0.0373	1.10	0.03236	0.00000	0.03236	0.00	<0.01	Na	59	Na	Na
12	0.10	995	8.29	3.32	695	0.0373	1.10	0.03292	0.00000	0.03292	0.00	<0.01	Na	118	Na	Na
24	0.20	704	5.87	2.35	404	0.0374	1.10	0.03292	0.00012	0.03304	0.00	<0.01	50	235	0.21	Na
36	0.30	574	4.78	1.91	274	0.0373	1.10	0.03260	0.00000	0.03260	0.00	<0.01	733	353	2.08	Na
48	0.40	497	4.14	1.66	197	0.0372	1.10	0.03260	0.00012	0.03272	0.00	<0.01	519	471	1.10	Na
Orifice	*Dia*	*37.95*	*mm*													
h (Θ=90°) (mm)	*h/H*	*r (mm)*	*r/H*	*r/R*	*L (mm)*	*V_{cap} (m^3)*	*V_{cap}/V_{rel}*	*V_{bund} (m^3)*	*V_{slosh} (m^3)*	*$V_{bund}+V_{slosh}$ (m^3)*	*Q*	*Q_f*	*Dyn_{base} (Pa)*	*$Stat_{base}$ (Pa)*	*Dyn/Stat base*	*Dyn/Stat cal*
6	0.05	1407	11.73	4.69	1107	0.0373	1.10	0.03276	0.00000	0.03276	0.00	<0.02	Na	59	Na	Na
12	0.10	995	8.29	3.32	695	0.0373	1.10	0.03276	0.00000	0.03276	0.00	<0.02	Na	118	Na	Na
24	0.20	704	5.87	2.35	404	0.0374	1.10	0.03240	0.00020	0.03260	0.01	<0.02	286	235	1.22	Na
36	0.30	574	4.78	1.91	274	0.0373	1.10	0.03224	0.00048	0.03272	0.01	<0.02	1547	353	4.38	Na
48	0.40	497	4.14	1.66	197	0.0372	1.10	0.03208	0.00060	0.03268	0.02	<0.02	675	471	1.43	Na

Chart 5.13 Asymmetric test results and empirical equations for overtopping for squat tank orifice releases

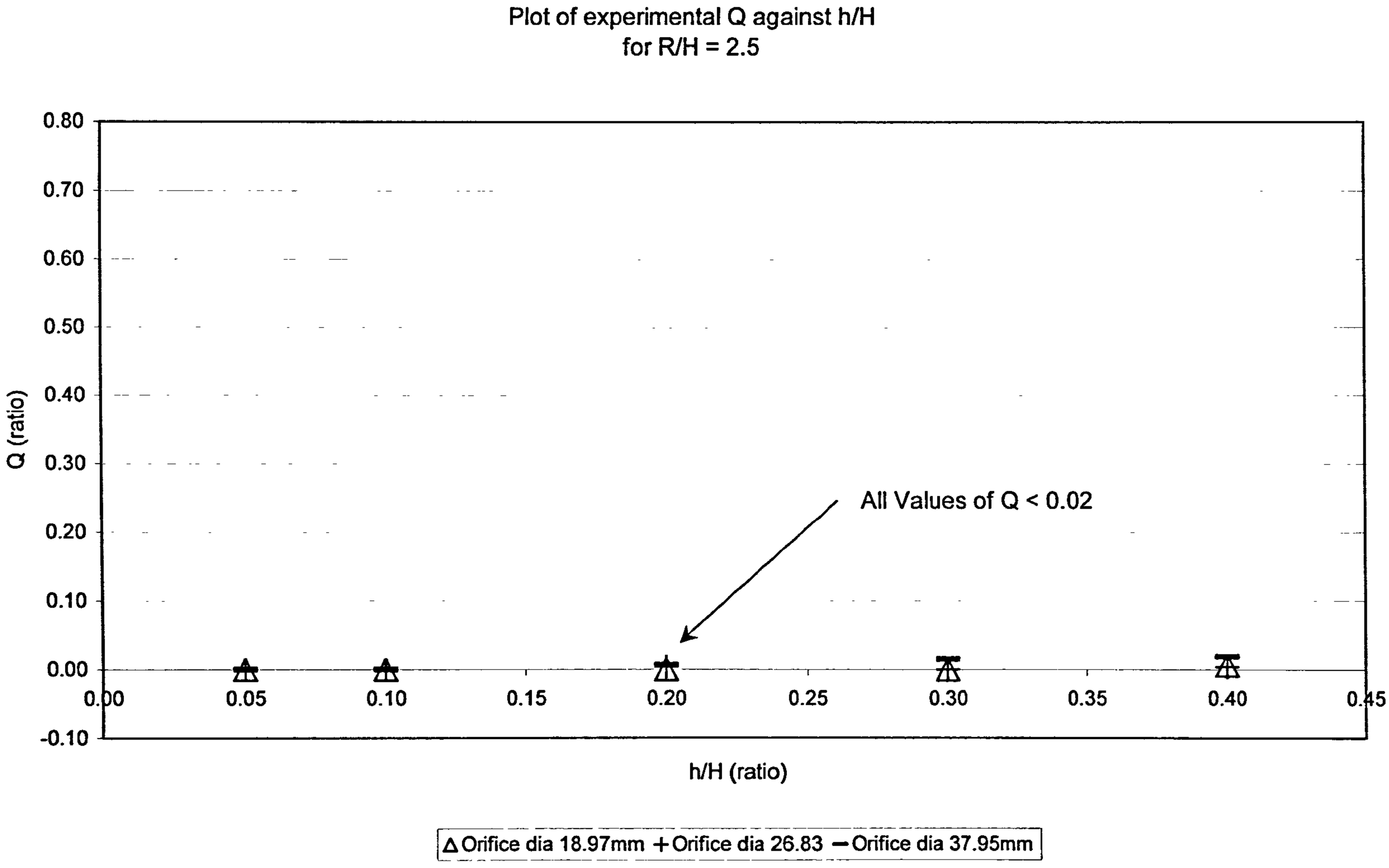

Table 5.19 Summary of results for asymmetric squat tank releases (slot with 110% nominal bund capacity)

R	*300*	*mm*	*H*	*120*	*mm*				*R/H*	*2.5*			*V_{rel}*	*0.03393*	*(m^3)*	*Theoretical*
Slot	*Width*	*157.08*	*mm*	*Height*	*7.20*	*mm*										
h (Θ=90°) (mm)	*h/H*	*r (mm)*	*r/H*	*r/R*	*L (mm)*	*V_{cap} (m^3)*	*V_{cap}/V_{rel}*	*V_{bund} (m^3)*	*V_{slosh} (m^3)*	*$V_{bund}+V_{slosh}$ (m^3)*	*Q*	*Q_f*	*Dyn_{base} (Pa)*	*$Stat_{base}$ (Pa)*	*Dyn/Stat base*	*Dyn/Stat cal*
6	0.05	1407	11.73	4.69	1107	0.0373	1.10	0.03024	0.00376	0.03400	0.11	0.04	Na	59	Na	Na
12	0.10	995	8.29	3.32	695	0.0373	1.10	0.03280	0.00036	0.03316	0.01	0.04	Na	118	Na	Na
24	0.20	704	5.87	2.35	404	0.0374	1.10	0.03152	0.00092	0.03244	0.03	0.02	843	235	3.59	Na
36	0.30	574	4.78	1.91	274	0.0373	1.10	0.03188	0.00048	0.03236	0.01	0.02	1225	353	3.47	Na
48	0.40	497	4.14	1.66	197	0.0372	1.10	0.03224	0.00036	0.03260	0.01	0.01	370	471	0.79	Na
Slot	*Width*	*157.08*	*mm*	*Height*	*21.60*	*mm*										
h (Θ=90°) (mm)	*h/H*	*r (mm)*	*r/H*	*r/R*	*L (mm)*	*V_{cap} (m^3)*	*V_{cap}/V_{rel}*	*V_{bund} (m^3)*	*V_{slosh} (m^3)*	*$V_{bund}+V_{slosh}$ (m^3)*	*Q*	*Q_f*	*Dyn_{base} (Pa)*	*$Stat_{base}$ (Pa)*	*Dyn/Stat base*	*Dyn/Stat cal*
6	0.05	1407	11.73	4.69	1107	0.0373	1.10	0.02288	0.01032	0.03320	0.31	0.29	Na	59	Na	Na
12	0.10	995	8.29	3.32	695	0.0373	1.10	0.02596	0.00716	0.03312	0.22	0.25	67	118	0.57	Na
24	0.20	704	5.87	2.35	404	0.0374	1.10	0.02704	0.00572	0.03276	0.17	0.17	315	235	1.34	Na
36	0.30	574	4.78	1.91	274	0.0373	1.10	0.02788	0.00476	0.03264	0.15	0.12	1120	353	3.17	Na
48	0.40	497	4.14	1.66	197	0.0372	1.10	0.03064	0.00256	0.03320	0.08	0.09	846	471	1.80	Na
Slot	*Width*	*157.08*	*mm*	*Height*	*36.00*	*mm*										
h (Θ=90°) (mm)	*h/H*	*r (mm)*	*r/H*	*r/R*	*L (mm)*	*V_{cap} (m^3)*	*V_{cap}/V_{rel}*	*V_{bund} (m^3)*	*V_{slosh} (m^3)*	*$V_{bund}+V_{slosh}$ (m^3)*	*Q*	*Q_f*	*Dyn_{base} (Pa)*	*$Stat_{base}$ (Pa)*	*Dyn/Stat base*	*Dyn/Stat cal*
6	0.05	1407	11.73	4.69	1107	0.0373	1.10	0.02288	0.01036	0.03324	0.31	0.31	Na	59	Na	Na
12	0.10	995	8.29	3.32	695	0.0373	1.10	0.02484	0.00856	0.03340	0.26	0.28	298	118	2.53	Na
24	0.20	704	5.87	2.35	404	0.0374	1.10	0.02504	0.00776	0.03280	0.24	0.23	651	235	2.77	Na
36	0.30	574	4.78	1.91	274	0.0373	1.10	0.02620	0.00688	0.03308	0.21	0.18	1118	353	3.17	Na
48	0.40	497	4.14	1.66	197	0.0372	1.10	0.02872	0.00440	0.03312	0.13	0.15	784	471	1.66	Na

Chart 5.14 Asymmetric test results and empirical equations for overtopping for squat tank slot releases

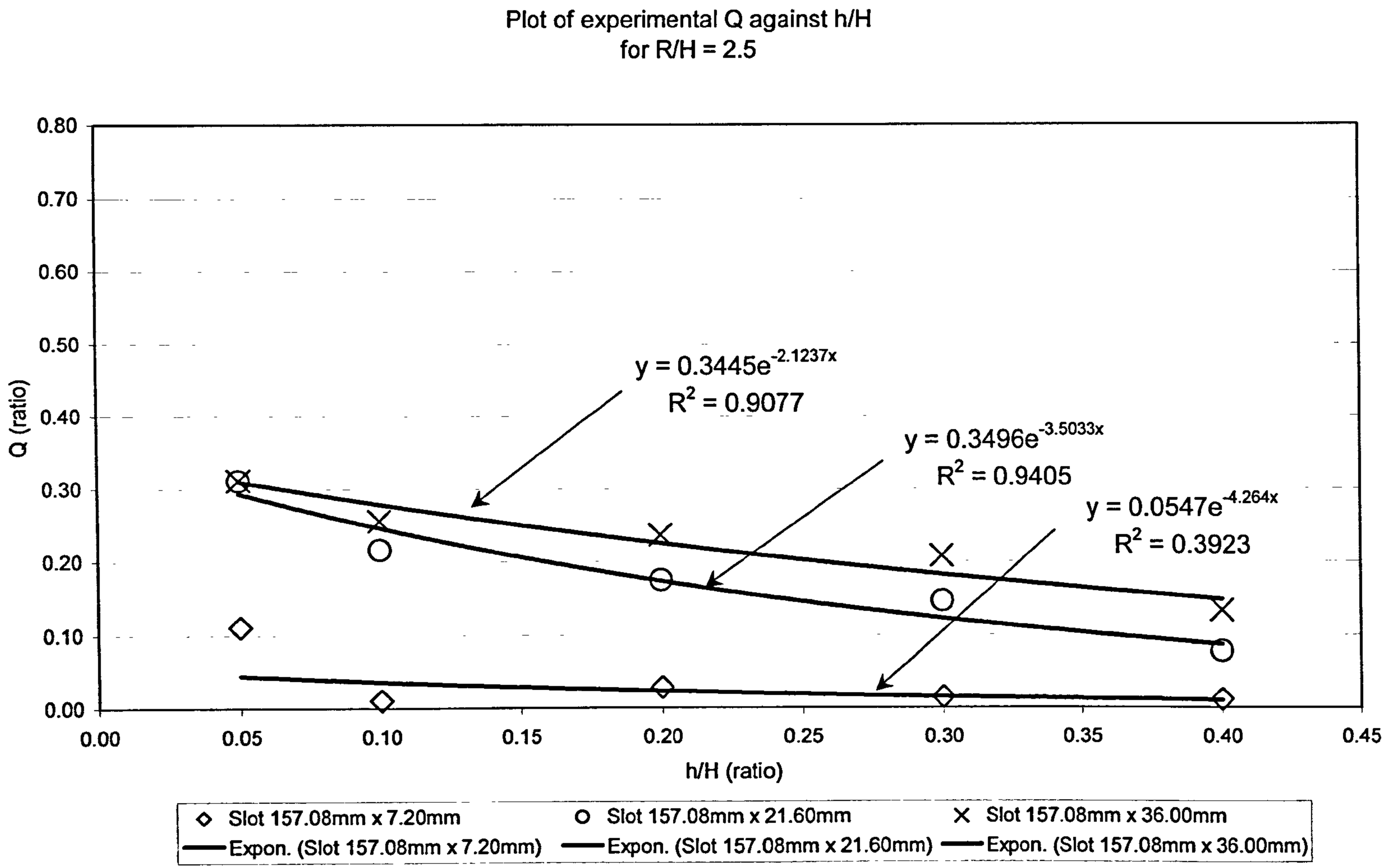

Table 5.20 Summary of results for asymmetric middle tank releases (orifice with 110% nominal bund capacity)

R	*300*	*mm*	*H*	*300*	*mm*				*R/H*	*1.0*			*V_{rel}*	*0.08482*	*(m^3)*	*Theoretical*
Orifice	*Dia*	*30.00*	*mm*													
h (Θ=90°) (mm)	*h/H*	*r (mm)*	*r/H*	*r/R*	*L (mm)*	*V_{cap} (m^3)*	*V_{cap}/V_{rel}*	*V_{bund} (m^3)*	*V_{slosh} (m^3)*	*$V_{bund}+V_{slosh}$ (m^3)*	*Q*	*Q_f*	*Dyn_{base} (Pa)*	*$Stat_{base}$ (Pa)*	*Dyn/Stat base*	*Dyn/Stat cal*
15	0.05	1407	4.69	4.69	1107	0.0933	1.10	0.07820	0.00532	0.08352	0.06	0.07	67	147	0.46	Na
30	0.10	995	3.32	3.32	695	0.0933	1.10	0.07224	0.01092	0.08316	0.13	0.07	301	294	1.02	Na
60	0.20	704	2.35	2.35	404	0.0934	1.10	0.08064	0.00184	0.08248	0.02	0.06	1937	589	3.29	Na
90	0.30	574	1.91	1.91	274	0.0932	1.10	0.07748	0.00648	0.08396	0.08	0.06	2227	883	2.52	Na
120	0.40	497	1.66	1.66	197	0.0931	1.10	0.07668	0.00660	0.08328	0.08	0.06	2876	1177	2.44	Na
Orifice	*Dia*	*42.43*	*mm*													
h (Θ=90°) (mm)	*h/H*	*r (mm)*	*r/H*	*r/R*	*L (mm)*	*V_{cap} (m^3)*	*V_{cap}/V_{rel}*	*V_{bund} (m^3)*	*V_{slosh} (m^3)*	*$V_{bund}+V_{slosh}$ (m^3)*	*Q*	*Q_f*	*Dyn_{base} (Pa)*	*$Stat_{base}$ (Pa)*	*Dyn/Stat base*	*Dyn/Stat cal*
15	0.05	1407	4.69	4.69	1107	0.0933	1.10	0.07904	0.00488	0.08392	0.06	0.09	76	147	0.52	Na
30	0.10	995	3.32	3.32	695	0.0933	1.10	0.07220	0.01208	0.08428	0.14	0.09	1596	294	5.43	Na
60	0.20	704	2.35	2.35	404	0.0934	1.10	0.07472	0.00744	0.08216	0.09	0.10	1612	589	2.74	Na
90	0.30	574	1.91	1.91	274	0.0932	1.10	0.07316	0.01072	0.08388	0.13	0.11	2128	883	2.41	Na
120	0.40	497	1.66	1.66	197	0.0931	1.10	0.07588	0.00808	0.08396	0.10	0.11	3222	1177	2.74	Na
Orifice	*Dia*	*60.00*	*mm*													
h (Θ=90°) (mm)	*h/H*	*r (mm)*	*r/H*	*r/R*	*L (mm)*	*V_{cap} (m^3)*	*V_{cap}/V_{rel}*	*V_{bund} (m^3)*	*V_{slosh} (m^3)*	*$V_{bund}+V_{slosh}$ (m^3)*	*Q*	*Q_f*	*Dyn_{base} (Pa)*	*$Stat_{base}$ (Pa)*	*Dyn/Stat base*	*Dyn/Stat cal*
15	0.05	1407	4.69	4.69	1107	0.0933	1.10	0.07192	0.01176	0.08368	0.14	0.15	725	147	4.93	4.20
30	0.10	995	3.32	3.32	695	0.0933	1.10	0.07140	0.01252	0.08392	0.15	0.15	1154	294	3.93	3.65
60	0.20	704	2.35	2.35	404	0.0934	1.10	0.07088	0.01160	0.08248	0.14	0.14	1280	589	2.17	2.75
90	0.30	574	1.91	1.91	274	0.0932	1.10	0.06868	0.01528	0.08396	0.18	0.14	1344	883	1.52	2.08
120	0.40	497	1.66	1.66	197	0.0931	1.10	0.07416	0.00992	0.08408	0.12	0.14	2521	1177	2.14	1.57

Chart 5.15 Asymmetric test results and empirical equations for overtopping for middle tank orifice releases

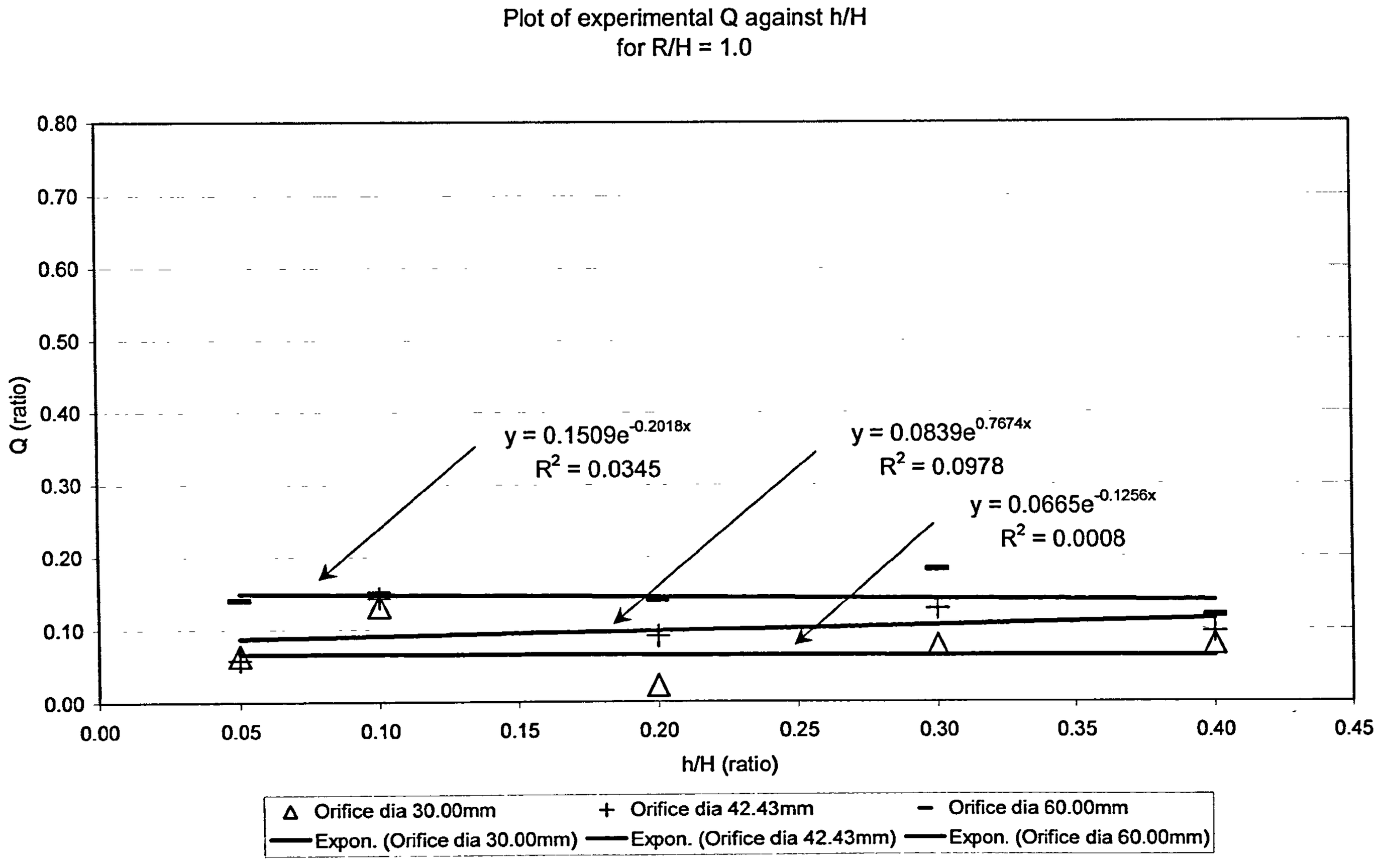

Chart 5.16 Asymmetric test results and empirical equations for the ratio Dyn/$Stat_{base}$ for middle tank orifice releases

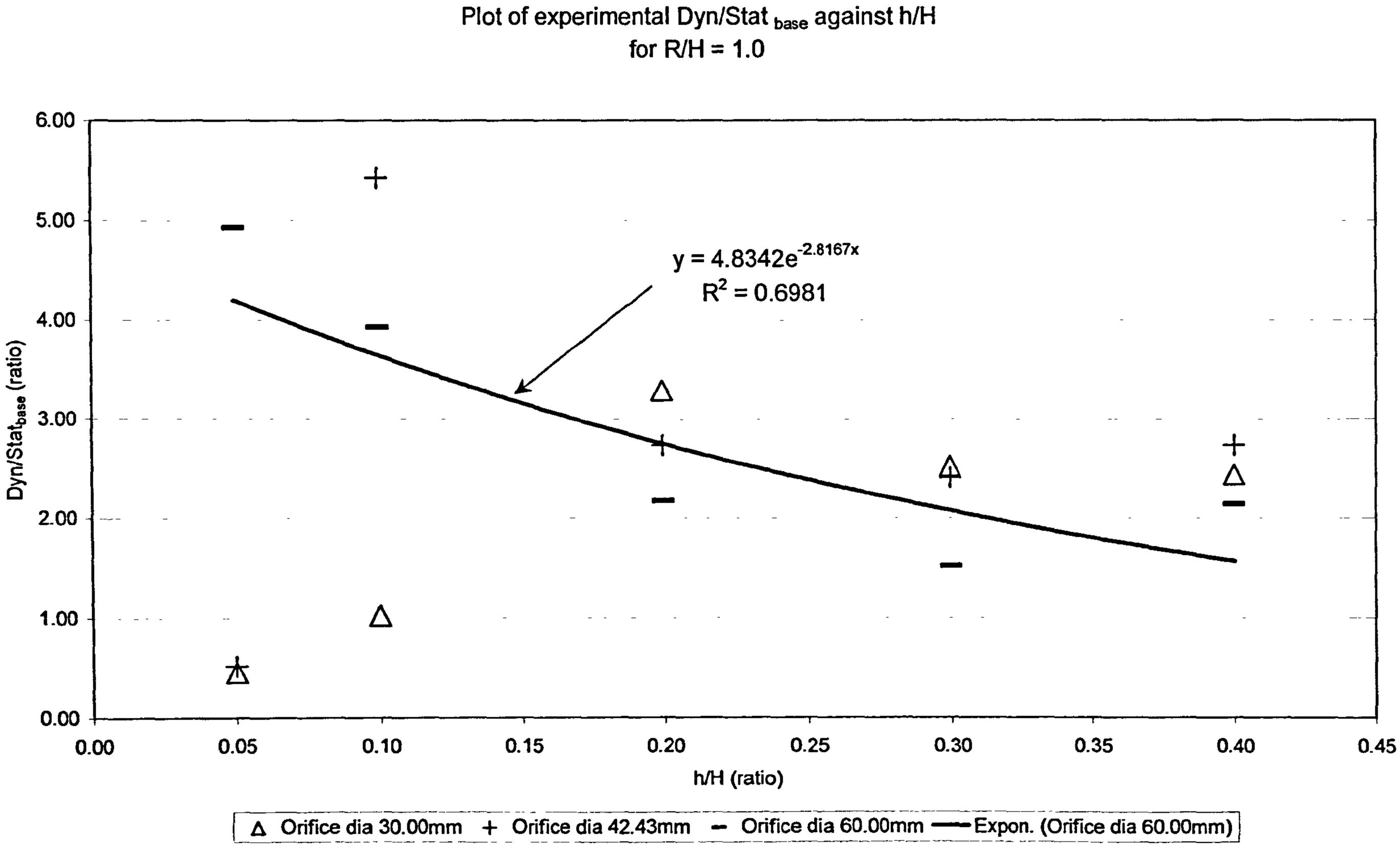

Table 5.21 Summary of results for asymmetric middle tank releases (slot with 110% nominal bund capacity)

R	*300*	*mm*	*H*	*300*	*mm*			*R/H*	*1.0*			*V_{rel}*	*0.08482*	*(m^3)*	*Theoretical*
Slot	*Width*	*157.08*	*mm*	*Height*	*18.00*	*mm*									
h (Θ=90°) (mm)	*h/H*	*r (mm)*	*r/H*	*r/R*	*L (mm)*	*V_{cap} (m^3)*	*V_{cap}/V_{rel}*	*V_{bund} (m^3)*	*V_{slosh} (m^3)*	*$V_{bund}+V_{slosh}$ (m^3)*	*Q*	*Q_f*	*Dyn_{base} (Pa)*	*$Stat_{base}$ (Pa)*	*Dyn/Stat base*	*Dyn/Stat cal*
15	0.05	1407	4.69	4.69	1107	0.0933	1.10	0.05560	0.02780	0.08340	0.33	0.32	483	147	3.29	3.78
30	0.10	995	3.32	3.32	695	0.0933	1.10	0.06196	0.02128	0.08324	0.26	0.24	1014	294	3.45	3.24
60	0.20	704	2.35	2.35	404	0.0934	1.10	0.07340	0.00988	0.08328	0.12	0.13	1909	589	3.24	2.37
90	0.30	574	1.91	1.91	274	0.0932	1.10	0.07908	0.00456	0.08364	0.05	0.07	1109	883	1.26	1.74
120	0.40	497	1.66	1.66	197	0.0931	1.10	0.08012	0.00380	0.08392	0.05	0.04	1649	1177	1.40	1.28
Slot	*Width*	*157.08*	*mm*	*Height*	*54.00*	*mm*									
h (Θ=90°) (mm)	*h/H*	*r (mm)*	*r/H*	*r/R*	*L (mm)*	*V_{cap} (m^3)*	*V_{cap}/V_{rel}*	*V_{bund} (m^3)*	*V_{slosh} (m^3)*	*$V_{bund}+V_{slosh}$ (m^3)*	*Q*	*Q_f*	*Dyn_{base} (Pa)*	*$Stat_{base}$ (Pa)*	*Dyn/Stat base*	*Dyn/Stat cal*
15	0.05	1407	4.69	4.69	1107	0.0933	1.10	0.04656	0.03644	0.08300	0.44	0.42	1091	147	7.42	5.83
30	0.10	995	3.32	3.32	695	0.0933	1.10	0.05260	0.03080	0.08340	0.37	0.38	1002	294	3.41	4.91
60	0.20	704	2.35	2.35	404	0.0934	1.10	0.05884	0.02476	0.08360	0.30	0.30	2497	589	4.24	3.47
90	0.30	574	1.91	1.91	274	0.0932	1.10	0.06672	0.01904	0.08576	0.22	0.23	1867	883	2.11	2.45
120	0.40	497	1.66	1.66	197	0.0931	1.10	0.06800	0.01624	0.08424	0.19	0.18	2197	1177	1.87	1.74
Slot	*Width*	*157.08*	*mm*	*Height*	*90.00*	*mm*									
h (Θ=90°) (mm)	*h/H*	*r (mm)*	*r/H*	*r/R*	*L (mm)*	*V_{cap} (m^3)*	*V_{cap}/V_{rel}*	*V_{bund} (m^3)*	*V_{slosh} (m^3)*	*$V_{bund}+V_{slosh}$ (m^3)*	*Q*	*Q_f*	*Dyn_{base} (Pa)*	*$Stat_{base}$ (Pa)*	*Dyn/Stat base*	*Dyn/Stat cal*
15	0.05	1407	4.69	4.69	1107	0.0933	1.10	0.04796	0.03520	0.08316	0.42	0.45	1265	147	8.61	6.01
30	0.10	995	3.32	3.32	695	0.0933	1.10	0.05028	0.03332	0.08360	0.40	0.41	1028	294	3.50	5.00
60	0.20	704	2.35	2.35	404	0.0934	1.10	0.05152	0.03160	0.08312	0.38	0.34	1948	589	3.31	3.47
90	0.30	574	1.91	1.91	274	0.0932	1.10	0.06044	0.02364	0.08408	0.28	0.28	1941	883	2.20	2.40
120	0.40	497	1.66	1.66	197	0.0931	1.10	0.06548	0.01804	0.08352	0.22	0.23	2237	1177	1.90	1.66

Chart 5.17 Asymmetric test results and empirical equations for overtopping for middle tank slot releases

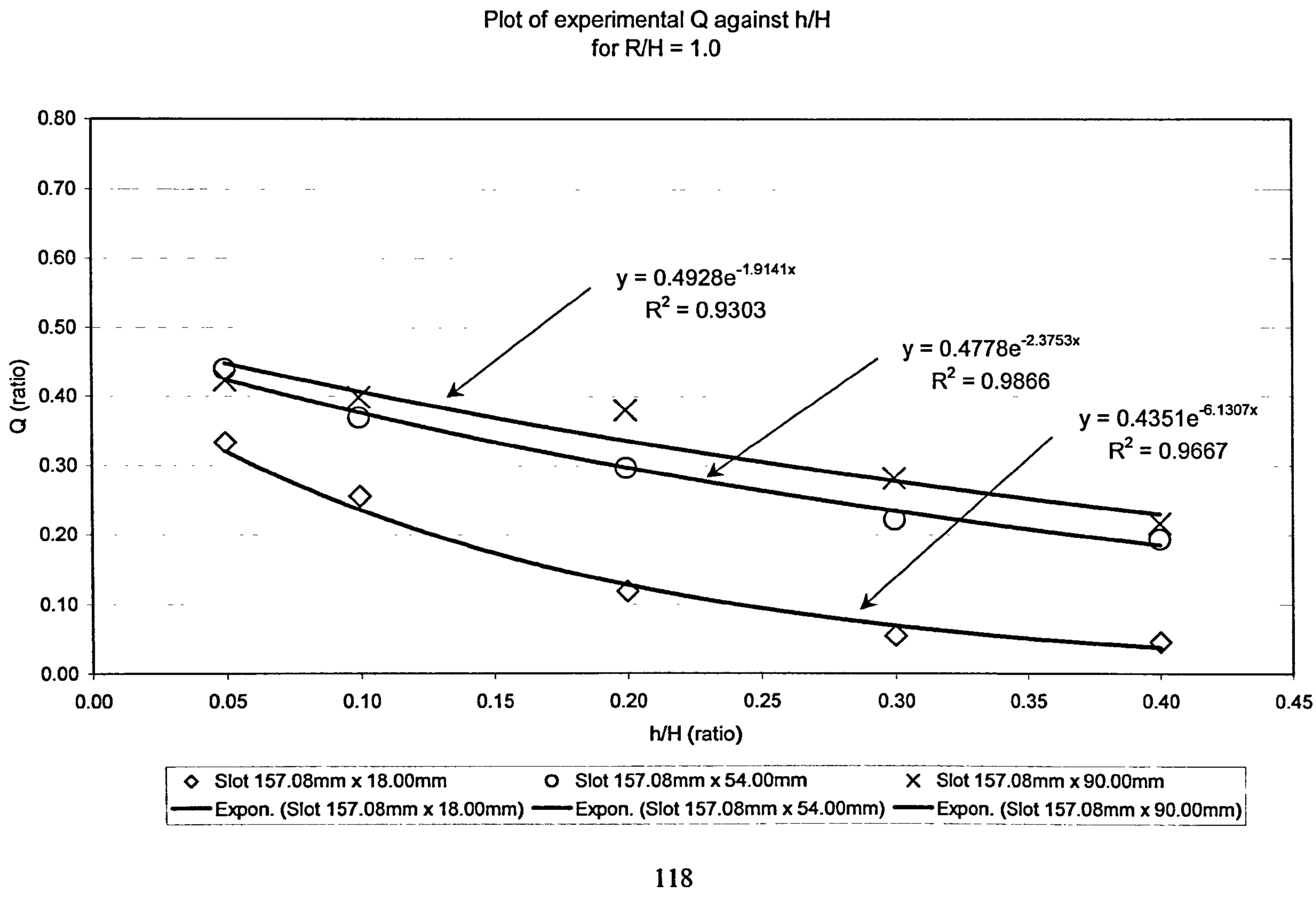

Chart 5.18 Asymmetric test results and empirical equations for the ratio Dyn/$Stat_{base}$ for middle tank slot releases

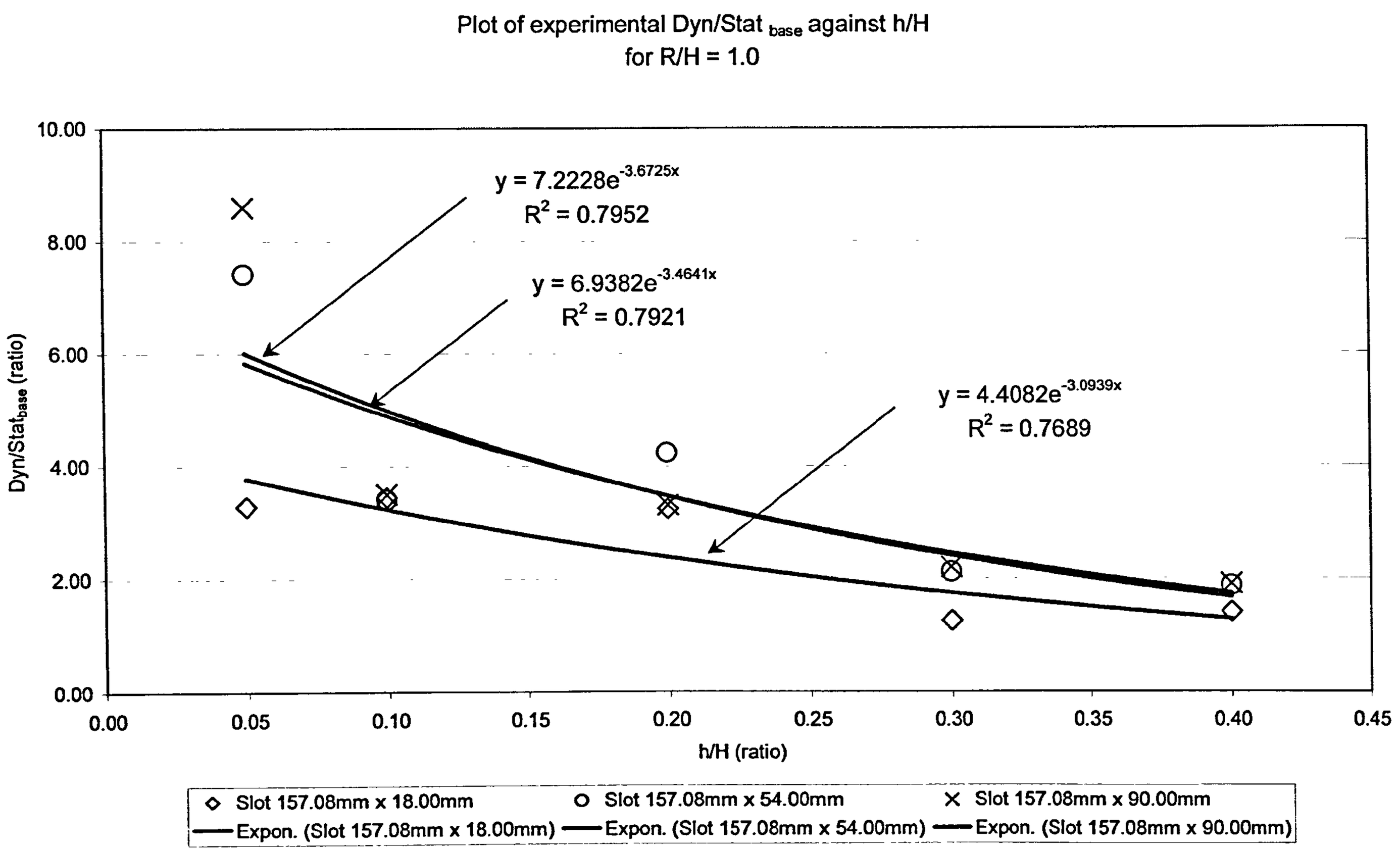

Table 5.22 Summary of results for asymmetric tall tank releases (orifice with 110% nominal bund capacity)

R	*300*	*mm*	*H*	*600*	*mm*				*R/H*	*0.5*			V_{rel}	*0.16965*	(m^3)	*Theoretical*
Orifice	*Dia*	*42.43*	*mm*													
h (Θ=90°) (mm)	*h/H*	*r (mm)*	*r/H*	*r/R*	*L (mm)*	V_{cap} (m^3)	V_{cap}/V_{rel}	V_{bund} (m^3)	V_{slosh} (m^3)	$V_{bund}+V_{slosh}$ (m^3)	*Q*	Q_f	Dyn_{base} *(Pa)*	$Stat_{base}$ *(Pa)*	*Dyn/Stat base*	*Dyn/Stat cal*
30	0.05	1407	2.35	4.69	1107	0.1866	1.10	0.12444	0.04484	0.16928	0.26	0.25	2353	294	8.00	7.15
60	0.10	995	1.66	3.32	695	0.1866	1.10	0.14012	0.02872	0.16884	0.17	0.20	2949	589	5.01	6.25
120	0.20	704	1.17	2.35	404	0.1868	1.10	0.15124	0.02036	0.17160	0.12	0.12	5991	1177	5.09	4.78
180	0.30	574	0.96	1.91	274	0.1863	1.10	0.15228	0.01636	0.16864	0.10	0.08	7453	1766	4.22	3.65
240	0.40	497	0.83	1.66	197	0.1862	1.10	0.16224	0.00692	0.16916	0.04	0.05	5946	2354	2.53	2.79
Orifice	*Dia*	*60.00*	*mm*													
h (Θ=90°) (mm)	*h/H*	*r (mm)*	*r/H*	*r/R*	*L (mm)*	V_{cap} (m^3)	V_{cap}/V_{rel}	V_{bund} (m^3)	V_{slosh} (m^3)	$V_{bund}+V_{slosh}$ (m^3)	*Q*	Q_f	Dyn_{base} *(Pa)*	$Stat_{base}$ *(Pa)*	*Dyn/Stat base*	*Dyn/Stat cal*
30	0.05	1407	2.35	4.69	1107	0.1866	1.10	0.12780	0.04140	0.16920	0.24	0.30	3023	294	10.28	6.76
60	0.10	995	1.66	3.32	695	0.1866	1.10	0.13020	0.03760	0.16780	0.22	0.24	2094	589	3.56	5.99
120	0.20	704	1.17	2.35	404	0.1868	1.10	0.13420	0.03464	0.16884	0.21	0.15	5368	1177	4.56	4.70
180	0.30	574	0.96	1.91	274	0.1863	1.10	0.14728	0.02092	0.16820	0.12	0.10	7578	1766	4.29	3.68
240	0.40	497	0.83	1.66	197	0.1862	1.10	0.16080	0.00756	0.16836	0.04	0.06	6657	2354	2.83	2.89
Orifice	*Dia*	*84.85*	*mm*													
h (Θ=90°) (mm)	*h/H*	*r (mm)*	*r/H*	*r/R*	*L (mm)*	V_{cap} (m^3)	V_{cap}/V_{rel}	V_{bund} (m^3)	V_{slosh} (m^3)	$V_{bund}+V_{slosh}$ (m^3)	*Q*	Q_f	Dyn_{base} *(Pa)*	$Stat_{base}$ *(Pa)*	*Dyn/Stat base*	*Dyn/Stat cal*
30	0.05	1407	2.35	4.69	1107	0.1866	1.10	0.11936	0.05036	0.16972	0.30	0.34	2084	294	7.09	4.58
60	0.10	995	1.66	3.32	695	0.1866	1.10	0.12524	0.04344	0.16868	0.26	0.28	1705	589	2.89	4.16
120	0.20	704	1.17	2.35	404	0.1868	1.10	0.12692	0.04260	0.16952	0.25	0.19	3057	1177	2.60	3.42
180	0.30	574	0.96	1.91	274	0.1863	1.10	0.14168	0.02668	0.16836	0.16	0.14	5534	1766	3.13	2.82
240	0.40	497	0.83	1.66	197	0.1862	1.10	0.15608	0.01288	0.16896	0.08	0.09	6002	2354	2.55	2.32

Chart 5.19 Asymmetric test results and empirical equations for overtopping for tall tank orifice releases

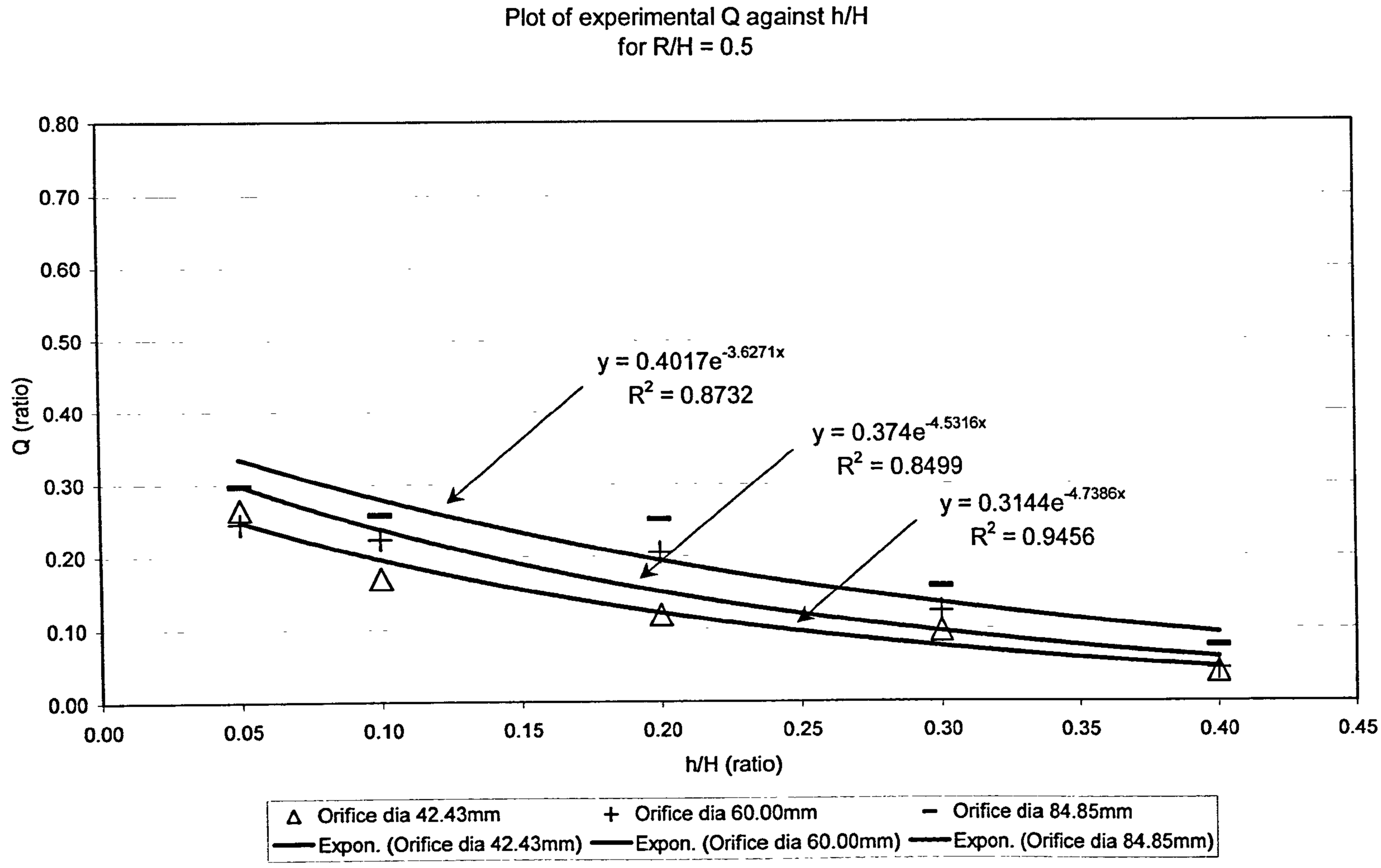

Chart 5.20 Asymmetric test results and empirical equations for the ratio Dyn/$Stat_{base}$ for tall tank orifice releases

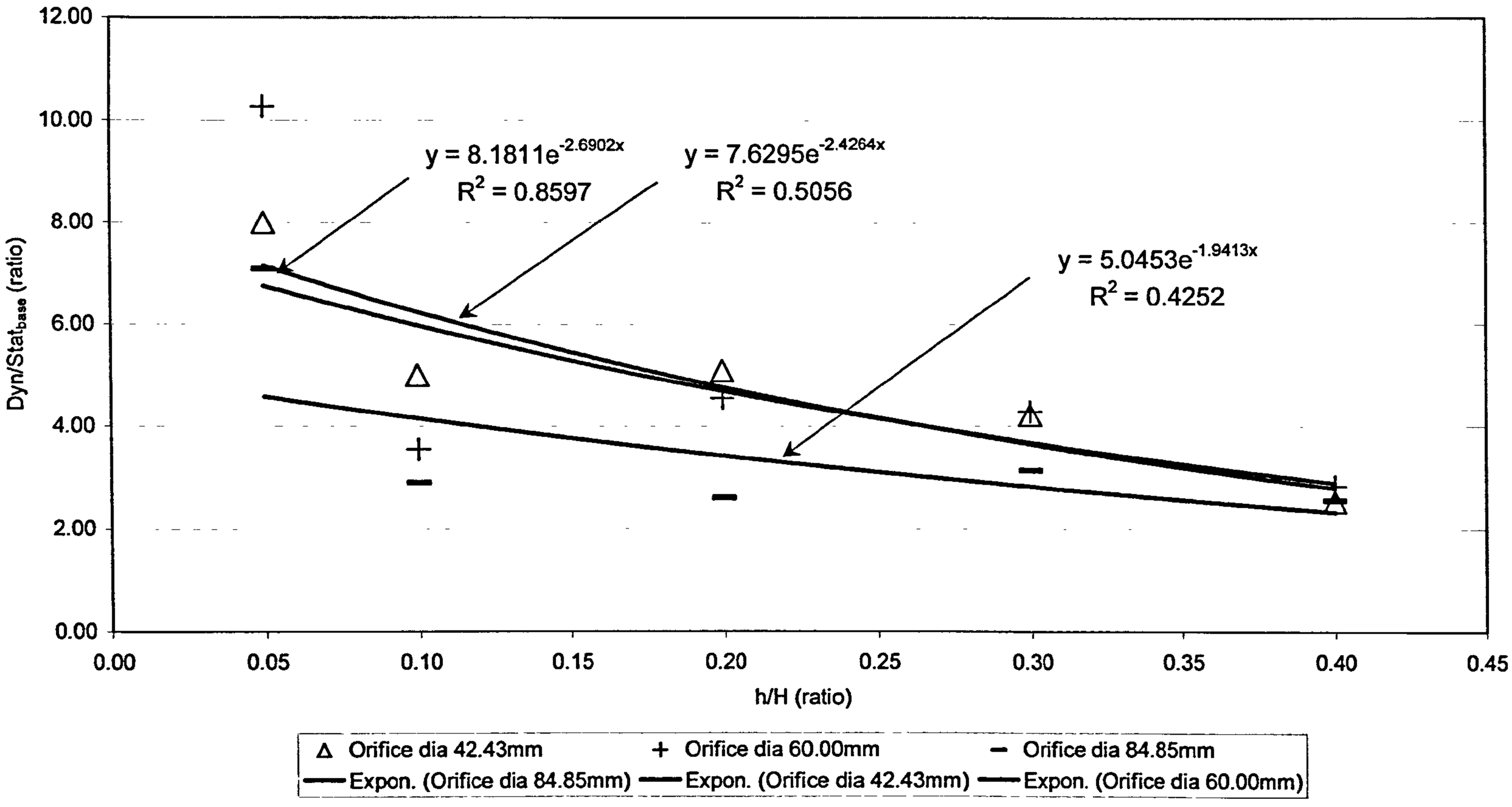

Table 5.23 Summary of results for asymmetric tall tank releases (slot with 110% nominal bund capacity)

R	*300*	*mm*	*H*	*600*	*mm*				*R/H*	*0.5*			*V_{rel}*	*0.16965*	*(m^3)*	*Theoretical*
Slot	*Width*	*157.08*	*mm*	*Height*	*36.00*	*mm*										
h (Θ=90°) (mm)	*h/H*	*r (mm)*	*r/H*	*r/R*	*L (mm)*	*V_{cap} (m^3)*	*V_{cap}/V_{rel}*	*V_{bund} (m^3)*	*V_{slosh} (m^3)*	*$V_{bund}+V_{slosh}$ (m^3)*	*Q*	*Q_f*	*Dyn_{base} (Pa)*	*$Stat_{base}$ (Pa)*	*Dyn/Stat base*	*Dyn/Stat cal*
30	0.05	1407	2.35	4.69	1107	0.1866	1.10	0.10004	0.06832	0.16836	0.41	0.36	1290	294	4.39	3.66
60	0.10	995	1.66	3.32	695	0.1866	1.10	0.12164	0.04656	0.16820	0.28	0.30	2048	589	3.48	3.19
120	0.20	704	1.17	2.35	404	0.1868	1.10	0.13760	0.03100	0.16860	0.18	0.21	1920	1177	1.63	2.42
180	0.30	574	0.96	1.91	274	0.1863	1.10	0.14412	0.02292	0.16704	0.14	0.14	2937	1766	1.66	1.84
240	0.40	497	0.83	1.66	197	0.1862	1.10	0.15100	0.01836	0.16936	0.11	0.10	4114	2354	1.75	1.39
Slot	*Width*	*157.08*	*mm*	*Height*	*108.00*	*mm*										
h (Θ=90°) (mm)	*h/H*	*r (mm)*	*r/H*	*r/R*	*L (mm)*	*V_{cap} (m^3)*	*V_{cap}/V_{rel}*	*V_{bund} (m^3)*	*V_{slosh} (m^3)*	*$V_{bund}+V_{slosh}$ (m^3)*	*Q*	*Q_f*	*Dyn_{base} (Pa)*	*$Stat_{base}$ (Pa)*	*Dyn/Stat base*	*Dyn/Stat cal*
30	0.05	1407	2.35	4.69	1107	0.1866	1.10	0.08772	0.07980	0.16752	0.48	0.48	2494	294	8.48	6.81
60	0.10	995	1.66	3.32	695	0.1866	1.10	0.09804	0.07044	0.16848	0.42	0.42	3195	589	5.42	5.60
120	0.20	704	1.17	2.35	404	0.1868	1.10	0.11468	0.05448	0.16916	0.32	0.32	3433	1177	2.92	3.78
180	0.30	574	0.96	1.91	274	0.1863	1.10	0.12392	0.04332	0.16724	0.26	0.25	3869	1766	2.19	2.56
240	0.40	497	0.83	1.66	197	0.1862	1.10	0.13744	0.03028	0.16772	0.18	0.19	5107	2354	2.17	1.73
Slot	*Width*	*157.08*	*mm*	*Height*	*180.00*	*mm*										
h (Θ=90°) (mm)	*h/H*	*r (mm)*	*r/H*	*r/R*	*L (mm)*	*V_{cap} (m^3)*	*V_{cap}/V_{rel}*	*V_{bund} (m^3)*	*V_{slosh} (m^3)*	*$V_{bund}+V_{slosh}$ (m^3)*	*Q*	*Q_f*	*Dyn_{base} (Pa)*	*$Stat_{base}$ (Pa)*	*Dyn/Stat base*	*Dyn/Stat cal*
30	0.05	1407	2.35	4.69	1107	0.1866	1.10	0.08416	0.08336	0.16752	0.50	0.55	2156	294	7.33	6.89
60	0.10	995	1.66	3.32	695	0.1866	1.10	0.08700	0.08296	0.16996	0.49	0.47	3352	589	5.69	5.69
120	0.20	704	1.17	2.35	404	0.1868	1.10	0.10676	0.06180	0.16856	0.37	0.34	4179	1177	3.55	3.89
180	0.30	574	0.96	1.91	274	0.1863	1.10	0.12284	0.04384	0.16668	0.26	0.24	4517	1766	2.56	2.65
240	0.40	497	0.83	1.66	197	0.1862	1.10	0.14260	0.02616	0.16876	0.16	0.17	4545	2354	1.93	1.81

Chart 5.21 Asymmetric test results and empirical equations for overtopping for tall tank slot releases

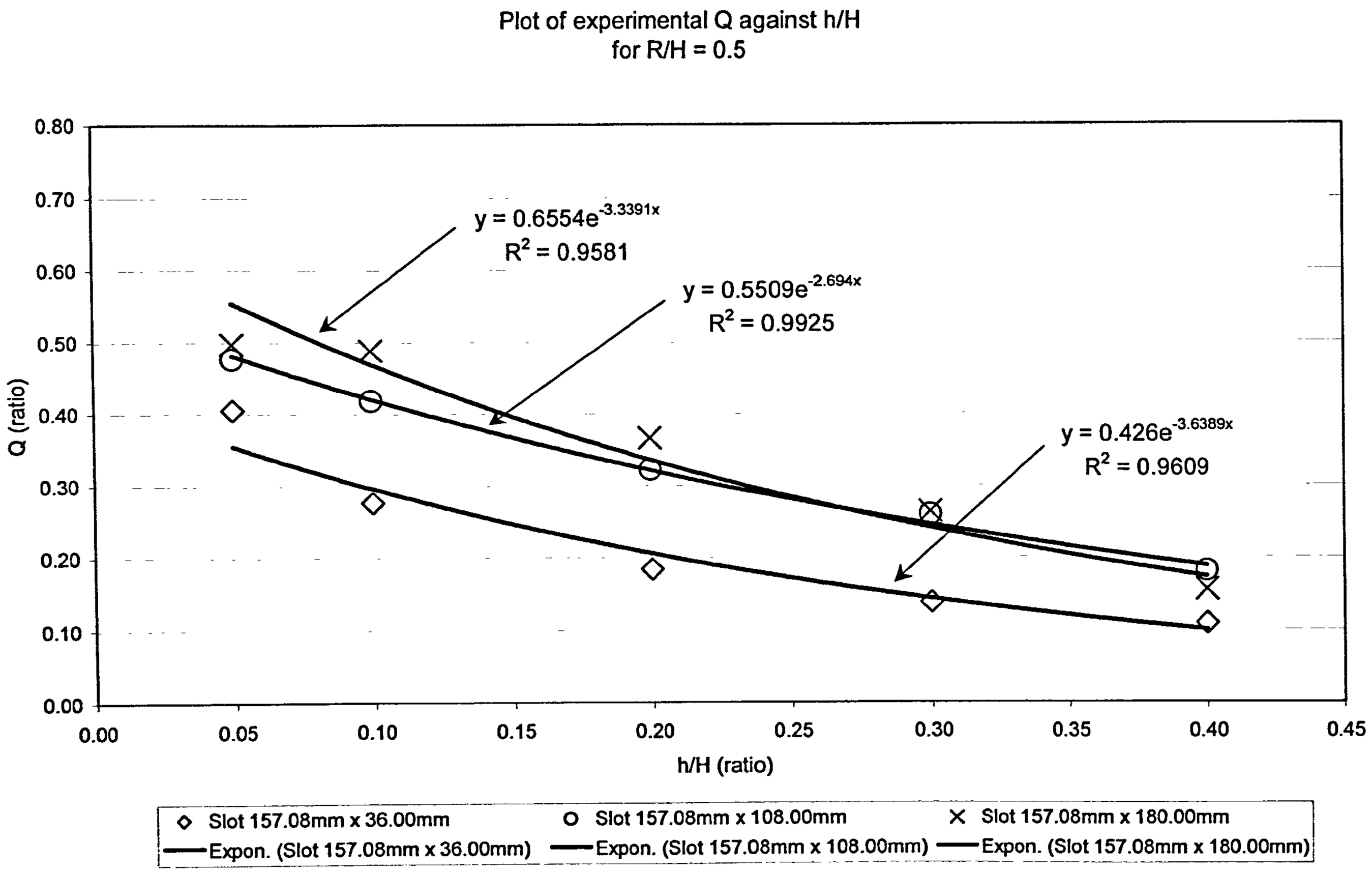

Chart 5.22 Asymmetric test results and empirical equations for the ratio Dyn/$Stat_{base}$ for tall tank slot releases

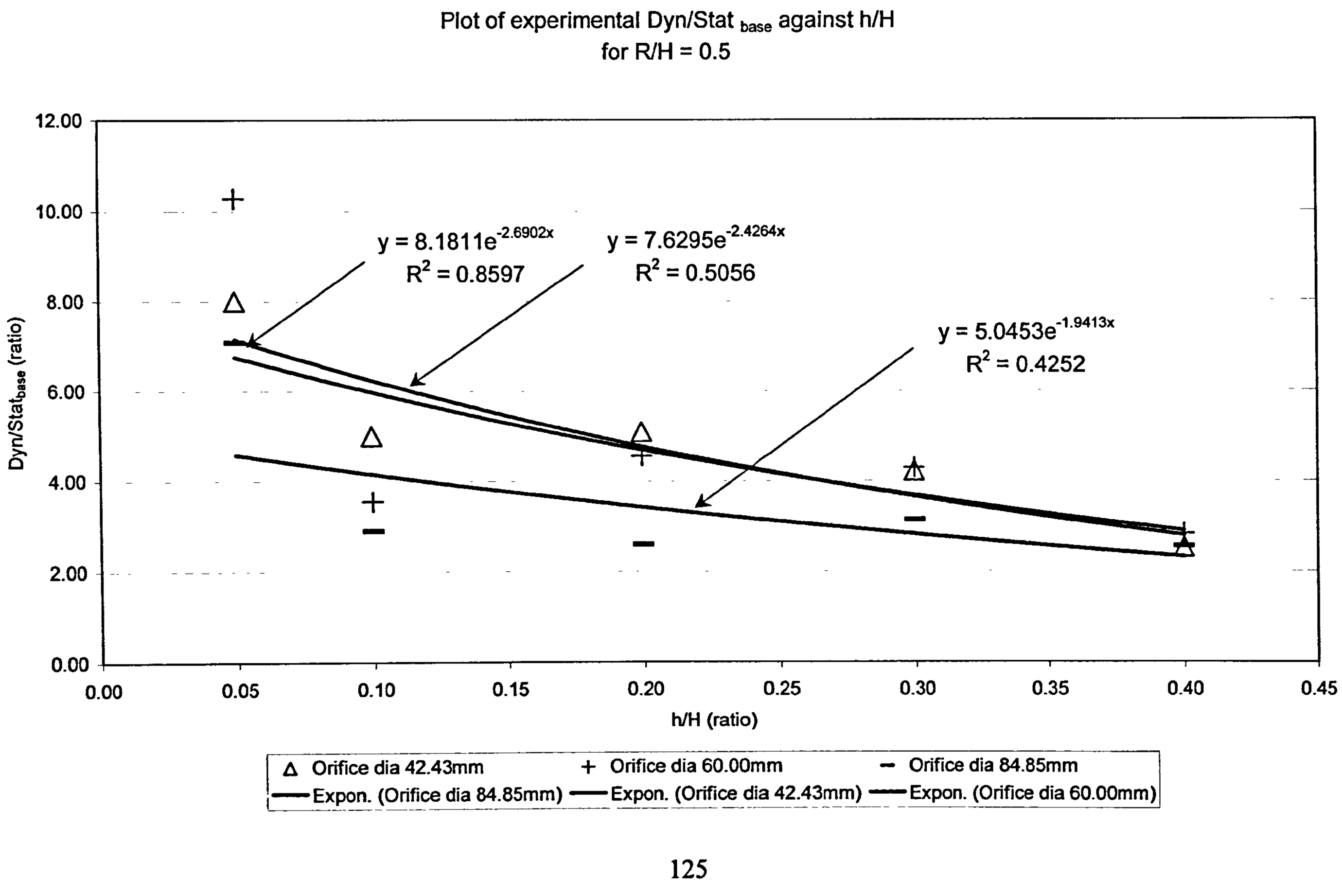

5.7 Interpretation of graphical results for asymmetric releases

The Charts 5.13 to 5.22 indicate both the quantity overtopping the bunds and the magnitudes of the dynamic pressures in terms of non-dimensional parameters for a bund capacity of 110 %. Again, the curves are derived from the best fit to the experimental data using the standard curve-fitting techniques available in Excel and the equations of the curve are shown along with the degree of fit, as indicated by R^2.

The dimensionless ratios used in the charts allow the equations to be used at any scale to predict both the amount of overtopping and the magnitude of the ratio of the dynamic to static pressures experienced due to an asymmetric failure of a bulk storage tank. The overtopping for squat tank orifice releases are all in the order of less than 2 % with the slot releases predicted form the equations indicated on the chart. The smallest slot used has the poorest degree of fit, mainly due to the apparent anomalous result for the smallest ratio of h/H. There are no predictions made for the dynamic pressure ratios in the cases of asymmetric releases for squat tanks.

For the overtopping related to middle tanks, the orifice releases all show a poor degree of fit and this can be attributed to effect of the eddy currents observed for certain configurations of tank and bund, particularly with the smallest orifice. The dynamic pressures also show a large degree of scatter and an empirical formula is only proposed for largest orifice. In the case of the slot releases for the middle tanks, the overtopping is reproducible with a good degree of fit, as are the pressure ratios, however there are some anomalous pressure results at the smaller values of h/H.

In the case of the overtopping for the tall tanks, the orifice releases are reproduced to a reasonable standard with a good degree of fit. The pressure ratios are less well reproduced for the orifice releases, again this is due to the results obtained for the lower values of h/H. The slot releases give good overtopping results across the range of apertures with a good degree of fit in all cases, however the pressure ratios are less well represented and have a lesser degree of fit. As in other cases, the degree of fit is compromised by the results obtained at lower values of h/H.

In general terms, the overtopping and pressure ratios increase along with the tank height and increase in potential energy, although there are some anomalies for both orifice and slot releases, possibly as a result of eddy currents produced due to the quadrant arrangement of the test rig. These anomalies were investigated to confirm the observations made during testing using a full 360° plastic barrel and bund arrangement constructed to the same scale as the test rig, but with a very basic rubber bung release allowing fluid to flow through the orifice. The data form these tests can be found in Tables 7.1.and 7.2 along with a more detailed discussion of the results in section 7.5.

Table 5.24 Example comparison of results for squat tank releases (0.5% area of release 110% nominal bund capacity) configuration identity B1 (h48)

Configuration identity	*Tank radius, R (mm)*	*Tank fluid depth, H (mm)*	*Bund radius, r (mm)*	*Bund height, h (mm)*	*Ratio of h/H*
B1(h48)	300	120	497	48	0.4

		Dynamic pressures		
Height from base (%)	*Static pressure (Pa)*	*Axisymmetric (Pa)*	*Asymmetric Orifice (Pa)*	*Asymmetric Slot (Pa)*
0	471	732	675	370
10	424	698	573	312
30	330	628	369	198
50	235	488	72	47
70	141	259	50	90
90	47	273	-11	-29
100	0			
Max Overtopping (%)		23.9	1.8	1.1

Chart 5.23 Example comparison of pressure and overtopping results for squat tank releases (0.5% area of release 110% nominal bund capacity) configuration identity B1 (h48)

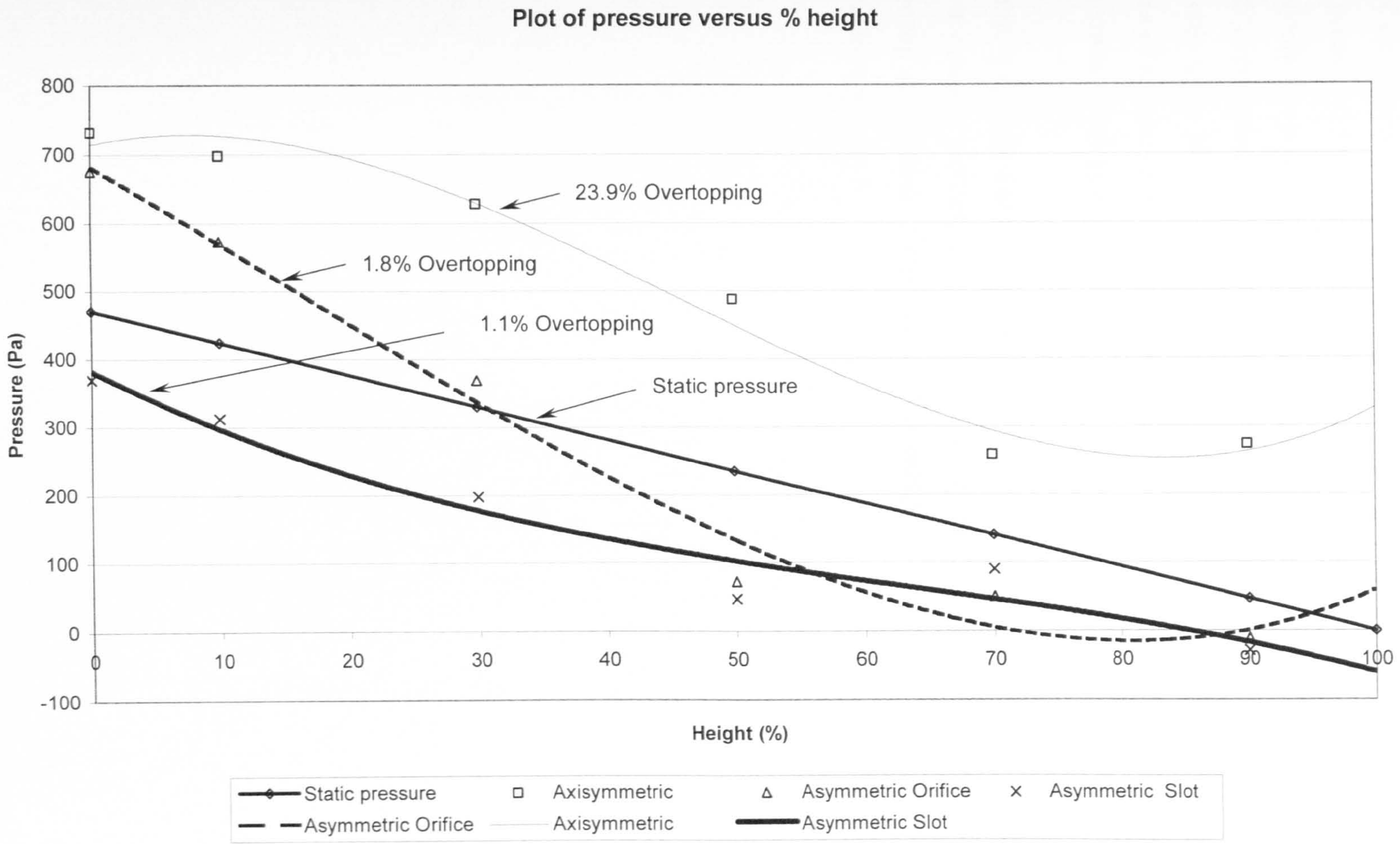

5.8 Interpretation of comparative graphical results for dynamic pressure profiles and overtopping

Table 5.24 and Chart 5.23 indicate the relationships between the various types of release in terms of the pressure profiles along the percentage height of the bund walls for asymmetric release areas of 0.5 % compared to the full axisymmetric release. For squat tank releases, the axisymmetric pressure profile is consistently above the normal static pressure designed for with overtopping of 23.9 %. The orifice release exhibits pressures above the static values only up to 30 % of the bund height and as such, the overtopping is only 1.8 %. In the cases of the slot release, the pressure profile is consistently below the static values and has the lowest overtopping of 1.1 %.

Generally, it appears that the greater the deviation of the dynamic pressure profiles above the static pressure profiles, the greater the overtopping, particularly if the deviation occurs near the top of the bund. These charts are examples taken from a more extensive range to be found in Appendix 6.

Table 5.25 Example comparison of overtopping results for middle tank orifice releases (various areas of release 110% nominal bund capacity)

Configuration identity	*Tank radius, R (mm)*	*Tank fluid depth, H (mm)*	*R/H*	*Bund capacity (%)*	*Angle of bund, Θ (°)*
Orifice releases	300	300	1.0	110	90

h/H	$Q_{0.125}$ *Orifice*	$Q_{0.250}$ *Orifice*	$Q_{0.500}$ *Orifice*	Q_{100} *Axisymmetric*
0.05	0.06	0.06	0.14	0.62
0.10	0.13	0.14	0.15	0.62
0.20	0.02	0.09	0.14	0.52
0.30	0.08	0.13	0.18	0.38
0.40	0.08	0.10	0.12	0.28

Chart 5.24 Example comparison of overtopping results for middle tank orifice releases (various areas of release 110% nominal bund capacity)

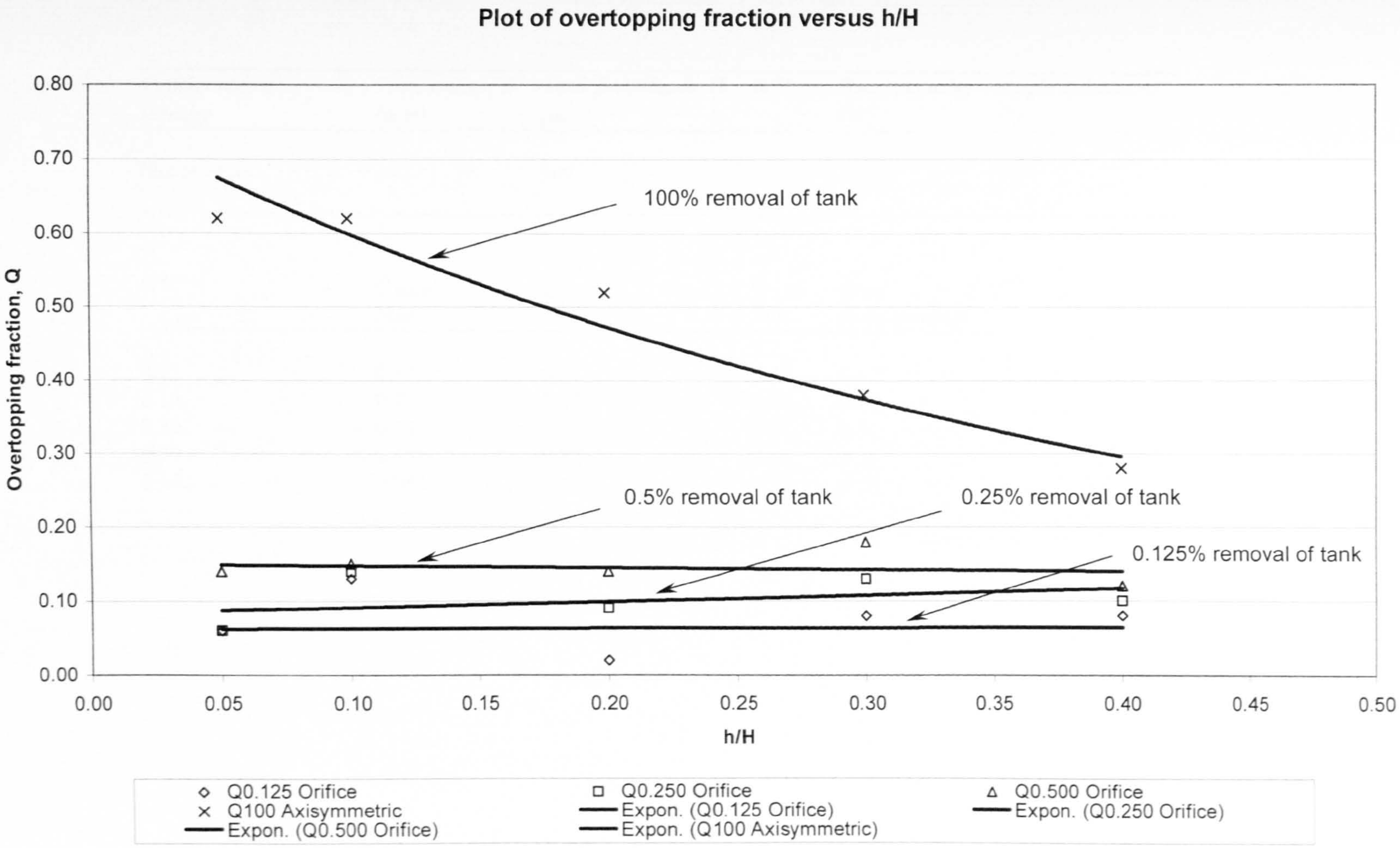

Table 5.26 Example comparison of overtopping results for middle tank slot releases (various areas of release 110% nominal bund capacity)

Configuration identity	*Tank radius, R (mm)*	*Tank fluid depth, H (mm)*	*R/H*	*Bund capacity (%)*	*Angle of bund, Θ (°)*
Slot releases	300	300	1.0	110	90

h/H	$Q_{0.500}$ *Slot*	$Q_{1.500}$ *Slot*	$Q_{2.500}$ *Slot*	Q_{100} *Axisymmetric*
0.05	0.33	0.44	0.42	0.62
0.10	0.26	0.37	0.40	0.62
0.20	0.12	0.30	0.38	0.52
0.30	0.05	0.22	0.28	0.38
0.40	0.05	0.19	0.22	0.28

Chart 5.25 Example comparison of overtopping results for middle tank slot releases (various areas of release 110% nominal bund capacity)

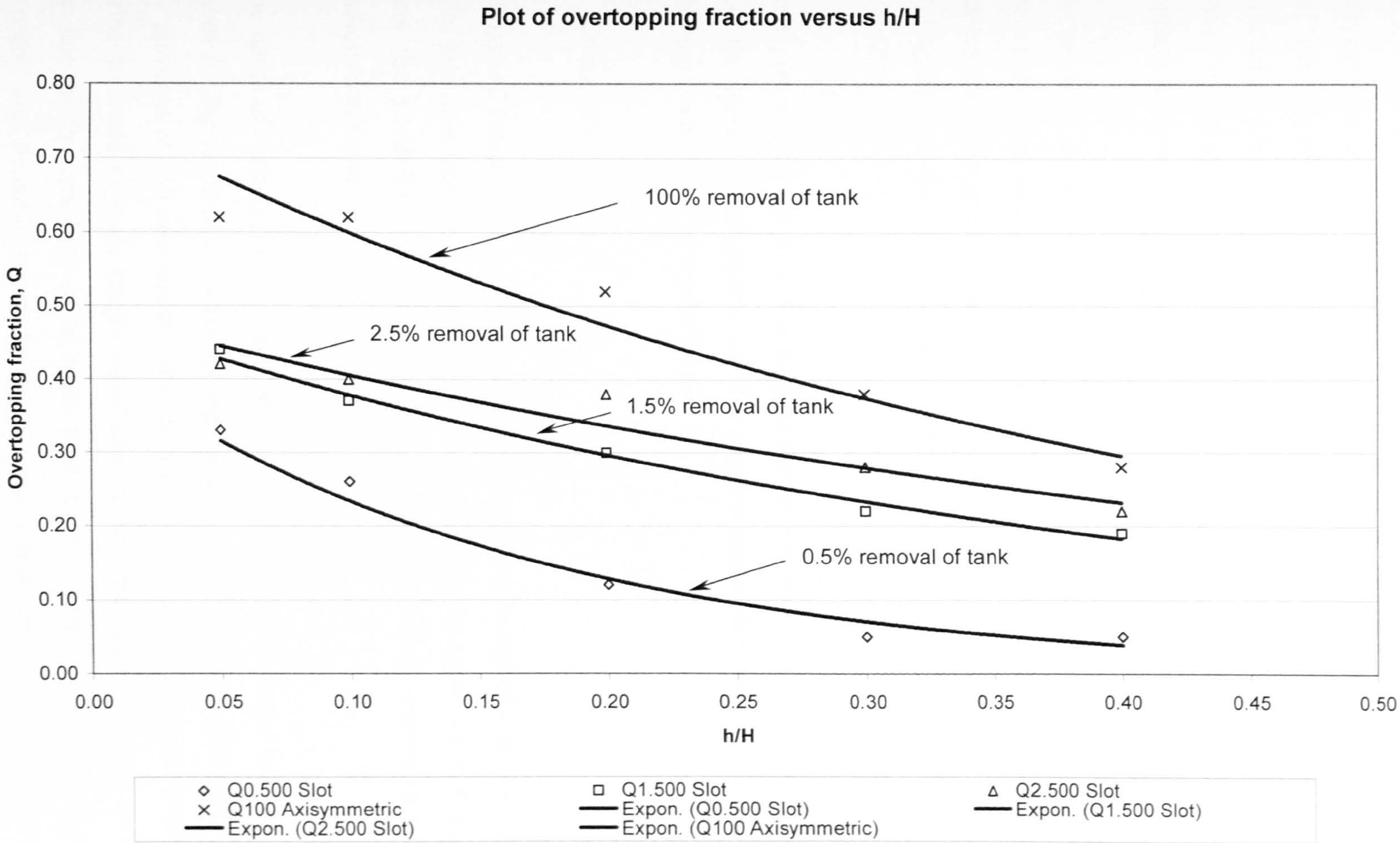

5.9 Interpretation of comparative graphical results for overtopping in terms of area of removal

Tables 5.25 and 5.26 together with Charts 5.24 and 5.25 indicate the relationships between the axisymmetric and asymmetric test results in term of the overtopping fraction and the ratio of h/H. In the case of orifice releases, the overtopping fractions are considerably lower (nominally less than 20 %) than those obtained for the full axisymmetric releases (28 to 62 %). It can be seen that the smaller the area of removal, the smaller the values of overtopping with respect to h/H.

For slot releases, the same observation is made and in all cases the overtopping fractions are lower than those obtained for the full axisymmetric releases (28 to 62 %), however the differences are not as great as those in the case of the orifice releases. The smaller area of removal again gives the smaller values of overtopping with the largest area giving a range of 22 to 42 %.

Generally, the smaller the area of release the smaller the overtopping fraction, however the shape of the aperture is of importance. The charts discussed are only examples taken from a fuller range to be found in Appendix 7.

5.10 Summary

The tables and charts in the summary of results indicate the extent of both overtopping and dynamic pressures that can occur post failure of a bulk storage tank. Upon inspection this presents the possibility of estimating the magnitude of such events using suitable correlations and equations.

For the range of variables investigated, the analysis of results proposes suitable empirical equations for the prediction of overtopping fractions and dynamic to static pressure ratios for the purposes of risk assessment. The equations and constants indicated for the various scenarios are valid over the ranges stated and exclude the ranges for high-collar bunds. This is due the fact that high-collar bunds pose much less of a problem in terms of both overtopping and dynamic pressures and are much less common than lower forms of bunding. This is directly related to the cost of the installation of high-collar bunds, which can be excessive and difficult to justify using current statistically based risk assessments.

CHAPTER 6

Analysis of Results

6.1 Introduction

The main aim of this investigation was to simulate various modes of failure over a wide range of tank and bund configurations and to determine the extent of the losses in terms of possible overtopping of the bunds and to quantify the magnitudes of the dynamic pressures exerted on the bunds. From the vast amount of data collected, empirical equations were derived based on dimensionless parameters, using curve-fitting techniques available within the Excel spreadsheet package. Tables 6.1 to 6.6 indicate the constants to be used for the various data sets based on mode of failure, tank type and bund capacity.

6.2 Correlations and equations for the prediction of overtopping fractions for axisymmetric failures

The test configurations sub-divided the tanks into three categories (squat, middle and tall). These groups are based on the ratios of tank radius to tank height giving the ratios of 2.5, 1.0 and 0.5 respectively. The equation produced (6.1) then requires the use of two constants (Table 6.1) to allow the prediction of losses. The constants allow for variations not only in tank configuration but also bund capacity. The equation is valid for the three-tank radius to tank height ratios of 2.5, 1, and 0.5 and for bund capacities ranging from 110 to 200 %.

The equation

$$Q = A\,exp\left[-B\left(\frac{h}{H}\right)\right] \qquad (6.1)$$

with A and B taking the values shown below (Table 6.1), is recommended to estimate the overtopping fraction. The equation is of the same form as that suggested by Clark et al (2001). The range of validity is $0.66 \leq (r - R) / R \leq 5.32$. It should be noted that high-collar bunds are excluded from the range of validity, as the overtopping fraction is negligible, usually less than 5 %, the bulk of which can normally be recovered from site. Omitting the high-collar bunds improves the quality of fit for the smaller bunds at greater

radii, where frictional forces start to affect the result, as evidenced by the reduction in impact velocities.

Table 6.1 Constants used in Equation 6.1 for prediction of losses for axisymmetric failures

Tank type	*Bund capacity (%)*	*A*	*B*
Squat	110	0.5789	2.0818
	120	0.5193	1.9671
	150	0.3978	2.0051
	200	0.1824	0.4972
Middle	110	0.7588	2.3529
	120	0.7306	2.3834
	150	0.6359	2.4451
	200	0.4814	2.1866
Tall	110	0.8873	3.1682
	120	0.8942	3.4692
	150	0.8244	3.4712
	200	0.7369	3.5240

6.3 Correlations and equations for the prediction of dynamic pressures for axisymmetric failures

Using the same test configurations as described in Section 6.2 the dynamic pressures at the base of the bund can be determined from the ratio of the dynamic pressures to static pressure, $Dyn/Stat_{base}$, which are evaluated from an equation of the same form as that used for calculation of the overtopping fractions.

The constants listed in Table 6.2 are used to predict the magnitude of the ratio $Dyn/Stat_{base}$ encountered with axisymmetric releases again using Equation 6.2. The configurations are again represented over various bund capacities with the three ratios of tank radius to tank height, R/H represented as 'squat', 'middle' and 'tall'.

$$Dyn/Stat_{base} = C\ exp\left[-D\left(\frac{h}{H}\right)\right] \qquad (6.2)$$

Table 6.2 Constants used in Equation 6.2 for prediction of dynamic pressures for axisymmetric failures

Tank type	*Bund capacity (%)*	*C*	*D*
Squat	110	28.9250	8.3704
	120	8.0669	4.2599
	150	10.9630	5.1350
	200	5.4911	3.0111
Middle	110	9.4121	4.5712
	120	8.4295	4.6397
	150	6.7030	4.3532
	200	7.4184	5.1410
Tall	110	9.8056	4.8587
	120	7.4835	4.3025
	150	8.2102	5.0004
	200	7.5531	5.2278

6.4 Correlations and equations for the prediction of overtopping fractions for asymmetric orifice failures

For asymmetric releases, the same ratios of R/H were employed, however only bund capacities of 110 % were investigated due to the additional complication of three orifice diameters being introduced with a range of validity of $0.66 \leq (r - R) / R \leq 3.69$. In cases where no empirical formula is proposed for the overtopping fraction, the constants in Table 6.3 are listed as 'Na'.

Table 6.3 Constants used in Equation 6.1 for prediction of losses for asymmetric orifice failures

Tank type	*Bund capacity (%)*	*Orifice dia (mm)*	*A*	*B*
Squat	110	18.97	Na	Na
		26.83	Na	Na
		37.95	Na	Na
Middle	110	30.00	0.0665	0.1256
		42.43	0.0839	0.7674
		60.00	0.1509	0.2018
Tall	110	42.43	0.3144	4.7386
		60.00	0.3740	4.5316
		84.85	0.4017	3.6271

6.5 Correlations and equations for the prediction of dynamic pressures for asymmetric orifice failures

Table 6.4 indicates the values of the constants C and D for the determination of the ratio *Dyn/Stat* $_{base}$ for the orifice releases. Again, where no empirical equation is proposed the values of C and D are listed as 'Na'.

Table 6.4 Constants used in Equation 6.2 for prediction of dynamic pressures for asymmetric orifice failures

Tank type	*Bund capacity (%)*	*Orifice dia (mm)*	*C*	*D*
Squat	110	18.97	Na	Na
		26.83	Na	Na
		37.95	Na	Na
Middle	110	30.00	Na	Na
		42.43	Na	Na
		60.00	4.8340	2.8167
Tall	110	42.43	8.1811	2.6902
		60.00	7.6295	2.4264
		84.85	5.0453	1.9413

6.6 Correlations and equations for the prediction of overtopping fractions for asymmetric slot failures

For the slot failures, values of A and B in Table 6.5 are listed throughout the configurations employed, making overtopping predictions possible in all the cases investigated for a range of $0.66 \leq (r - R) / R \leq 3.69$.

Table 6.5 Constants used in Equation 6.1 for prediction of losses for asymmetric slot failures

Tank type	*Bund capacity (%)*	*Slot height (mm)*	*A*	*B*
Squat	110	7.20	0.0547	4.2640
Slot width		21.60	0.3496	3.5033
157.08mm		36.00	0.3445	2.1237
Middle	110	18.00	0.4350	6.1307
Slot width		54.80	0.4778	2.3753
157.08mm		90.00	0.4928	1.9141
Tall	110	36.00	0.4260	3.6389
Slot width		108.00	0.5509	2.6940
157.08mm		180.00	0.6554	3.3391

6.7 Correlations and equations for the prediction of dynamic pressures for asymmetric slot failures

Table 6.6 gives values of C and D for the determination of $Dyn/Stat_{base}$ for slot releases with the 'squat' tanks having no empirical formulae.

Table 6.6 Constants used in Equation 6.2 for prediction of dynamic pressures for asymmetric slot failures

Tank type	*Bund capacity (%)*	*Slot height (mm)*	*C*	*D*
Squat	110	7.20	Na	Na
Slot width		21.60	Na	Na
157.08mm		36.00	Na	Na
Middle	110	18.00	4.4082	3.0939
Slot width		54.80	6.9382	3.4641
157.08mm		90.00	7.2228	3.6725
Tall	110	36.00	4.2077	2.7650
Slot width		108.00	8.2802	3.9153
157.08mm		180.00	8.3413	3.8197

6.8 Dimensional analysis

The method of dimensional analysis is valid for comparison of the same phenomenon at different scales and speeds. Common forms of non-dimensional groups used in fluid mechanics are Reynolds number, the Froude number, the Mach number and the Webber number. The magnitude of the forces exerted on the escaping fluid depends on the mean velocity, on the size of the release (length or depth), on the fluid viscosity and density and on the gravitational acceleration. Gravity is important, as any changes in fluid level involve a gravity force tending to cause acceleration or a deceleration as the release progresses. It is important that the length in the model is taken at the same point as the full size prototype so that a suitable scale can be determined.

The problem is therefore a function of Reynolds number and the Froude number.

Reynolds number, R_e:

$$R_e = \frac{ul}{\mu/\rho} \tag{6.3}$$

Froude number, F_r:

$$F_r = \frac{u}{(gl)^{1/2}} \tag{6.4}$$

Where, u = velocity, l = length, μ = viscosity, ρ = density of liquid & g = acceleration due to gravity

The frictional forces cannot be reproduced using the same scale as the gravitational forces due to the problems with viscosity scales. The scale of the model test rig was chosen to allow the effects of friction to be ignored, thus leaving the gravitational forces to be correctly modelled (Francis, 1975).

This gives:

$$\frac{u_m}{(gl_m)^{1/2}} = \frac{u_p}{(gl_p)^{1/2}}$$

The scaling law for velocities is therefore :

$$\frac{u_m}{u_p} = \left(\frac{l_m}{l_p}\right)^{1/2} \quad as\ g\ is\ a\ constant \tag{6.5}$$

Where, u_m = velocity in model & u_p = velocity in prototype

l_m = model length & l_p = length in prototype

6.9 Summary

The empirical equations derived from the experimental data require validation and their performances are checked by initial comparison with the measured data they were developed to represent. As to the potential usefulness the equations, this can best be determined from their ability to reproduce results produced from a reliable source. The problem with this approach is that no definitive set of data has been previously established and comparisons with various sources are therefore required to determine the accuracy of any predictions made. The seminal works originally identified will therefore form the basis for comparison for the orders of magnitude for overtopping, wave celerity and dynamic pressures with the Ashland Oil spill (1988) used as a case study.

CHAPTER 7

Performance of Empirical Formulae and Case Studies

7.1 Historical approaches for modelling

Various methodologies have been employed in an effort to suitably quantify the losses in the event of the failure of a bulk storage tank; these include the application of pure mathematics, physical modelling and more recently computational fluid dynamics (CFD). Each method has its merits, however an underlying fact remains that some form of validation is required to ensure a rigorous approach and to give a level of confidence in the resulting predictions.

The recent and ever developing field of computer hardware and software has made CFD a more viable option for the analysis of free surface flow, which is complicated by the instability of the complex algorithms used in the computation together with the demands made on the processors. Today, such software is able to run simulations more efficiently on high speed dual-core processors or even able to share the work between several machines using parallel processing techniques.

One of the main problems encountered with the use of commercially available generic CFD packages is the problem of accurately evaluating the overtopping fraction, given the mixing of the liquid with air during the initial release and subsequent bund impact. The volume fraction (liquid/air) contained within each cell has to be determined and the sum of the cells overtopping the bund calculated, based on an assessment of a suitable minimum value for the fraction of liquid in each cell. This causes inherent errors in the determination of the overtopping fraction, as the magnitude is dependent on the value used for the minimum volume fraction for the individual cells. Thus, the overtopping fraction is sensitive to changes in the cell volume fraction used as the trigger to be counted in the final summation of the cells moving out of the bund boundary.

As far as modelling a wide range of data sets, there seems to be little evidence that CFD has been used to build suitable mathematical models for the purposes of loss prediction and risk assessment. The general use of such tools appears to be limited to individual cases and specific scenarios. Hence there is a need for complementary work in the field of

physical modelling and the development of empirical formulae to aid in the development of such packages. The work of Ivings and Webber (2007) in the development of 'SPLOT' using the data and empirical formulae produce by Atherton (2005) is one example where major advances are being made. The additional modelling work carried out in this research will further reinforce the material published by Atherton (2005), especially with regard to the determination of the dynamic pressures for both axisymmetric and asymmetric releases.

7.2 Correlations and equations for the prediction of overtopping fractions and dynamic pressures

The performance of the empirical equations for overtopping and dynamic pressures formulated from the collected data sets is investigated in the following sections. The equations have been developed using curve-fitting techniques and algorithms available in Excel and the degree of fit determined using R^2 (where R is the correlation coefficient). They are evaluated against the measured values from which they were derived as well as the equations suggested by other researchers. The final assessment uses various experimental data sets; CFD model results and case studies in an attempt to further validate the work.

Chart 7.1 Example performance of empirical equations versus experimental results for overtopping for middle tank axisymmetric releases (various bund capacities)

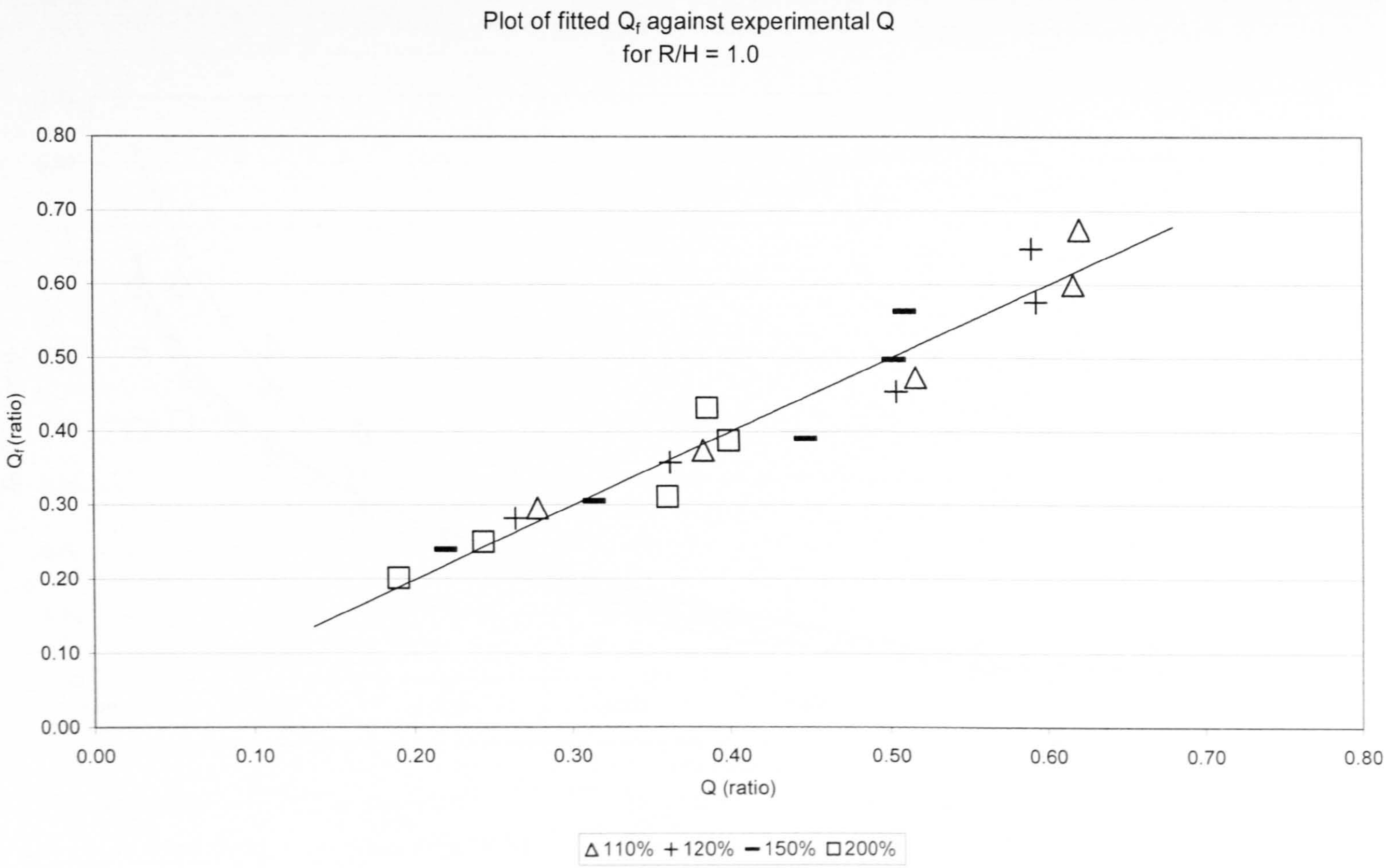

Chart 7.2 Example predictions using Clark and Hirst equations for overtopping in relation to experimental results for middle tank axisymmetric releases (various bund capacities)

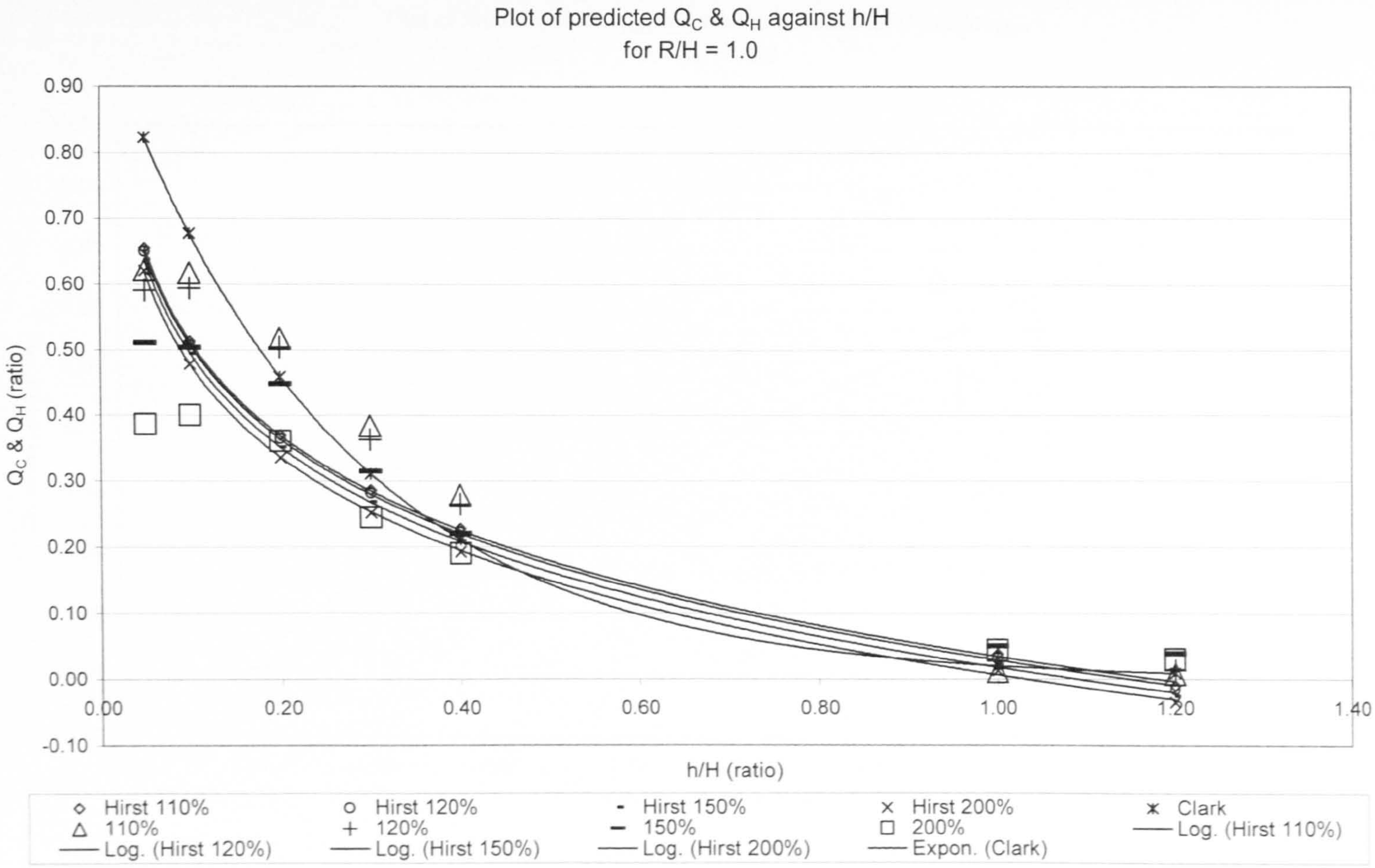

Chart 7.3 Example performance of empirical equations versus experimental results for the ratio $Dyn/Stat_{base}$ for middle tank axisymmetric releases (various bund capacities)

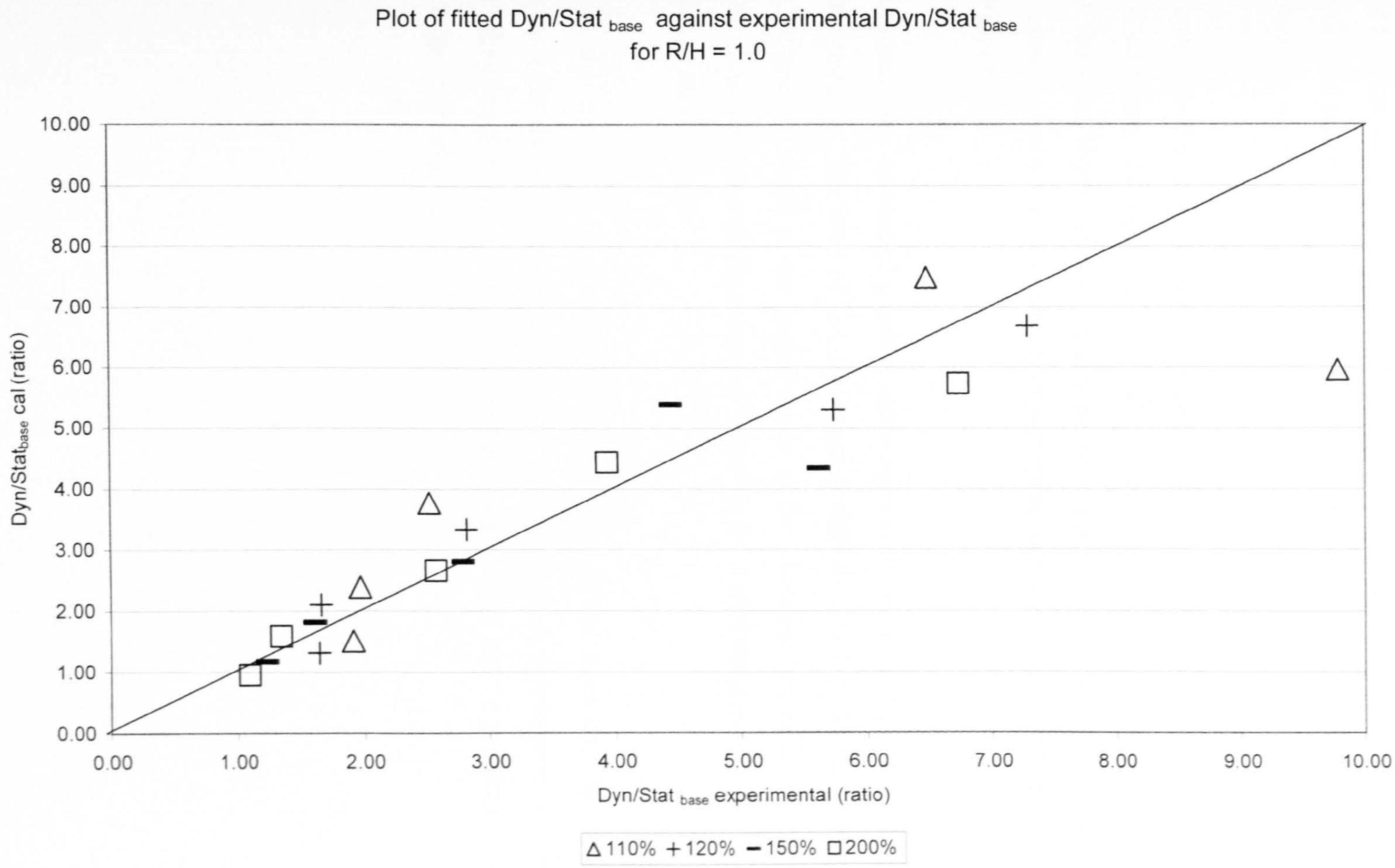

7.3 Interpretation of graphical results for the performance of the empirical equations for axisymmetric releases

Chart 7.1 shows a plot of the calculated overtopping fraction against the measured overtopping fraction for axisymmetric middle tank releases and indicates a good level of fit with only minimal scatter. The empirical equation is therefore a reasonable representation of the overtopping fractions for the configurations considered.

Chart 7.2 represents the predictions of overtopping fractions against h/H for axisymmetric releases and compares the new experimental results to the equations proposed by Clark (2001) and Hirst in Thyer (2002). It can be seen that both sets of equations show a reasonable approximation of the data, however there are significant differences at the smaller values of h/H.

Chart 7.3 indicates the calculated pressure ratios against the measured pressure ratios for axisymmetric releases. The level of fit is again acceptable over most of the range, however there is an anomalous result at the higher range of the pressures considered, where the calculated result underestimates the measured value for the 110% bund capacity relating to one of the lower ratios of h/H.

Generally, in the case of axisymmetric releases, the empirical equations for both the overtopping and the dynamic pressures perform relatively well in representing the results from which they were derived. As such they are suitable for use in predicting values within the ranges investigated.

Chart 7.4 Example performance of empirical equations versus experimental results for overtopping for middle tank asymmetric orifice releases (110% bund capacity)

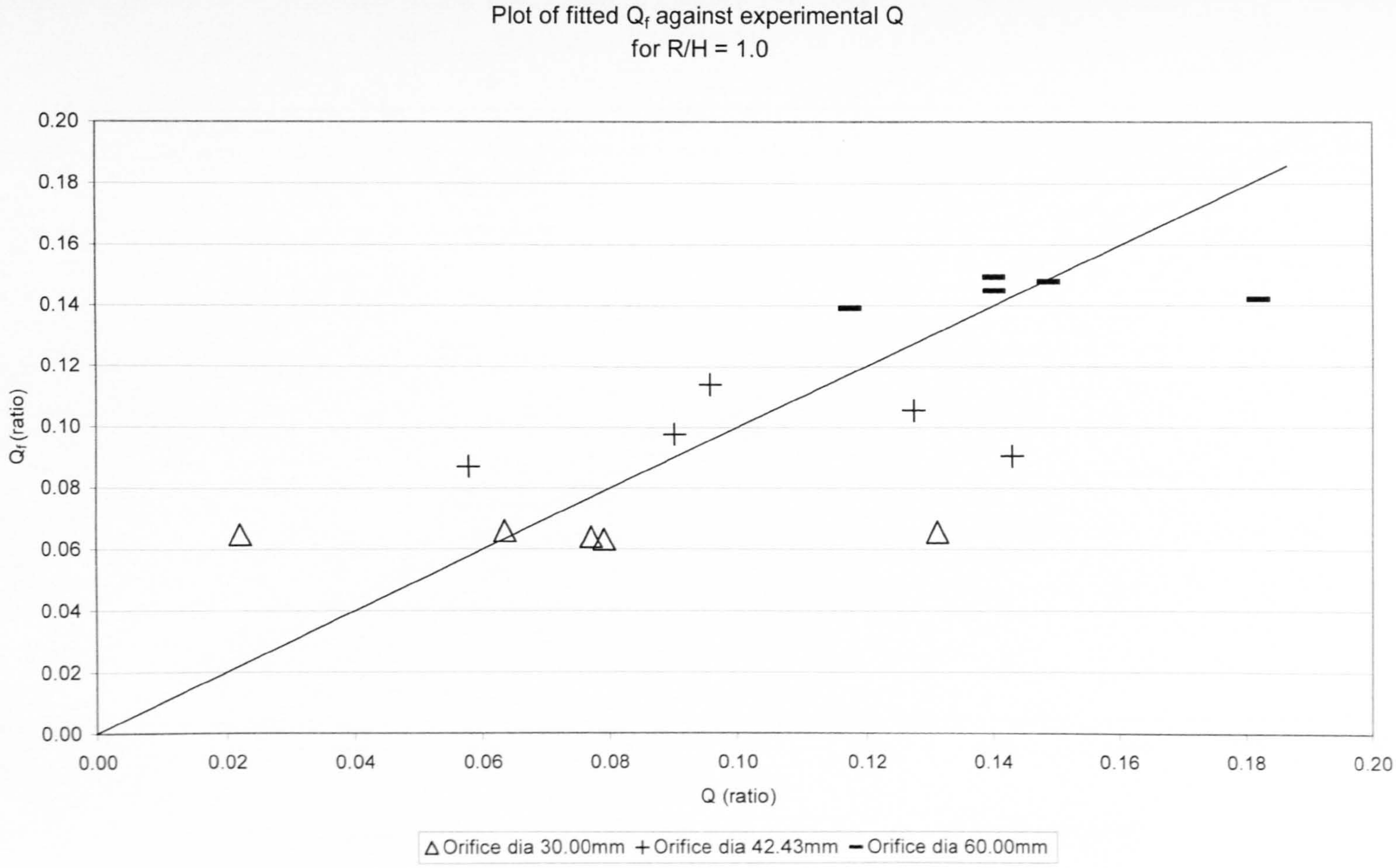

Chart 7.5 Example performance of empirical equations versus experimental results for overtopping for middle tank asymmetric slot releases (110% bund capacity)

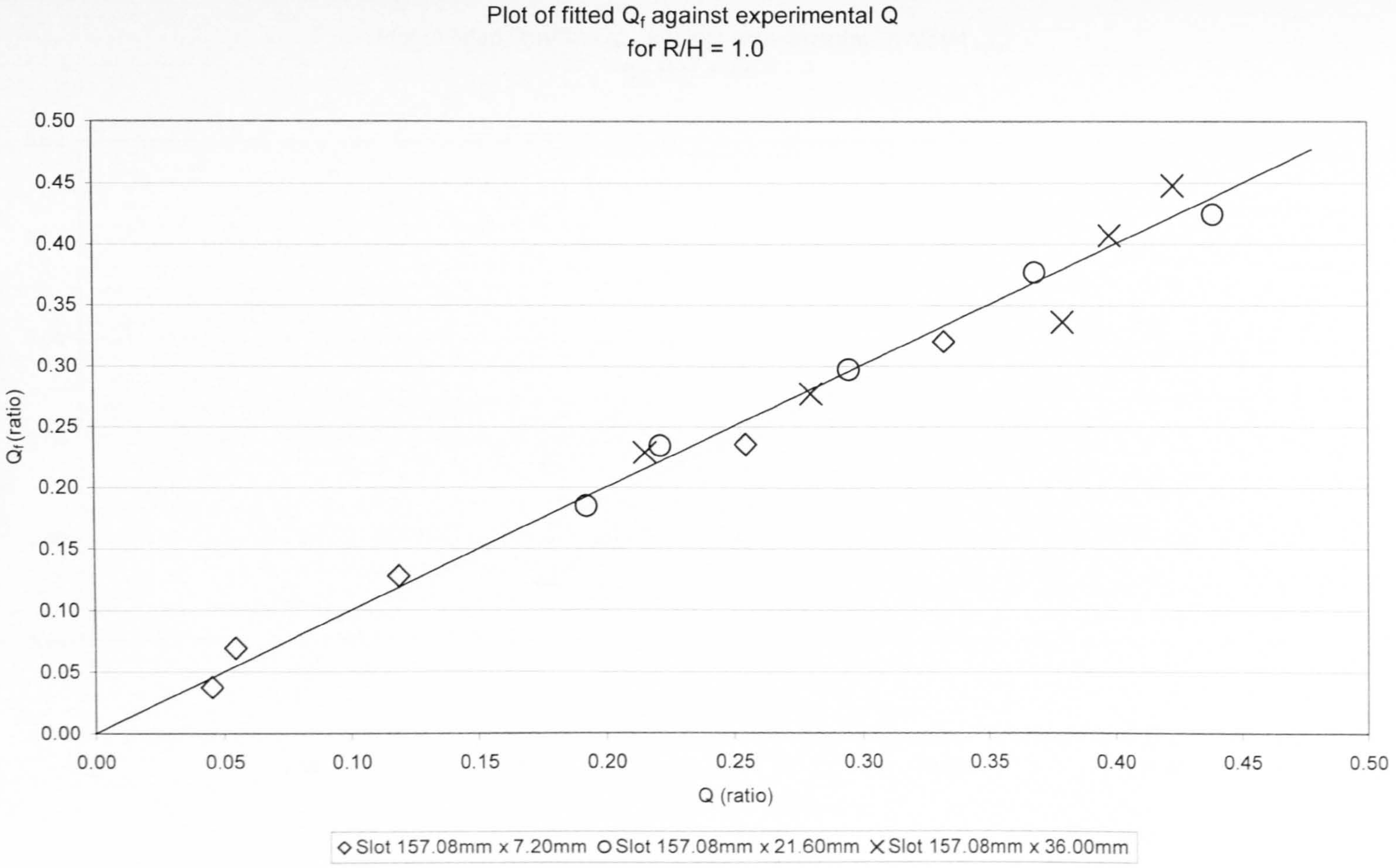

Chart 7.6 Example performance of empirical equations versus experimental results for the ratio $Dyn/Stat_{base}$ for middle tank asymmetric orifice releases (110% bund capacity)

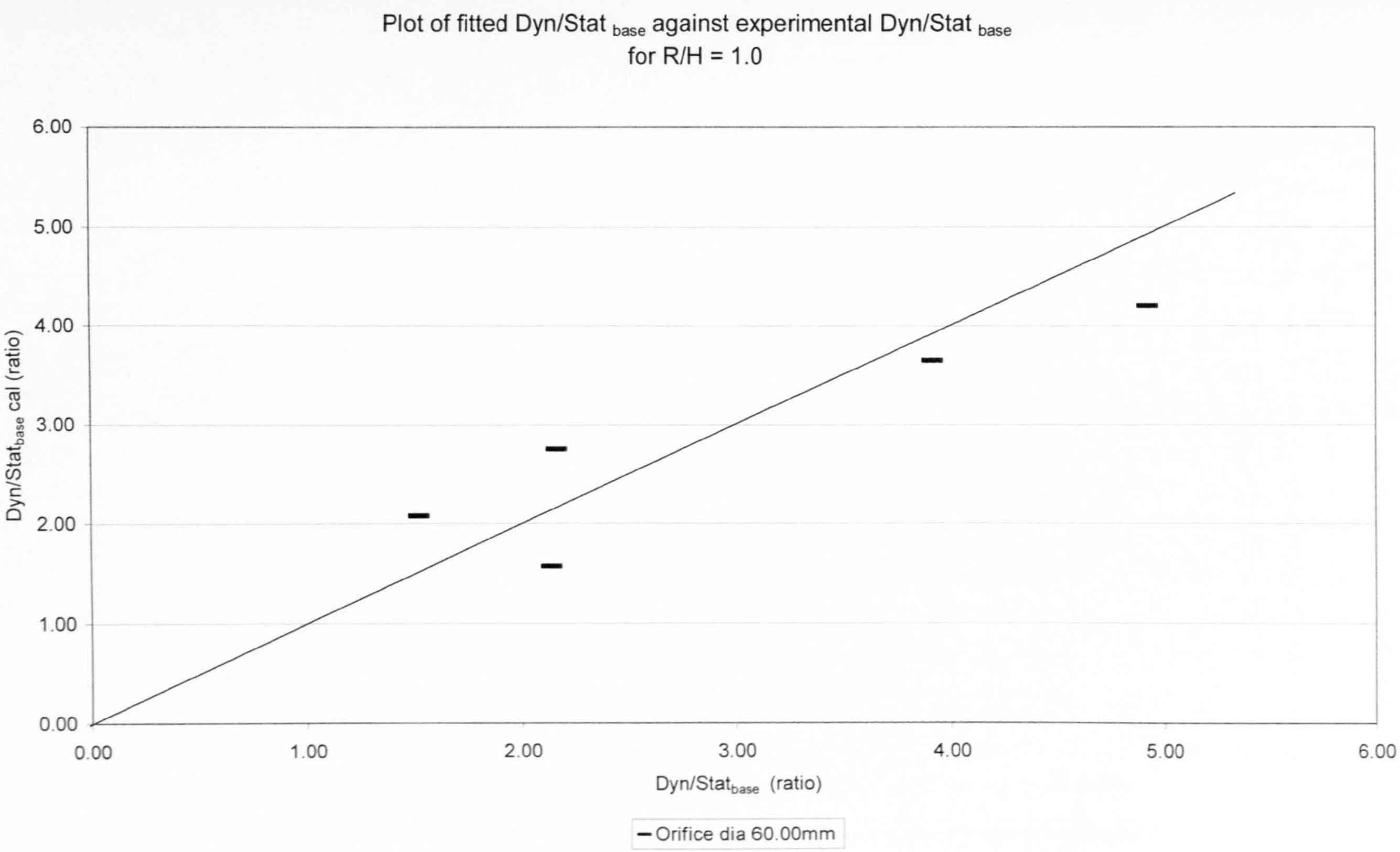

Chart 7.7 Example performance of empirical equations versus experimental results for the ratio $Dyn/Stat_{base}$ for middle tank asymmetric slot releases (110% bund capacity)

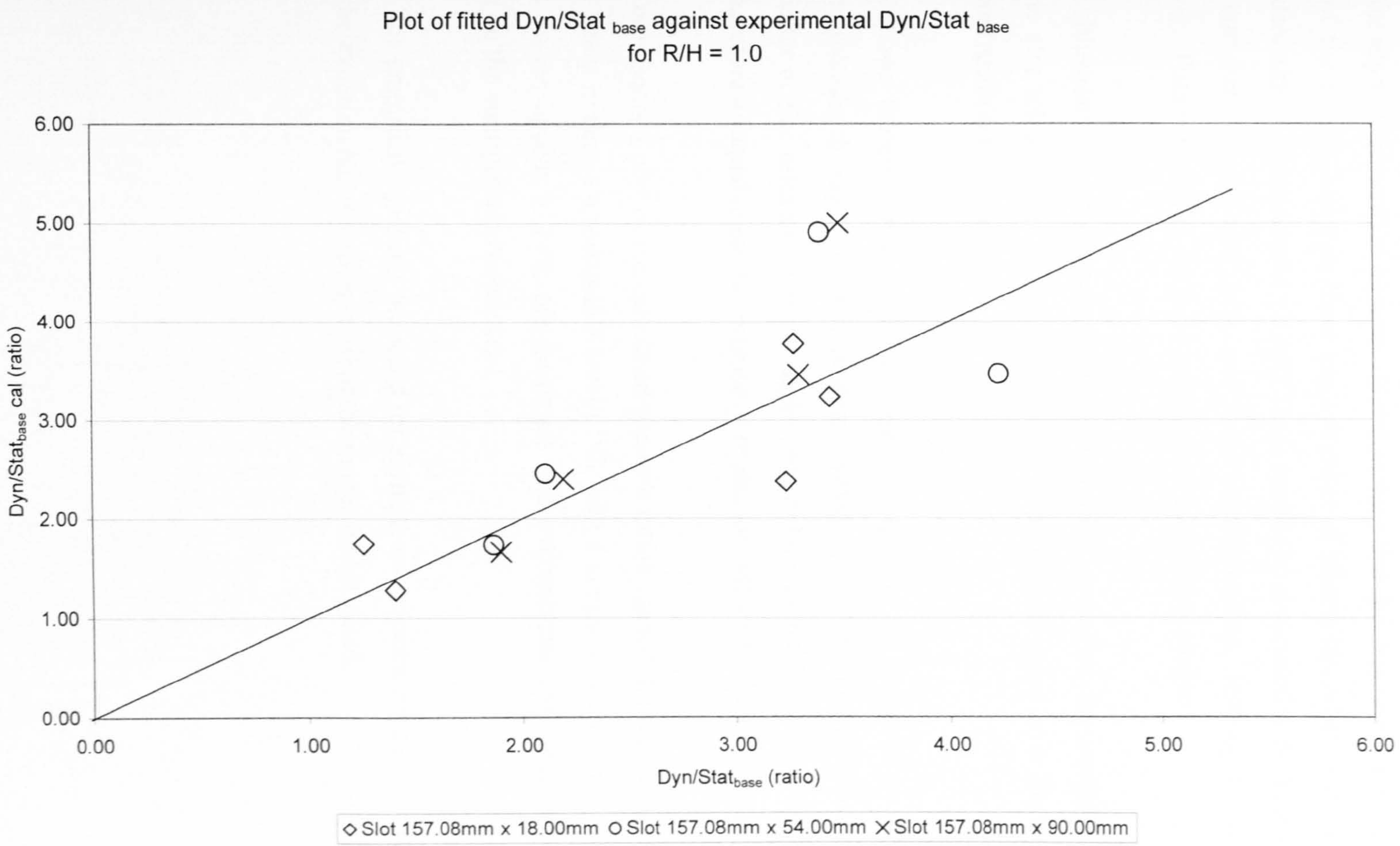

7.4 Interpretation of graphical results for the performance of the empirical equations for asymmetric releases

Chart 7.4 indicates a plot of calculated overtopping fractions against measured overtopping fractions for asymmetric orifice releases. It can be seen that the degree of fit is reasonable for most of the results, however there are a number of anomalies, where the calculated values underestimate the measured values. These tend to be associated with the generation of eddy currents at particular tank and bund configurations, leading to additional overtopping. These anomalies are to be investigated later in this chapter.

Chart 7.5 illustrates the performance of the empirical equations for overtopping for asymmetric slot releases and shows the fit to be exceptionally good over the complete range of configurations considered.

Chart 7.6 shows the performance of the empirical equation for the pressure ratios for asymmetric releases through a 60 mm diameter orifice. There are no equations proposed for the smaller orifice releases. The fit can be seen to be reasonable for an orifice of this size and therefore acceptable for the purpose of prediction within the range investigated.

Chart 7.7 represents a plot of the calculated pressure ratios against the measured pressure ratios and again indicates a reasonable level of fit with a couple of anomalies, where the calculated values appear to both underestimate and overestimate the measured values, depending on the configuration considered.

Generally, the empirical equations proposed for asymmetric releases, appear to reasonably represent the experimental data over most of the ranges investigated.

Table 7.1 Overtopping results for middle tank asymmetric 30mm diameter orifice (0.25%) release for 360°geometrey (110% bund capacity)

Configuration identity	*Tank radius, R (mm)*	*Tank fluid depth, H (mm)*	*R/H*	*Bund radius, r (mm)*	*Bund height, h (mm)*	*h/H*
Orifice releases	300	300	1.0	995	30	0.1

	360° Volume released	*0.08482*	*(m^3)*
Test number	*Depth retained (mm)*	*Volume retained (m^3)*	*Q*
1	26.0	0.08087	0.05
2	26.0	0.08087	0.05
3	27.0	0.08398	0.01
4	26.5	0.08242	0.03

Table 7.2 Overtopping results for middle tank asymmetric 60mm diameter orifice (0.25%) release for 360°geometrey (110% bund capacity)

Configuration identity	*Tank radius, R (mm)*	*Tank fluid depth, H (mm)*	*R/H*	*Bund radius, r (mm)*	*Bund height, h (mm)*	*h/H*
Orifice releases	300	300	1.0	574	90	0.3

	360° Volume released	*0.08482*	*(m^3)*
Test number	*Depth retained (mm)*	*Volume retained (m^3)*	*Q*
1	74.5	0.07711	0.09
2	75.0	0.07763	0.08
3	75.0	0.07763	0.08
4	74.5	0.07711	0.09

7.5 Interpretation of the results for 360° asymmetric orifice releases

Tables 7.1 and 7.2 illustrate the results from an additional investigation into the effect of the eddy currents observed in a number of the orifice releases in the quadrant of the test rig. The results show that the overtopping is in fact exaggerated by the generation of the eddy currents due to the quadrant arrangement used in the test rig. In the case of the 30 mm diameter orifice, the additional overtopping due to the eddy currents is approximately 2.6 times that measured in the 360 ° test. For the 60 mm diameter orifice, the additional overtopping equates to approximately 2 times that measured in the 360 ° test.

In both cases, the empirical formulae for the overtopping give a better approximation the 360 ° test results and therefore give a reasonable indication of the actual overtopping, reducing the effects of the eddy currents that are generated as a result of the test rig geometry.

7.6 Comparison with Henderson (1966) dam-break theory

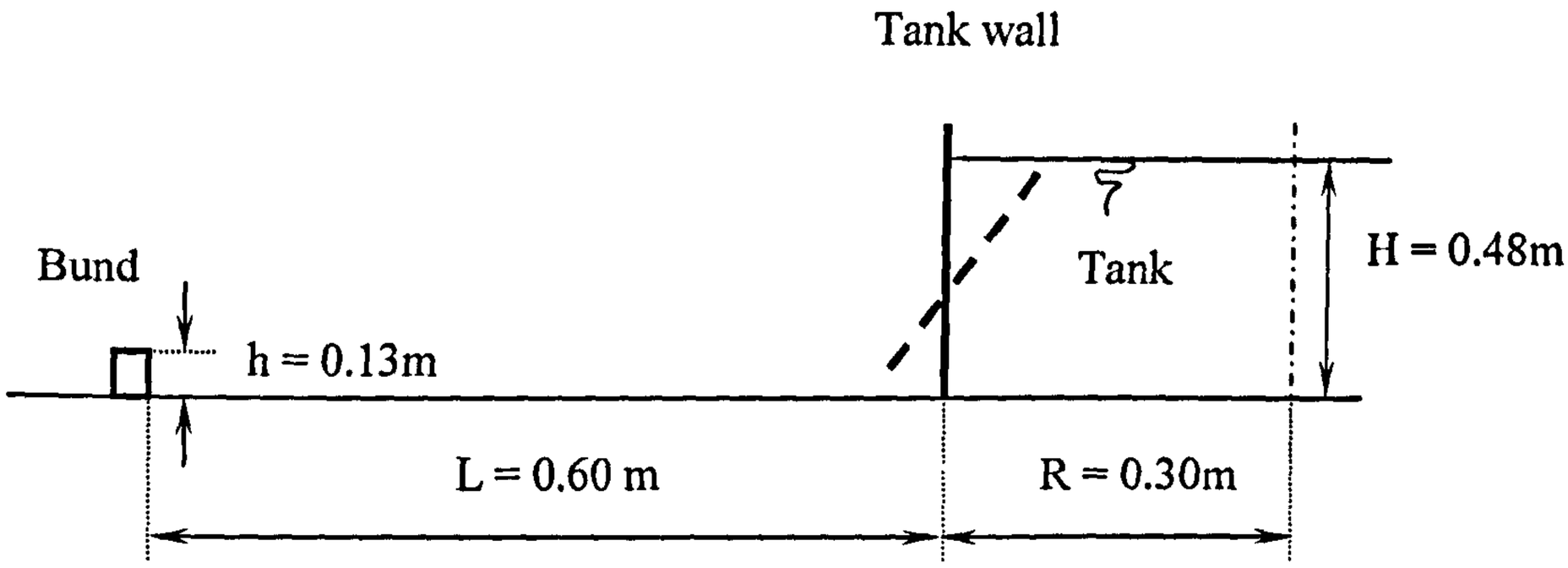

Figure 7.1 An axisymmetric release using Henderson (1966) dam-break theory

Using Featherstone (1988) Equation 4.1:

$$At\ x = 0, y = \frac{4}{9}H$$

$$V_1 = \frac{2}{3}g^{1/2}H^{1/2}$$

$$V_1 = \frac{2}{3} \times 9.81^{1/2} \times 0.48^{1/2}$$

$$V_1 = 1.45\ ms^{-1}$$

Consider the pressure on the bund at impact using momentum (Francis 1975):

$$F = \rho A V_2^{\,2}$$

Dynamic pressure :

$$Dyn = \frac{F}{A} = \rho V_2^{\,2}$$

$$Assuming\ V_1 = V_2$$

$$Dyn = 1000 \times 1.45^2$$

$$Dyn = 2102\ Pa$$

Considering bund geometry:

$$\frac{h}{H} = \frac{0.13}{0.48} = 0.27$$

$$\frac{R}{H} = \frac{0.3}{0.48} = 0.625$$

Volume released :

$$V_{rel} = \pi R^2 H$$

$$V_{rel} = \pi \times 0.3^2 \times 0.48$$

$$V_{rel} = 0.13572\ m^3$$

Bund capacity :

$$V_{cap} = \pi r^2 h$$

$$V_{cap} = \pi \times 0.9^2 \times 0.13$$

$$V_{cap} = 0.33081\ m^3$$

$$\frac{V_{cap}}{V_{rel}} = \frac{0.33081}{0.13572} = 2.437 \text{ or } \quad 243.7\ \%$$

Using experimental test data:

A 200 % bund capacity with R/H = 0.5.

Using the dynamic pressure Equation 6.2:

$$Dyn/Stat_{\ base} = C\ e^{-D(h/H)}$$

$$Dyn/Stat_{\ base} = 7.5531\ e^{-5.2278(0.27)}$$

$$Dyn/Stat_{\ base} = 1.84$$

Based on the hydrostatic head for the model bund :

$$Dynamic\ pressure = 1.84\rho gh$$

$$Dynamic\ pressure = 1.84 \times 1000 \times 9.81 \times 0.13 = 2346\ Pa$$

Comparing dynamic pressures: The values obtained from the theoretical and empirical formulae are similar in magnitude and generally compare well with a difference of 11.6 % based on the theoretical result. The dam-break theory assumes continuity using velocity at centreline of tank wall along with conservation of momentum, which is not the case, as the released liquid will initially accelerate due to the falling head and then decelerate due to frictional effects. This will depend on the separation distance, L between the tank wall and the bund together with the roughness of the fluid/ground interface with the dynamic pressure at impact varying accordingly.

7.7 Comparison with Greenspan and Young (1978) experimental channel models for determination of overtopping fractions

Example 1

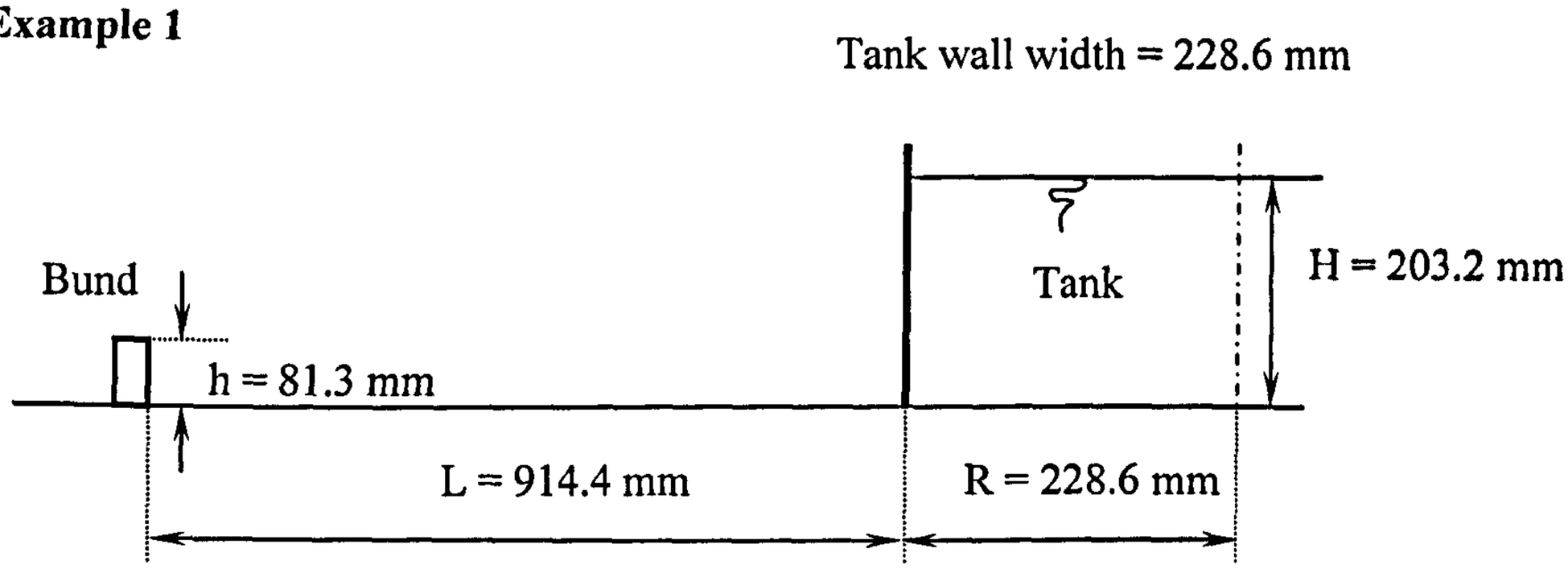

Figure 7.2 The Greenspan and Young (1978) channel model

From the data given, assuming h/H = 0.4 & L/R = 4.0 the chart for flow over a containment dyke, Fig. 10 from Greenspan and Young (1978) gives an overtopping fraction, Q = 0.24 or 24 %.

Considering bund geometry:

$$h = 0.4 \times H$$

$$h = 0.4 \times 203.2$$

$$h = 81.3\ mm$$

Hence,

$$\frac{R}{H} = \frac{228.6}{203.2} = 1.125$$

Volume released :

$$V_{rel} = 0.2286 \times 0.2286 \times 0.2032$$

$$V_{rel} = 0.01062\ m^3$$

Bund capacity :

$$V_{cap} = 0.2286 \times (0.9144 + 0.2286) \times 0.0813$$

$$V_{cap} = 0.02124\ m^3$$

$$\frac{V_{cap}}{V_{rel}} = \frac{0.02124}{0.01062} = 2.00\ or \quad 200\ \%$$

Using experimental test data:

A 200 % bund capacity with R/H = 1.0 & h/H = 0.4.

Using the Overtopping Equation 6.1:

$$Q_f = Ae^{-B(h/H)}$$

$$Q_f = 0.4814e^{-2.1866(0.4)}$$

$$Q_f = 0.20 \quad or \quad 20\,\%$$

Comparing overtopping: The empirical equation for overtopping based on axisymmetrical results under-estimates the magnitude of the experimental value obtained with a difference of -16.7 % expressed in terms of the Greenspan and Young (1978) data. The fact that the experimental results are based on channel releases will influence the magnitudes of any overtopping data sets obtained due to the enclosed channel sides preventing the spread of the fluid flow after release. The ensuing flow will therefore be at a greater, more uniform depth across the width of the bore prior to the impact and subsequent overtopping of the bund, thus exaggerating the magnitude of the overall result. The differences found between the channel and small-scale cylinder results were reported to be minimal (< 5 %) and a combination of the increased height of bore along with the increased wetted perimeter, allowing friction to reduce the celerity of the bore, may sufficiently account for this.

Using a bund capacity of half the previous example by halving the bund height and maintaining the parameter L/R:

Example 2

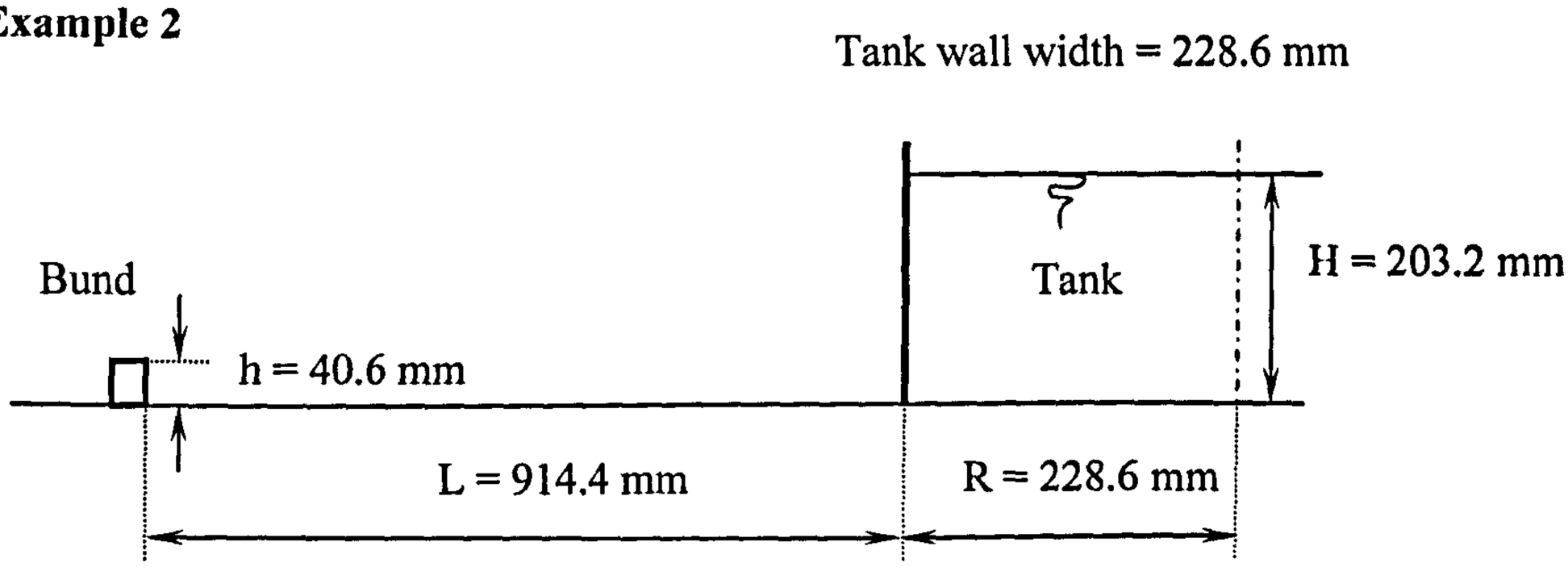

Figure 7.3 Greenspan and Young (1978) channel model with reduced bund height

From the data given, assuming h/H = 0.2 & L/R = 4.0 the chart for flow over a containment dyke, Fig. 10 from Greenspan and Young (1978) gives an overtopping fraction, Q = 0.49 or 49 %.

Considering bund geometry:

$$h = 0.2 \times H$$

$$h = 0.2 \times 203.2$$

$$h = 40.6\ mm$$

Hence,

$$\frac{R}{H} = \frac{228.6}{203.2} = 1.125$$

Volume released :

$$V_{rel} = 0.2286 \times 0.2286 \times 0.2032$$

$$V_{rel} = 0.01062\ m^3$$

Bund capacity :

$$V_{cap} = 0.2286 \times (0.9144 + 0.2286) \times 0.0406$$

$$V_{cap} = 0.01061\ m^3$$

$$\frac{V_{cap}}{V_{rel}} = \frac{0.01061}{0.01062} = 0.10\ or \quad 100\ \%$$

Using experimental test data:

A 110 % bund capacity with R/H = 1.0 & h/H = 0.2.

Using the overtopping Equation 6.1:

$$Q_f = Ae^{-B(h/H)}$$
$$Q_f = 0.7588e^{-2.3529(0.2)}$$
$$Q_f = 0.47 \quad or \quad 47\,\%$$

Comparing overtopping: The magnitude of the empirical result again under-estimates the overtopping by –4.1 % based on the experimental value. This is consistent with the previous findings, however the difference is reduced. The fact that the bund height has been halved; the increase in overtopping is to be expected due to a reduced capacity with the bund presenting a much smaller obstacle to the flow. The other consideration is that the empirical formulae is based on a slightly larger bund capacity than that of the experimental configuration, this will reduce the calculated overtopping fraction and will partially account for the reduced difference in magnitude.

7.8 Comparison with Greenspan and Johansson (1981) experimental cylinder models for axisymmetric releases.

Example 1

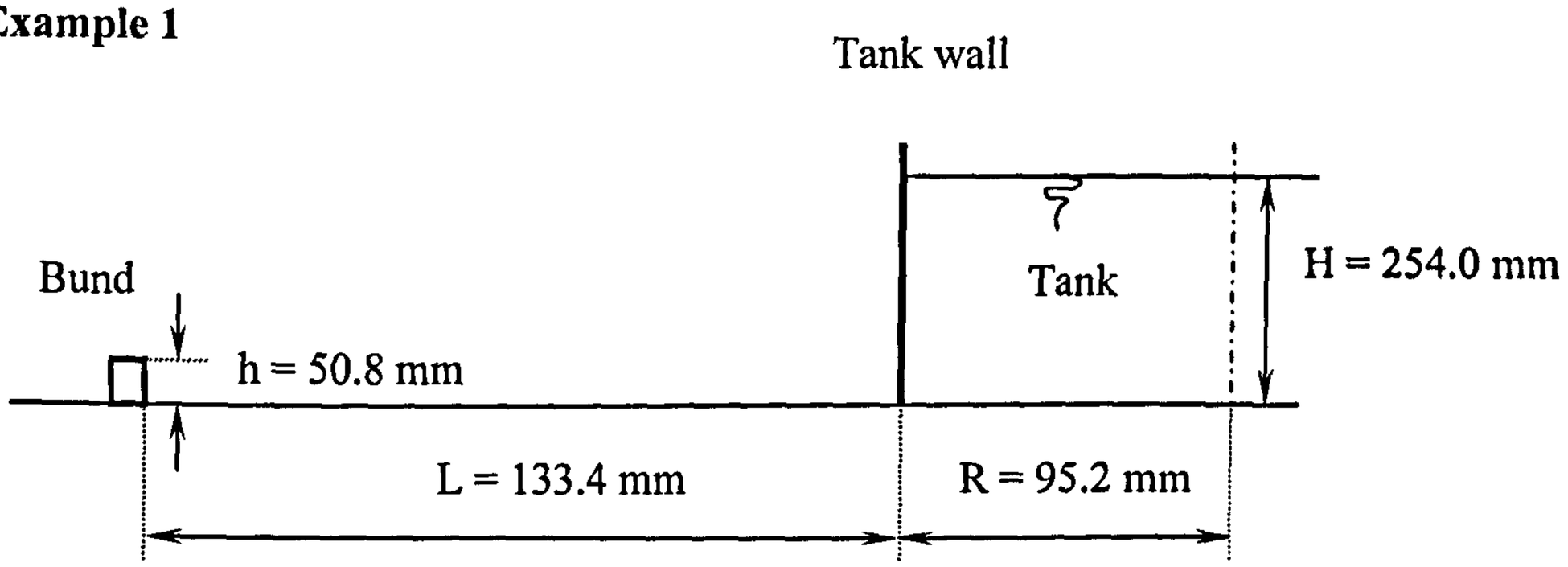

Figure 7.4 The Greenspan and Johansson (1981) axisymmetric cylinder model

From the data given, assuming h/H = 0.2, r = 228.6 mm & h = 50.8 mm, the chart for flow over a containment dyke, Fig. 2a from Greenspan and Johansson (1981) gives an overtopping fraction, Q = 0.43 or 43 %.

Considering bund geometry:

$$\frac{h}{H} = 0.2$$

$$H = \frac{h}{0.2} = \frac{50.8}{0.2}$$

$$H = 254\ mm$$

Hence,

$$\frac{R}{H} = \frac{95.2}{254} = 0.38$$

Volume released :

$$V_{rel} = \pi R^2 H$$

$$V_{rel} = \pi \times 0.0952^2 \times 0.254$$

$$V_{rel} = 0.00723\ m^3$$

Bund capacity :

$$V_{cap} = \pi r^2 h$$

$$V_{cap} = \pi \times 0.2286^2 \times 0.0508$$

$$V_{cap} = 0.00834\ m^3$$

$$\frac{V_{cap}}{V_{rel}} = \frac{0.00834}{0.00723} = 1.153\ or \quad 115.3\ \%$$

Using experimental test data:

A 120 % bund capacity with R/H = 0.5 & h/H = 0.2.

Using the overtopping Equation 6.1:

$$Q_f = Ae^{-B(h/H)}$$

$$Q_f = 0.8942e^{-3.4692(0.2)}$$

$$Q_f = 0.45 \quad or \quad 45\,\%$$

Comparing overtopping: In the case of the cylindrical model, the empirical formula gives a slightly higher result than the experimental value quoted by Greenspan and Johansson (1981) with a difference of 4.6 %. The empirical result is based on a slightly larger bund capacity, with larger tank radius to tank height ratio, in which case it would be expected that the calculated overtopping fraction would be less than the experimental value. One possible consideration is the scale of the two physical models with the Greenspan and Johansson (1981) model being of a much smaller size it is more susceptible to frictional effects due to surface roughness. It has long been established in hydraulic modelling that small-scale models must have extremely smooth surfaces to avoid issues with experimental error in flow analogies being induced due to excessive friction between the fluid/solid interfaces (Francis, 1975).

Using a tank height of half the previous example and changing r and h/H:

Example 2

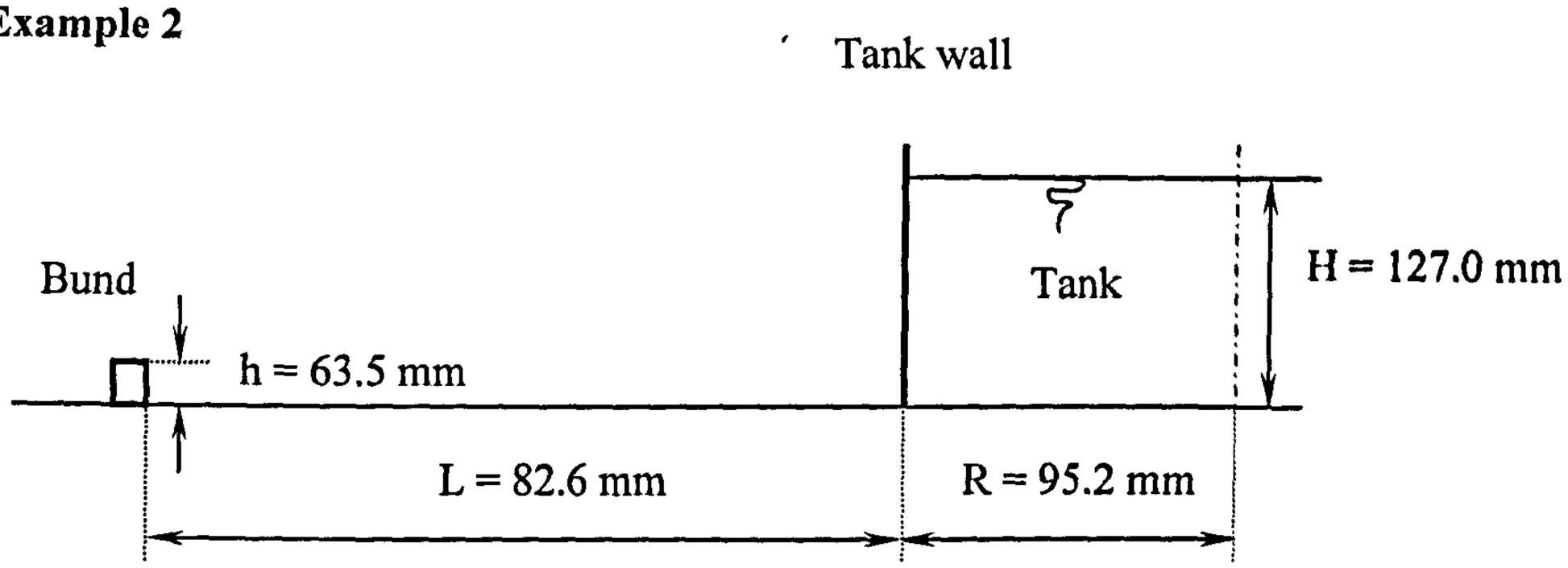

Figure 7.5 The Greenspan and Johansson (1981) axisymmetric cylinder model with reduced tank height

From the data given, assuming h/H = 0.5, r = 177.8 mm & h = 63.5 mm, the chart for flow over a containment dyke, Fig. 2a from Greenspan and Johansson (1981) gives an overtopping fraction, Q = 0.22 or 22 %.

Considering bund geometry:

$$\frac{h}{H} = 0.5$$

$$H = \frac{h}{0.5} = \frac{63.5}{0.5}$$

$$H = 127.0\ mm$$

Hence,

$$\frac{R}{H} = \frac{95.2}{127.0} = 0.75$$

Volume released :

$$V_{rel} = \pi R^2 H$$

$$V_{rel} = \pi \times 0.0952^2 \times 0.127$$

$$V_{rel} = 0.00362\ m^3$$

Bund capacity :

$$V_{cap} = \pi r^2 h$$

$$V_{cap} = \pi \times 0.1778^2 \times 0.0635$$

$$V_{cap} = 0.00631\ m^3$$

$$\frac{V_{cap}}{V_{rel}} = \frac{0.00631}{0.00362} = 1.743 \text{ or } \quad 174.3\ \%$$

Using experimental test data:

A 150 % bund capacity with R/H = 1.0 & h/H = 0.5.

Using the overtopping Equation 6.1:

$$Q_f = Ae^{-B(h/H)}$$
$$Q_f = 0.63592e^{-2.4451(0.5)}$$
$$Q_f = 0.19 \quad or \quad 19\,\%$$

Comparing overtopping: In this example, the empirical formula under-estimates the overtopping by -13.6 % based on the result form the experimental model. When considering the smaller bund capacity on which the empirical result is based, it would be anticipated that the overtopping fraction should be higher. On closer inspection, the ratio of tank radius to tank height, R/H is smaller for the experimental test rig indicating a taller tank. A relatively taller tank would have more potential energy and hence more kinetic energy on release, assuming conservation of energy principles are applied. This would result in an increased level of overtopping due to greater velocity and increased dynamic pressure.

7.9 Comparison with Greenspan and Johansson (1981) experimental cylinder models for asymmetric releases.

Example 1

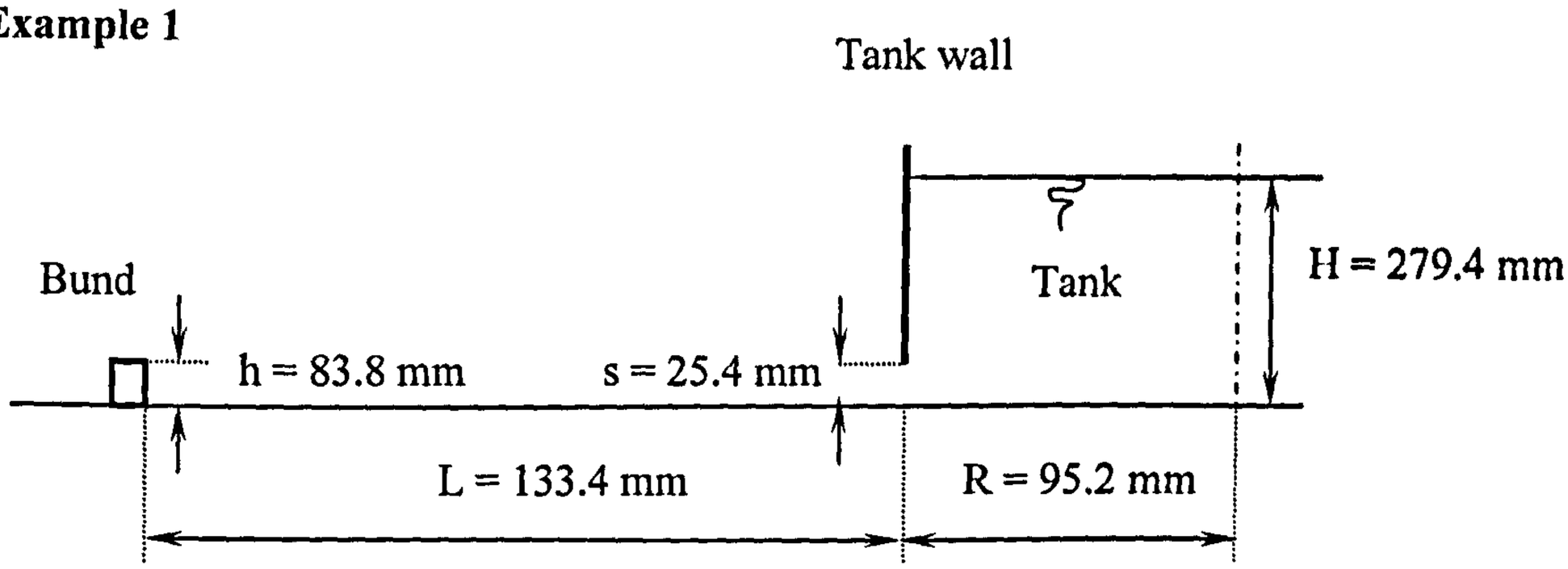

Figure 7.6 The Greenspan and Johansson (1981) asymmetric cylinder model

From the data given for a vertical bund, assuming h/H = 0.3, r = 228.6 mm for a slot height of 25.4 mm, Table 1 from Greenspan and Johansson (1981) for flow over a containment dyke gives an overtopping fraction, Q = 0.13 or 13 %.

Considering bund geometry:

$$\frac{h}{H} = 0.3$$

$$h = 0.3 \times H$$

$$h = 0.3 \times 279.4$$

$$h = 83.8\ mm$$

$$\frac{R}{H} = \frac{95.2}{279.4} = 0.34$$

Volume released :

$$V_{rel} = \pi R^2 H$$

$$V_{rel} = \pi \times 0.0952^2 \times 0.2794$$

$$V_{rel} = 0.00796\ m^3$$

Bund capacity :

$$V_{cap} = \pi r^2 h$$

$$V_{cap} = \pi \times 0.2286^2 \times 0.0838$$

$$V_{cap} = 0.01376\ m^3$$

$$\frac{V_{cap}}{V_{rel}} = \frac{0.01376}{0.00796} = 1.729 \text{ or } \quad 172.9\,\%$$

For a slot height, s = 25.4 mm over a 30° sector:

$$\textit{Release area :}$$

$$A_{rel} = \frac{30}{360} \times 2\pi Rs$$

$$A_{rel} = \frac{30}{360} \times 2 \times \pi \times 95.2 \times 25.4$$

$$A_{rel} = 1266.10\ mm^2$$

$$\textit{Total area :}$$

$$A_{tot} = 2\pi RH$$

$$A_{tot} = 2 \times \pi \times 95.2 \times 279.4$$

$$A_{tot} = 167125.69\ mm^2$$

$$\textit{Percentage ares of release :}$$

$$A_{\%} = \frac{A_{rel}}{A_{tot}} \times 100$$

$$A_{\%} = \frac{1266.10}{167125.69} \times 100$$

$$A_{\%} = 0.76\ \%$$

Using experimental test data:

A 110 % bund capacity with R/H = 0.5 & h/H = 0.3 for a 0.5% area of release.

Using the overtopping Equation 6.1:

$$Q_f = Ae^{-B(h/H)}$$

$$Q_f = 0.4260e^{-3.6389(0.3)}$$

$$Q_f = 0.14 \quad or \quad 14\ \%$$

Comparing overtopping: In the case of an asymmetric release, the empirical formula agrees very well with the Greenspan and Johansson (1981) model with a difference of 7.7% based on the experimental value. It is to be expected that the empirical overtopping fraction would be greater due to the smaller bund capacity (110 %) on which the equation is based, however this is partially offset by the relatively larger release area (0.76 %) and the relatively taller tank (R/H =0.34) used in the case of the physical model.

Now using a larger area of release with no change in other parameters.

Example 2

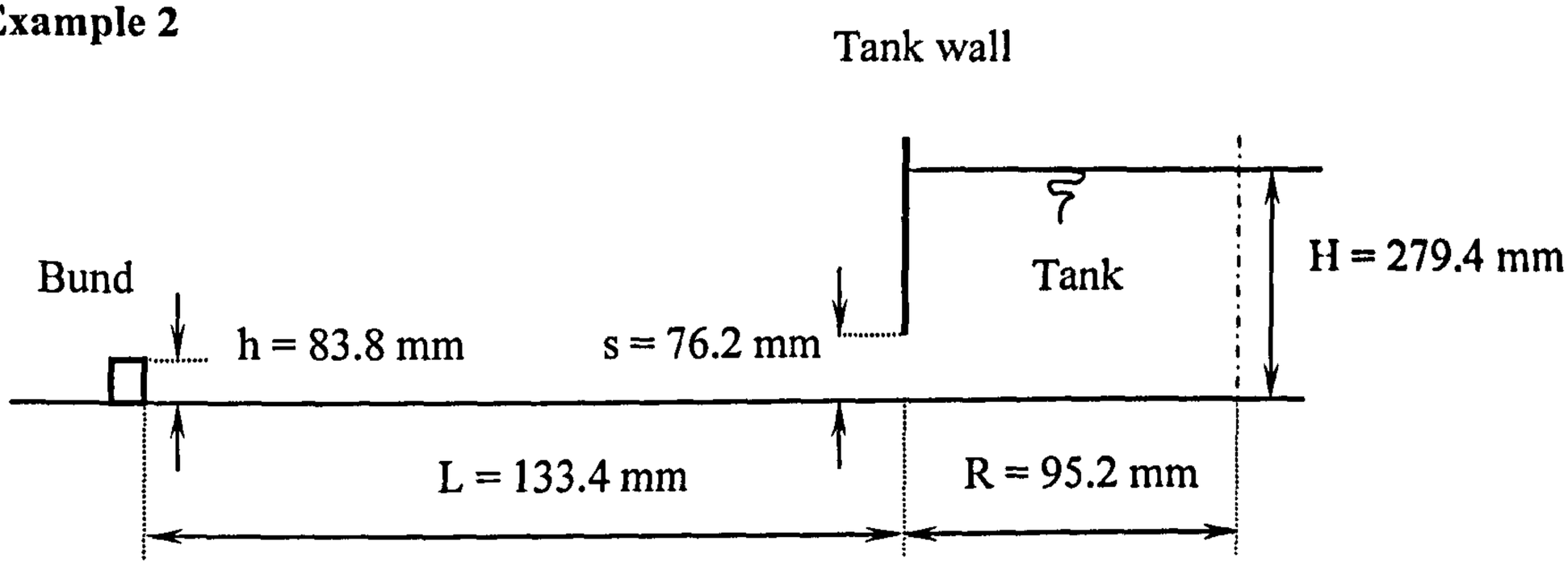

Figure 7.7 The Greenspan and Johansson (1981) asymmetric cylinder model with enlarged slot release

From the data given for a vertical bund, assuming h/H = 0.3, r = 228.6 mm for a slot height of 76.2 mm, Table 1 from Greenspan and Johansson (1981) for flow over a containment dyke gives an overtopping fraction, Q = 0.18 or 18 %.

Considering bund geometry:

For a slot height, s = 76.2 mm over a 30° sector.

Release area :

$$A_{rel} = \frac{30}{360} \times 2\pi Rs$$

$$A_{rel} = \frac{30}{360} \times 2 \times \pi \times 95.2 \times 76.2$$

$$A_{rel} = 3798.31\ mm^2$$

Total area :

$$A_{tot} = 2\pi RH$$

$$A_{tot} = 2 \times \pi \times 95.2 \times 279.4$$

$$A_{tot} = 167125.69\ mm^2$$

Percentage ares of release :

$$A_{\%} = \frac{A_{rel}}{A_{tot}} \times 100$$

$$A_{\%} = \frac{3798.31}{167125.69} \times 100$$

$$A_{\%} = 2.27\ \%$$

Using experimental test data:

A 110 % bund capacity with R/H = 0.5 & h/H = 0.3 for a 2.5% area of release.

Using the overtopping Equation 6.1:

$$Q_f = Ae^{-B(h/H)}$$
$$Q_f = 0.6554e^{-3.3391(0.3)}$$
$$Q_f = 0.24 \quad or \quad 24\,\%$$

Comparing overtopping: In this case the size of the aperture has been increased and as such the experimental overtopping fraction is greater. This is reflected in the empirical result with a difference of 33.3 % between the two values based on the experimental model. On inspection of the parameters used, there is a clear difference in the relative release areas with the empirical result based on a larger aperture (2.5 %). It must also be considered that the empirical expression is based on a smaller bund capacity (110 %) rather than the much larger Greenspan and Johansson (1981) bund capacity of 172.9 %. With these issues considered, it is not surprising that there is a notable difference in the two overtopping results and illustrates the limitations of the empirical data with only the 110% bund capacity investigated for asymmetric releases.

7.10 Case history – Ashland Oil, Floreffe, Pennsylvania, USA, 2nd January 1988.

Based on upper and lower estimates and approximate calculations by Wilkinson (1991), the following comparisons have been made considering upper and lower bounded solutions. The information contained in the report gives the following data:

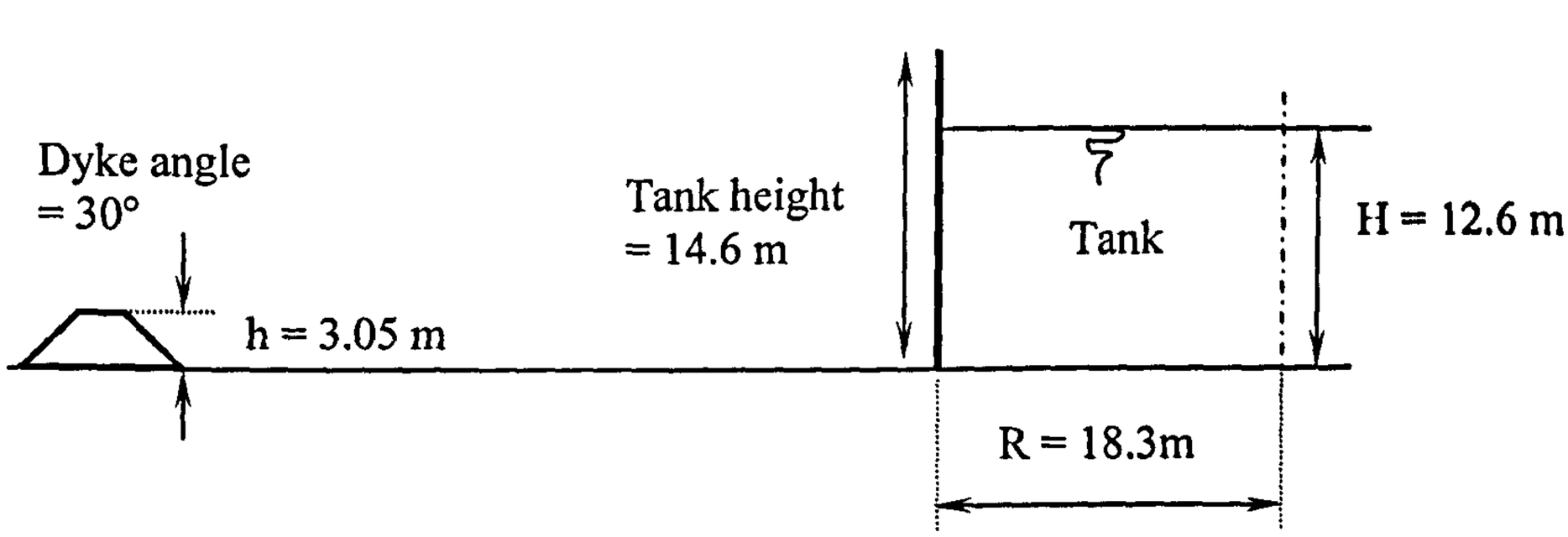

Figure 7.8 Wilkinson (1991) model for overtopping in the Ashland Oil spill (1988)

Volume released was estimated as 3.5 million US gallons or $V_{rel} = 13249\ m^3$ (1 US gallon $= 3.7854 \times 10^{-3}\ m^3$).

Estimated volume retained by the secondary containment was determined to be between 1 and 2 million gallons with the dyke slope estimated at 30°.

Min $V_{bund} = 3785\ m^3$ and max $V_{bund} = 7571\ m^3$.

Using tank and bund geometry:

$$V_{rel} = \pi R^2 H$$

$$H = \frac{V_{rel}}{\pi R^2}$$

$$H = \frac{13249}{\pi \times 18.3^2} = 12.6\ m$$

$$\frac{h}{H} = \frac{3.05}{12.6} = 0.24$$

$$\frac{R}{H} = \frac{18.3}{12.6} = 1.45$$

Estimated range of overtopping:

Minimum overtopping :

$$Q = \frac{(13249 - 7571)}{13249}$$

$$Q = 0.43 \quad or \quad 43\,\%$$

Maximum overtopping :

$$Q = \frac{(13249 - 3785)}{13249}$$

$$Q = 0.71 \quad or \quad 71\,\%$$

Using experimental test data:

For a vertical bund with a 150 % bund capacity (based on a bund capacity of 172.9 % for the nearest Greenspan and Johansson (1981) configuration) with R/H = 1.0 & h/H = 0.24.

Using the overtopping Equation 6.1:

$$Q_f = Ae^{-B(h/H)}$$

$$Q_f = 0.6359e^{-2.4451(0.24)}$$

$$Q_f = 0.35 \quad or \quad 35\,\%$$

Due the fact that a vertical bund has been used for the comparison an engineering judgement approach using data from the Greenspan and Johansson (1981) is applied to modify the overtopping result.

$$\theta = 30° \quad \frac{h}{H} = 0.234 \quad Q = 0.67$$

$$\theta = 90° \quad \frac{h}{H} = 0.250 \quad Q = 0.35$$

Conversion factor from 90°to 30° :

$$K = \frac{0.67}{0.35} = 1.9143$$

Modified overtopping, Q_m for LJMU result :

$$Q_m = 1.9143 \times 0.35$$

$$Q_m = 0.67 \quad or \quad 67\,\%$$

Comparing overtopping: Due to the nature of the dyke profile in the case study (30° slope), it is not possible to calculate an overtopping fraction directly from the empirical formula and a modification has to be made for comparison purposes. This modification seems to be justifiable as the difference between the overtopping fractions is minimal giving an under-estimate of –5.6 % based on the upper bounded result estimated by Wilkinson (1991). On inspection of the data used for the modification, it can be seen that the Greenspan and Johansson (1981) data yields the exactly the same result (0.35) as the empirical formula for the overtopping fraction when considering a vertical bund.

7.11 Comparison with Trbojevic and Slater (1989) finite difference model

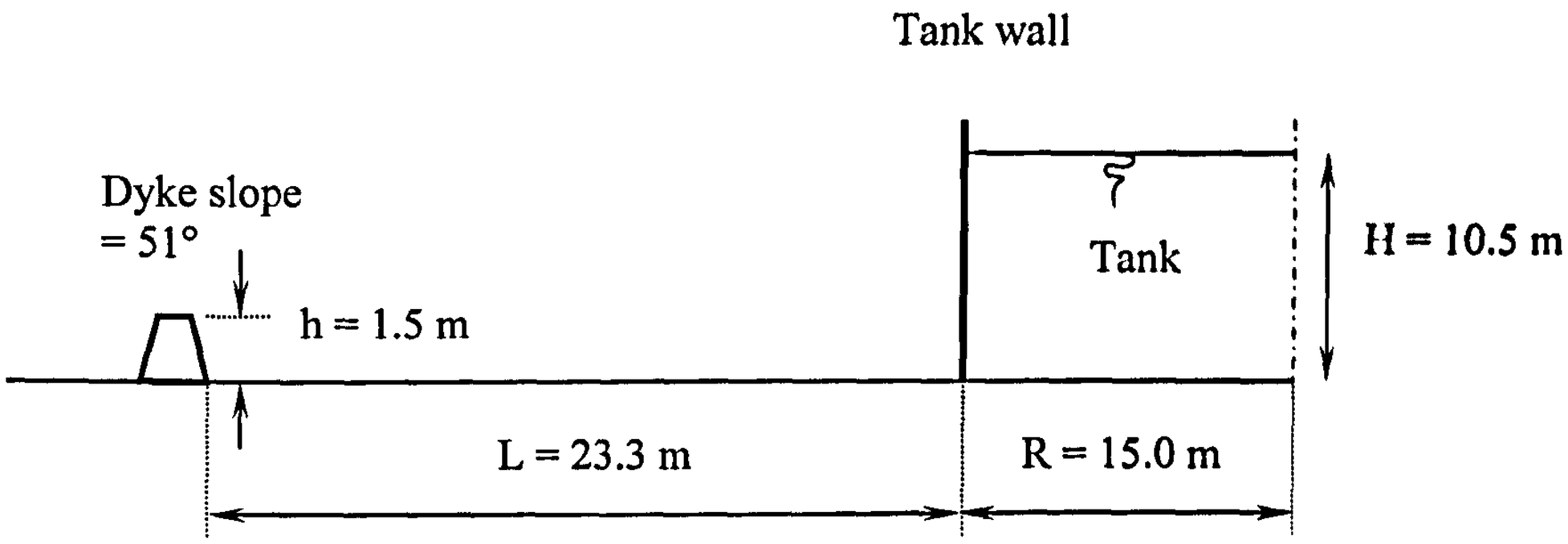

Figure 7.9 The Trbojevic and Slater (1989) finite difference model

Given the time from release to prior to impact as 2 seconds, a velocity of 14.6 ms^{-1} is quoted as being reached using the finite difference model.

Using Newton's equations of motion:

$$v = u + at$$

$$u = 0$$

$$v = at \tag{7.1}$$

Also:

$$s = ut + \frac{1}{2}at^2$$

$$u = 0$$

$$s = \frac{1}{2}at^2$$

$$a = \frac{2s}{t^2} \tag{7.2}$$

Combining (7.1) & (7.2):

$$v = \frac{2s}{t^2}t$$

$$v = \frac{2s}{t} \tag{7.3}$$

Using the time at impact of 2.5027 seconds and applying Equation 7.3:

$$v = \frac{2 \times 23.3}{2.5027} = 18.62 ms^{-1}$$

From Michels et al (1988) using Equation 4.5, theoretically:

$$u = 2g^{1/2}H^{1/2}$$
$$u = 2 \times 9.81^{1/2} \times 10.5^{1/2}$$
$$u = 20.30\ ms^{-1}$$

Experimentally, using Equation 4.6:

$$u = 1.4g^{1/2}H^{1/2}$$
$$u = 1.4 \times 9.81^{1/2} \times 10.5^{1/2}$$
$$u = 14.21\ ms^{-1}$$

From Fig. 4 in Trbojevic and Slater (1989), the dynamic pressure maxima near the base of the bund = 0.36 Bar.

Tank and Bund geometry:

$$\frac{R}{H} = \frac{15.0}{10.5} = 1.43$$
$$\frac{h}{H} = \frac{1.5}{10.5} = 0.14$$

Volume released :

$$V_{rel} = \pi R^2 H$$
$$V_{rel} = \pi \times 15.0^2 \times 10.5$$
$$V_{rel} = 7422.0\ m^3$$

Bund capacity :

$$V_{cap} = \pi r^2 h$$
$$V_{cap} = \pi \times (23.3 + 15.0)^2 \times 1.5$$
$$V_{cap} = 6912.6\ m^3$$
$$\frac{V_{cap}}{V_{rel}} = \frac{6912.6}{7422.0} = 0.93 \quad or \quad 93\%$$

Using experimental test data:

A 110 % bund capacity with R/H = 1.0 & h/H = 0.1

i.e. Configuration identity E1 (h30):

Impact velocity, u = 3.55 ms^{-1}

Separation distance, L = 695 mm

Using dimensional analysis, Equation 6.5 (Francis, 1975):

Where, u_m = velocity in model & u_p = velocity in prototype

l_m = model length & l_p = length in prototype

$$\frac{u_m}{u_p} = \left(\frac{l_m}{l_p}\right)^{1/2}$$

$$u_p = \frac{u_m}{\left(\frac{l_m}{l_p}\right)^{1/2}}$$

$$u_p = \frac{3.55}{\left(\frac{695}{23300}\right)^{1/2}} = 20.55\ ms^{-1}$$

Using the dynamic pressure Equation 6.2:

$$Dyn/Stat_{base} = C\, e^{-D(h/H)}$$

$$Dyn/Stat_{base} = 9.4121\, e^{-4.5712(0.14)}$$

$$Dyn/Stat_{base} = 4.96$$

Based on the hydrostatic head for the model bund :

$$Dynamic\ pressure = 4.96 \rho g h$$

$$Dynamic\ pressure = 4.96 \times 850 \times 9.81 \times 1.5 = 62038\ Pa$$

$$Dynamic\ pressure = 62.038\ kPa \quad or \quad 0.62\ Bar$$

Comparing velocities: The quoted velocity of 14.6 ms^{-1} after 2 seconds has been determined before impact with the bund and the use of Newton's equations of motion applied to the position of the bore at the exact time of impact indicates that the celerity of the wave was higher and therefore still accelerating. Using the theoretical and experimental equations from Michels et al (1988), the range of upper and lower velocity

values determined encompass the magnitude of the value calculated using Newton's equations of motion. Comparison with the value estimated using the dimensional analysis from the model results indicates reasonable correlation both with the theoretical equation from Michels et al (1988) and with the value determined from Newton's equations of motion. The difference between the Newtonian value derived from the Trbojevic and Slater (1989) data and the value given by the dimensional analysis is 10.4 %.

Comparing dynamic pressures: The dynamic pressure maxima near the base of the bund (0.36 Bar) is quoted as being approximately 3.5 times the static pressure based on the density of Diesel fuel. Applying the empirical formula gives a $Dyn/Stat_{base}$ ratio of 4.96, which equates to a dynamic pressure of 0.62 Bar. The difference in magnitude between theses two pressures is 72.2 % based on the reported value, which is very significant. The parameters R/H and h/H are suitably similar, however the major factor in the significantly larger dynamic stress in the case of the empirical solution is that the equation is based on vertical bund modelling data. The dynamic pressure on the sloping dyke would be very different from that on a vertical bund and a reduced order of magnitude is to be expected given the that the momentum will carry the flow more easily over the inclined dyke and present less of an obstacle.

7.12 Comparison with Kleefsman et al (2004) dam break experiment

By using the scale diagram and the data provide by Kleefsman et al (2004) the dimensions shown in fig. 7.1 were elicited. The following calculations were made to determine the velocity of the wave with the charts used to evaluate the dynamic pressures at the front impact face:

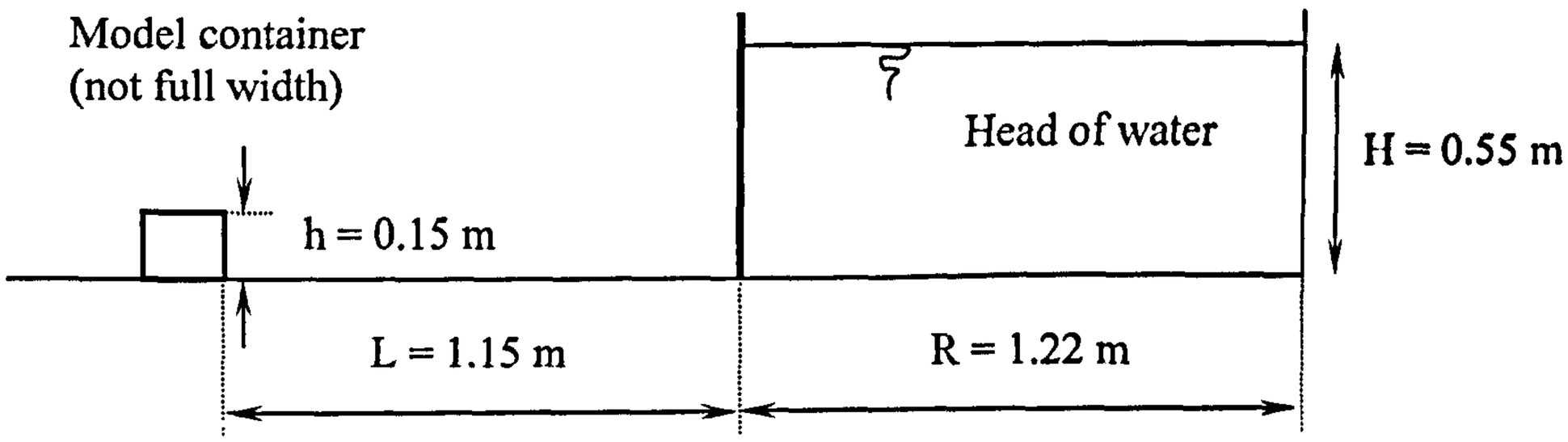

Figure 7.10 The Kleefsman et al (2004) dam-break model

Given the time from release to just prior to impact as 0.40 seconds and the time from release to the wave front surging up the wall as 0.56 seconds it is deduced that the time at impact is approximately 0.42 seconds.

Using equation (7.3):

$$v = \frac{2 \times 1.15}{0.42} = 5.48\ ms^{-1}$$

From the pressure charts, the dynamic pressure near the base of the front face:

Instantaneous peak value = 11400 Pa

Post peak value = 4000 Pa

Dynamic pressure at the upper third of the front face:

Instantaneous peak value = 6500 Pa

Post peak value = 3900 Pa

From Michels et al (1988) using Equation 4.5, theoretically:

$$u = 2g^{1/2}H^{1/2}$$
$$u = 2 \times 9.81^{1/2} \times 0.55^{1/2}$$
$$u = 4.64\ ms^{-1}$$

Experimentally, using Equation 4.6:

$$u = 1.4g^{1/2}H^{1/2}$$
$$u = 1.4 \times 9.81^{1/2} \times 0.55^{1/2}$$
$$u = 3.25\ ms^{-1}$$

Comparing to circular tank and bund geometry:

$$\frac{R}{H} = \frac{1.22}{0.55} = 2.22$$
$$\frac{h}{H} = \frac{0.150}{0.55} = 0.27$$

Volume released :

$$V_{rel} = 1.0 \times 1.22 \times 0.55$$
$$V_{rel} = 0.6710\ m^3$$

'Bund capacity':

$$V_{cap} = 1.0 \times (1.22 + 1.15) \times 0.15$$
$$V_{cap} = 1.3035\ m^3$$
$$\frac{V_{cap}}{V_{rel}} = \frac{1.3035}{0.6710} = 1.94 \quad or \quad 194\,\%$$

Using experimental test data:

For a 200 % bund capacity with R/H = 2.5 & h/H = 0.3

i.e. Configuration identity C4 (h36)

Impact velocity, u = 2.62 ms^{-1}

Separation distance, L = 475 mm

Using dimensional analysis, Equation 6.5 (Francis, 1975):

Where, u_m = velocity in model & u_p = velocity in prototype

l_m = model length & l_p = length in prototype

$$\frac{u_m}{u_p} = \left(\frac{l_m}{l_p}\right)^{1/2}$$

$$u_p = \frac{u_m}{\left(\frac{l_m}{l_p}\right)^{1/2}}$$

$$u_p = \frac{2.62}{\left(\frac{475}{1150}\right)^{1/2}} = 4.08 ms^{-1}$$

Using the dynamic pressure Equation 6.2:

$$Dyn/Stat_{base} = C\, e^{-D(h/H)}$$

$$Dyn/Stat_{base} = 5.4911\, e^{-3.0111(0.27)}$$

$$Dyn/Stat_{base} = 2.44$$

Based on the hydrostatic head for the model container :

$$Dynamic\ pressure = 2.44 \rho g h$$

$$Dynamic\ pressure = 2.44 \times 1000 \times 9.81 \times 0.15 = 3590\ Pa$$

Comparing velocities: The velocity determined from the dam-break experiment is based on an estimate made from the bore position with respect to time. Using the Michels (1988) theoretical and experimental formulae gives a reduced estimate for the impact velocity in both cases with the dimensional analysis approach producing a magnitude between these two values. The dimensional analysis produces an under-estimate of –25.5 % based on the experimental result and is possibly related to the manner of the fluid release. The door in the channel is quoted as being opened by a falling weight, which is unable to accelerate the door sufficiently fast enough to allow a standing head of liquid to fall under gravity. This means that on initial opening of the door, the fluid escaping through the gap would be forced out at higher pressure with the rest of the fluid following behind as the gap increased.

Comparing dynamic pressures: Considering the recorded dynamic pressures near the base of the model container, the instantaneous peak value is in excess of three times the post impact value. This can be attributed to the momentum of the fluid being distributed around the model container, as unlike the bund scenario, the fluid as able to pass the container on either side mainly undisturbed (Fig. 7.11). This addition momentum, which suffers no change in direction, will contribute to sudden increased pressure prior to the normal build up of fluid behind the model container. A more suitable comparison for the dynamic pressures would therefore be made with the post peak impact value. The measured post peak value of 4000 Pa compares more favourably with the empirical solution of 3590 Pa, giving an under-estimate of –10.2 %.

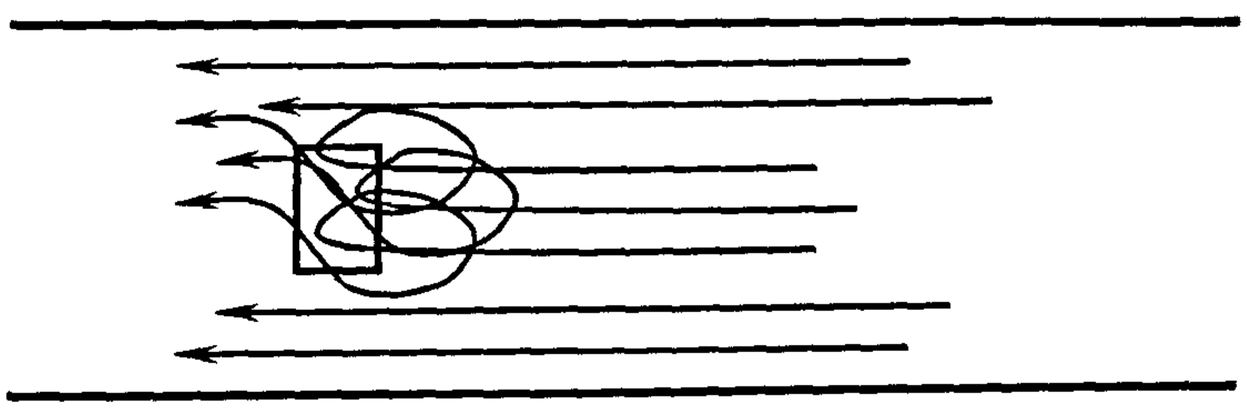

Figure 7.11 Plan view of model container with flow pattern

7.13 Comparison with CFD results supplied by Logistique France – Risques Industriels (2007) derived from information from Total France.

Table 7.3 contains results derived from a series of CFD models created for the investigation of dynamic pressures on bund walls as a result of simulated catastrophic failures of the primary containment based on actual site data (Louise, 2007). For comparison purposes the CFD predicted ratios of dynamic pressure to static pressure, *Dyn/Stat* $_{base}$ are indicted along with those predicted by the new empirical equations with the percentage differences calculated. Where the same configurations have been run a number of times using different modelling techniques and meshes, a mean value has been calculated.

Table 7.3 Comparison of empirical results with CFD results for dynamic pressures

Study referenece	*R (m)*	*H (m)*	*R/H*	*r (m)*	*h (m)*	*h/H*	*Bund capacity (%)*	*Dyn/Stat $_{base}$ (CFD)*	*Dyn/Stat $_{base}$ (LJMU)*	*Difference (%)*	*Mean Dyn/Stat $_{base}$ (CFD)*	*Difference (%)*
A	18.0	14.0	1.29	24.0	3.5	0.25	44.4	1.73	3.00	73.51		
B	6.0	12.0	0.50	8.5	3.0	0.25	50.2	3.40	2.91	-14.40		
C	6.0	11.0	0.55	8.0	2.4	0.22	38.8	3.80	3.40	-10.61		
D	9.0	12.0	0.75	12.5	2.4	0.20	38.6	4.50	3.77	-16.17		
E	26.0	19.0	1.37	29.0	2.5	0.13	16.4	5.30	5.16	-2.68		
F	21.0	10.0	2.10	24.0	2.5	0.25	32.7	1.90	3.57	87.81		
G	4.5	9.0	0.50	9.5	1.5	0.17	74.3	4.38	4.36	-0.39	4.12	5.96
H	4.5	9.0	0.50	9.5	1.5	0.17	74.3	3.54	4.36	23.25		
I	4.5	9.0	0.50	9.5	1.5	0.17	74.3	5.01	4.36	-12.91		
J	4.5	9.0	0.50	9.5	1.5	0.17	74.3	3.54	4.36	23.25		
K	6.0	9.0	0.67	9.0	1.5	0.17	37.5	4.96	4.36	-12.04	4.25	2.66
L	6.0	9.0	0.67	9.0	1.5	0.17	37.5	3.54	4.36	23.25		
M	6.0	9.0	0.67	8.0	1.5	0.17	29.6	5.30	4.36	-17.68	4.42	-1.29
N	6.0	9.0	0.67	8.0	1.5	0.17	29.6	3.54	4.36	23.25		

Comparison of dynamic pressures: The individual scenarios for the various tank and bund configurations modelled using CFD techniques indicate a large degree of variation when compared to the empirical results derived from the experimental data. This can be attributed to a number of various modelling techniques being employed with various mesh densities and VOF algorithms in an attempt to identify a satisfactory simulation of a bulk storage tank failure and the magnitude of the dynamic/static pressure ratio. Where a number of simulations for the same scenario have been recorded, the mean values of $Dyn/Stat_{base}$ have been calculated and re-compared the empirical solutions. On inspection this method gives a more favourable comparison between the values of –1.29 to 5.96 %. These results are indicative of the range of values that can be obtained using CFD modelling, particularly with problems involving free surface flow.

7.14 Summary

In general terms, the performance of the empirical equations justifies their use in the prediction of both the overtopping fractions and dynamic pressures obtained for the range of configurations for which they were developed. The orders of magnitude for the results are similar in the vast majority of cases, which provides a sufficient degree of confidence to allow reasonable predictions to be made for the purposes of risk assessment and spill management.

The overriding issues that are evident from the orders of magnitude obtained for both overtopping and dynamic pressures have severe implications for designers, operators and managers of large-scale bulk storage facilities. The discussion of the results and implications for stakeholders regarding the design and construction of secondary containment further emphasises the need for greater understanding and vigilance when evaluating risk and preparing safety reports.

CHAPTER 8

Discussion of Results and Implications for Stakeholders

8.1 Reasons for bunding

Barnes (1990) states that the object of bunding is to retain any spilled liquid from the primary storage tank/tanks in order that it may be dealt with in a controlled manner by evaporation in specially designed catchments, by foam blanketing or other suitable measures. There are two major reasons for providing bunding around a bulk storage vessel, firstly for reasons of safety and secondly for economic reasons, due to the high cost of the material being stored. With regard to safety, the risks associated with the stored material upon release may relate to flammability, toxicity along with possible corrosive and reactive properties.

In general, most of the arguments covered relate to atmospheric storage vessels sited in chemical plants, where relatively weak thin-shelled tanks are provided with full bunding. In the case of pressure vessels containing liquefied flammable gas, bunds tend not to be utilised, as they would contribute to the problem of any leak by trapping large volumes of vapour.

8.1.1 Construction of bunds

In most failure scenarios the escaping fluid normally contacts the floor of the bunded area, except possibly in the case of a spigot/jetting failure, where the fluid may completely clear the bund. The floor of the bunded area therefore needs careful consideration in terms of permeability to resist possible losses due to seepage as well as moisture content with respect to boiling rates for refrigerated liquid gases. The bund walls and floors need to withstand the possibility of thermal shock in the case of cryogenic liquids being stored and correct material selection is of great importance.

The main materials used in the construction of floors and bunds are earth and concrete, however variations include steel bunds and crushed rock. In most cases, even with a concrete bund the floor area will be constructed from levelled and compacted earth/clay with coefficients of permeability mostly not known or even considered.

For reactive/corrosive materials the floor and internal face of the bund may require special surface preparation/finishes to prevent damage in the event of a spill and specialised concrete mixes have been developed to withstand exposure to acids.

8.1.2 Bund capacity

The recommendations for the capacity of bunded areas vary greatly and nominal bund capacities range from 50 to 150 % based on actual measurements taken from operational facilities. With capacities greater than 100 %, there is no guarantee of total containment, as evidenced by sudden catastrophic tank failures accompanied by large bund overtopping fractions. Failures involving spigot flow/jetting may make the volume of the bunded area irrelevant if the tank to bund separation distance is inadequate.

8.1.3 Bund height and profile

Changes in the Codes of Practice have gone from restrictions on bund height of about 2 m to no restrictions in order to allow for high collar bunds, while in the USA, a minimum height of 1.5 m is usually stipulated. There are a number of views taken as to the required height of a bund; a possible catastrophic failure of a bulk storage tank would merit the use of a high collar bund to restrict overtopping. Others argue that such forms of construction would restrict access for fire fighting, requiring specialist equipment.

For bunds with sloping sides or dykes, there is a possibility of increased losses due to the angle of construction presenting a reduced barrier to fluid flow with low distant bunds allowing greater overtopping than taller closer installations. Hence, the volume of containment is less important than the ratio of the bund height to that of the fluid height contained in the tank.

8.2 Overtopping for axisymmetric releases

The magnitude of the overtopping results clearly indicate a problem with the current guidelines for the design of secondary containment as substantial levels of overtopping are obtained in most of the cases studied with the exception of high collar bunds. Apart from the initial impact and the resulting surge over the bund, the shock waves generated at the bund are reflected back only to return causing additional overtopping.

The results from the experimental overtopping measurements are consistent for each test configuration and indicate a serious problem if full secondary containment is to be relied upon in the event of a catastrophic tank failure. This is in direct agreement with similar results found by other researchers, where large overtopping fractions have been found both experimentally and by computational methods.

A conclusion from earlier work, supported by the new work, is that the fraction that escapes the confines of the bund is mainly a function of h/H and generally increases if h/H is reduced and the bund moved further away from the tank to maintain the same bund volume. However, a feature seen in the new work is that beyond a certain point the overtopping fraction begins to decrease. This is because surface friction begins to affect the results at larger spreading distances, where the velocities tend to be reduced.

With regard to the height of the overtopping wave, the level to which the main body of fluid reaches is in some cases higher than the original tank level prior to release. A main feature of the breaking wave is the separation layer that develops giving rise to the flight of droplets from the leading edge or crest of the wave as indicated in the video capture photograph in section 4. The height these droplets can attain generally reaches a level at least three times the original tank level, with the smallest droplets travelling even higher, especially in the case of the high collar bunds. The vertical nature of the bund face contributes greatly to this effect, as the forward horizontal momentum of the fluid is violently interrupted and a sudden change in the direction of the fluid takes place as it rapidly accumulates behind the bund, eventually surging upwards and forwards over the bund.

Reflected waves contribute to the final overtopping fraction, however this has been shown to be minor with impacts after the first one accounting for only 5 to 6% of the total, as in the case of the initial trials configuration (Table 5.4). Greenspan and Young (1978) also found that 5% of the total overtopping was from sloshing after the initial impact. The action of these 'sloshings' becomes more significant when (r – R) is small and h is large as in the case of high collar bunds, however the total overtopping is minimal in these cases.

Comparison between the smaller scale Greenspan and Johansson (1981) test data and test data obtained in this investigation for overtopping suggests a good level of agreement, with slightly more scatter associated with the squat tank results, particularly at greater separation distances. An improved level of agreement for overtopping is observed in the

case of both middle and tall tank releases, again with some scatter occurring at larger separation distances in the case of the middle tank results. It therefore seems that the effects of scale are not overly apparent in terms of the overtopping results, which is interesting as the effects of friction at smaller scales should lead to slightly smaller overtopping fractions.

The 'square' and 'rectangular' bunds investigated had overtopping fractions very similar to those of 'circular' bunds with the same area and height, slightly greater (52-55% versus 49%) for a squat tank, slightly smaller (47-50% versus 52%) for a middle tank, and in good agreement (48-50% versus 49%) for a tall tank (Table 5.10).

8.3 Overtopping for asymmetric releases

Comparisons made between orifice and slot releases of the same area of release indicate that for squat tanks, the orifice release gives a greater magnitude in overtopping for smaller separation distances and taller bunds. This situation changes as the separation distance increases and the bund wall height is reduced, when the slot release gives greater overtopping. The same is true for all ranges of R/H, middle and tall tank configurations included as illustrated in Table 5.24 and Chart 5.23 with full results in Appendix 6.

The size of the aperture is also of importance with regard to overtopping with larger apertures giving greater overtopping fractions. This is true for both orifice and slot releases with the time of emptying being an obvious factor (Tables 5.25 to 5.26 and Charts 5.24 to 5.25 with full results in Appendix 7). The trends obtained for overtopping in relation to asymmetric releases compare well to the results for slot releases published by Greenspan and Johansson (1981).

The resulting overtopping for the asymmetric releases is less than that obtained for the axisymmetric releases in all cases. This can be explained by a combination of factors depending on the size and shape of the aperture, the height of fill in the tank, the emptying time and the separation distance, L between the tank and the bund. In the majority of cases the separation distance is sufficient to allow the spigot/jet to impact the bund floor resulting in a spreading out of the flow, thus reducing the energy prior to impact with the bund. This leads to the localised build up of fluid behind the bund, which then ultimately surmounts the bund resulting in overtopping. There are exceptions to this type of behaviour and in certain cases the fluid fails to build to a height capable of overtopping the

bund and builds in depth in the bunded area with the formation of eddy currents between the bund and the sides of the spill table. These eddy currents eventually grow in magnitude and converge on the still emerging flow from the tank suddenly leading to an upward surge in the jet, which subsequently causes overtopping of the bund (Fig. 8.1).

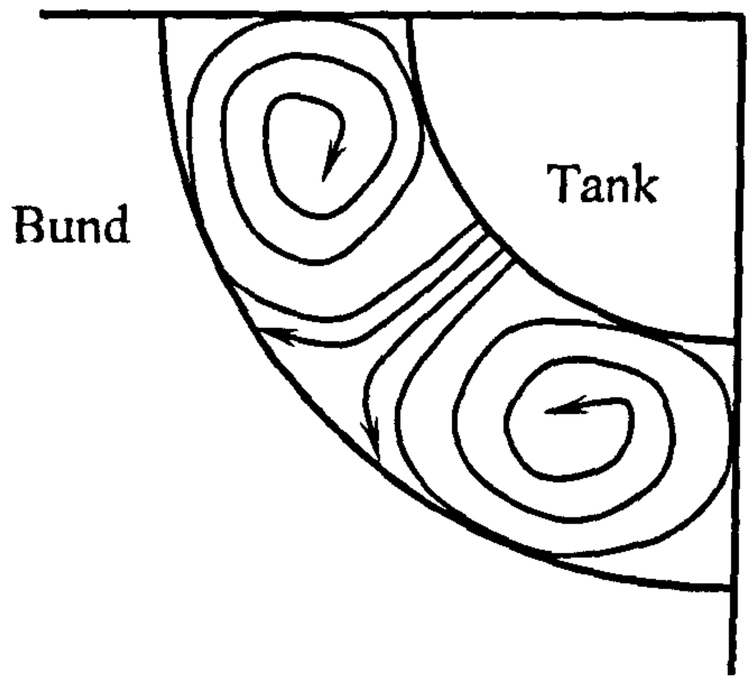

Figure 8.1 Plan view of spill table with eddy currents

There are a couple of configurations vulnerable to this type of phenomenon at certain values of h/H for all values of R/H, particularly in the case of the orifice releases. It was theorised that the geometrical configuration of the test rig was influencing the overtopping result and therefore it was decided to model two particular cases using full 360° geometries (Tables 7.1 and 7.2). This was achieved using a simple plastic barrel and concentric bund arrangement incorporating a rubber bung, which was pulled free from the orifice allowing the water to escape.

The results obtained confirmed the initial observations and the overtopping fraction was reduced with the surging fluid spreading around the bund area, rather than forming eddy currents and meeting at a position diametrically opposed to the release point prior to overtopping the bund. Comparison with the original results found that in the case of the 30 mm diameter orifice the overtopping fraction was reduced by approximately 64 % with the 90 mm diameter orifice; the reduction was approximately 38 %. This meant that the results recorded in the original quadrant test rig for the affected configurations were anomalous and that the observed localised increases in overtopping were generated as a direct result of the eddy currents. This is reflected in the quality of the fit for some of the orifice results in the empirical equations derived for asymmetric overtopping.

8.4 Avoiding overtopping

The amount of fluid overtopping the bund in the event of a significant release can vary greatly depending on the design of the secondary containment. The inclined faces of dykes may be easily vaulted or fluid may rapidly pile-up against the face of a vertical bund, subsequently flowing over the top. The resulting strong shock waves return to the original position of the tank causing further losses due to reflected waves in a so-called 'sloshing' action.

The dependence of overtopping on h/H rather than volume of containment seems clear and as h increases for the same value of H, the overtopping fraction reduces. This leads to the conclusion that high collar bunds would be the most effective way of preventing overtopping in the event of a catastrophic tank failure. A major problem with this, is the asymmetric dynamic loading, which has been determined to be up to 6 times the normal static loading condition. This obviously has implications for the design strength of high collar bunds, with many existing facilities having been designed based on static loading only. Suggestions for the possible mitigation of existing facilities include the construction of earthen berms to add support and increasing the thickness of the walls with the use of additional reinforced concrete (Barnes, 1990).

8.5 Dynamic pressures for axisymmetric releases

It is clear from the results in this report and from work carried out by previous researchers that the current design for bunds is in question with respect to containment of spillage from a sudden catastrophic failure of the primary storage. The problem of overtopping is not the only issue and the actual mechanical integrity of the bund is also in question when the magnitudes of the dynamic pressures are considered. The dynamic pressure profiles obtained in the experimental results (Charts 5.1, 5.3 and Appendix 2) are very different than those used in the normal hydrostatic design, being of generally greater magnitude but shorter duration. Structural response calculations would be needed to determine the significance, but there is a *prima facie* possibility of the collapse of the bund leading to a total failure of the secondary containment to retain any of the fluid released.

The results from the dynamic pressure transducers take a little interpretation in terms of identifying true signals and those generated by the impact of the overtopping waves striking the sensor bodies and cables. Comparison with video footage using frame-by-

frame analysis (Plate set 5.2) was used to confirm the timings of the wave impacts and identify the time periods to be used for sampling. Data logger gains were selected to ensure that sensible signals were within the ranges selected, thus avoiding any signal truncation due to excessive voltages. The largest dynamic/static pressure factors are found in the case of the smaller bund heights h, at the larger bund radii r, for each of the nominal bund capacities of 110 %, 120 %, 150 % and 200 %. These configurations also give rise to the largest overtopping fractions indicating the obvious relationship between the overtopping fraction and the associated dynamic pressures exerted on the bund. Upon examination of the local dynamic pressure maxima and static pressure profiles (Charts 5.2, 5.4 and Appendix 2) it can be seen that when the plot of dynamic pressure values falls below that of the static values, then overtopping fraction is reduced, the larger the difference the smaller the volume of fluid escaping the bund. Conversely, with dynamic values falling above the static pressure plot, the level of the overtopping fraction is increased, with large deviations leading to significant fluid loss over the bund. At the point where the difference in the envelope of bund pressure maxima is at a minimum i.e. the dynamic pressure profile is close to that of the static profile, then the overtopping fraction is at a minimum for non-high collar bunds. This corresponds to h = 48 mm for squat tank releases, h = 120 mm for middle tank releases and finally h = 240 mm for tall tank releases. This may be as expected in terms of overtopping, however a direct link between the overtopping fraction and the dynamic pressures is now clearly established. In the case of high collar bunds, the dynamic/static ratios are all less than 1 and hence have the smallest overtopping fractions, as would be expected.

The 'rectangular' bunds (Appendix 3) gave mixed results in terms of the dynamic pressures calculated at the base. In the case of the triangular configuration, the dynamic pressure was lower than that calculated for the circular equivalent for squat tanks but larger for middle and tall tank releases. The square configuration again gave a lower result than the circular for the squat tanks, but higher results for middle and tall tanks. Finally, the rectangular bund gave a lower result for the squat tank releases, but higher for middle and tall tanks when compared to their circular equivalents.

8.6 Dynamic pressures for asymmetric releases

Comparison of orifice and slot apertures with the same release area (0.5 %) Table 5.24 and Chart 5.23 indicate variations in dynamic pressures at the base with the orifice creating larger pressures in the majority of cases. This variation is related to the length of the

perimeter of the aperture, the contraction and the relative discharge coefficients together with the fill level of the tank. It should be noted that large dynamic pressures at the base do not necessarily correlate to high overtopping fractions, with overtopping being directly related to the difference between the static and dynamic pressure profiles. In cases where there is a larger difference between local static and dynamic near the top of the bund, the overtopping fraction is substantially increased. Local dynamic pressure maxima occur at various positions along the bund height as a result of the bore profile on impact and the way in which the fluid builds and is propelled up the face of the bund. In a number of cases there are negative pressures produced on the bund as a large amount of fluid impacts at the base of the bund and suddenly changes direction to run along the inner face before overtopping. This effect is due to the relative motion between the solid surface of the wall and the surrounding fluid and the accompanying drag forces.

The magnitudes of the dynamic pressures vary greatly across the range of configurations considered, however factors as high as 10.27 times the static pressure have been determined. In most cases the dynamic pressure is substantially above the normal static design pressure with values in excess of 2 times the static pressure being common.

8.7 Wave heights for axisymmetric releases

The wave monitoring probes have inherent problems with respect to establishing constant datum positions and hence were calibrated against initial tank fill levels for each test using Excel. These datum variations were due to temperature changes and the build up of contamination on the stainless steel probes. Other problems were experienced with the high collar bunds, as the reading from the probe located at the bunds tended to give wave heights in excess of the probe length. This was due to the large amounts of spray formed and the electrical connections at the probe being compromised. The results from the probes are useful in terms of determining the time between fluid release and initial impact with the bund, as the probe separation distance corresponds to the bund radius, **r**, this enables the average velocity of the wave to be estimated. In the case of this investigation these velocities have been calculated in terms of impact velocities with the distance travelled calculated from the tank wall directly to a point at the bund. The probes were also useful in allowing the investigation of the point of intersection, where the falling tank contents level is equal to that accumulated at the inner face of the bund. An estimate of the maximum wave height at the bund was also possible giving a comparison with the dynamic pressure at the base of the bund.

Assuming the dynamic pressure consists of an instantaneous hydrostatic head and an associated velocity head an estimate can be made of the maximum instantaneous hydrostatic head using the maximum wave height at the bund. A number of areas of interest were highlighted by the results from the wave monitoring probes including the apparent relationship between the position of the point of intersection for equal tank and bund wave heights and the position of the maximum dynamic pressures with respect to time. This relationship is particularly true in the case of the non-high collar bunds, where the positions of the maximum wave heights at the bunds lag the positions of the maximum dynamic pressures.

Examination of the video footage on a frame-by-frame basis (25 frames per sec) and comparison with the measured data, led to the observation that the hydrostatic element of the maximum dynamic pressure due to the instantaneous height of fluid occurred due to a mass of fluid building at the bund. This occurred prior to the formation of the separation layer as the surge moved upwards and forwards overtopping the bund. Hence the maximum wave height consists of an element of fluid, which has upwards and forwards momentum eventually forming the separation layer, leading to the expulsion of elongated fingers of fluid and finally the ejection of droplets. As is the case with the 'crown' of liquid formed by a single droplet splashing onto a surface or into a liquid pool.

The nature of the wave impact means that the full height of the wave does not contribute to the instantaneous hydrostatic element of the maximum dynamic pressure, as only part of the height has a gravitational component at that instant in time. The part of the wave with the gravitational component corresponds to the point of intersection of the fluid height in the tank and the developing wave at the bund, where both levels are equal. This means that the potential energy due to the level in the tank is equal to that of the wave building at the bund just prior to the formation of the observed separation layer.

With respect to high collar bunds, this is not always the case and for the larger bund heights, the intersections occur after the positions of maximum dynamic pressures. Conversely, in the case of the smaller bunds at the larger radii, the points of intersection occur before the positions of the maximum dynamic pressures. This illustrates the interplay of the hydrostatic and velocity heads, which form the dynamic pressures, with the smaller bund heights unable to oppose the full heights of the approaching surge profiles, thus significant dynamic pressures and overtopping result, even with reduced instantaneous wave heights. This situation changes for the largest bund radii considered due to friction

with the base of the spill table, where velocities are reduced enough to actually cause a slight reduction in the overtopping fraction.

When considering the 'rectangular' bunds, in the case of squat and middle tanks, all the configurations gave intercept and maximum wave heights lower than those found for the equivalent circular configuration. The tall tank releases gave mixed results with the triangular configuration having a greater intercept height and smaller maximum height. The square configuration gave a smaller intercept height and a greater maximum height and finally, the rectangular configuration having lower intercept and maximum heights.

8.8 Wave heights for asymmetric releases

The wave monitor was not utilised for the asymmetric releases due to the nature of the directional flow and the possible physical interference of the probe with the fluid jet. Video recordings were used to verify impact times and in cases where the dynamic pressure sensors failed to pick up a meaningful signal, the frame rate and number of frames to collision with the bund were used to establish impact velocities.

8.9 Bund effectiveness

Davies et al (1996) published findings on bund effectiveness in preventing escalation of tank farm fires and examined a number of case studies. There are a large number of incidents recorded on the Major Hazard Incident Database (MHIDAS), where bund overtopping was known be a contributory factor in the escalation of the incident. The database gives the following reasons for failure of the bund to contain losses from the storage vessel:

- Overtopping due to the fluid surge.
- Structural failure of the bund due to dynamic loading from stored liquid.
- Structural failure due to impact form pieces of the original storage vessel.
- Overfilling due to fire fighting operations.
- Open drain valves.
- Holes in the bund due to the passage of pipe work etc.
- Multiple tank failures within a single bunded area.
- 'Rocketing' of tanks containing flammables.

No incidents of 'spigot' flow over the bund were recorded on the MHIDAS database, although cases have been reported in the past.

From the analysis of vessels involving flammable releases both with and without bunds, 314 out of 376 or 84 % of releases ignited with the proportion falling to 31 out of 51 or 61 % in the case of bunded tanks. Hence, in cases specifically relating to the presence of bunds, there was a probability of 0.61 that the bund was ineffective. For cases involving the fire spreading to include other tanks, bunded vessels yielded a figure of 20 out of 51 or 39 %, with unbunded vessels quoted as 4 out of 5 or 80 %.

On further analysis, the probability of a bund failing to contain the release was 12 out of 15 or 0.80 for tanks in a shared bund and 7 out of 17 or 0.41 for singly bunded tanks. Tanks within common bunds spread the incident to a significantly greater extent than those in single bunds.

8.10 Emergency spill management

There are a number of possible routes for spills to enter rivers eventually leading to the sea with the immediate response of authorities concerning the adverse effects on human health. The type of chemical and quantities involved will determine the type of response with the longer-term efforts concentrated on avoidance of environmental impact on a wider-scale, particularly relating to species in the human food chain.

The toxicity, bioaccummulability and degradability of a particular compound, must be considered along with physical and chemical data in order to predict the outcome on the environment. The spreading at sea will take various forms depending on the time from the original spill migrating from the surface through various depths of suspension before finally reaching the seabed as degradation takes place.

The sensitivity of various regions can be mapped and areas particularly at risk can be identified e.g. fish spawning fields. As data is collected and resources mapped a process of mathematical modelling can be employed to determine pre and post spill situations. Such tools are valuable in terms of training and can assist in the decision making process in the event of a real spill.

In post spill situations there is a great need to evaluate the environmental hazard both during and after the spill and an environmental impact assessment is an essential

requirement to predict the possible outcomes of a major release. Part of the process considers possible transport routes and the potential fate of the chemicals released before they finally degrade to inorganic compounds deposited in sediment or they are combated by some other means. The chemical, physical and biological properties of various compounds involved in the spill and the actual conditions of the spill area will have to be processed before the necessary course of action can be determined. A diagrammatic representation of the process can be seen in Fig. 8.2.

In the case of a compound that is a fast precipitator and a danger to humans, then evacuation of areas that could be affected should be considered. For chemicals that dissolve in the water column or float on the surface, then efforts will have to be made to determine the effects on pelagic and bottom feeding organisms in both the short and long-term. The short-term effects on food sources for human consumption will be the initial focus of efforts with the log-term effects on the total ecosystem being a secondary consideration.

The very nature of a spill at sea can make any response difficult and in some cases a meaningful solution can be severely limited if not impossible. Efforts should be made to minimise the effects of such spills and avoid unnecessary environmental damage with suitably prepared guidance and advice given to those facing possible exposure as stated by Bender in Bockholts and Heidebrink (1988).

Figure 8.2 Chemical spills at sea

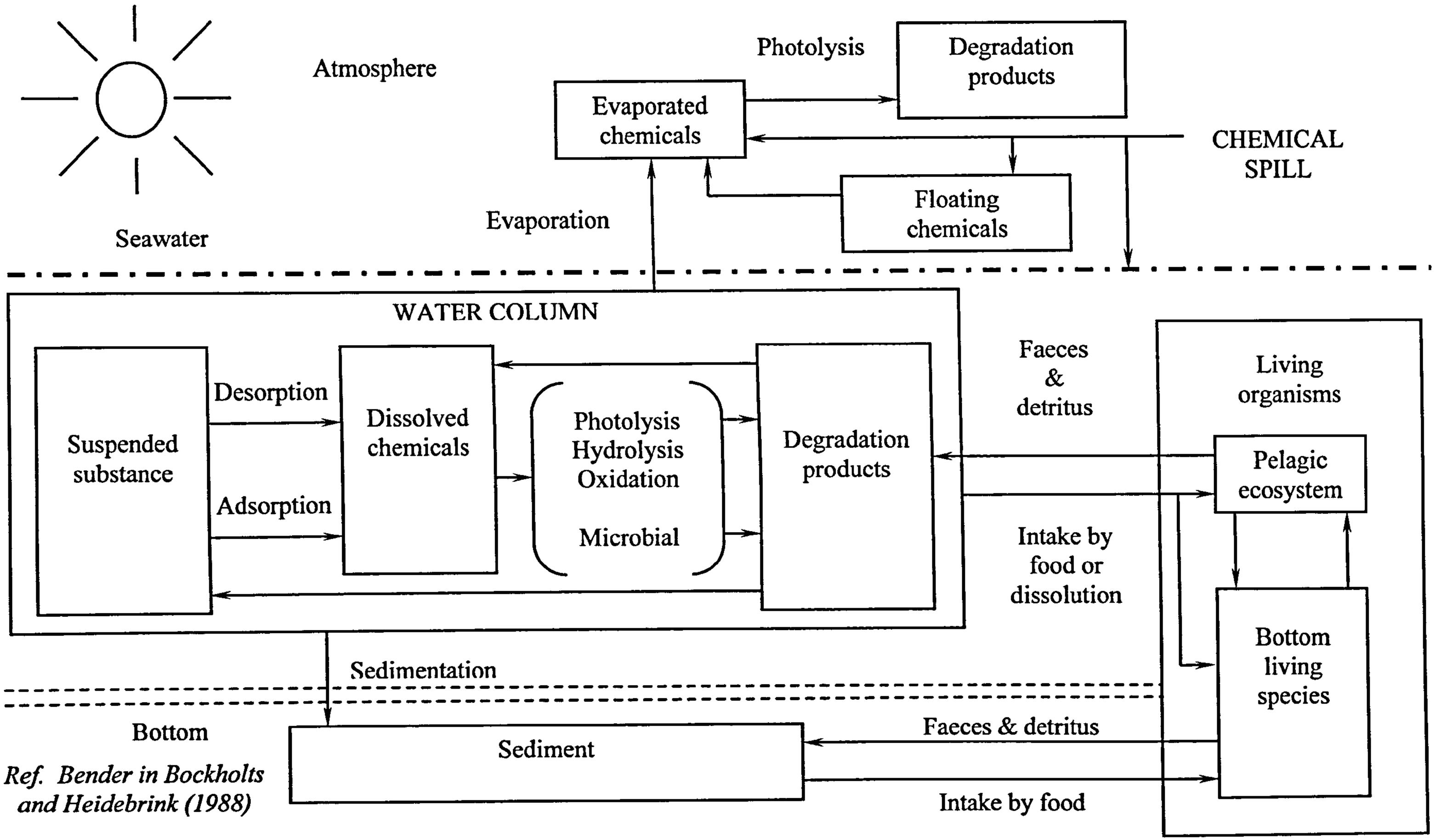

8.10.1 Case study – Ashland Oil spill (1988)

The Ashland Oil spill on 2nd January 1988 was one of the largest releases of oil in to the environment ever recorded in the USA with the total response time being in excess of a month. The response required the combined efforts of government, industry and the public. Nearly 4 million US gallons of Diesel fuel was released after the catastrophic failure of the bulk storage tank at the Ashland Oil Company terminal in Floreffe, Pennsylvania. The oil and tar tank farm was located approximately 200 yards (183 m) from the Monongahela River and the surge of escaping oil, which passed easily over the bunds of the facility entered into a near-by storm sewer. The spill in turn led to approximately 750,000 US gallons entering the Monongahela River with drastic consequences.

Estimates place most of the oil entering the river within two hours of the initial failure of the tank with difficulties encountered in shutting off the drainage access and outfall points. There were a number of factors that conspired to make an accurate assessment difficult, firstly the spill took place during the hours of darkness, secondly all electrical and communications equipment at the oil storage facility had been cut off as a safety precaution and the emergency evacuation of near-by residents collectively added to cause overall confusion. This made effective initial response to the spill mostly ineffective with access to the site limited and information confused and conflicted.

The speed of flow for the river was estimated at 3.2 kmh^{-1}, however the actual rate was 1.76kmh^{-1} with the flow rate decreasing as the temperatures fell over the next few days. The predictions of plume movement were difficult to access with the variable flow rate and emulsified oil was mixed and distributed throughout the water column. The emulsified oil made the containment booms of limited use and cleanup crews were unable to effectively deploy the booms in an effort to collect oil downstream of the spill. The extreme cold period hampered all efforts to contain and cleanup the spill with conditions on the river increasing the risk of hypothermia to the exposed crews, which meant that ultimately all crews were withdrawn from the river on day four. The formation of ice on the river acted to contain patches of the spill and interfered with the installation of additional booms and sorbent materials in other areas, which also further complicated the assessment of plume development. It was also theorised that the cold temperatures may have stabilised the oil emulsion increasing the threat of subsurface contamination, threatening the water utility intake pipes used to service populations adjacent to the river.

Employees of the oil company had provided prompt and efficient notification of the spill to the National Response Center (NRC) and local emergency response agencies. The NRC then informed the US Coast Guard, who ultimately notified the USEPA of the spill. The local authorities acted to reroute traffic and attempted to block off the storm drains as a direct means of the spill entering the river.

In terms of federal response, the US Coast Guard acted to close the river to commercial traffic and mobilised their National Strike Force, trained to deal with environmental emergencies and waterways. The USEPA arrived on site at first light and provided directions to the Technical Assistance Team, who provided engineering and scientific advice on the spill.

The Monongahela River drains into the Allegheny River with their confluence creating the Ohio River and details provided by emergency response agencies allowed treatment procedures to be put in place and storage facilities to be utilised before the contamination reached intake pipes. Using a combination of water conservation measures and bottled water, vital supplies were maintained in a number of areas, however commercial premises were affected.

The process of river monitoring involved three elements, definition of the mass of the spill and tracking of its progress, determination of the effects on wildlife and testing of water samples at the intakes. Attempts at tracking the plume combined information from fly-bys, testing at treatment plants and reports from lock and dam employees. Sampling at surface water and ground water intakes took place at regular intervals with analysis for volatile organics, total organic carbon and fuel oil.

The numerous cleanup operations covered approximately 30 miles of river with specialist equipment and alternative oil recovery systems employed from all around the world. A number of processes were proposed and trials were initiated in a few instances to assess suitability and effectiveness of the technology. Teams were established to collected oil-soaked waterfowl, however it was estimated that 2,000 to 4,000 birds had been killed as a result of the spill. The spill affected a number of other water borne species including fish and mussels and multiple studies were initiated to determine the long-term adverse effects of test subjects placed in cages down stream from the discharge (Laskowski and Voltaggio in Bockholts and Heidebrink, 1988).

8.11 Implications for stakeholders

The problems facing stakeholders in the event of a major spill are clearly on an enormous scale and if such events can be prevented or minimised, then this will bring obvious advantages. There will be less material escaping and therefore a reduced commercial loss of product, with a much more limited release to the surrounding environment, which will in turn lead to reduced environmental damage and lower costs in terms of any clean up.

There is a need for better communication of developments in the field of bulk storage and probably a requirement for greater application of such developments through possible legislation. This is necessary in both terms of improved methods of risk assessment and in terms of providing adequate secondary containment to account for the possibility of catastrophic failures of the primary storage. Only by a unified effort to respond to such issues will the necessary improvements be made and the lessons properly learned from the past. Dissemination of the findings from this research and of the empirical equations is to be carried out through peer reviewed journal publication in the months following the completion of this thesis. It is envisaged that this will have a subsequent impact within the industry and possibly lead to better regulation and design in an effort to reduce the possibility of major spills and devastating effects on the environment.

The importance of this research is clear in so far as it not only confirms the issues identified in the literature with regard to potential overtopping and the possible effects of the dynamic pressures generated, but also quantifies the magnitude of the problems over a wide range of configurations in common use. The equations proposed by Clark (2001) and Hirst in Thyer et al (2002) are suitable in terms of representing axisymmetric overtopping over the limited scale and range of configurations investigated (Tables 5.12 to 5.17, Chart 7.2 and Appendix 8). These equations, were, however never intended to represent asymmetric overtopping and are therefore restricted in their range of application.

The new empirical equations derived in this investigation were based on data elicited at a much larger scale, over an extended range of configurations with consideration of both axisymmetric and asymmetric modes of failure. The innovative approach of this work in the evaluation of the dynamic pressures generated by such failures has made it possible to derive similar empirical equations for the purposes of prediction. This gives a powerful, yet simple method of assessing not only the possible losses due to overtopping, but also the

physical integrity of existing secondary containment, when exposed to the sudden impact of the escaping fluid.

For operators and statutory bodies alike, this provides relatively simple methods of assessing the potential risks at existing facilities and will aid in the development of mitigation methods for sites found at risk. For issues of land use planning, this work allows identification of possible areas at risk in terms of major spill events if existing regulations and recommendations are adhered to in the development of future installations.

8.12 Summary

The existing design and construction of bund walls is clearly in question with regard to providing satisfactory levels of containment in the event of a failure of the primary containment vessel. This is not the only issue and in many cases the inherent factors of safety against the pressures experienced in such an event leave many bunds falling woefully short of expectation and in severe danger of complete structural failure.

Mitigation of overtopping alone may not adequate in the majority of cases and reinforcement techniques will have to be employed to strengthen existing bunds if they are to be relied upon in the unlikely, yet distinctly possible event of a catastrophic failure. A number of recommendations are proposed to for both further investigation and modifications to existing tank and bund designs with the aim of providing adequate protection across the range of foreseeable accident scenarios.

CHAPTER 9

Conclusions and Recommendations

9.1 Summation

This project investigated the catastrophic and partial failure of bulk storage vessels in the process industries by designing and constructing a suitable test facility. The investigation included conducting many hundreds of tests on various tank and bund configurations under differing modes of failure to determine the major parameters involved in the quantification of bund wall overtopping and dynamic pressures along with the associated wave velocities.

The main results from this research indicate that, although rare, the possibility exists that a bulk storage tank may fail and that considerable stored material can overtop the secondary containment. The volume of fluid lost over the bund/dyke depends on a number of variables, however the principal parameter in the determination of the magnitude of the overtopping is the ratio h/H.

The vast amount of data collected has made it possible to derive empirical formulae to predict the magnitude of both the overtopping and dynamic pressures likely to be experienced under a wide range of scenarios. These empirical equations have been checked to ensure they reasonably represent the experimental results from which they were derived and validated against previous research data including a suitable case study.

For overtopping, Equation 6.1:

$$Q = A\,exp\left[-B\left(\frac{h}{H}\right)\right]$$

With A and B taking values as recommended in Chapter 6

For dynamic pressures, Equation 6.2:

$$Dyn/Stat_{base} = C\ exp\left[-D\left(\frac{h}{H}\right)\right]$$

With C and D taking values as recommended in Chapter 6

It is the large number of configurations, the detail of the recorded results and the determination of the dynamic pressures that make this research novel in its approach to this long-standing problem. The development of the predictive equations give a simplified method of assessing the risks posed by existing facilities and allows a more accurate method of determining the performance of modified/new structures.

The major impact of this work is the quantification of the potential losses given the various types of tank failure identified and the extent to which such losses can quickly escalate to create a major incident that can have long-lasting implications. There is clear evidence that the measures currently employed are inadequate to provide complete containment given the types of failures possible, as supported by the findings in this research and the number of recorded incidents on a worldwide basis. This has serious implications for operators, regulators and planning authorities and suggests that an urgent review of major facilities should be undertaken with the express consideration of catastrophic tank failures along with other forms of major breaches.

The aim and objectives of this research have therefore been realised and problems identified in the literature have been addressed. There is now a valid method of assessing the problem of bulk storage tank failure, which has been evaluated against work by previous researchers and case studies. Comparison with the seminal works of Greenspan and Young (1978) and Greenspan and Johansson (1981) has proven the empirical equations derived to be suitable in their application for the prediction of overtopping. This was further reinforced by the satisfactory performance of the equations when applied to the case history of the Ashland Oil incident, Floreffe, Pennsylvania, USA, 2nd January 1988, where the equation suitably predicted the overtopping within the reported range of actual losses once adapted for an inclined dyke.

The performance of the equation for dynamic pressure was also suitably validated against the work of Henderson (1966) and Featherstone (1988) using the dam-break analogy. This was further underpinned by comparison with the work of Trbojevic and Slater (1989) using their finite difference model results and taking the slope of the dyke used in to account. Perhaps, one of the most unlikely analogies was that made with the work of Kleefsman et al (2004), where wave impacts were investigated on containers placed on the deck of a ship. Although the comparison gave rise to differing flow patterns, there were surprising similarities in the results obtained.

Comparisons with results from the CFD analysis carried out by Louise (2007) on bulk storage tanks operated by Total France, gave rise to varied results in term of the expected dynamic pressures. This was attributed to the different methods of analysis employed on each of the test configurations using the CFD package and once the mean values were calculated, a satisfactory comparison was made. The work of Ivings and Webber (2007) stands as further testament to the quality of the data collected in this research, with their application of the findings of Atherton (2005) in the development of their novel CFD package 'SPLOT'.

9.2 Overtopping

It has been established from the literature that even though the probability of a catastrophic tank failure is extremely low, the possibility of major loss of costly materials, infrastructure and life along with long-lasting damage to the environment, make this research of vital importance to stakeholders.

The overtopping fractions possible in the event of a catastrophic (axisymmetric) failure of the primary containment have been established and their magnitudes give cause for concern to any operators who are relying on the bunds to provide full secondary containment in such circumstances. For high-collar bunds the overtopping fraction is only a few % but for non high-collar bunds the overtopping fractions vary from 14 to 24 % at best, depending upon the initial tank fill levels and considering the larger height bunds at the closer bund radii, at the various bund capacities. For bunds of 110 % nominal capacity overtopping fractions up to 70 % were obtained (Table 5.10). This represents a considerable loss of fluid over the secondary containment with the possibility of formidable environmental impact on the area surrounding the bund, and human impact if that area is populated.

Where spigot (asymmetric) failures are concerned, using a 110 % bund capacity, the overtopping fraction varies from 0 to 2 % at best for orifice releases and from 1 to 31 % for slot releases. In the case of tall tanks, the overtopping fraction can be as high as 50 % for slot releases (Table 5.11).

It has thus been demonstrated that the present bund design criteria produce structures that are unable to contain the spills resulting from catastrophic tank failures, the amount of spillage depending upon the individual configurations used, even if those structures are not damaged by the impact.

9.2.1 Alternative design approach

CIRIA, C598 by Cassie and Seale (2003) states that while the 110 % design criterion provides a good starting point, operators need to assess their own particular circumstances in terms of the characteristics of their installation and surrounding land use. Once this has been carried out, decisions should be made as to the extent of additional measures that need to be taken, whether to increase bund capacities or provide containment measures as is considered reasonably practicable. It is reasonable to assume that a review of such measures is particularly important in the event of retrofitting and/or refurbishment and should be the result of a rigorous risk assessment.

CIRIA Report R164 (1997) is recommended as an alternative method for estimation of bund capacity and takes into account a number of factors in an effort to improve the overall performance of the secondary containment:

- The total storage capacity of the tank/tanks in the bunded area.
- The amount of rain fall that could possibly collect in a 24-hour period prior to a failure and for a period of 8 hours post failure, based on a 10 year period.
- An allowance for fire fighting requiring the bund to be of an adequate size, incorporating a recommended freeboard of 100 mm for foam.
- An allowance for surges in the event of a catastrophic tank failure, nominally a freeboard of 250 mm should be allowed, however this is not based on any particular detailed analysis and in the case of earthen dykes should be increased to 750 mm.

The bund capacity calculations allow for the volume of fluid retained within the tank, up to the height of the bund with allowances made for pipes, equipment and other permanent items within the bunded area. Physical or practical limitations to the size of a bund may reduce the capacity available to a value below that required. Various options are available to overcome the problem including reducing the storage tank capacity or constructing a containment system incorporating dedicated containment drainage and/or underground/remote storage. The most important factor is that the level of containment should be in direct response to the risk associated with the materials being stored. This will depend mostly on the risk assessment using both environmental and heath and safety factors. Environmental issues are decided on the best practical environmental option with health and safety problems rendered as low as reasonably practicable.

Even though the recommendations made above go some way to addressing the existing problems, they do not give a method of assessing the level of risk and make suggestions that are not based on any suitably detailed analysis. The suggestion of increasing the bund capacity has only a minor effect on reducing the overtopping, as has been shown in this research, where bund capacities of 200 % still give rise to significant overtopping fractions (Table 5.1). The dynamic pressures on the bund from the accompanying surge are implied, but not quantified and yet again, no recommendations are made as to a method of undertaking a 'rigorous risk assessment'.

9.3 Dynamic pressures

The dynamic pressures on the bunds have also been established. They have been linked to the overtopping fractions and in some cases are of significant magnitudes when compared to the hydrostatic pressures at the base of the bunds. For axisymmetric releases, the pressures on the bunds can be much greater than those normally employed for design purposes and were found to be mostly in excess of 6 times the hydrostatic pressure at the base (Table 5.10). Normally, bund design only considers the hydrostatic pressures, however the dynamic pressure distributions are very different to the hydrostatic pressure profiles, with variations of local dynamic pressure maxima. In the case of the smaller bunds, large variations in the dynamic/static pressure ratios were calculated, in one case the ratio was indicated to be as high as 16.45. However, such values are subject to interpretation due to the method of extrapolation and the positions of the sensors used to compute the dynamic pressures at the base.

When considering asymmetric releases, dynamic/static pressure ratios in excess of 3 are common for orifice type apertures with the maximum value calculated as 10.27. For slot type apertures, values in excess of 3 are again common with a maximum value of 8.59 recorded (Table 5.11).

The mechanical integrity of current bund design has to be questioned if the bunds are relied upon to provide secondary containment in the event of a sudden catastrophic failure of the primary containment. A catastrophic breach in the secondary containment due to the impact of a surge would be disastrous in terms of the total loss of any containment leading to a major incident of possible overwhelming environmental and human proportions.

9.4 Wave heights

The waves generated by a catastrophic tank failure can be considerable in terms of their height, and may reach heights greater than that of the original level of tank fill, with the potential to cause damage to adjoining tanks and equipment. The resulting tsunami can be far reaching with the separation layer and eventual droplet formation throwing fluid over vast distances. Details of recorded maximum wave heights can be found in the tables for the worst-case dynamic pressures and the charts for dynamic pressures and wave heights (Tables 5.3 and 5.6 and Charts 5.1 and 5.3 with full results in Appendices 2 and 3).

9.5 Bund structural design and integrity

To allow for maximum containment of hazardous liquids and protection of the environment, the inner faces of bunds should be impermeable. This can be achieved by careful consideration of the construction materials and the methods employed for connection of the structural elements to provide a continuous seal capable of preventing leaks. The most common materials used in the construction process are concrete, brickwork and block-work. In the case of concrete, which is reasonably impermeable, lining may be required depending on the reactivity of the liquid being retained. Brickwork and block-work are not normally considered as impermeable, although the use of considered bonding techniques can reduce porosity, lining are nearly always required.

The type of lining will again depend on the reactivity of the materials, however chemical resistant resins, bituminous coatings or sheet linings are common. Maintenance of linings

is essential and the durability of the materials used together with the level of environmental exposure should be used to prevent degradation.

The design of any bund should carefully consider the possibility of adverse loading conditions to ensure the necessary structural integrity throughout its life. The normal design criteria of withstanding the maximum volume they contain is no longer adequate as confirmed by a number of mathematical and experimental studies have shown. This will pose a particular problem with bund walls constructed from brick and block, which are normally structurally inferior to reinforced concrete bunds and will probably not survive the impact of a surging wave resulting from a catastrophic tank failure (Cassie and Seale, 2003).

9.6 Recommendations for reducing overtopping including modification of the bund

The effect of ground conditions will obviously cause variations in the speed of the wave approaching the bund, especially with porous ground materials, where the volume released will decrease as fluid is absorbed. Further work could be undertaken:

- To evaluate the overtopping fractions based on porous/roughened ground conditions again using similar test configurations used in this investigation.
- To investigate the use of remedial works to modify existing bunding arrangements using inward facing deflectors or profiles to redirect the vertical and forward motion of the wave backwards and reduce the overtopping fraction.

9.7 Recommendations for dynamic pressures

Any directional release of fluid under the jetting scenario would lead to the likelihood of some form of mechanical failure of the bund itself due to the localised high impact. All bunds are susceptible to dynamic loading under primary storage catastrophic failure conditions, with higher dynamic/static pressure ratios occurring for smaller height bunds at larger radii.

Further work could be undertaken:

- To further investigate the dynamic pressures experienced by low-level bunds at larger radii, with careful consideration given to more accurate determination of the dynamic pressures at the base of the bunds, given the limitations of scale and the physical size of any sensors used.

9.8 Recommendations for wave heights

The importance of the action of the resulting wave of fluid striking the bund has been established to some degree in this research, the nature of the overtopping wave in relation to the dynamic pressures being observed in some detail. Further work could be undertaken:

- To reproduce the experimental work undertaken with emphasis on more detailed measurements on the actions of the overtopping waves in direct relation to the dynamic pressures generated on the bunds.

9.9 Recommendations for modification of the storage vessel

It is important to consider the function of the storage vessel in providing primary containment and any possible improvements in design that may reduce the damaged caused in the event of a catastrophic failure. A research programme has recently been approved by LJMU to investigate the feasibility of possible mitigation measures using a number of design options. It is planned to compare the performance of any feasible designs to the newly obtained test data. Further work could be undertaken:

- To investigate the possibility of modifications to the primary containment in order to substantially reduce the overtopping fraction and dynamic pressures without the need to modify existing bunding arrangements.

9.10 Site-specific modelling

The work undertaken has been limited to considering a single tank surrounded by a single bund wall. Further work could be undertaken, for example:

- To study the effect on the overtopping fraction of having other tanks within the same bund. The positions of adjacent tanks can act to reduce the overtopping fraction by providing a physical obstacle to the escaping wave of fluid. Previous incidents have shown that there is a possibility of close proximity tanks sustaining impact damage and further adding to the quantity of escaping fluid.
- To study the effects of buildings or natural features of the terrain outside the bund in diverting the overtopped fluid. The ground levels and other features of the site can act to concentrate or divert the flow of overtopped fluid with directed flow having sufficient energy to cause considerable damage to structures or plant in areas surrounding the bund.
- To study retention in an adjacent bund or bunds following a catastrophic failure. Considerable quantities of fluid can be collected by neighbouring bunds in the event of significant overtopping of the bund containing the original source of failure.
- To study the optimum design of an additional 'tertiary' bund or flow diverter. An additional bund surrounding the secondary containment area can limit the quantity of fluid escaping to the site in the event of overtopping of the main bund. The size and position of an additional bund could be identified using existing tank and bund parameters. The possible use of diverters to control the direction of any spills could be investigated, particularly where damage to items of important plant needs to be considered.

9.11 Progress on recommendations

A number of researchers including Greenspan and Johansson (1981) have proposed varying modifications to the profile of the secondary containment as a means of reducing losses in the event of a tank failure. Recent work undertaken at LJMU in 2007 has investigated a range of possible improvements, both to the primary and secondary containment, the full details of which are to be published over the next two years. This work has concentrated on retaining the bund capacity of 110 %, as it has already been shown, counter to some arguments, that simply increasing the capacity of the secondary containment does not prevent substantial losses occurring in the event of a tank failure (Atherton 2005). The most productive in terms of loss reduction have been termed MOTIF (Mitigation Of Tank Instantaneous Failure) and COAST (Catastrophic Overtopping Alleviation of Storage Tanks), both of which are the subject of a current patent application.

MOTIF is a modification to the design of the storage vessel; it involves the installation of a low level internal baffle, the dimensions of which are governed by the type of tank to which the modification is made. The purpose of the baffle is to reduce the velocity of any escaping liquid that would be released in the event of a catastrophic tank failure. COAST incorporates a specially designed deflector fitted to the top of the bund wall capable of withstanding any wave impact. If added to an existing bund this would marginally increase the overall capacity of the secondary containment. If however, the modification is incorporated into the design of a new secondary containment system, then 110 % capacity remains more than adequate. It is the shape of the additional deflector, which is of significance in preventing overtopping rather than the overall dimensions of the structure.

The findings of this research and the evolution of MOTIF and COAST are to be modelled using advanced CFD software as part of an investigation of the possibility of developing a decision support tool for the process industry and regulators. It is envisaged that such a tool will be based on an Excel spreadsheet enabling a relatively quick method of carrying out a site-specific risk assessment and evaluating a suitable method of mitigation if required.

9.12 Summary

The range and weight of evidence provided in terms of the performance of secondary containment under all foreseeable modes of failure is difficult to refute, yet facilities continue to be constructed without due consideration of all the facts. The statistical approach to the probability of a tank failure has its place in the assessment of risk, yet given the magnitude of losses and the extensive short and long-term environmental impact of such failures, assessment criteria must merit the consideration of a more deterministic approach.

The development of effective and practicable mitigation is only one consideration in the reduction of losses and a range of hazards will always be present, given the nature of the process industry and the complexity of the systems employed. Careful land use planning and the correct selection of future sites in terms of locally sensitive areas must also be a major factor together with geographical, topographical and geological considerations.

REFERENCES

1. Akatashi, H. and Kobayashi, H. (2006) *Fire of Petroleum Tank etc. by Niigata Earthquake.* Failure Knowledge Database. http://shippai.jst.go.jp/en/Detail?fn=0&id=CB1012035&kw=Niigata+earthquake+1964 [Accessed 6 November 2006].
2. American Petroleum Institute. (2001) *Tank Inspection, Repair, Alteration and Reconstruction Third Edition.* API 653-2001.
3. Anderson, B.O. and Lindley, J. (1992) *Ammonia Tank Failure in Lithuania.* Loss Prevention Bulletin, Part :107 pp:11-15.
4. Atherton, W. (2005) *An Experimental Investigation of Bund Wall Overtopping and Dynamic Pressures on the Bund Wall Following Catastrophic Failure of a Storage Vessel.* Research Report 333, HSE Books, ISBN 0-7176-2988-0.
5. Barnes, D.S. (1990) *The design of bunds.* SRD R 500. ISBN 0-85356338 – 1.
6. BBC News UK. (2005) *Massive blaze rages at fuel depot.* http://newsvote.bbc.co.uk/mpapps/pagetools/print/news.bbc.co.uk/1/hi/uk/4517962.stm [Accessed January 2006].
7. Bender, K. in Bockholts, P. and Heidebrink, I. (1988) *Chemical Spills and Emergency Management at Sea.* Pages 277 – 283, Kluwer Academic Publishers. ISBN: 0-7923-0052-1.
8. British Standards Institute. (2004) *Specification for the design of site built, vertical, cylindrical, flat-bottomed, above ground, welded, steel tanks for the storage of liquids at ambient temperature above ground.* BS EN 14015:2004. ISBN 0 580 45461 4.
9. Buncefield Adeyfield Community Forum. (2006) *Meeting held on 22 May 2006 at Adeyfield Major incident.* http://www.dacorum.gov.uk/pdf/Mins%20Adeyfield%20Community%20Forum.pdf [Accessed May 2006].
10. Buncefield Major Incident Investigation Board. (2006) *The Buncefield Investigation: Second Progress Report.* http://www.buncefieldinvestigation.gov.uk/reports/report2.pdf [Accessed April 2006].
11. Cassie, S. and Seale, L. (2003) *Chemical Storage Tank Systems – Good Practice.* CIRIA, C598. London. ISBN 0 86017 598 7.
12. Churchill Controls. (1977) *Wave Monitor Manual.* Churchill Controls Ltd. Berks. England.

13. CIRIA. (1997) *Design of Containment Systems for the Prevention of Water Pollution from Industrial Incidents.* Report R164.
14. Clark, S.O., Deaves, D.M., Lines, I.G. and Henson, L.C. (2001) *Effects of Secondary Containment on Source Term Modelling.* HSE Books, Norwich. ISBN 0 7176 1955 9.
15. Cronin, P.S. & Evans, J.A. (2002) *A Series of Experiments to Study the Spreading of Liquid Pools with Different Bund Arrangements.* HSE Contract Research Report 405/2002, Prepared for the Health and Safety Executive by Advantica Technologies Ltd. ISBN 0 7176 225 X.
16. Cuperus, N.J. (1980) *Developments in cryogenic storage tanks.* 6th Int. Conf. on Liquefied Natural Gas. Kyoto, Japan, Session II, paper, 13.
17. Davies, T., Harding, A.B., McKay, I.P., Robinson, R.G.J. and Wilkinson, A. (1996) *Bund Effectiveness in Preventing Escalation of Tank Farm Fires.* Process Safety and Environmental Protection. Vol: 74B, pages: 88-93. ISBN/ISSN: 09575820.
18. Department of Environmental Protection. (1988) *Storage Tank Collapse Sends 500,000 Gallons of Diesel Fuel into Monongahela River.* Ashland Oil Tank Rupture, Pennsylvania. http://www.depweb.state.pa.us/heritage/cwp/view.asp?a=3&q=444629 [Accessed January 2004].
19. Environment Agency. (2005) *Buncefield – what's happening?* http://www.environment-agency.gov.uk/yourenv/857406/1242738/ [Accessed January 2006].
20. Environment Agency. (1999) *Spotlight on business environmental performance.*
21. Featherstone, R.E. (1988) *Civil Engineering Hydraulics.* BSP Professional Books. Oxford, England.
22. Federal Public Service – Employment, Labour & Social Dialogue. (2006) *Safety Alert: Rupture of an (atmospheric) Crude Oil Storage Tank.* Document No CRC/ONG/013 – E, Version 1.
23. Francis, J.R.D. (1975) *Fluid Mechanics for Engineering Students.* Fourth Edition. Edward Arnold (Publishers) Ltd. London, Great Britain. ISBN: 0-7131-3331-7.
24. Greenspan, H.P. and Johansson, A.V. (1981) *An Experimental study of Flow Over an Impounding Dike.* Studies in Applied Mathematics. 64: 211-233.
25. Greenspan ,H.P. and Young, R.E. (1978) *Flow over a Containment dyke.* J. Fluid Mech., Vol. 87, Part 1, 179-192.
26. Henderson, F.M. (1966) *Open Channel Flow.* MacMillan. New York.

27. HSE Hazardous Installations Directorate. (2000) *Secondary Containment.* Technical Measures document. http://www.hse.gov.uk/comah/sragtech/techmeascontain.htm [Accessed July 2003].
28. Ivings, M.J., and Webber, D.M. (2007) *Modelling bund overtopping using a shallow water CFD model.* Journal of Loss Prevention in the Process Industries. 20: 38– 44.
29. Kistler. (2000) *Universal Pressure Transducers.* Kistler Instruments Ltd. USA.
30. Kleefsman, K.M.T. Fekken, G. Veldman, A.E.P. (2004) *An improved Volume-of-fluid method for wave impact problem.* Paper No. 2004 – JSC – 365.
31. Laskowski, S.L. and Voltaggio, T.C. in Bockholts, P. and Heidebrink, I. (1988) *Chemical Spills and Emergency Management at Sea.* Pages 421 – 434, Kluwer Academic Publishers. ISBN: 0-7923-0052-1.
32. Louise, K. (kilian.louise@total.com), 20 Dec 2007. *RE: Dynamic pressure and height of bund.* E-mail to W. Atherton (w.atherton@ljmu.ac.uk).
33. Michels, H.J., Richardson, S.M. and Sharifi, T. (1988) *Catastrophic Failure of Storage Tanks.* I CHEM. E. symposium series No 110.
34. MSN News. (No date) http://msnbc.msn.com/id/9365607 [Accessed 28/02/2006].
35. Murphy Oil Corporation. (No date). http://www.murphyoilcorp.com/im/ [Accessed 10/11/2006].
36. Persson, H. & Lönnormark, A. (2004) *Tank Fires, Review of fire incidents 1951 – 2003.* Brandsforsk project 513-021. ISBN 91-7848-987-3.
37. Pettitt, G. and Waite, P. (2003) *Bund design to prevent overtopping.* I. Chem. E. symposium series No. 149 – 2003. ISBN/ISSN: 03070492.
38. Rouzsky, N. (1983) *Second Int. Conf. on Cryogenic Concrete.* Amsterdam. Cited in Thyer, A.M., Hirst, I.L. and Jagger, S.F. (2002) *Bund Overtopping – the consequence of catastrophic tank failure.* Journal of Loss Prevention in the Process Industries. Elsevier.
39. Seveso II Directive. (1996) *COUNCIL DIRECTIVE 96/82/EC of 9 December 1996 on the control of major-accident hazards involving dangerous substances.* http://eurlex.europa.eu/LexUriServ/LexUriServ.do?uri=CELEX:31996L0082:EN:HTML [Accessed 5 March 2004].
40. Statutory Instrument No. 743. (1999) *The Control of Major Accident Hazards Regulations 1999.* http://www.opsi.gov.uk/si/si1999/19990743.htm [Accessed March 2006].

41. Statutory Instrument No. 1088. (2005) *The Control of Major Accident Hazards (Amendment) Regulations 2005.* http://www.opsi.gov.uk/si/si2005/20051088.htm [Accessed March 2006].
42. Thyer, A.M., Hirst, I.L. and Jagger, S.F. (2002) *Bund Overtopping – the consequence of catastrophic tank failure.* Journal of Loss Prevention in the Process Industries. Elsevier.
43. Thyer, A.M. and Jagger, S.F. (1997) A *Review of Data and Models Available for Estimating the Extent of Bund Overtopping.* Health and Safety Laboratories. Buxton, England.
44. Thyer, A.M., Jagger, S.F., Atherton, W. and Ash, J.W. (2005) *A Review of Catastrophic Failures of Bulk Liquid Storage Tanks.* Draft paper for publication. Journal of Loss Prevention in the Process Industries. Elsevier.
45. Thyer, A.M. and MacMillan, A.J.R. (1998) *Bund Overtopping Data Correlation.* Health and Safety Laboratories Buxton, England.
46. Trbojevic, V.M. and Slater, D. (1989) T*ank Failure Modes and Their Consequences.* Plant/Operations Progress. Vol. 8. No 2.
47. US Chemical Safety & Hazard Investigation Board. (No date) *CBS to Conduct Full Investigation of Fatal Oilfield Incident at Partridge-Raleigh Oilfield in Raleigh, Mississippi.* http://www.csb.gov/index.cfm?folder=news_releases&page=news&NEWS_ID=295 [Accessed October 2006].
48. US Chemical Safety & Hazard Investigation Board. (No date) *CBS Issues Preliminary Findings in BP Texas City Refinery Accident; Investigators Present Data in Public Meeting.* http://www.csb.gov/index.cfm?folder=news_releases&page=news&NEWS_ID=259 [Accessed February 2006].
49. US Chemical Safety & Hazard Investigation Board. (2002) *Refinery Incident.* Report No. 2001-05-I-DE http://www.csb.gov/completed_investigations/docs/DS-MotivaIR-090602.pdf [Accessed October 2006].
50. United States Environmental Protection Agency. (1997) *Catastrophic Failure of Storage Tanks.* Office of Solid Waste and Emergency Response. US.
51. United States Environmental Protection Agency. (1998) *Chemical Accident Investigation Report* – EPA 550-R-98-001.
52. United States Environmental Protection Agency. (2000) *Oil spill program update.* 3 (2).

53. United States Environmental Protection Agency. (2001) *Rupture Hazard from Liquid Storage Tanks.*" Office of Solid Waste and Emergency Response.

54. Wilkinson, A. (1991) *Bund Overtopping – The Consequences Following Catastrophic Failure of Large Volume Liquid Storage Vessels.* SRD/HSE R530. HMSO, England. ISBN 0-853563586.

BIBLIOGRAPHY

1. ADAS National Building Design Team. (2000) *Bunds for Agricultural Fuel Oil Tanks.* Guidance on Construction, repair and Maintenance, Note No: CGN009. The Ministry of Agriculture, Fisheries and Food.
2. Baldock, T.E., Swan, C. and Taylor, P.H. (1996) *A laboratory study of non-linear surface waves on water.* Phil. Trans. R. Soc. Vol: 354, Part: 1704, Pages: 649 – 676. London, Great Britain.
3. Bulk Transporter. (2003) *Ruptured steam pipe catalyst for Vopak tank collapse.* http://bulktransporter.com/news/transportation_ruptured_steam_pipe/index.html [Accessed July 2006].
4. Buncefield Investigation. (2006) *Latest News.* http://www.buncefieldinvestigation.gov.uk/press/news.htm [Accessed October 2006].
5. Buncefield Investigation. (2006) *Press Release.* http://www.buncefieldinvestigation.gov.uk/press/b06005.htm [Accessed December 2006].
6. Buncefield Major Incident Investigation Board. (2006) *The Buncefield Investigation: Progress report.* http://www.buncefieldinvestigation.gov.uk [Accessed March 2006].
7. Buncefield Major Incident Investigation Board. (2006) *The Buncefield Investigation: Third progress report.* http://www.buncefieldinvestigation.gov.uk [Accessed May 2006].
8. Buncefield Major Incident Investigation Board. (2006) *The Buncefield Investigation: Initial report.* http://www.buncefieldinvestigation.gov.uk [Accessed August 2006].
9. Buncefield Major Incident Investigation Board. (2007) *Recommendations on the design and operation of fuel storage sites.* http://www.buncefieldinvestigation.gov.uk [Accessed April 2007].
10. Buncefield Major Incident Investigation Board. (2007) *Recommendations on the emergency preparedness for, response to and recovery from incidents.* http://www.buncefieldinvestigation.gov.uk [Accessed August 2007].
11. Buncefield Major Incident Investigation Board. (2007) *Explosion Mechanism Advisory Group report.* http://www.buncefieldinvestigation.gov.uk [Accessed September 2007].

12. Buncefield Standards Task Group. (2007) *Final Report: Safety and environmental standards for fuel storage sites.* http://www.hse.gov.uk/comah/buncefield/bstgfinalreport.pdf [Accessed August 2007].
13. Chaplin, J.R. and Flintham, T.P. (1992) *Breaking wave forces on a vertical Cylinder.* HSE, Offshore Technology Report. HMSO, London.
14. CIRIA. (No date) *Concrete Bunds for Oil Storage Tanks.* CIRIA/Environment Agencies Joint Guidelines. http://www.ciria.org.uk [Accessed July 2003].
15. City of Charles Sturt Environmental Project Officer (No date) *Bunding.* City of Charles Sturt, South Australia.
16. City of Mitcham (No date) *Storm water Management – Bunding information.* CWMB Fact Sheet No 9. South Australia.
17. Environment Agency. (2004) "*Above Ground Oil Storage Tanks: PPG2.* Pollution Prevention Guidelines. http://www.environment-agency.gov.uk/commondata/acrobat/ppg02feb04_126893.pdf [Accessed July 2003].
18. European Fertilizer manufacturers Association. (2002) R*ecommendations for the Safe and Reliable Inspection of Atmospheric, Refrigerated Ammonia Storage Tanks – Description of Specific Areas of Concern.* EFMA Publications. http://www.etma.org/publications/Amonia%20tank%20inspection/Section%203.asp [Accessed July 2003].
19. European Fertilizer manufacturers Association. (2002) *Recommendations for the Safe and Reliable Inspection of Atmospheric, Refrigerated Ammonia Storage Tanks Appendix 3.* EMFA Publications. http://www.etma.org/publications/Amonia%20tank%20inspection/Appendix%203.asp [Accessed July 2003].
20. HSE. (2005) *COMAH background.* http://www.hse.gov.uk/comah/background/comah99.htm [Accessed October 2005].
21. HSE. (2005) *COMAH index.* http://www.hse.gov.uk/comah/index.htm [Accessed October 2005].
22. Lees, F.P. (1996) *Hazard Identification and Control.* Loss Prevention in the Process Industries. Vol: 2, 2nd Edition.
23. Lemonick M.D. (1988) *Nightmare on the Monongahela.* Time. http://www.time.com/time/magazine.article/0,9171,966480,00.html [Accessed February 2008].

24. National Response Center. (2002) *NRC Background.* http://www.nrc.uscg.mil/nrcback.html [Accessed July 2007].
25. National Response Center. (2002) *Statistics – Incident Type 1991 – 1999.* http://www.nrc.uscg.mil/incident91-96.html [Accessed February 2008].
26. National Response Center. (2007) *Statistics – Incident Type 2000 – 2007.* http://www.nrc.uscg.mil/incident97-02.html [Accessed February 2008].
27. National Response Center. (2007) *Statistics – Incident Causes 1991 – 1999.* http://www.nrc.uscg.mil/causes1991-1999.html [Accessed February 2008].
28. National Response Center. (2007) *Statistics – Incident Causes 2000 – 2007.* http://www.nrc.uscg.mil/causes2000-2007.html [Accessed February 2008].
29. New South Wales EPA. (2001) *Designing and constructing bunds.* Bunding and Spill Management. Australia. http://www.environment.nsw.gov.au/mao/bundingspill.htm#designing [Accessed July 2003].
30. Steel Tank Institute. (2004) *New AST Inspection Standard Committee Plans for July Meeting.* Tank Talk. Vol 19, Number 2. http://list.steeltank.com/display2.aspx?SID=be4caf6e-ab1b-480a-995c-ffcc731e6143&N=118 [Accesses July 2003].
31. Sutcliffe, R.B. (No date) *How to survive a bund inspection.* Environmental Efficiency Consultants. Ireland.
32. Swift, R.H. (1989) *Prediction of Breaking Wave Forces on Vertical Cylinders.* Coastal Engineering. Vol: 13, Pages: 97 – 116.
33. US Chemical Safety and Hazard Investigation Board. (2007) *Statement from Carolyn W. Merrit, Chairman and CEO, US Chemical Safety Board, on the Release of the BP Refineries Independent Safety Review Panel Report.* CBS News Release. http://www.csb.gov/index.cfm?folder=news_releases&page=news&NEWS_ID=331 [Accessed February 2007].
34. Venugopal, V., Wolfram, J. and Linfoot, B.T. (2005) *The properties of extreme waves.* HSE Research Report 401. HSE books.

PUBLICATIONS

Atherton, W. (2005) *An experimental investigation of bund wall overtopping and dynamic pressures on the bund wall following catastrophic failure of a storage vessel.* Research Report 333. HSE Books. ISBN 0-7176-2988-0.

PAPERS

Thyer, A.M., Jagger, S.F., Atherton, W., Ash, J.W. (2005) *A Review of Catastrophic Failures of Bulk Liquid Storage Tanks.* Draft paper for publication. Journal of Loss Prevention in the Process Industries. Elsevier.

Atherton, W. (2006) *Catastrophic Failure of Storage tanks & Secondary Containment.* The Liverpool Conference in Built Environment and Natural Environment – First Annual Conference. http://www.ljmu.ac.uk/BLT/BUE_Docs/atherton.pdf

Atherton, W., Ash, J.W. (2006) *The Design & Manufacture of a Large Scale Test Facility for Modelling & Measuring the Losses Incurred in the Event of a Catastrophic Failure of a Bulk Storage Tank.* GERI Annual Research Symposium.

Atherton, W., Ash, J.W. (2007) *Review of Failures, Causes & Consequences in the Bulk Storage Industry.* The Liverpool Conference in Built Environment and Natural Environment – Second Annual Conference.

Ash, J.W., Atherton, W. (2007) *Current Overtopping Data; its Implications for Industry, the Environment & the Need for Mitigation.* The Liverpool Conference in Built Environment and Natural Environment – Second Annual Conference.

Atherton, W., Ash, J.W., Alkhaddar, R.M. (2006) *An Empirical Study into Overtopping & Dynamic Pressures on a Bund Wall Post Catastrophic Failure of a Storage Vessel & Methods of Mitigation.* I. Chem. E. 12th International Symposium – 'Loss prevention & Safety Promotion in the Process Industries.' Edinburgh 2007. ISBN 978-0-85295-508-6.

Atherton, W., Ash, J.W. and Alkhaddar, R.M. (2007) *The Modelling of Spills Resulting from the Catastrophic Failure of Above Ground Storage Tanks and the Development of Mitigation.* 2008 International Oil Spill Conference. Savannah, Georgia, USA.